Stony Brook University

Inhibition of Delta-induced Notch signaling using fucose analogs

A Dissertation Presented

by

Michael Schneider

to

The Graduate School

in Partial Fulfillment of the

Requirements

for the Degree of

Doctor of Philosophy

in

Molecular and Cellular Pharmacology

Stony Brook University

May 2017

Stony Brook University

The Graduate School

Michael Schneider

We, the dissertation committee for the above candidate for the

Doctor of Philosophy degree, hereby recommend

acceptance of this dissertation.

Dr. Robert S. Haltiwanger – Dissertation Advisor
Adjunct Professor, Department of Biochemistry and Cell Biology

Dr. Geoffrey D. Girnun - Chairperson of Defense
Associate Professor, Department of Molecular and Cellular Pharmacology

Dr. David Talmage
Professor, Department of Molecular and Cellular Pharmacology

Dr. R. Scott Powers
Professor, Department of Pathology

This dissertation is accepted by the Graduate School

Charles Taber
Dean of the Graduate School

Abstract of the Dissertation

Inhibition of Delta-induced Notch signaling using fucose analogs

by

Michael Schneider

Doctor of Philosophy

in

Molecular and Cellular Pharmacology

Stony Brook University

2017

Notch is a cell surface receptor that controls cell fate decisions in metazoans. Notch signaling is regulated by *O*-glycans attached to epidermal growth factor-like (EGF) repeats in its extracellular domain. Protein *O*-fucosyltransferase 1 (POFUT1) is responsible for the addition of *O*-fucose to EGF repeats and is essential for Notch signaling. Constitutive activation of Notch is associated with a variety of human malignancies. Therefore, tools for the inhibition of Notch are being sought for the development of cancer therapeutics. Towards this end, we screened L-fucose analogs for their effects on Notch signaling. Treatment with 6-alkynyl and 6-alkenyl fucose reduced Notch ligand binding and Notch signaling induced by Notch ligands Dll1 and Dll4, but not Jag1. Inhibition was partially rescued by Fringe elongation of inhibitory fucose analogs. The inhibitory analogs effectively prevented Notch-dependent T-cell differentiation, inhibited glioma cell proliferation and inhibited Notch signaling in T-ALL associated Notch mutants. Additionally, we examined the role of *O*-fucosylation in a human patient's congenital disorder resulting from a mutation in *POFUT1*, hepatocellular carcinoma, and regulation of a protein associated with Weill- Marchesani-like syndrome. Finally, we characterize the function of a novel *O*-glucose modification found on Notch EGF repeats.

To my mother, father, brothers, and sister for their enduring love and support.

Table of Contents

List of Figures/Tables/Illustrations

List of Abbreviations

EGF	Epidermal growth factor-like
POFUT	Protein *O*-fucosyltransferase
DLL	Delta-like ligand
JAG	Jagged ligand
GlcNAc	*N*-Acetylglucosamine
GalNAc	*N*-Acetylgalactosamine
GMD	GDP-mannose 4,6 dehydratese
ER	Endoplasmic reticulum
FUT	Fucosyltransferase
RBC	Red blood cell
vWF	von Willebrand Factor
LTP	Long term potentiation
NCAM	Neural cell adhesion molecule
LAD2	Leukocyte Adhesion Deficiency II
CDG	Congenital disorder of glycosylation
ADCC	Antibody dependent cellular cytotoxicity
mAb	Monoclonal antibody
CLL	Chronic lymphocytic leukemia
T-ALL	T-cell acute lymphoblastic
EGFR	Epidermal growth factor receptor
VEGF	Vascular endothelial growth factors
AFP	α-Fetoprotein
BPH	Benign prostatic hyperplasia
TSR	Thrombospondin type 1 repeat
DDD	Dowling Degos Disease
ADAMTS	A Disintegrin and Metalloproteinase with Thrombospondin motifs
B3GLCT	β3-Glucosyltransferase
LFNG	Lunatic Fringe
MFNG	Manic Fringe
RFNG	Radical Fringe
DMEM	Dulbecco's Modified Eagle Medium
OptiMEM	Optimum Minimum Essential Medium
PBS	Phosphate buffered saline
TBS	Tris-buffered saline
BCS	Bovine calf serum
FBS	Fetal bovine serum
Ni-NTA	Nickel-nitrilotriacetic acid
EIC	Extracted ion chromatogram
BSA	Bovine serum albumin
DIC	Digital interference contrast
Cax	Compact axial skeleton
hFA9	Human coagulation factor IX

m/z	Mass to charge ratio
kD	KiloDalton
bp	Base pair
TLC	Thin layer chromatography
GSI	γ-Secretase inhibitor
MO	Morpholino
ECD	Extracellular domain
LC/MS	Liquid Chromatography/Mass Spectrometry
HPLC	High performance liquid chromatography
MFI	Mean fluorescence intensity
RLU	Relative luciferase units
LSK	Lineage-Sca1^{+}ckit^{+}
2F-Fuc	2-Fluoro-fucose
CADASIL	Cerebral Autosomal-Dominant Arteriopathy with Subcortical Infarcts and Leukoencephalopathy
PNGase F	Peptide:*N*-glycosidase F
EV	Empty vector
WT	Wild type
SEM	Standard error of the mean
CSC	Cancer stem cells
OSCC	Oral squamous cell carcinoma
HEY	Hairy/enhancer-of-split related with YRPW motif protein
HES	Hairy and enhancer-of-split
aCGH	Comparitive genomic hybridization array
HCC	Hepatocellular carcinoma
L2K	Lipofectamine 2000
PEI	Polyethylenimine
RT-qPCR	Real time-quantitative polymerase chain reaction
FACS	Fluorescence-activated cell sorting
WMS	Weill-Marchesani Syndrome
EOGT	EGF Domain Specific *O*-linked *N*-Acetylglucosamine Transferase
POGLUT	Protein *O*-Glucosyl Transferase
mNotch	Mouse Notch
FL	Full length
TM	Transmembrane

Acknowledgments

I am greatly indebted to many individuals for support rendered during my PhD years, but none more so than the PI of my lab and my primary academic advisor, Dr. Bob Haltiwanger. Bob remained patient, supportive and encouraging throughout the past four years. His immense knowledge and strong guidance was invaluable throughout my research and writing. I truly could not imagine having a better advisor and mentor for my Ph.D. (except perhaps a version of Bob who stayed at Stony Brook).

I was always able to turn to the rest of my thesis committee: Dr. Geoffrey Girnun, Dr. Scott Powers and Dr. David Talmage. Only now can I fully appreciate what I was asking each of you when I invited you to serve on my committee. I thank you all for so unselfishly devoting your time and energy to the meticulous review of this project and more so, for the contribution that you have all made to my academic maturation. Equal thanks go to Dr. Jian Cao, who provided much help and many valuable insights.

Sincere thanks also must go to Dr. Miguel Garcia-Diaz, Dr. Stella Tsirka and Odalis Hernandez of Stony Brook's amazing Pharmacology graduate program. The strength of your work and efforts has built the framework for many graduate students, like myself, to gain an understanding and appreciation for science and its potential applications, especially important to me as I begin to look forward to my career in both medicine and science. My journey got started through my participation in Stony Brook's Medical Scientist Training Program, which has become synonymous with the leadership that program director, Dr. Michael Frohman has so brilliantly provided. When things seemed most desperate, Dr. Frohman was always the voice of reason and the vote of confidence that helped to maintain focus and perspective. While Mike directs the program, Carron Kaufman is instrumental in actually running it and I am forever indebted to her for her assistance and kindness.

I am also grateful to all of my MSTP compatriots who first embarked on this course with me six years ago and with whom I have now bonded for a lifetime. Thanks also to so many other friends, mentors and colleagues whom I have met along the way including all of the other members of the Haltiwanger lab, past and present. In particular, Dr. Hideyuki Takeuchi has generously shared his data, wisdom and hands-on assistance. Dr. Bernadette Holdener and Rich Grady always made sure that I had a welcome home and a running lab in the Life Sciences Building. Dr. Beth Harvey ensured that I always had a friend in the lab as she remained almost to the very end and it was always a question as to who would be the one to turn off the lights for the final time. Unfortunately, I won.

Last, but certainly not least, I want to thank my family. My siblings, Jason, Evan and Gemma, for their enduring support, confidence and love. My mother, for always being my problem solver and ensuring that the important things always get done. And my father, who has always been an inspiration to me and role model for the path that I have chosen.

Curriculum Vitae

EDUCATION

2011-present	Stony Brook University School of Medicine, Stony Brook, NY Medical Scientist Training (MD/PhD) Program PhD candidate, Lab of Dr. Robert Haltiwanger Pharmacology Graduate Program
2007-2011	Duke University, Durham, NC B.S. in Biology, minor in Chemistry Final GPA: *3.67;* Graduated with distinction in biology

RESEARCH EXPERIENCE

Research Assistant/ Independent Study Student (May 2009 – May 2011)

Duke Human Vaccine Institute – Laboratory of Laurent Verkoczy, PhD

Used a transgenic mouse model to evaluate the role of the HIV MPER epitope in possible immune tolerance to HIV. Used flow cytometry, FlowJo analysis, PCR, Southern blotting, harvested organs. Lab presentations, senior honors thesis completed.

Independent Study Student (Fall 2005 – Spring 2008)

Roslyn High School – Research Mentor Allison Wesley, PhD

Studied "Factors Influencing Students' Decisions to Use Athletic Performance Enhancing Substances." Won Regional Finalist in the Young Epidemiology Scholars (YES) competition and received a scholarship.

AWARDS/HONORS

2007	National Merit Scholarship Award
2007-2011	Young Epidemiology Scholars (YES) Scholarship
2007-2011	Dean's List (4x out of 6 eligible semesters)
2011	Graduation with Distinction in Biology
2015	Student Travel Award, Society for Glycobiology

POSTER PRESENTATIONS AND PUBLICATIONS

Schneider M & Verkoczy L. Characterization of MPER transgenic mice. Annual Duke University Biology Poster Symposium. 2011. Durham, NC. Poster.

Schneider M, Sawey E, Powers S, & Haltiwanger RS. A Role for POFUT1 in hepatocellular carcinoma. ICBD&D Stony Brook University, 2013. Stony Brook, NY. Poster.

Schneider M, Sawey E, Powers S, & Haltiwanger RS. POFUT1 promotes hepatocellular carcinoma tumorigenesis via Notch signaling. Notch signaling in development, regeneration & disease, Gordon Research Conference, 2014. Lewiston, ME. Poster.

Schneider M, Takeuchi H, Wu P, Haltiwanger RS. Using fucose analogs as inhibitors of Notch. Annual Meeting of the Society for Glycobiology, San Francisco, CA, 2015. Poster.

Schneider M, Takeuchi H, Nordstroem L, Wu P, Haltiwanger RS. Development of fucose analogs as ligand specific inhibitors of Notch. Notch signaling in development, regeneration & disease. Gordeon Research Conference 2016, Lewiston, ME. Poster.

Schneider M. Notch signaling in development, regeneration & disease. Gordon Research Seminar. 2016, Lewiston, ME. Discussion Leader.

Hubmacher D, **Schneider M**, Berardinelli S, Takeuchi H, Willard B, Reinhardt D, Haltiwanger RS, Apte S. Unusual life cycle and impact on microfibril assembly of ADAMTS17, a secreted metalloprotease mutated in genetic eye disease. *Scientific Reports*. In Press.

Schneider M, Kumar V, Nordstroem L, Feng L, Takeuchi H, Stanley P, Wu P, Haltiwanger RS. Inhibition of Delta-induced Notch signaling using fucose analogs. Submitted.

Chapter 1: Introduction

1.1 Fucose and fucose metabolism

Fucose is an unusual carbohydrate that is present in a variety of glycolipids and glycoproteins produced by mammalian cells. It is unique in having an L-configuration, whereas all other naturally occurring sugars in mammals exist in the D-conformation (Fig. 1.1). It is also structurally distinct in lacking a hydroxyl group on its C-6 carbon. A study of 3299 mammalian oligosaccharides revealed that fucose was found in 7.2% of oligosaccharides studied, second only to sialic acid, making fucose a relatively common component of carbohydrate modifications on proteins and lipids (1).

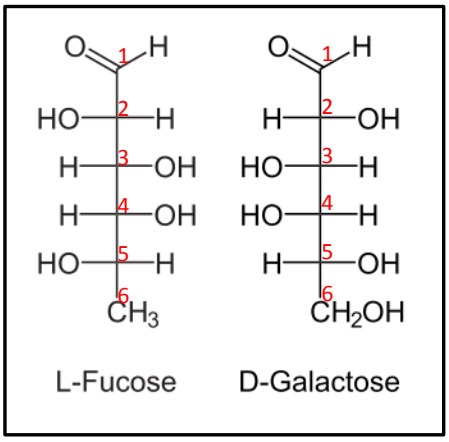

Figure 1.1: Fischer projection formula of L-fucose. The six carbons of fucose are labeled. Note that most naturally occurring sugars, such as galactose, are present in the D-configuration, as can be determined by the arrangement of the hydroxyl-group bound to the C-5 carbon. Note further that the C-6 carbon lacks a hydroxyl group. L-Fucose can also be described as 6-deoxy-L-galactose.

Fucose can be incorporated into the terminal portions of *N*-, *O*- or lipid-linked oligosaccharide chains, can modify the core of complex-type *N*-linked glycans, or can be linked directly to serine or threonine residues on some proteins. *N*-Linked glycans are extremely structurally diverse, but all contain a 5-saccharide core with an *N*-acetylglucosamine (GlcNAc) attached to the amide nitrogen of asparagine within the appropriate consensus sequence (Asn-X-Ser/Thr) of target proteins (2). Two types of *O*-linked glycans can be modified with fucose: mucin type *O*-linked glycans are initiated by the attachment of *N*-acetylgalactosamine (GalNAc) to the hydroxyl group of a serine or

threonine; alternatively fucose can be directly attached to serine or threonine residues within the appropriate consensus sequence. There are 13 known fucosyltransferases responsible for the synthesis of these fucosylated glycans (Fig. 1.2). The modifications made by these enzymes play an important role in a variety of biological systems, many of which are discussed here. Knockout of three of these fucosyltransferases, FUT8, POFUT1 and POFUT2, are lethal to mice, demonstrating their biologic importance (3-5).

All fucosyltransferases utilize a nucleotide-charged form of fucose (GDP-fucose) to modify target proteins or lipids. In mammals, GDP-fucose is synthesized through two pathways – the *de novo* synthesis pathway and the fucose salvage pathway (Fig. 1.3). The *de novo* pathway synthesizes GDP-fucose from GDP-mannose through a three-step reaction catalyzed by two enzymes, GDP-mannose 4,6 dehydratase (GMD) and GDP-keto-6-deoxymannose 3,5 epimerase (the FX protein) (6, 7). It is estimated that ~90% of GDP-fucose in mammals is generated by the *de novo* pathway under ordinary circumstances (8). The fucose salvage pathway utilizes free fucose derived from dietary sources or added to culture medium (9, 10). Fucose is transported across the plasma membrane through a poorly understood mechanism, likely L-fucose specific facilitated diffusion (11). A two-step mechanism catalyzed by two alternative enzymes then converts fucose to GDP-fucose (12). Once synthesized, GDP-fucose is transported into the lumen of the Golgi or endoplasmic reticulum (ER) to be used by the fucosyltransferases. The Golgi transporter has been identified (SLC35C1), mutations in which result in the human disorder Leukocyte Adhesion Deficiency Type II (see below) (13). An ER-localized GDP-fucose has been identified in *Drosophila* (14), but the human ortholog of this gene has been shown to be a UDP-xylose/GlcNAc transporter (15). Other candidates for a human ER GDP-fucose candidate

transporter have been reported (16), but this remains an open question. Fucose metabolism has been previously reviewed in detail (17). The remainder of this introduction will summarize what is known about the physiological and pathophysiological significance of fucose. Several very recent observations and their potential implications will be emphasized.

1.2 Terminal Fucosylation

Terminal fucosylation is a common modification found on many *N*-linked glycans, mucin-type *O*-linked glycans and glycolipids. The processing and maturation of these glycan chains is quite complex and is carried out by the concerted action of a staggering number of enzymes. Ten fucosyltransferases (FUT1-7, FUT9-11) are responsible for the addition of terminal fucose to these oligosaccharide chains. These enzymes are all localized to the Golgi apparatus and add fucose to oligosaccharides by α(1,2)-linkage to a terminal galactose or α(1,3/4)-linkage to a subterminal GlcNAc to generate blood group and Lewis antigens (Fig. 1.2). Many serve redundant functions and due to these redundancies, despite the biological importance of these modifications, loss of function for any one of these enzymes is not lethal in mice.

Common Name(s)	Abbreviation	Representative Major Product(s)
H blood group α2fucosyltransferase	FUT1^	
Secretor (Se) blood group α2fucosyltransferase	FUT2^	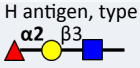
Fuc-TIII α3/4fucosyltransferase Lewis blood group fucosyltransferase	FUT3^	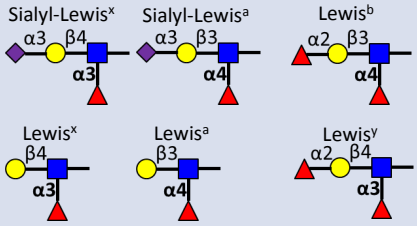
Fuc-TIV α3fucosyltransferase ELAM-1 ligand fucosyl transferase	FUT4^	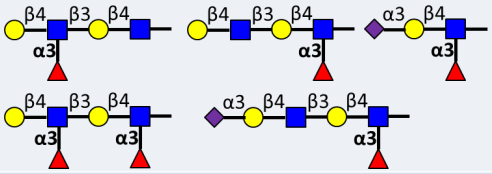
Fuc-TV α3fucosyltransferase	FUT5^	
Fuc-TVI α3fucosyltransferase	FUT6^	
Fuc-TVII α3fucosyltransferase	FUT7^	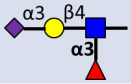
Fuc-TVIII α6fucosyltransferase	FUT8‡	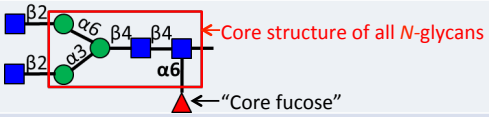
Fuc-TIX α3fucosyltransferase	FUT9^	
Fuc-TX α3fucosyltransferase	FUT10^	
Fuc-TXI α3fucosyltransferase	FUT11^	
Protein *O*-fucosyltransferase 1	POFUT1 / FUT12	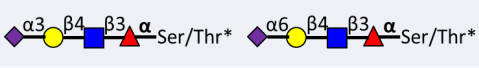
Protein *O*-fucosyltransferase 2	POFUT2 / FUT13	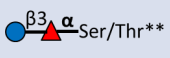

Figure 1.2: List of thirteen known fucosyltransferases in humans. Major representative products of each fucosyltransferase are listed. The linkage of the fucose added by each enzyme appears in **bold.** ^These enzymes can add fucose to oligosaccharide chains on glycolipids, *N*-linked glycans or mucin-type *O*-linked glycans. ‡This enzyme only adds core fucose to *N*-linked glycans *These modifications are only observed in *O*-fucose consensus sequences on epidermal growth factor-like (EGF) repeats ($C^2XXXX(S/T)C^3$). **This modification is only observed in *O*-fucose consensus sequences on Thrombospondin-1 type repeats (TSRs) ($C^{1-2}XX(S/T)C^{2-3}$). This figure was adapted from a figure made by Dr. Esam Al-Shareffi.

ABO blood groups

The ABO blood group antigens are perhaps the most-well known fucosylated glycans. Two α(1,2)-fucosyltransferases, the H-transferase (FUT1) and the Secretor (Se) transferase (FUT2), synthesize the structure known as the H-antigen by adding fucose to terminal galactose residues (18). The H-transferase is expressed in erythroid precursors and is responsible for the generation of H-antigen on red blood cells. The Se transferase is expressed in epithelial tissues and salivary glands and is responsible for the formation of H-antigen in saliva and other bodily secretions. Individuals without at least one copy of a functional FUT2 gene are considered non-secretors and do not produce soluble H-antigen.

ABO locus-encoded glycosyltransferases can modify the H-antigen to generate A and B antigens in A, B or AB blood type individuals. In O blood type individuals, only unmodified H-antigen is expressed. These antigens are highly immunogenic and are found in high quantities on glycoproteins and glycolipids in red blood cells (RBCs). As a result, they notoriously prevent successful blood transfusions between incompatible individuals.

Patients lacking functional copies of both α(1,2)-FucT enzymes (FUT1 and FUT2), display the rare "Bombay phenotype" (present in only ~0.01% of the population) (19), and are entirely deficient in type A, type B and H blood group antigens (20). These individuals contain robust anti-A, anti-B and anti-H antibody titers and can only receive blood transfusions from other Bombay individuals (21). Similarly "para-Bombay" individuals lack functional copies of FUT1, but still have functional Se transferase (FUT2 gene product), resulting in the absence of blood group antigens only in RBCs (22). These individuals may have low titers of antibodies against the H-antigen, but can typically receive normal blood transfusions without complication (23). Aside from potential issues with blood

transfusions, these individuals appear unaffected, prompting questions about the physiological importance of these antigens.

Although the functional significance of ABO antigen expression remains unclear, ABO blood type has been linked with other processes, suggesting medical importance beyond blood typing. ABO blood type and ability to secrete soluble H-antigen have been linked with plasma von Willebrand Factor (vWF) levels, a protein vital to the process of blood coagulation (24). Consequently, these characteristics are also related to vWF disease and other related coagulopathies. ABO blood type has also been linked to increased risk for several types of cancer (25-27), possibly suggesting a role in the immunogenicity of tumors and the associated opportunity for host recognition. The blood groups also appear to affect susceptibility to a number of pathogens (28-31) (discussed further below), suggesting that variation in blood types among individuals in a population might help to prevent the spread of disease.

Host-microbe interactions

Blood group antigens fucosylated by the Se transferase and Lewis fucosyltransferase (FUT3) also play an important role in mediating host-microbe interactions. *Heliobacter pylori*, a pathogen that can lead to peptic ulcer disease and gastric cancer, utilizes host expression of the Lewis^b antigen, generated by the joint action of the Se and Lewis fucosyltransferases, to recognize and attach to the gastric epithelial tissue (29). Other pathogens including *Norovirus* (30, 32) and *Vibrio cholera* (31) also take advantage of specific blood group antigens to attach to host cells. Additionally, *Bacteroides thetaiotaomicron*, a prominent resident of the human intestinal tract, can sense low fucose

availability in the gut and induce expression of host fucosyltransferases. It is able to harvest fucose from secreted oligosaccharides using α–fucosidases (32). Other bacteria exploit the release of free fucose by *B. thetaiotaomicron* using their own fucose sensors (33).

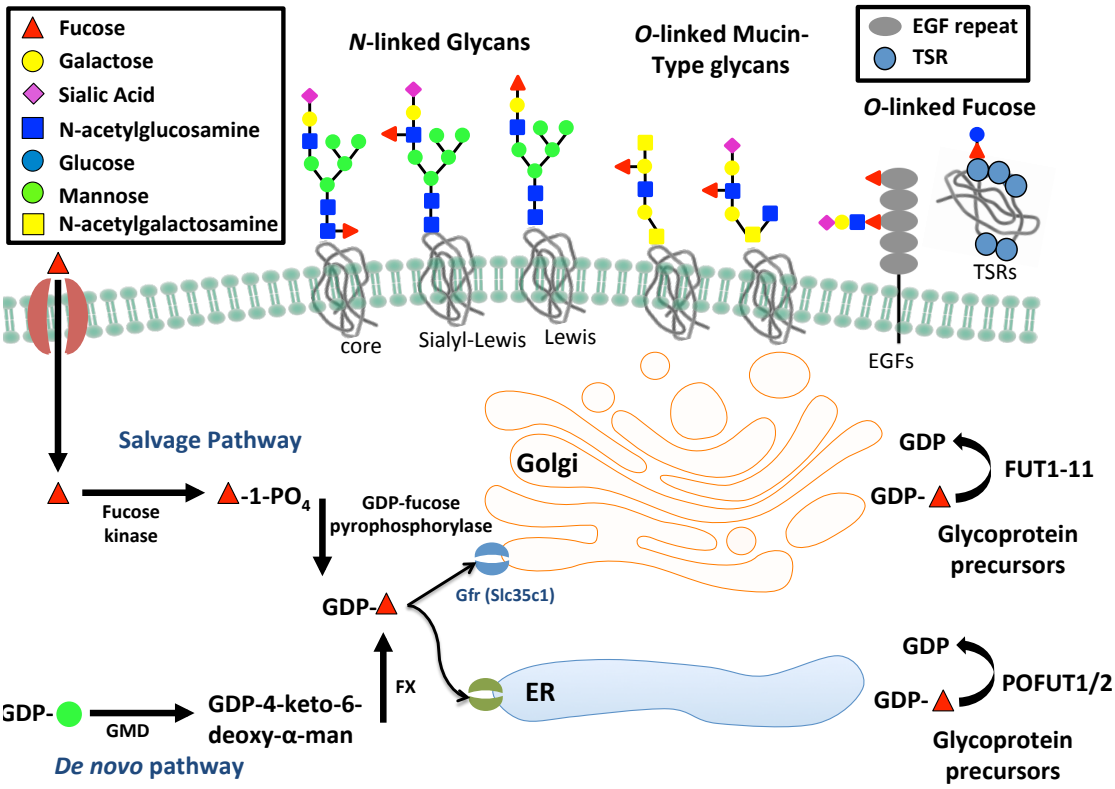

Figure 1.3: Fucose metabolism pathways and variation in types of fucosylated glycans. This figure illustrates the *de novo* fucose synthesis pathway, which converts GDP-mannose to GDP-fucose and the fucose salvage pathway, which converts free fucose taken up from outside the cell to GDP-fucose. GDP-fucose can then be taken up into the Golgi apparatus by the GDP-fucose transporter (Slc35c1) and possibly into the endoplasmic reticulum (ER) by an as-yet unknown transporter (possibly Slc35c2), (56). Proteins are then modified with GDP-fucose and other carbohydrates within the Golgi and ER and can then be secreted or expressed on the cell surface. A variety of types of fucose modifications are shown.

Fucosyltransferases also play an important role in maintaining the gut microbiome. The activity of Se fucosyltransferase promotes normal microbial diversity and composition in the gut (34). Its up-regulation during sickness serves as a protective mechanism to increase tolerance to infection and maintain host-microbiome symbiosis (35, 36).

Inactivating FUT2 mutations, seen in about 20% of the human population (37, 38), result in a non-secretor phenotype that is associated with a distinct community of bacteria in the gut. Among the notable distinctions in non-secretors is an increased association with the genus *Prevotella*, which can promote breakdown of the gut's mucus barrier (39, 40). Additionally, bacteria thought to promote good intestinal health including members of the *Lactobalcillus* and *Bifidobacterium* genera are decreased in non-secretors (39, 41). This abnormal gut microbiome composition can result in dysregulation of the local immune response (42) and is associated with increased risk of Crohn's disease (43-45).

Learning, memory and cognitive processes

Synaptic plasticity, neurite outgrowth and neuron morphology are regulated by fucosylation and are responsible for many cognitive processes including learning and memory. It was initially recognized that fucosylation of structures in the hippocampus was a component of learning and long-term potentiation (LTP) (46). Further, injections of L-fucose enhanced LTP in the rat brain (47). Additional work demonstrated that fucose α(1,2)-linkages formed by FUT1 and FUT2 were directly involved in synapse formation and neurite outgrowth (48). These fucose modifications can also direct neurite migration and mediate pathfinding for sensory neurons, including those in the olfactory bulb (49, 50).

One glycoprotein involved in these processes that has been well characterized is Synapsin I, a protein involved in neurotransmitter release and formation of new synapses. Fucosylation regulated turnover and stability of this protein (51). Fucosylation of neural cell adhesion molecule (NCAM) has also been suggested to regulate its function (52, 53). More recent work suggests that a wide array of olfactory bulb proteins involved in cell

adhesion, ion and solute transport, ATP binding, synaptic vesicle formation, and cell signaling are all modified with α(1,2)-fucose (54). Fucosylation of these proteins contribute to olfactory bulb development (54).

Leukocyte rolling and extravasation

Leukocyte trafficking is a process mediated by selectins and their counter-receptors (reviewed previously in (55)). E-, P-, and L-selectins are expressed in platelets (P-selectin), leukocytes (L-selectin), and endothelial cells (E- and P-selectins) allowing for their adhesion to oligosaccharide containing ligands expressed by specialized endothelial cells lining post-capillary venules. Mucin-type *O*-linked glycans can make up ~70% of these ligands by mass and are heavily decorated with fucose (55, 56). Two α(1,3) fucosyltransferases, encoded by the FUT4 and FUT7 genes, are responsible for the addition of these fucose residues (57). Inactivation of FUT7 in particular causes a severe deficit in selectin-dependent endothelial cell adhesion and lymphocyte homing (58). Fucose modifications on glycolipid E-selectin receptors are required for neutrophil extravasation during inflammation (58, 59).

Leukocyte Adhesion Deficiency II (LAD2), a rare congenital disorder of glycosylation (CDG) caused by mutation of the gene encoding a GDP-fucose transporter in the Golgi apparatus (SLC35C1), exemplifies the importance of fucose in leukocyte trafficking. LAD2 is characterized by immunodeficiency, leukocytosis without pus formation, mental retardation, and growth retardation, all directly attributed to the absence of neutrophil sialyl Lewis^X, of which fucose is an essential component (60). Dietary supplementation with fucose can reduce symptoms of LAD2 in some patients (61, 62), including some with

mutations causing complete inactivation of Slc35c1 (63), suggesting that at high concentrations GDP-fucose might be transported to the Golgi by the more recently described Slc35c2 (16) or other as yet unknown transporters (Fig. 1.3).

Cancer metastasis

As a byproduct of their role in promoting selectin-mediated rolling and adhesion, Sialyl Lewis antigens play an important role in promoting cancer migration and metastasis (64). These antigens are upregulated in a variety of cancer types including lung (65), breast (66) and colorectal (67, 68) cancers and serve as positive prognostic factors for increased risk of metastasis (69). Studies have even shown that elimination of fucose from these antigens with an α-L-fucosidase can impair their ability to roll within endothelial tissue and decrease cancer cell invasion (70). Additionally, one study demonstrated that preventing terminal fucosylation by knocking down FUT1 and FUT4 inhibits tumor growth (71).

Altered fucosylation has also been implicated in affecting TNF-related apoptosis inducing ligand (TRAIL) activity in colon cancer, a ligand important for promoting destruction of oncologenically transformed cells. Although the precise role for fucose in the regulation of this signaling pathway remains unclear (72), defects in the *de novo* synthesis of GDP-fucose caused increased tumor growth and metastasis of colon cancer in mice (73).

Fertilization and Development

Fucosylated *N*-linked glycans in the zona pellucida facilitate sperm binding in a variety of mammalian species (74-76), including humans (77). Fucosylated Lewis^X antigens also promote cell-cell adhesion in early stage embryos (78). Fuc-TIX (*FUT9* gene product),

responsible for the generation of Lewis^X in the brain, plays an important role in neural development and promotes normal migration of motor neuron progenitors (79). *Fut9* knockout in mice results in development of anxiety like behavior (80). Additionally, knockout of *Fut2* in mice resulted in altered hepatic vasculature and hepatic fibrosis resulting in microcirculatory disturbances and sensitivity towards bile salt toxicity (81).

1.3 Core Fucosylation

Core fucosylation is the most common type of fucose modification that occurs exclusively on *N*-linked glycans. Like terminal fucosylation, core fucosylation occurs in the Golgi and is characterized by α(1,6)-linkage to the innermost GlcNAc of the *N*-glycan core (Fig. 1.2). However, while enzymes responsible for terminal fucosylation catalyze the formation of redundant linkages, FUT8 is the sole enzyme responsible for catalyzing this reaction. *Fut8* knockout mice lack core fucose, and while born with no apparent anomalies, about 70% die within three days of birth due to major developmental growth and respiratory defects (5, 82). Survivors display severe growth retardation and emphysema-like changes in the lungs. Core fucosylation of α3β1 integrin also plays a critical role in kidney and lung organogenesis (83).

Inflammation and the immune system

Core fucosylation plays several important roles in regulating the immune system. Perhaps of greatest interest is the observation that antibody dependent cellular cytotoxicity (ADCC) is inhibited by the presence of fucose on the Fc region of IgG1 antibodies. Core fucose on IgG1 *N*-linked glycans causes a 50-100 fold reduction in binding

to FcγRIIIa (CD16), an Fc receptor found on the surface of natural killer cells and macrophages that is partially responsible for crosslinking these immune effector cells with antibody bound cells targeted for destruction (84). A co-crystal structure demonstrated that the addition of this core fucose causes a steric clash that weakens carbohydrate-carbohydrate interactions required for high affinity receptor recognition (85). This observation is of particular importance because therapeutic antibodies, used in the treatment of cancer and other diseases, can be generated without this core fucose to significantly enhance their potency (84, 86).

Several pharmaceutical companies have begun to take advantage of this knowledge and glycoengineered monoclonal antibodies (mAb) are being developed for therapeutic purposes (87). Two afucosylated mAbs have already been approved by the FDA for use in cancer patients: mogamulizumab and obinutuzumab. Mogamulizumab targets chemokine receptor 4 (CCR4), an important signal transducer that is upregulated in T-cell leukemia and lymphoma (88, 89). Obinutuzumab is an afucosylated mAb against CD20, an antigen found on developing B-cells, and has been effective for the treatment of chronic lymphocytic leukemia (CLL). Rituximab, a mAb also targeting CD20, has been approved for use in autoimmune diseases and CLL since 1997. However, obinutuzumab has been shown to be more effective in CLL treatment due more effective promotion of ADCC (90). Inspired by these successes, drug companies have continued development of similarly glycoengineered mAbs and have more than 20 currently in clinical trials (91-94).

Additionally, inflammatory cytokine TGFβ1 and α3β1 require core fucose to function (5, 83). Down-regulation of these signaling pathways causes enhanced matrix metalloproteinase expression and inflammation. Lack of core fucosylation also disrupts

epidermal growth factor receptor (EGFR) (95) and vascular endothelial growth factors (VEGF) mediated signaling (96). Core fucosylation is vital for appropriate growth factor receptor signaling (5, 82).

Cancer and cancer biomarkers

Many fucosylated oligosaccharides on proteins can serve as important cancer biomarkers (97, 98). Elevated α-fetoprotein (AFP) levels are a well-established marker for hepatocellular carcinoma. Unfortunately, elevated AFP is not entirely specific for cancer and may also be associated with other forms of benign liver disease (i.e. cirrhosis, hepatitis). Only in hepatocellular carcinoma, however, is the fraction of core fucosylated AFP elevated, making this a more reliable biomarker for cancer (99, 100). In prostate cancer, prostate-specific antigen (PSA) is another well-established 'tumor-specific' biomarker that lacks true specificity as it may also be elevated in benign prostatic hyperplasic (BPH), a very common diagnostic confounder. In patients with prostate cancer, the fraction of core fucosylated PSA is significantly increased relative to patients with BPH (101), again increasing the value of this biomarker. Increases in core fucosylation of serum proteins have also been associated with increased risk of metastasis in prostate cancer (102). In pancreatic cancer, core fucosylated haptoglobin is another potential biomarker for cancer detection (103, 104). Pancreatic cancer has a very poor prognosis largely due to lack of reliable early detection methods, so the discovery and development of more reliable detection biomarkers would be of tremendous clinical utility (105).

Additionally, increased core fucosylation of *N*-glycans on E-cadherin and integrins has been shown to decrease cell adhesion and promote cell migration and metastasis in

cancer (106, 107). Increased expression of FUT8 promotes this mechanism causing for increased tumor growth and metastasis in non-small cell lung cancer (NSCLC) and ovarian cancer (108, 109). FUT8 inhibitors might rationally be developed as anti-neoplastic agents in this context.

1.4 O-Linked Fucosylation

Fucose can also be added directly to serine or threonine residues on proteins by two protein *O*-fucosyltransferases: POFUT1 or POFUT2. POFUT1 is responsible for the addition of fucose to epidermal growth factor-like (EGF) repeats containing the consensus sequence $C^2XXXX(S/T)C^3$, where C^2 and C^3 are the second and third conserved cysteines of the EGF repeat and X represents any amino acid (110, 111) (Fig. 1.4a). EGF repeats can also be modified with *O*-glucose and *O*-GlcNAc at distinct consensus sequences. POFUT2 is responsible for similar modifications on thrombospondin type 1 repeats (TSRs) with the consensus sequence $C^1XX(S/T)C^2$ in group 1 TSRs and $C^2XX(S/T)C^3$ in group 2 TSRs (112-114) (Fig. 1.4b). TSRs can also be modified with C-mannosylation of tryptophans. Both EGF repeats and TSRs contain six conserved cysteines, which form three disulfide bonds that are crucial for the structure of these motifs. POFUT1 and POFUT2 only modify properly folded EGF repeats or TSRs, respectively (113, 115). Over 100 proteins contain EGF repeats with consensus sequences for *O*-fucose modification (116) (Table 1.1) and about 50 proteins contain TSRs with *O*-fucose consensus sequences (117) (Table 1.2). Modification of many of these proteins remains unconfirmed and much remains to be determined about the role of *O*-fucose on these proteins. Unlike the other fucosyltransferases, the protein *O*-fucosyltransferases are localized in the endoplasmic reticulum (112, 118). The fact that

POFUT1 and POFUT2 only modify properly folded modules and are ER-localized has led to the hypothesis that both enzymes participate in quality control (119).

O-Fucosylation of EGF repeats

The Notch family of receptors has more predicted *O*-fucose sites than any other protein (see Table 1.1) (120). *Pofut1* knockout is embryonic lethal in mice. These knockout mice show severe growth retardation during early embryogenesis, particularly in somite formation. Neural tube, cardiac, and blood vessel defects are also evident in these mice (121) – all phenotypes associated with defects in Notch signaling. POFUT1 also plays a critical role in mediating other Notch dependent processes including promotion of T-cell differentiation during lymphopoiesis (122). Results from many groups reveal that POFUT1 is essential for normal Notch-ligand binding and Notch signaling (4, 118, 123-125). A recently reported Notch-DLL4 co-crystal structure has additionally shown that at least one fucose on EGF repeat 12 of the extracellular domain of Notch1 directly interacts with the Notch activating ligand DLL4, demonstrating the importance of these fucose residues at the interface of protein-protein interactions (126). In addition to its fucosyltransferase activity, the *Drosophila* homolog of POFUT1, Ofut1, also acts as a chaperone for Notch protein folding (118), although it is not clear that this function is conserved in mammalian systems (124).

Fringe enzymes can elongate *O*-fucose residues with an *N*-acetylglucosamine (GlcNAc) to further regulate Notch signaling (Fig. 1.4a) (127). Fringe was originally described in *Drosophila*, where it was recognized that mutations in *fringe* caused a Notching phenotype in wings (128). Further work demonstrated that Fringe is an

important regulator of Notch signaling (129, 130). While *Drosophila* express only one Fringe enzyme, there are three mammalian homologues (Lunatic Fringe, Manic Fringe and Radical Fringe) (131). Fucose elongation by any of the three Fringes causes an increase in Notch signaling mediated by members of the Delta-like ligand (Dll) family, but can have variable effects on signaling initiated by the Jagged (Jag) family of ligands in mammals (125, 132). These enzymes play extremely important roles in regulating Notch signaling throughout development. For instance, Lunatic Fringe is required for normal somitogenesis (133, 134). Recent work has demonstrated that addition of GlcNAc by Fringe to Notch's extracellular domain create a "Fringe-mediated Notch code," where modifications at specific EGF repeats can either enhance Dll-mediated signaling or inhibit Jag-mediated Notch signaling (125, 135).

While POFUT1 is predicted to modify many other proteins based on consensus sequences, modification of most of these proteins has not been confirmed (Table 1.1). Dysregulation of POFUT1 activity has, however, been shown to play an important role in several disorders and processes involving other proteins. Heterozygous mutations in POFUT1 have been associated with a rare dermatologic condition, Dowling-Degos Disease (DDD), characterized by pigmentation abnormalities (136, 137). *O*-Fucosylation of EGF repeats also appears to play an important role in allowing agrin to cluster acetylcholine receptors (138). Amplification of POFUT1 has also been implicated as a prognostic marker and potential drug target for several cancer types including breast cancer (139), oral squamous cell carcinoma (140), and hepatocellular carcinoma (141, 142).

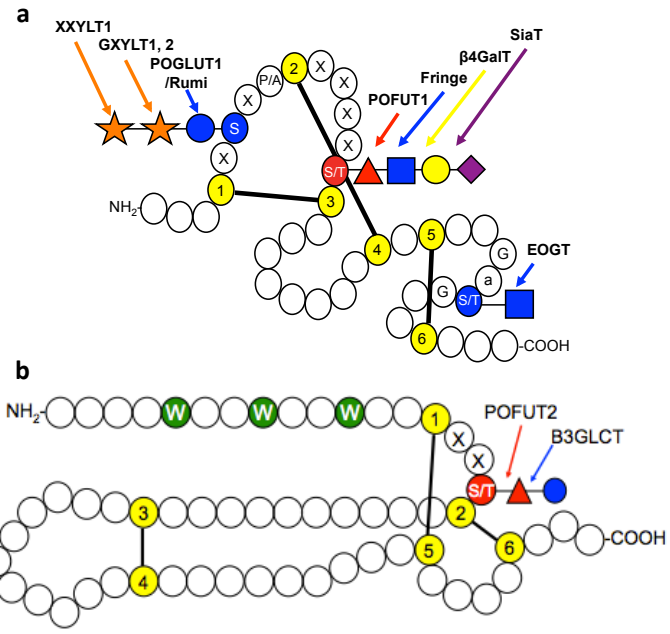

Figure 1.4: Cartoon showing key features of EGF repeats and TSRs. (a) Cartoon showing a single EGF repeat. Each circle represents one amino acid. Conserved cysteines (yellow) are numbered and disulfide bonds are indicated. *O*-Glucose and *O*-GlcNAc sites are shaded blue and the *O*-fucose site is shaded red. Enzymes responsible for the addition of each sugar are indicated. (b) Cartoon showing a typical TSR. Conserved cysteines (yellow) and disulfide bonds are indicated. *C*-Mannose sites are shown in green and the *O*-fucose site is shaded red. (S) Serine; (T) Threonine; (G) Glycine; (W) Tryptophan; (X) any amino acid.

O-Fucosylation of TSRs

Like *Pofut1*, knockout of *Pofut2* in mice is embryonic lethal with severe defects in gastrulation, indicating its importance in development (3). A recent report strongly suggests that ADAMTS9 is the target protein responsible for these defects, as knockout of *Adamts9* resulted in a phenotype essentially identical to *Pofut2* knockout (143). Other target proteins play an important role in regulating cell proliferation, migration and differentiation. *O*-Fucosylation of CCN1, which is required for its secretion, has been shown to be vital to these processes (144, 145). Additionally, members of the A Disintegrin and Metalloproteinase with ThromboSpondin motifs (ADAMTS) family of metalloproteinases play critical roles in mediating angiogenesis, extracellular structuring, inflammation, and other developmental processes (146). Several proteins in this family also depend on *O*-fucosylation for their secretion (143, 147-150). One of the affected proteins, ADAMTS13, is particularly noteworthy as its deficiency results in thrombotic thrombocytopenic purpura (TTP), a life threatening hematologic disorder (149). More work will be needed to

determine the importance of *O*-fucosylation for processes mediated by other specific proteins.

O-Fucose residues on TSRs can be elongated with glucose by β3-glucosyltransferase (B3GLCT) further promoting secretion of target proteins. Mutations in this enzyme cause the human disease Peters Plus Syndrome (PPS), characterized by a number of defects in the eye chambers, limbs and intellectual development (151). Elimination of B3GLCT activity results in reduced secretion of some, but not all of the proteins regulated by POFUT2 modification (147). A recent report from our lab suggests that the carbohydrate modifications added by POFUT2 and B3GLCT serve as a novel quality control system that recognizes and stabilizes properly folded TSRs. POFUT2 recognizes and sequentially fucosylates properly folded TSRs in the ER allowing B3GLCT to bind and add glucose to these TSRs. The data suggests that addition of these sugars stabilizes the folded form of the TSR, removing it from a folding cycle in the ER. Once all TSRs on a protein have been processed the protein can exit the ER (147).

1.5 Fucose analogs

The development of fucose analogs has revolutionized the study of fucose and fucosyltransferases by providing a valuable tool for modifying, tracking and inhibiting fucosylation of proteins. As early as 1992, it was recognized that the Lewis fucosyltransferase could tolerate GDP-fucose modified at the C-6 position by even a large structure and that this could be used as a powerful tool for labeling lipids and proteins that incorporated this modified form of fucose (152). Taking advantage of this enzymatic promiscuity, researchers have developed a strategy using fucose analogs with an azide or

alkyne group at the C-6 position to metabolically label fucosylated proteins. Once incorporated into target proteins, "click"-chemistry can be used to attach fluorophores or other groups. This strategy has allowed for successful *in vivo* imaging of fucose in several model organisms (153, 154), bacteria (155) and cell culture (156, 157). Others have used this strategy to tag fucosylated proteins with biotin allowing for their identification using anti-biotin or streptavidin probes for Western blot or isolation using a streptavidin pulldown (158, 159), potentially allowing for the identification of unknown fucosylated proteins. These tools continue to develop, as one group recently showed that 7-alkynyl fucose is more efficiently utilized by FUT8 than 6-alkynyl fucose (160). This type of development could ultimately allow for more efficient and/or targeted labeling of glycoproteins.

In addition to their utility for identifying and tracking fucosylated proteins, fucose analogs have also been developed as potential inhibitors of fucosyltransferases. Carbohydrate analogs have already been approved for the treatment of lysosomal storage disorders, diabetes and are being developed for potential use in other diseases (161). As discussed above, fucose plays an important role in many cancer types and other disorders, so the development of fucosyltransferase inhibitors might serve as a valuable clinical tool. Several groups have begun screening and developing inhibitors towards this end (162-165). One group used click chemistry to generate fucose analogs with a variety of different groups "clicked" on and screened them as potential fucosyltransferase inhibitors, identifying several candidates (166). Fucose analogs that inhibit transfer of fucose by several fucosyltransferases including FUT4, 7, and 8 can be used to prevent selectin-mediated cell migration, a process that plays an important role in cancer metastasis (167,

168). Similar inhibitors are orally active and slow tumor cell proliferation in mice (169). Additionally, taking advantage of the role fucosylation plays in regulating learning and memory, fucose analogs have been used to cause reversible amnesia and inhibition of long-term memory formation (170-172).

1.6 Aims of this dissertation

As indicated above, much is known about the critical roles fucose and other carbohydrates play in regulating protein function. This knowledge has led to the development of many novel or improved therapeutics. It remains important to continue to identify new roles for carbohydrates and new methods to study and manipulate carbohydrate modifications. In this dissertation I addressed two major aims: (1) to better understand the role *O*-linked fucose plays in regulating protein activity and (2) to identify and characterize the function of novel *O*-linked glucose modifications on Notch receptors.

As a part of the first aim, I investigated the use of fucose analogs as inhibitors of Notch signaling (Chapter 3). I also examined the effect of a novel congenital mutation, causing decreased enzymatic activity of POFUT1, on Notch signaling (Chapter 4) and began to examine the effect of amplified *POFUT1* on hepatocellular carcinoma (Chapter 5). I also used mass spectrometry to map *O*-fucose and *O*-glucose sites on mouse Notch3 (Chapter 6). Finally, I investigated the importance of fucose in regulating secretion of ADAMTS17 (Chapter 7). In the second aim, I used mass spectrometry to identify novel *O*-glucose sites on mouse Notch3. I also began to characterize the importance of the novel *O*-glucose modification in regulating Notch receptor function (Chapter 8).

Name and UNIPROT ID	Consensus / total	Known human pathology (if any)
AGRIN (O00468)	2/4	Myasthenia, limb-girdle, familial (LGM) (173, 174)
ATRAID (Q6UW56)	1/1	---
CD93 (Q9NYP3)	1/5	---
CD97 (P48960)	1/5	---
CELSR1 (Q9NYQ6)	2/8	Neural tube defects (NTD) (175)
CELSR2 (Q9HCU4)	2/7	---
CELSR3 (Q9NYQ7)	2/8	---
CFC1 (P0CG37)	1/1	Heterotaxy, visceral, 2, autosomal (HTX2); Transposition of the great arteries dextro-looped 2 (DTGA2); Conotruncal heart malformations (CTHM) (176, 177)
CFC1B (P0CG36)	1/1	---
CNTNAP5 (Q8WYK1)	1/2	---
CRB1 (P82279)	8/19	Retinitis pigmentosa 12 (RP12); Leber congenital amaurosis 8 (LCA8); Pigmented paravenouschorioretinal atrophy (PPCRA) (178-180)
CRB2 (Q5IJ48)	8/15	---
CSPG2 (P13611)	2/2	Wagner vitreoretinopathy (WGVRP) (181, 182)
CUBN (O60494)	4/7	Recessive hereditary megaloblastic anemia 1 (RH-MGA1) (183, 184)
DLK1 (P80370)	3/6	---
DLK2 (Q6UY11)	1/6	---
DLL1 (O00548)	4/8	---
DLL3 (Q9NYJ7)	2/6	Spondylocostaldysostosis 1, autosomal recessive (SCDO1) (185)
DLL4 (Q9NR61)	5/8	---
DNER (Q8NFT8)	6/10	---
EDIL3 (O43854)	1/3	---
EGF (P01133)	1/9	Hypomagnesemia 4 (HOMG4) (186)
EGFL7 (Q9UHF1)	1/2	---
EGFLAM (Q63HQ2)	2/3	---
EMR1 (Q14246)	4/6	---
EMR2 (Q9UHX3)	1/5	---
EYS (Q5T1H1)	11/27	Retinitis pigmentosa 25 (RP25) (187-190)
F7 (P08709)	1/2	Factor VII deficiency (FA7D) (191-196)
F9 (P00740)	1/2	Hemophilia B (HEMB); Thrombophilia, X-linked, due to factor IX defect (THPH8) (197-200)
F12 (P00748)	1/2	Factor XII deficiency (FA12D); Hereditary angioedema 3 (HAE3) (201-204)

FAT1 (Q14517)	2/5	---
FAT2 (Q9NYQ8)	1/2	---
FAT3 (Q8TDW7)	3/4	---
FAT4 (Q6V0I7)	5/6	Van Maldergem syndrome 2 (VMLDS2) (205)
FBLN1 (P23142)	1/9	Complex type of synpolydactyly; Associated with human breast cancer (206, 207)
FBLN7 (Q53RD9)	1/3	---
FBN2 (P35556)	1/47	Arthrogryposis, distal 9 (DA9) (208-213)
FBN3 (Q75N90)	1/44	---
HABP2 (Q14520)	1/3	---
HGFAC (Q04756)	2/2	---
JAG1 (P78504)	11/16	Alagille syndrome 1 (ALGS1); Tetralogy of Fallot (TOF) (214-216)
JAG2 (Q9Y219)	9/16	---
LRP1 (Q07954)	5/22	---
LRP1B (Q9NZR2)	4/14	---
LTBP2 (Q14767)	1/20	Glaucoma 3, primary congenital, D (GLC3D); Microspherophakia and/or megalocornea, with ectopialentis and with or without secondary glaucoma (MSPKA); Weill-Marchesani syndrome 3 (WMS3)(217-219)
MEGF6 (O75095)	1/27	---
MEGF8 (Q7Z7M0)	2/5	Carpenter syndrome 2 (CRPT2) (220)
MEGF10 (Q96KG7)	2/15	Myopathy, early-onset, areflexia, respiratory distress, and dysphagia (EMARDD)(221, 222)
MEGF11 (A6BM72)	2/14	---
MMRN1 (Q13201)	1/1	Factor V Quebec (223)
NCAN (O14594)	2/2	---
NELL1 (Q92832)	1/5	---
NID2 (Q14112)	1/5	---
NOTCH1 (P46531)	20/36	Aortic valve disease 1 (AOVD1) (224)
NOTCH2 (Q04721)	20/36	Alagille syndrome 2 (ALGS2); Hajdu-Cheney syndrome (HJCYS) (225-227)
NOTCH2NL (Q7Z3S9)	5/6	---
NOTCH3 (Q9UM47)	14/34	Cerebral arteriopathy with subcortical infarcts and leukoencephalopathy (CADASIL); Myofibromatosis, infantile 2 (IMF2)(228-231)
NOTCH4 (Q99466)	18/29	---
PAMR1 (Q6UXH9)	1/1	---
PEAR1 (Q5VY43)	1/9	---
PGBM (P98160)	3/4	Schwartz-Jampel syndrome (SJS1); Dyssegmental dysplasia Silverman-Handmaker type (DDSH)(232, 233)

PGCB (Q96GW7)	1/1	---
PROC (P04070)	1/2	Thrombophilia due to protein C deficiency, autosomal dominant (THPH3) and autosomal recessive (THPH4) (234-236)
PROZ (P22891)	1/2	---
RELN (P78509)	2/8	Lissencephaly 2 (LIS2) (237)
SLIT1 (O75093)	2/9	---
SLIT2 (O94813)	3/7	---
SLIT3 (O75094)	3/9	---
SNED1 (Q8TER0)	10/15	---
SREC2 (Q96GP6)	1/7	Van den Ende-Gupta syndrome (VDEGS) (238)
STAB1 (Q9NY15)	3/16	---
STAB2 (Q8WWQ8)	6/17	---
SUSD1 (Q6UWL2)	2/3	---
SVEP1 (Q4LDE5)	4/9	---
TEN1 (Q9UKZ4)	1/8	---
TEN2 (Q9NT68)	2/8	---
TEN4 (Q6N022)	2/8	---
TIE1 (P35590)	1/3	---
TPA (P00750)	1/1	Increased activity results in excessive bleeding; Defective release results in thrombosis or embolism. (239)
TSP3 (P49746)	1/3	---
UMOD (P07911)	3/3	Familial juvenile hyperuricemic nephropathy 1 (HNFJ1); Medullary cystic kidney disease 2 (MCKD2); Glomerulocystic kidney disease with hyperuricemia and isosthenuria (GCKDHI)(240, 241)
UMODL1 (Q5DID0)	1/3	---
UROK (P00749)	1/1	Quebec platelet disorder (QPD) (242)
VASN (Q6EMK4)	1/1	---
VWA2 (Q5GFL6)	2/2	---
VWDE (Q8N2E2)	3/7	---
WIF1 (Q9Y5W5)	2/5	---

Table 1.1: List of putative human gene targets of POFUT1. Potential targets of POFUT1 are listed based on a ScanProsite database search of all human proteins containing EGF repeats that also contain the $C^2XXXX(\underline{S/T})C^3$consensus sequence for *O*-fucosylation cross-referenced with the Uniprot database. Splice variants were not considered. The number of EGF repeats containing the consensus sequence/total number of EGF domains is listed, as well as any known human pathologies associated with the putative targets. Confirmed POFUT1 targets are listed in boldface. This table was adapted from a table made by Dr. Esam Al-Shareffi.

Name and UNIPROT ID	Consensus / total	Known human pathology (if any)
ADAMTS1 (Q9UHI8)	3/3	---
ADAMTS2 (O95450)	2/4	Ehlers-Danlos syndrome 7C (EDS7C) (243)
ADAMTS3 (O15072)	2/4	---
ADAMTS4 (O75173)	1/1	---
ADAMTS5 (Q9UNA0)	2/2	---
ADAMTS6 (Q9UKP5)	3/5	---
ADAMTS7 (Q9UKP4)	5/8	---
ADAMTS8 (Q9UP79)	2/2	---
ADAMTS9 (Q9P2N4)	12/15	---
ADAMTS10 (Q9H324)	3/5	Weill-Marchesani syndrome 1 (244, 245)
ADAMTS12 (P58397)	6/8	---
ADAMTS13 (Q76LX8)	7/8	Thrombotic thrombocytopenic purpura, congenital (TTP) (149, 246-249)
ADAMTS14 (Q8WXS8)	2/4	---
ADAMTS15 (Q8TE58)	3/3	---
ADAMTS16 (Q8TE57)	6/6	---
ADAMTS17 (Q8TE56)	4/5	Weill-Marchesani-like syndrome (250)
ADAMTS18 (Q8TE60)	4/5	Microcornea, myopic chorioretinal atrophy, and telecanthus (MMCAT) (251)
ADAMTS19 (Q8TE59)	4/5	---
ADAMTS20 (P59510)	11/15	---
ADAMTSL1 (Q8N6G6)	8/9	---
ADAMTSL2 (Q86TH1)	6/7	Geleophysic dysplasia 1 (252)
ADAMTSL3 (P82987)	8/10	---
ADAMTSL4 (Q6UY14)	2/6	Ectopialentis 2, isolated (ECTOL2) (253); Ectopialentis et pupillae (ECTOLP) (254)
ADAMTSL5 (Q6ZMM2)	1/1	---
BAI1 (O14514)	4/5	---
BAI2 (O60241)	4/4	---
BAI3 (O60242)	4/4	---
C6 (P13671)	1/3	Complement component 6 deficiency (C6D) (255)
CILP2 (Q8IUL8)	1/1	---
CTGF (P29279)	1/1	---
CYR61 (O00062)	1/1	---
HMCN1 (Q96RW7)	6/6	Age-related macular degeneration 1 (ARMD1) (256)
ISM1 (B1AKI9)	1/1	---
NOV (P48745)	1/1	---
PPN (O95428)	4/5	---

PROP (P27918)	4/7	Properdin deficiency (PFD) (257-259)
SEM5A (Q13591)	2/7	---
SEM5B (Q9P283)	2/5	---
SPON1 (Q9HCB6)	5/6	---
SSPO (A2VEC9)	10/24	---
THS7A (Q9UPZ6)	4/15	---
THS7B (Q9C0I4)	4/18	---
THSD1 (Q9NS62)	1/1	---
THSD4 (Q6ZMP0)	3/6	---
TSP1 (P07996)	3/3	---
TSP2 (P35442)	3/3	Intervertebral disc disease (IDD) (260)
WISP1 (O95388)	1/1	---
WISP2 (O76076)	1/1	---
WISP3 (O95389)	1/1	Progressive pseudorheumatoidarthropathy of childhood (PPAC) (261)

Table 1.2: List of putative human gene targets of POFUT2. Potential targets of POFUT2 are listed based on a ScanProsite database search of all human proteins containing TSRs that also contain the $CX_{2\text{-}3}(\underline{S/T})C_2G$ consensus sequence for *O*-fucosylation cross-referenced with the Uniprot database. Splice variants were not considered. The number of TSRs containing the consensus sequence/total number of TSR domains is listed, as well as any known human pathologies associated with the putative targets. Confirmed POFUT2 targets are indicated in boldface. This table was adapted from a table made by Dr. Esam Al-Shareffi.

Chapter 2: Materials and Methods

2.1 Expression Constructs

Mouse Notch1 (mNotch1) expression plasmid containing EGF1-18 with C-terminal Myc-His6 tags (pSecTag2, Invitrogen) was described previously (262). The plasmid expressing full-length mNotch1 (mN1; pcDNA1-mN1-myc) was generously provided by Dr. Jefferey Nye (263). The plasmid expressing full-length mNotch2 (mN2; pTracer-CMV-mN2-Flag) was kindly provided by Dr. Shigeru Chiba (264). Fringe plasmids SEAP (EV) and Lfng-AP were previously described (127). The TP-1 luciferase reporter construct (Ga981-6) was a gift form Dr. Georg Bornkamm and the gWIZ β-galactosidase construct was from Gene Therapy Systems. A plasmid expressing GFP (pEGFP-N1) was from Clontech. Note that "N1" in this plasmid name refers to a Not1 restriction site following the GFP coding region. T-ALL mutant plasmids were a gift from Dr. Stephen Blacklow. The construct used for POFUT1 overexpression has been previously described (265). For RNAi experiments the LPE retroviral vector (Mirimus) was used (266). The plasmid expressing full length mNotch3 fused with GFP (pEGFP) (267) and the secreted extracellular domain of mNotch3 (pSecTag2) (268) have been previously described. Plasmids used for ADAMTS17 site mapping and secretion assays have been described (269) (described in Chapter 7).

2.2 Cell culture

HEK293T, NIH3T3 (NIH3T3 CRL-1658), U-87 MG (HTB-14), T98G (CRL-1690), and A172 (CRL-1620) cells were obtained from the American Type Culture Collection (ATCC)(Manassas, VA). These cells were authenticated and tested for mycoplasma contamination by ATCC at the time of purchase. U2OS WT and *POFUT1* knockout cells were generously provided by Dr. Steven Blacklow (Harvard Medical School). L cells stably

expressing Jagged1 (Jag1) or Delta-like 1 (Dll1) were a gift of Dr. Gerry Weinmater (UCLA). MS5 cells stably expressing Delta-like 4 (Dll4) were a gift from Dr. Stephen Blacklow. HEK293T, NIH3T3, L cells, MS5 cells, and U2OS cells were grown in Dulbecco's modified Eagle's medium (DMEM)(Invitrogen) supplemented with 10% bovine calf serum. U87MG and T98G cells were grown in minimum essential media (Invitrogen) supplemented with sodium pyruvate, essential amino acids and fetal bovine serum. A172 and HepG2 cells were cultured in DMEM supplemented with fetal bovine serum. Skin derived fibroblasts were grown in DMEM-low glucose (Invitrogen) supplemented with 10% FBS. All cells were grown at 37°C in a humidified incubator at 5% CO_2.

2.3 Production of sugar and sugar analog-modified proteins

HEK293T cells were co-transfected with plasmids encoding mouse N1 EGF1-18-MycHis (2 μg) and either SEAP (EV) or Lfng-AP (Lfng) (1 μg); mouse N3 EGF1-34 (2 μg) and either SEAP (EV), Lfng-AP (Lfng), Mfng-AP (Mfng), or Rfng-AP (Rfng) (1 μg); or ADAMTS17 1C or 25P constructs (2 μg) in a 10 cm plate containing 8 mL media using 6 μl of PEI reagent (polyethyleneimine)(270) per 1 μg of DNA mixed with 100 μl of OPTI-MEM (Invitrogen) per 1 μg of DNA. Cells were washed with PBS and media was changed to OPTI-MEM containing 50 μM of the appropriate fucose analog after 6 hours for fucose analog experiments or pure OPTI-MEM (Invitrogen) for other experiments. Four days later the media was collected and protein was purified using Ni-NTA resin (Qiagen) and eluted with 250 mM imidazole as described previously (271). For analysis of protein *O*-fucosylation, ADAMTS17 constructs 1C and 25P were transiently expressed in HEK293T cells and proteins were purified from conditioned medium using Ni^{2+}-NTA resin (Qiagen). The

purified proteins were reduced, alkylated, and subjected to digestion with trypsin or chymotrypsin (Promega, Madison, WI).

2.4 Glycoproteomic analysis of purified Notch and ADAMTS17 protein

Affinity-purified protein from each culture condition was reduced, alkylated and digested (in-gel) with trypsin, chymotrypsin or V8 as described previously (262, 271). The resulting peptides were analyzed by nano LC-MS/MS using Agilent nano-HPLC-CHIP system coupled to a model 6340 Ion Trap mass spectrometer as described (262, 271). *O*-Fucosylated and *O*-glucosylated peptides were identified by neutral loss searches and semi-quantitative Extracted Ion Chromatograms (EICs) of selected ions were generated to compare relative amounts of relevant glycoforms of each peptide (262, 271). EICs were smoothed using a Gaussian algorithm.

2.5 Cell-based co-culture Notch reporter assay

NIH3T3 cells (0.5 x 10^4 cells/well) were seeded in a 24-well tissue culture plate and co-transfected with 0.1 μg of pcDNA1-mN1-myc or pTracer-mN2-Flag, and either 0.05 μg of SEAP (EV) or Lfng-AP (Lfng) plasmid (0.1 μg Lfng-AP was used in Dll1-N2 experiments to better evaluate the effects of Fringe), along with 0.12 μg of TP-1 luciferase Notch signaling reporter construct and 0.06 μg of gWIZ β-galactosidase construct for transfection efficiency normalization using Lipofectamine 2000 (Invitrogen), according to the manufacture's instructions. After 4 hours, media were changed to media containing the appropriate peracetylated fucose analog (50 μM, unless otherwise specified) or DMSO. Then L-cells stably expressing Jag1 or Dll1, or MS5 cells stably expressing Dll4, were overlaid on the

NIH3T3 transfectants at a density of 1.5 x 10^5 cells/well. Cells were lysed after an additional 24 hour culture and luciferase and β-galactosidase assays were performed based on the manufacture's instructions (Luciferase Assay system, Promega) as described previously (262, 272). Three biological replicates were performed in at least two independent experiments (total n≥6, as indicated in figure legends).

Similar assays were performed with T-ALL constructs in U2OS cells. Briefly, U2OS cells were plated in 24 well plates at 0.5 x 10^4 cells/well and incubated overnight. Cells were transfected with EV, human WT Notch1 or T-ALL mutant Notch1 plasmids (0.1 μg), TP-1 Notch luciferase reporter (0.12 μg) and gWIZ β-galactosidase (0.06 μg). Cells were washed, lysed and luciferase and β-galactosidase were performed, as above. Cells were incubated for 4 h and media was changed to either normal growth media or normal growth media with Dll1-expressing L-cells (1.5 x 10^5 cells/well). Three biological replicates were performed in at least two independent experiments (total n≥6, as indicated).

For signaling assays in glioma cells, glioma cell lines were plated in 24 well plates at 0.5 x 10^4 cells/well. Cells were incubated overnight and transfected with TP-1 Notch luciferase reporter (0.12 μg) and gWIZ β-galactosidase (0.06 μg). After 4 h cells were co-cultured with Dll1 expressing L-cells and were incubated for 24 additional hours. Cells were lysed and endogenous Notch activity was measure, as above.

2.6 Notch ligand coated plate induction assay of Notch signaling

24-well tissue culture plates were coated with Dll1-Fc (R&D Systems, 3970-DL-050), Dll4-Fc (Sino Biological, 10171-H02H-50) or Jag1-Fc (R&D Systems, 599-JG-100) (4 μg/mL per well for each ligand) in PBS for 2 hours at room temperature. NIH3T3 cells (0.5

x 10^5 cells/well) were plated in ligand-coated wells and incubated overnight. Transfection of control and Notch reporter constructs, media changes, β-galactosidase, and luciferase reporter assays were carried out, as above. Three biological replicates were performed for each condition (n=3).

2.7 Cell surface Notch expression

HEK293T cells were co-transfected 1.5 μg of either EV or pcDNA-N1-MycHis, and 0.4 μg of GFP (pEGFP-N1) in a 3.5-cm plate using PEI transfection reagent. After 4 hours in culture, media was changed to media containing 50 μM of the appropriate peracetylated fucose analog or DMSO. At 28-30 h post-transfection, the cells were dissociated with cold PBS pH 7.4 containing 1% bovine serum albumin, (BSA) and resuspended in 1 mM $CaCl_2$, 1% BSA and 0.05% NaN_3 in Hanks' balanced salt solution (Gibco). Cells were incubated with 100 μl of anti-mN1 (ECD) antibody (R&D systems, AF5267) at 10 μg/ml for 1 h at 4°C. Cells were washed with the binding buffer and then incubated with PE-anti-sheep IgG (1:100; Santa Cruz, SC-3757) for 30 min at 4°C. After two washes with binding buffer, the cells then were analyzed with a FACSCalibur (BD, Bioscience) flow cytometer. The gate was set to collect the GFP positive population of 30,000 events for each sample and analyzed using FlowJo software (ver. 9.4.10). Three independent experiments were performed for each condition (n=3).

2.8 Cell-based Notch ligand binding assay

HEK293T cells (8.5 x 10^5 cells/well) were seeded in a 3.5 cm culture plate and co-transfected with 1.5 μg of pcDNA1-mN1-myc, 0.4 μg of GFP and 0.75 μg of either SEAP (EV)

or Lfng-AP (Lfng) using PEI reagent. After 4 hours in culture, media was changed to media containing 50 μM of the appropriate peracetylated fucose analog or DMSO. Cells were dissociated 24-28 hours post-transfection with cold PBS pH 7.4 containing 1% bovine serum albumin (BSA). Cells were then resuspended in binding buffer (1 mM $CaCl_2$, 1% BSA and 0.05% NaN_3 in Hanks' balanced salt solution, pH 7.4, Gibco). Dll1-Fc (R&D Systems, 3970-DL-050), Dll4-Fc (Sino Biological, 10171-H02H-50) or Jag1-Fc (R&D Systems, 599-JG-100) (each at 0.5 μg/mL) were pre-clustered with fluorescent secondary antibody PE-goat anti-mouse IgG (1:100; Invitrogen, P-852) or PE-anti-human IgG (1:100; Jackson Immuno Research, 109155-098) for 30 min at 4°C. Cells were incubated with clustered ligands at 4°C. After 1 hour, the cells were washed twice with binding buffer and analyzed using a FACSCalibur (BD, Bioscience) flow cytometer. The gate was set to collect 30,000 GFP-positive events for each sample and analyzed using FlowJo software (ver. 9.4.10). Experiments were performed at least three independent times (n≥3, as indicated in figure legends).

For reverse binding assays, HEK293T cells were transfected with 1.5 μg of full-length mDll1 (pTracer) and 0.4μg of GFP, as above. Cells were dissociated and incubated with 0.5 μg/mL of soluble Notch1-Fc chimera, containing EGF repeats 1-13 (R&D Systems, 5267-TK-050), for 1 hour. Cells were washed in binding buffer and incubated with PE-anti-human IgG (1:100; Jackson Immuno Research, 109155-098). Cells were then washed twice and analyzed, as above. Three independent experiments were performed for each condition (n=3).

2.9 Mutagenesis of O-fucosylation and O-glucosylation sites

O-Fucosylation site mutants at EGF repeats 8, 12, or both of the pcDNA1-mN1myc plasmid were provided by Dr. Shinako Kakuda (125). Mutations were designed to eliminate the modified residue (threonine to valine) within the *O*-fucosylation consensus sequence, CXXXX(S/T)C (273). The mutants were confirmed by DNA sequencing.

Primer	Sequence (5' to 3')
mN1 S435A Fwd	CTCAACACACTGGGTGCTTTTGAGTGCCAGTG
mN1 S435A Rev	CACTGGCACTCAAAAGCACCCAGTGTGTTGAG
mN3 S415A Fwd	GTGTGAATACACAGGGCGCATTCTTGTGCCAATG
mN3 S415A Rev	CATTGGCACAAGAATGCGCCCTGTGTATTCACAC
Pofut1 S162L Fwd	CAACAAGTTGGAGCTTTTTACAGGCATTTCCTT
Pofut1 S162L Rev	AAAGCTCCAACTTGTTGAAACTCACATGAAACTGAT

Table 2.1: Primers used for site directed mutagenesis of Notch receptors.

Site directed mutagenesis was also used to generate mutants for novel *O*-glucose sites on mouse Notch1 and mouse Notch 3. The QuikChange II XL Site-Directed Mutagenesis Kit (Agilent Technologies) was used according to the manufacturer's protocol. Mutants were confirmed using DNA sequencing of the entire plasmid. The S162L mutant was generated similarly by Dr. Hideyuki Takeuchi. Primers used for mutagenesis are shown in Table 2.1.

2.10 Glioma and hepatocellular carcinoma cell MTT assay

Cells were plated in 96-well plates at 3,000 cells per well and were grown in the presence of experimental compounds or DMSO for 96 hours. To assay proliferation at the end of an experiment, one-tenth volume of 3-(4,5-dimethylthiazol-2-yl)-2,5-diphenyltetrazolium bromide reagent (Vybrant Cell Proliferation Assay Kit, ThermoFisher) was added to each well and incubated at 37 °C. After 4 hours, 100 µL of SDS buffer (Vybrant

Cell Proliferation Assay Kit, ThermoFisher) was added to each well and the absorbance at 570 nm measured using a plate reader, as per manufacturer's instructions.

2.11 RT-qPCR assays for cancer cells and patient fibroblast

RNA was isolated from cells using TRIzol (Thermo Fisher Scientific) according to manufacturer's protocol. RNA was quantified following purification and SuperScript II Reverse Transcriptase (Thermo Fisher Scientific) was used to generate cDNA according to manufacturer's protocol. cDNA was quantified and used for RT-qPCR analysis. The SYBR Green Real-Time PCR kit was used with 1 µg cDNA and 1 µg primers (Table 2.2). Mixtures were added to wells of a 384 well plate and run on the Light Cycler 480 (Roche) for 40 cycles. The $2^{-\Delta\Delta CT}$ method was used for analysis of results. At least three technical replicates were run for each condition.

RT-qPCR Primer	Sequence (5' to 3')
mGAPDH Fwd	CCAATGTGTCCGTCGTGGATCT
mGAPDH Rev	GTTGAAGTCGCAGGAGACAACC
mHEY1 Fwd	TACCCAGTGCCTTTGAGAAG
mHEY1 Rev	AACCCCCAAACTCCGATAGTC
mHES1 Fwd	CTACCCCAGCCACTGTCAAC
mHES1 Rev	ATGCCGGGAGCTATCTTTCT
hPofut1 Fwd	AACAGCTCTTCAAAGGGAAG
hPofut1 Rev	ACAGTTGCCAATAAAGTGGT
hGAPDH Fwd	ACATCGCTCAGACACCATG
hGAPDH Rev	ATGACAAGCTTCCCGTTCTC
hHES1 Fwd	TCAACACGACACCGGATAAA
hHES1 Rev	CCGCGAGCTATCTTTCTTCA
hHEY1 Fwd	TGAGCTGAGAAGGCTGGTAC
hHEY1 Rev	ATCCCAAACTCCGATAGTCC
hNotch1 Fwd	AGGACCTCATCAACTCACACGC
hNotch1 Rev	CGTTCTTCAGGAGCACAACTGC
hNotch2 Fwd	TTTGGCAACTAACGTAGAAACTCAAC
hNotch2 Rev	TGCCAAGAGCATGAATACAGAGA

hNotch3 Fwd	AAGGACGTGGCCTCTGGT
hNotch3 Rev	TCAGGCTCTCACCCTTGG
hNotch4 Fwd	CAGCCCAAGCAGATATGTAAGGA
hNotch4 Rev	CGTCCAACCCACGTCACA
hLfng Fwd	ACGTCTTCATCGCTGTCAAG
hLfng Rev	CTCATCTTCCCCGTCAGTG
hMfng Fwd	GGGAAACTCAACGTCATTAAGC
hMfng Rev	AGCAGTTCAGGATTCATCGG
hRfng Fwd	AGCAGACGTTTATCTTCACCG
hRfng Rev	AACTTCTCATACTCCACGGAC
hPOGLUT2 Fwd	ATTCAGGCAGTGGATACATCAG
hPOGLUT2 Rev	TGAAGGACCCATCTTTTCGG
hPOGLUT3 Fwd	CCCGGAGGTGCTGGTCA
hPOGLUT3 Rev	GACCGCCTGCAGGTAGAAAT
mPOGLUT2 Fwd	CGTTGGCTTTAGGATTTTCATGG
mPOGLUT2 Rev	AGATCGGCTGAATGTTGGAG
mPOGLUT3 Fwd	TGAAATTTTGCTGTCACTGGC
mPOGLUT3 Rev	AGCCACACCAGGAAATGATAG

Table 2.2: RT-qPCR primer sequences used in this dissertation.

2.12 Statistical analysis

For signaling and binding assays two-way ANOVAs were used to assess significance. Tukey's post-hoc test was used to evaluate differences between individual treatment conditions. Statistically identical conditions were grouped together in graphs. Sidak's multiple comparisons test was used to evaluate significance between –Fng and +Lfng conditions. Student t-tests were used to assess significance for T-cell differentiation assays. All statistical tests were carried out using Prism 7 software (Graphpad).

2.13 Viral transduction and selection of infected cells

To generate shRNA virus, LinX-A retroviral producing cells were plated at 10 x 10^5 cells/well in 3.5 cm dishes and were transfected with anti-POFUT1 shRNA constructs using

1 µg plasmid and 6 µL PEI. Media was changed to fresh media after 4 h. After an additional 48 h incubation period media was collected and filtered with a 0.22 micron filter. This supernatant was then added to HEK 293T cells plated at 70% confluence. After 48 h media was changed to fresh media with 2 µg/mL puromycin to select for successfully transduced cells.

Following puromycin selection, fluorescence-activated cell sorting (FACS) was used to select cells expressing the highest levels of GFP. A FACSAria III cell sorter (BD Biosciences) was used to collect the top 10% of GFP expressing cells. Selected cells were cultured, passaged and used for further experiments.

2.14 Fluorescence microscopy

In order to examine levels of GFP expression in cells the Nikon Eclipse Ti-S florescence microscope was used to observe cells. The digital interference contrast (DIC) setting was used to observe all cells and a FITC lens was used to observe GFP expressing cells.

2.15 ADAMTS17 secretion assays

To determine the impact of *O*-fucosylation on ADAMTS17 secretion, control, *POFUT2* and *B3GLCT* knockout cells were generated (by Stephen Berardinelli and Hideyuki Takeuchi). Cells were plated in 3.5 cm plates and co-transfected with 1C, 25P, or full length ADAMTS17 constructs (1 µg) and human IgG (0.5 µg). Media was changed to OPTI-MEM after 4 hours and was collected after an additional 24 hours. Cells were lysed in 1% NP-40 with a protease inhibitor and lysates were collected. The media and lysates were analyzed

by reducing SDS-PAGE followed by Western blotting with anti-myc (9E10) and anti-hIgG (Rockland). Results from control HEK293T cells were compared with HEK293T cells with CRISPR-Cas9 mediated knockout of *POFUT2* or *B3GLCT*, using co-transfected IgG as a control as recently described (274).

2.16 Zebrafish embryo experiments (Wu lab, Einstein)

All Zebrafish (*Danio rerio*) were maintained following standard procedures and embryos were staged as previously described (275). AB and casper fish [*roy*^{a9}*;mitfa*^{w2} (*AB*)] (276) were used as wild type fish. The SuH:GFP transgenic line [*Tg(TP1bglob:gfp)*^{um13}] (277) was maintained in an AB background. The towhead (*twd*)^{rw685} mutant (79) was maintained by intercross. Only healthy Zebrafish larva with normal shape and behavior, as judged by pre-established criteria (275), were analyzed. Larvae were assigned randomly to treatment conditions. The gmds Morpholino was used at 2 ng per embryo, as previously described (79). GDP-fucose and GDP-fucose analogs were re-suspended in pure water at 20-60 mM and 60 pmol of each analog was injected into embryos at the 1-cell stage. After reaching the desired developmental stages (48 hpf), embryos were mounted to the desired position in 1.5% methyl-cellulose in E3 medium. Images were taken using an Olympus SZ16 fluorescent dissecting microscope and Microfire digital camera (Olympus). To ensure that each embryo had one allele of GFP-Notch reporter, heterozygous or homozygous [*Tg(TP1bglob:gfp)*^{um13}] fish were crossed to wild type AB fish. The progeny were collected and injected as described above. At 48 hpf, GFP-positive embryos were collected and each fish was put into one well of a 96-well plate. A group of 60 embryos was treated for each condition. The final number of survived Zebrafish larva ranged from 23 to 48 due to

different fertilization rates. Since the treatments of different GDP-fucose analogs created 100% penetrance, no statistical methods were used to determine required sample size. All Zebrafish maintenance and usage was performed with the full compliance of ethical regulation and was approved by the Institutional Animal Care and Use Committee (IACUC) of Albert Einstein College of Medicine.

2.17 In vitro Pofut1 and Lfng glycosyltransferase assays (Dr. Hideyuki Takeuchi, Stony Brook)

In vitro glycosyltransferase assays were performed as previously described (265). The first EGF repeat from human factor IX (hFA9) was expressed in *E. coli* BL21 (DE3) cells and purified by Ni-NTA affinity chromatography and subsequently, reverse phase HPLC. For *in vitro O*-fucosylation, a 30-μl reaction mixture contained 50 mM HEPES pH 6.8, 10 mM MnCl2, 10 μM hFA9, 200 μM GDP-fucose analogs, and approximately 300 ng of recombinant mouse Pofut1. The reaction was performed at 37°C overnight. Reaction products were purified by reverse phase HPLC (Agilent Technologies, 1200 Series) equipped with a C18 column (10 x 250 mm, Vydac) with a linear gradient of solvent B (80% acetonitrile and 0.1% trifluoroacetic acid (TFA)) from 10% to 90% in solvent A (0.1% TFA) for 60 min, monitoring absorbance at 214 nm. Peak fractions were dried down in a SpeedVac centrifuge and analyzed by mass spectrometer as described above. For Lfng reactions, hFA9 modified with fucose analogs were quantitated with a BCA Protein assay (Thermo Fisher) with BSA as a standard, and used as acceptor substrate. The 10-μl enzymatic reaction with Lfng contained 50 mM HEPES pH 6.8, 10 mM $MnCl_2$, 0.5% Nonidet P-40, the indicated amounts of acceptor substrate, 0.25 μM UDP-[^{3}H]GlcNAc (Perkinelmer,

1.46 TBq/mmol), 20 μM UDP-GlcNAc and 1 μg of recombinant Lfng. The reaction was performed at 37°C for 20 min and stopped by adding 900 μl of 100 mM EDTA pH 8.0. The samples were loaded onto a C18 cartridge (100 mg, Agilent Technologies). After the cartridge was washed with 5 ml of water, the EGF repeat was eluted with 1 ml of 80% methanol. Incorporation of [^{3}H]-GlcNAc into the EGF repeat was determined by scintillation counting of the eluate. Reactions without substrates were used as background control.

2.18 Purification of LSK cells from bone marrow (Stanley lab, Einstein)

LSK cells were purified from bone marrow of FVB littermates, 2 males and 2 females, chosen at random. The first experiment was performed with an FVB female heterozygous for each of three Fringe genes (*Lfng*, *Mfng* and *Rfng*) (278). Mice were housed in a barrier facility, allowed to eat and drink ad libitum, and used in experiments at 8-10 weeks of age. All experiments were performed with permission from the Albert Einstein Institutional Use and Animal Care Committee. Since only FVB mice were used, no blinding was performed. Briefly, bone marrow cells were prepared by crushing the femur, tibia, hips and vertebrae of FVB mice in cold Flow Buffer (PBS pH 7.4 lacking cations, containing 4% FBS and 100 U/ml penicillin/streptomycin). Cells were incubated in 5 ml RBC lysis buffer (0.15 M NH_4Cl, 10 mM $KHCO_3$, 0.1 mM EDTA, pH 7.2–7.4) for 3 min before adding 40 ml Flow Buffer. After centrifugation at 1200 rpm for 10 min at 4 °C, cells were counted using a Coulter counter. Approximately 1.5 x 10^8 cells were incubated with 3 μl FcR blocking solution (rat-anti-mouse CD16/CD32) in 250 μl Flow Buffer on ice for 15 min and then depleted of Lineage$^+$ cells using biotin-conjugated antibodies against B220 (1:100; clone

RA3-6B2), CD11b (1:500; clone M1/70), Gr-1 (1:500; clone RB6-8C5), CD4 (1:200; clone GK1.5), CD8α (1:200; clone 53-6.7), CD3ε (1:100; clone 145-2C11), Ter119 (1:100; clone TER-119), and CD19 (1:100; clone 6D5) (all biotinylated antibodies were from Biolegend) in a final volume of 300 µl Flow Buffer. After 30 min on ice, cells were washed with 10 ml cold Flow Buffer and the pellet resuspended in 9 ml cold Flow buffer to which 1 ml anti-biotin microbeads (Life Technology) was added. After rotation for 30 min at 4 °C, bead-coated cells were removed by magnetic separation. Lineage-depleted cells were incubated with anti-Sca-1-PE (1:50; Biolegend, clone D7), anti-cKit-APC (1:50; BD Pharmingen, clone–1B8) and streptavidin-PE-Cy7 (1:200; Biolegend) in a final volume of 300 µl Flow Buffer. After 30 min on ice, cells were washed with 10 ml cold Flow buffer, the pellet resuspended in 300 µl Flow Buffer containing 4,6-diamidino-2-phenylindole, dihydrochloride (DAPI; 1:1000). Live, DAPI-negative, $Lin^{-}Sca1^{+}cKit^{+}$ (LSK) cells were collected by cell sorting using an Aria flow cytometer (BD Biosciences), and analyzed using FlowJo™ (FlowJo, LLC) software.

2.19 LSK cell differentiation assay (Stanley lab, Einstein)

OP9-GFP, OP9-Dll1 and OP9-Dll4 cells(279) were kindly provided by Cynthia Guidos and were cultured in α-Minimum Essential Medium (MEM, Gibco), supplemented with 10% FBS (Hyclone), 100 U/mL penicillin/streptomycin. OP9-GFP, OP9-Dll1 and OP9-Dll4 cells were plated in 24-well plates (Corning) in 1 ml MEM, supplemented with 20% heat-inactivated FBS (Hyclone), 100 U/mL penicillin/streptomycin and 25 ng/ml Amphotericin B (Gibco), to achieve ~90% confluency after 24 hour. Co-cultures were initiated by overlaying LSK cells (3×10^3 per well) in 1 ml MEM containing 5 ng/mL Flt3-L and 1 ng/mL

IL-7 (both from Preprotech, Rocky Hill, NJ). Compound **9** or **10** in DMSO was added to co-cultures to a final concentration of 25 μM and an equal volume of DMSO was added to control wells. Plates were incubated at 37°C in a humidified atmosphere with 5% CO_2. Every 2 days, half the medium was refreshed to maintain the final concentration of DMSO, **9** or **10**. On day 8, co-cultures were harvested by forceful pipetting, filtered through a 40 micron cell strainer, and centrifuged at 1200 rpm for 5 min at room temperature. Cell pellets were fixed in 4% *paraformaldehyde* (PFA) in PBS (pH 7.4, lacking cations) for 15 min at room temperature, and stored at 4ºC.

For flow cytometry, fixed cells were washed with 1 ml cold FACS binding buffer (FBB; Hanks' balanced salt solution (HBSS), 2% bovine serum albumin (BSA), 0.05% sodium azide, pH 7.2–7.4) by centrifugation for 5 min at 1200 rpm. Cells were resuspended in 90 μl FBB containing 1 μl Fc block (rat-anti-mouse CD16/CD32), and incubated for 15 min on ice. Antibody diluted in FBB (10 ml final volume) was added, and the tube was incubated for 30 min at 4°C. To detect differentiated T-cells, CD44-PE (1:200; clone-IM7, eBioscience) and CD25-PerCPCy5.5 (1:200; clone-PC61.5, eBioscience) and for B-cells CD19-PE-Cy7 (1:100; clone–6D5, Biolegend) were used. Cells were washed twice in 1 ml FBB and transferred to a 5 ml Polystyrene round bottom tube in 250 μl FBB. Immunofluorescence of GFP-negative (non-stromal) cells was analyzed using FACSCalibur (BD Biosciences), and data were analyzed using FlowJo software (FlowJo, LLC). One of four FVB mice gave reduced numbers of CD25+ cells and is not included in the analysis shown in Figure 3.10. However, when the data are normalized to DMSO control, the results for the 4 mice were qualitatively similar (compound **9** (Ac-GDP-Fuc) averaged 0.97+/-0.15 for Dll1

and 1.11+/-0.11 for Dll4 and compound **10** averaged 0.0+/-0.002 for Dll1 and 0.01+/-0.003 for Dll4.

2.20 Synthesis of GDP-fucose and GDP-fucose analogs (Wu lab, Einstein)

GDP-fucose and GDP-fucose analogs were prepared following the protocol reported in (280). Crude reaction products were purified by Bio-Gel P2 gel filtration chromatography (1.5 × 75 cm) and eluted with H_2O. GDP-L-fucose or analog containing fractions from P2 separation were pooled and evaporated to a volume of 3 ml under reduced pressure (20 mbar) at 25°C (no more than 30 °C). HPLC separation was performed on a C18 column (ES Industries; Epic C18 5µ 120 Å 20 ×250 mm) at a flow rate of 20 mL/min. The gradient had the following steps: 0-20 min, 100-98% phosphate-buffer; 20-21 min, 98-10% phosphate-buffer; 21-25 min, 10% phosphate-buffer; 25-26 min, 10-100% phosphate-buffer; 26-30 min, 100% phosphate-buffer. The GDP-L-fucose or analog containing fractions were collected (between 11-16 min), pooled, and concentrated under reduced pressure (20 mbar) at 25°C (no more than 30 °C). For the desalting, a gel filtration on a Sephadex G-10 column (GE Health and Life Sciences) was used.

2.21 Synthesis of peracetylated fucose analogs (Wu lab, Einstein)

Peracetylated L-fucose (Carbosynth, 24332-95-4), 2-fluoro-L-fucose (Calbiochem, 344827-10MG), and L-galactose (Carbosynth, 604-69-3) and all other chemical reagents and solvents were obtained from commercial sources and used without further purification except for the following: Anhydrous THF was obtained using a Pure Solv™ AL-258 solvent purification system and pyridine was dried over activated 4 Å molecular sieves.

Chromatography was performed on a Teledyne ISCO CombiFlash R_f 200i using disposable silica cartridges. Analytical thin layer chromatography (TLC) was performed on Merck silica gel plates and compounds were visualized using ceric ammonium molybdate (CAM) stain. NMR spectra were recorded on a Bruker DRX 300 or 600 spectrometers. ^{1}H chemical shifts (δ) are reported relative to tetramethyl silane (TMS, 0.00 ppm) as internal standard. Mass spectra were recorded on a Shimadzu LCMS 2010EV (direct injection).

Synthesis

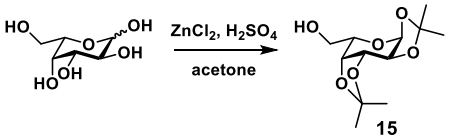

1,2:3,4-Di-O-isopropylidene-α-L-galactopyranose (15): Acetone (33 mL), zinc chloride (1.21 g, 8.88 mmol, 1.6 equiv.) and H_2SO_4 (0.03 mL, 0.056 mmol, 0.1 equiv.) were added to a flask that was then purged with argon. L-Galactose (1 g, 5.55 mmol, 1 equiv.) was added and the reaction mixture stirred at room temperature for 15 hours. TLC analysis (hexanes/EtOAc 1:1; CAM) showed full conversion and the reaction was quenched with sodium carbonate (3 g) and water (6 mL). Stirring continued for 10 minutes and the solids was filtered and rinsed with acetone. Concentration *in vacuo* gave the title compound in quantitave yield (152).

TLC: R_f = 0.27 (Hexanes/EtOAc 1:1; CAM). **^{1}H NMR (300 MHz, $CDCl_3$)** δ 5.58 (d, *J* = 5.1 Hz, 1H), 4.62 (dd, *J* = 7.9, 2.4 Hz, 1H), 4.34 (dd, *J* = 5.1, 2.4 Hz, 1H), 4.28 (dd, *J* = 7.9, 1.6 Hz, 1H), 3.96 – 3.83 (m, 2H), 3.85 – 3.71 (m, 1H), 2.38 (d, *J* = 8.8 Hz, 1H), 1.55 (s, 3H), 1.46 (s, 3H), 1.34 (s, 6H).

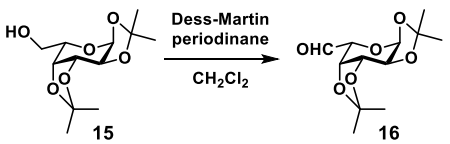

1,2:3,4-Di-O-isopropylidene-α-L-galacto-hexadialdo-1,5-pyranose (16): A solution of alcohol **15** (1.57 g, 6.03 mmol, 1 equiv.) in CH_2Cl_2 (50 mL) was cooled in an ice/water bath. Dess-Martin periodinane (3.38 g, 7.97 mmol, 1.32 equiv.) was added in portions over 8 minutes. After 3 hours, TLC analysis (hexanes/EtOAc 1:1, CAM) indicated full conversion and the reaction mixture was diluted with Et_2O (60 mL) and quenched with sat. aq. $NaHCO_3$ (60 mL) and $Na_2S_2O_3$ (2.5 g). The resulting biphasic mixture was stirred vigorously until both phases became clear. The phases were separated and the organic layer was washed with sat. aq. $NaHCO_3$ (50 mL) and brine (50 mL). The combined aqueous phases were back-extracted with CH_2Cl_2 (50 mL) and combined extracts were dried over $MgSO_4$ and filtered thought celite. Concentration *in vacuo* gave aldehyde **16** (1.48 g, 5.73 mmol, 95%) in acceptable purity (281).

TLC: R_f = 0.52 (Hexanes/EtOAc 1:1; CAM). **^{1}H NMR (300 MHz, $CDCl_3$)** δ 9.62 (s, 1H), 5.67 (d, *J* = 4.9 Hz, 1H), 4.65 (dd, *J* = 7.8, 2.4 Hz, 1H), 4.60 (dd, *J* = 7.8, 2.1 Hz, 1H), 4.39 (dd, *J* = 4.9, 2.4 Hz, 1H), 4.19 (d, *J* = 2.1 Hz, 1H), 1.51 (s, 3H), 1.45 (s, 3H), 1.35 (s, 3H), 1.32 (s, 3H).

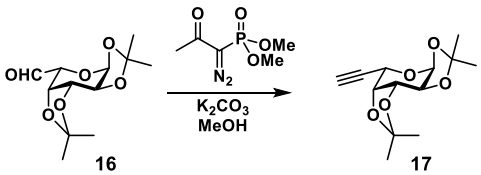

6,7-Dideoxy-1,2:3,4-Di-O-isopropylidene-α-L-galacto-hept-6-ynopyranose (17): Methanol (20 mL), K_2CO_3 (412 mg, 2.98 mmol, 2 equiv.), and dimethyl (1-diazo-2-oxopropyl)phosphonate (384 mg, 2.00 mmol, 1.34 equiv.) were added to a flask containing aldehyde **16** (385 mg, 1.49 mmol, 1 equiv.) under argon. After 15 hours, TLC analysis (Hexanes/EtOAc 1:1; CAM) showed full conversion. The reaction mixture was transferred to a separatory funnel and diluted with water (100 mL). The product was extracted with EtOAc (3 × 30 mL), and the combined organic phases were dried (Na_2SO_4), filtered and

concentrated. Column chromatography (12 g silica, gradient of 0-20% EtOAc in hexanes) gave pure alkyne **17** (282).

TLC: R_f = 0.56 (Hexanes/EtOAc 1:1; CAM). **^{1}H NMR (300 MHz, $CDCl_3$)** δ 5.55 (d, *J* = 5.0 Hz, 1H), 4.67 – 4.56 (m, 2H), 4.37 – 4.25 (m, 2H), 2.54 (d, J = 2.3 Hz, 1H),), 1.55 (s, 3H), 1.54 (s, 3H), 1.39 (s, 3H), 1.34 (s, 3H).

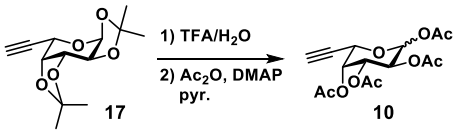

6,7-dideoxy-1,2,3,4-tetraacetate-L-galacto-hept-6-ynopyranose (10): A vial with alkyne (38 mg, 0.15 mmol) was cooled in an ice/water bath and a pre-cooled mixture of water (0.2 mL) and TFA (1.8 mL) was added. After 30 minutes, TLC analyses (hexanes:EtOAc 1:1 and CH_2Cl_2:MeOH 4:1, CAM) showed full conversion. The reaction mixture was co-evaporated with PhMe (3 × 2 mL) and dried *in vacuo*. The crude tetra-ol was dissolved in pyridine (1 mL) and DMAP (18 mg, 0.15 mmol, 1 equiv.) and acetic anhydride (0.5 mL, 5.3 mmol, 36 equiv.) were added. Stirring continued overnight and the mixture was diluted with EtOAc (5 mL) and transferred to a separatory funnel. Washing with 1 M HCl (2 × 5 mL) and sat .aq. $NaHCO_3$ (5 mL), followed by drying (Na_2SO_4) and removing of volatiles gave crude product which was purified by column chromatography (4 g silica, gradient of 0-75% EtOAc in hexanes). Tetraacetate **10** (39 mg, 0.11 mmol, 76%) was isolated as an anomeric mixture of both pyranosides and furanosides (156).

TLC: R_f = 0.09 (Hexanes/EtOAc 3:1; CAM). **^{1}H NMR (300 MHz, $CDCl_3$; Major signals)** δ 6.41 (d, J = 3.0 Hz), 6.35 (d, J = 4.6 Hz), 5.51 (dd, J = 3.5, 1.4 Hz), 5.07 (d, J = 3.4 Hz), 4.90 (ddd, J = 2.3, 1.5, 0.7 Hz), 4.61 (dd, J = 2.2, 1.4 Hz), 4.42 (dd, J = 6.4, 4.6 Hz), 4.23 (dd, J = 8.4, 5.6 Hz), 2.52 (s), 2.51 (s), 2.50 (s), 2.49 (s), 2.22 (s), 2.21 (s), 2.17 (s), 2.12 (s), 2.12 (s), 2.02 (s), 2.01 (s). **ESI-MS:** calc'd for $C_{15}H18NaO_9$ $(M+Na)^+$ 365.1 found 364.9.

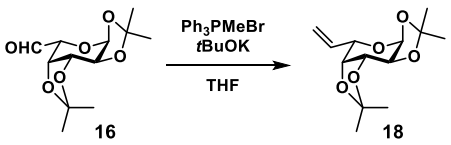

6,7-Dideoxy-1,2:3,4-Di-O-isopropylidene-α-L-galacto-hept-6-enopyranose (18): Methyltriphenyl-phosphonium bromide (389 mg, 1.09 mmol, 3.3 equiv.) and THF (3 mL) were added to an oven dried Schlenk flask under argon. The flask was cooled in an ice/water bath and *t*BuOK (111 mg, 0.99 mmol, 3 equiv.) was added to give a bright yellow mixture. After stirring for 60 minutes, a solution of aldehyde **16** (85 mg, 0.33 mmol, 1 equiv.) in dry THF (3 mL) was added drop-wise. After stirring for 90 minutes, sat. aq. $NaHCO_3$ (3 mL) was added to quench the reaction. The product was extracted with Et_2O (3 × 3 mL) and the combined organic phases were dried over $MgSO_4$, filtered and concentrated. The alkene **18** (46 mg, 0.18 mmol, 54%) was obtained after column chromatography (4 g silica, gradient of 0-85% EtOAc in hexanes) (283).

TLC: R_f = 0.53 (Hexanes/EtOAc 3:1; CAM). **^{1}H NMR (300 MHz, $CDCl_3$)** δ 5.93 (ddd, J = 17.4, 10.6, 6.0 Hz, 1H), 5.58 (d, J = 5.0 Hz, 1H), 5.37 (dt, J = 17.4, 1.6 Hz, 1H), 5.28 (dt, J = 10.6, 1.5 Hz, 1H), 4.62 (dd, J = 7.9, 2.4 Hz, 1H), 4.31 (m, 2H), 4.23 (dd, J = 7.8, 2.0 Hz, 1H), 1.54 (s, 3H), 1.47 (s, 3H), 1.35 (s, 6H).

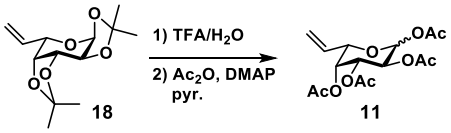

6,7-dideoxy-1,2,3,4-tetraacetate-L-galacto-hept-6-enopyranose (11): A vial with alkene **18** (40 mg, 0.16 mmol) was cooled in an ice/water bath and a pre-cooled mixture of water (0.2 mL) and TFA (1.8 mL) was added. After 45 minutes, TLC analyses (hexanes:EtOAc 1:1 and CH_2Cl_2:MeOH 4:1, CAM) showed full conversion. The reaction mixture was co-evaporated with PhMe (2 × 2 mL) and dried *in vacuo*. The crude tetra-ol was dissolved in pyridine (1 mL) and DMAP (2 mg, 0.016 mmol, 0.1 equiv.) and acetic

anhydride (0.5 mL, 5.3 mmol, 34 equiv.) were added. Stirring continued overnight and the mixture was diluted with EtOAc (5 mL) and transferred to a separatory funnel. Washing with 1 M HCl (2 × 5 mL) and sat .aq. $NaHCO_3$ (5 mL), followed by drying (Na_2SO_4) and removing of volatiles gave crude product which was purified by column chromatography (4 g silica, gradient of 0-40% EtOAc in hexanes). Tetraacetate **11** (43 mg, 0.13 mmol, 80%) was isolated as an anomeric mixture of both pyranosides and furanosides (283).

TLC: R_f = 0.15 (Hexanes/EtOAc 3:1; CAM). **^{1}H NMR (600 MHz, $CDCl_3$; Major signals)** δ 6.44 (d, J = 2.9 Hz), 6.33 (d, J = 4.6 Hz), 5.78 – 5.63 (m), 5.27 (ddt, J = 12.2, 10.7, 1.3 Hz), 5.12 (dd, J = 10.4, 3.4 Hz), 4.68 – 4.61 (m), 4.33 (dt, J = 5.2, 1.4 Hz), 2.16 (s), 2.14 (s), 2.13 (s), 2.13 (s), 2.05 (s), 2.05 (s), 2.03 (s), 2.01 (s), 2.00 (s). **ESI-MS:** calc'd for $C_{15}H_{20}NaO_9$ $(M+Na)^+$ 367.3 found 368.0.

Chapter 3: Inhibition of Delta-induced Notch signaling using fucose analogs

3.1 Introduction

The Notch signaling pathway is highly conserved across all metazoa and plays important roles in cell fate determination during development and in adult tissue homeostasis (284-286). In mammals there are four Notch receptor homologs (Notch1-4) and five Notch ligands: Jagged (Jag) 1, 2 and Delta-like (Dll) 1, 3 and 4 (285). Notch signaling is initiated upon binding of Notch ligand to Notch receptor leading to a cascade of events that ultimately culminates in the cleavage of the Notch intracellular domain (NICD) by a γ-secretase. NICD then translocates to the nucleus, where it regulates transcription of target genes (287).

Given the critical role that Notch plays in tissue development and maintenance, it is not surprising that defects in Notch signaling lead to several human disorders. As early as 1991, it was shown that the breakpoint of a defining chromosomal translocation seen in T-cell lymphoblastic leukemias occurs within the Notch1 gene (288). Since then, excessive Notch signaling has been implicated in a wide range of human cancers including cervical, renal, lung, hepatocellular, hematologic, and neurologic malignancies (289-291). Initial efforts to inhibit Notch signaling in the treatment of these cancers had focused largely on the development of γ-secretase inhibitors (GSIs), small molecules that prevent NICD cleavage and thereby block Notch signaling. Unfortunately, this strategy has not been successful to date, largely due to dose limiting gastrointestinal and other side effects (292). Alternative anti-Notch therapeutic strategies which are now in development include the use of monoclonal antibodies targeting either specific Notch homologues (293) or Notch ligands that induce signaling (294-296), with the hopes that these may prove more selective and less toxic.

The Notch extracellular domain (NECD) consists of up to 36 tandem epidermal growth factor-like (EGF) repeats including those that interact directly with ligands (126, 297). EGF repeats with appropriate consensus sequences are post-translationally modified with *O*-glycans, initiated by *O*-fucose, *O*-glucose, or *O*-GlcNAc (120, 298). Protein *O*-fucosyltransferase 1 (Pofut1) is responsible for the addition of *O*-fucose to EGF repeats with an *O*-fucose consensus sequence (C^2-X-X-X-X-(S/T)-C^3 where S/T is the modified amino acid, C^2 and C^3 are the second and third conserved cysteines of the EGF repeat, and X represents any amino acid) and is an essential component of Notch signaling during embryogenesis (4). Members of the Fringe family of enzymes often extend the *O*-fucose modification by the addition of GlcNAc to further regulate Notch activity (127, 299).

Considering the critical role of *O*-fucosylation for Notch function, we hypothesized that inhibition or interference with the normal *O*-fucosylation process might lead to the development of anti-Notch therapeutics. Recent work has demonstrated that peracetylated fucose derivatives are metabolized to their corresponding GDP-fucose analogs within cells by exploiting a promiscuous fucose salvage pathway (157, 167, 169). The presence of some of these analogs causes feedback inhibition of the *de novo* biosynthesis of GDP-fucose, which thereby inhibits fucosylation of oligosaccharide chains on target proteins, resulting in altered behavior of these glycoproteins (167, 169). One such analog, peracetylated 6-alkynyl fucose (**10**), is tolerated by *O*-fucosyltransferases and was previously shown to be incorporated into a single Notch EGF repeat (159).

Here, we report the synthesis of a small panel of fucose analogs and evaluate whether they can be used to affect Notch activity. We demonstrate that some GDP-fucose analogs inhibit Notch signaling when injected into Zebrafish embryos. We have developed

peracetylated versions of these inhibitory analogs, which are taken up by cells and successfully incorporated into Notch EGF repeats, where they disrupt Delta-, but not Jagged-induced Notch signaling. Additionally, we show that Lunatic Fringe (Lfng) can elongate fucose analogs and thereby partially rescue Notch signaling. Finally, we demonstrate that these analogs inhibit Notch dependent T-cell differentiation and cancer cell proliferation. Fucose analogs thus represent a novel alternative approach to anti-Notch signaling therapeutics.

3.2 *Identification of fucose analogs that inhibit Notch signaling in Zebrafish*

We generated a panel of GDP-fucose derivatives with different substituents at the 6-carbon position (Fig. 3.1a). In order to screen for analogs with an inhibitory effect on Notch signaling, we utilized transgenic Zebrafish Tg(Tp1bglob:eGFP)^{um14} embryos expressing a Notch reporter (GFP under the control of DNA bound by NICD) (277). GDP-fucose analogs were injected into the yolk sac of embryos at the one cell stage and GFP fluorescence was visualized to monitor Notch signaling at 48 hours post-fertilization (Fig. 3.1c). The analogs in our panel had a range of effects on Notch signaling. As expected, untreated and natural GDP-fucose (**1**) treated embryos expressed relatively high levels of GFP indicating robust Notch signaling. Inhibition of GDP-fucose biosynthesis by knocking down GDP-mannose-4,6-dehydratase (gmds MO) (79) served as a positive control for Notch inhibition, and effectively reduced Notch signaling (Fig. 3.1c, bottom left panel). Analogs **2** and **5** did not cause any substantial reduction in Notch signaling compared to negative controls. By contrast, compounds **7** and **8** caused a partial reduction in GFP levels, whereas compounds

3, **4** and **6** with the C-6 ethynyl, ethenyl or OH substituent respectively, had the greatest inhibitory effect, almost entirely eliminating the GFP Notch reporter signal (Fig. 3.1c).

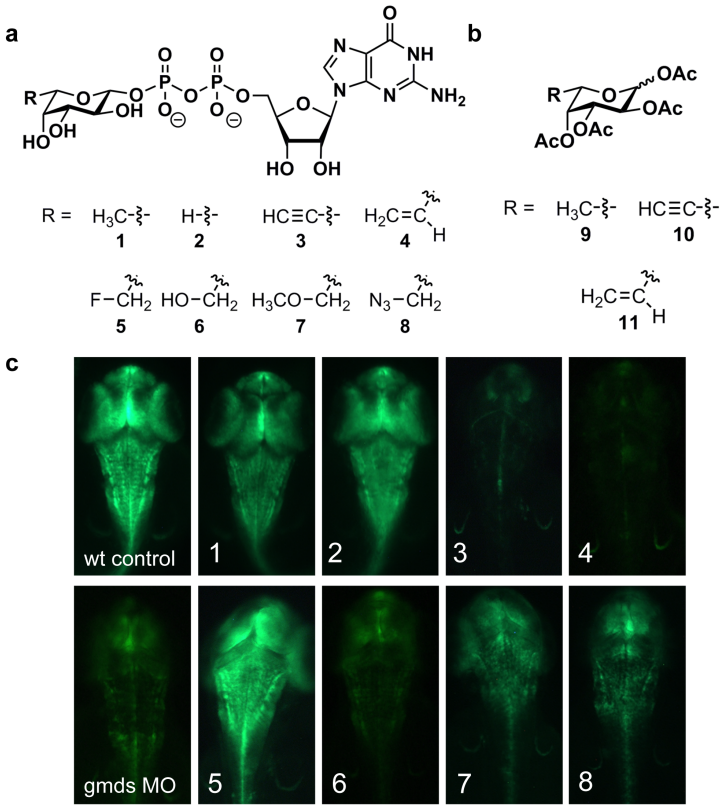

Figure 3.1: Effects of fucose analogs on Notch signaling in Zebrafish embryos. Numbered structures of (a) GDP-fucose analogs screened as potential inhibitors of Notch signaling and (b) acetylated fucose analogs selected for further analysis in cell culture systems. (c) Transgenic Zebrafish embryos expressing a GFP fluorescent Notch signaling reporter showed that some injected GDP-fucose analogs, indicated in each panel, reduced Notch signaling. Knock down of GDP-mannose-4,6-dehydratase (*gmds* MO) to inhibit endogenous GDP-fucose biosynthesis was used as a positive control for the effect of eliminating Notch *O*-fucosylation. Scale bar represents 0.5 mm. Performed by Wu lab, Einstein.

3.3 Fucose analogs are utilized by Pofut1 and incorporated into Notch EGF repeats

Based on previous literature describing the importance of fucose for Notch activation (4, 300) and the effects of sugar analogs in other systems (167, 169, 301-303), we hypothesized that one of two possible mechanisms is likely responsible for the inhibitory function of synthetic GDP-fucose derivatives on Notch signaling (Fig. 3.1c); either the analogs inhibit the transfer of fucose by Pofut1 resulting in unmodified EGF repeats *or* the analogs are transferred by Pofut1, and when incorporated into EGF repeats, interfere with Notch signaling. In order to address this question, we examined selected

analogs from the no effect (**1**, **2**), partial effect (**8**), and high effect (**3**, **6**) groups for their ability to affect Pofut1 transferase activity. All five GDP-analogs were efficiently incorporated into an EGF repeat from human factor 9 (hFA9) after overnight incubation with purified Pofut1 (Fig. 3.2a). However, kinetic analysis over a 20 min incubation period showed that fucose analogs were incorporated into the hFA9 EGF repeat to a lesser extent than control GDP-fucose (Fig. 3.2b). Additionally, Lunatic Fringe (Lfng) was able to efficiently add GlcNAc to each fucose analog-modified hFA9 EGF repeat (Fig. 3.2c).

Having shown that GDP-fucose analogs were substrates for Pofut1 *in vitro,* we next investigated their ability to be incorporated into EGF repeats of Notch receptors in cultured cells. To this end, the most potent fucose analog inhibitors of Notch signaling in Zebrafish were peracetylated (Fig. 3.1b), to increase cell membrane permeability(167), and tested in cell culture systems. The success of this approach requires that a peracetylated analog be taken up by cells, efficiently converted to the corresponding GDP derivative and transported into the endoplasmic reticulum for utilization by Pofut1 (167, 169). In Figure 3.1, we injected GDP-fucose analogs directly, bypassing the need for conversion of analogs to their corresponding GDP derivatives.

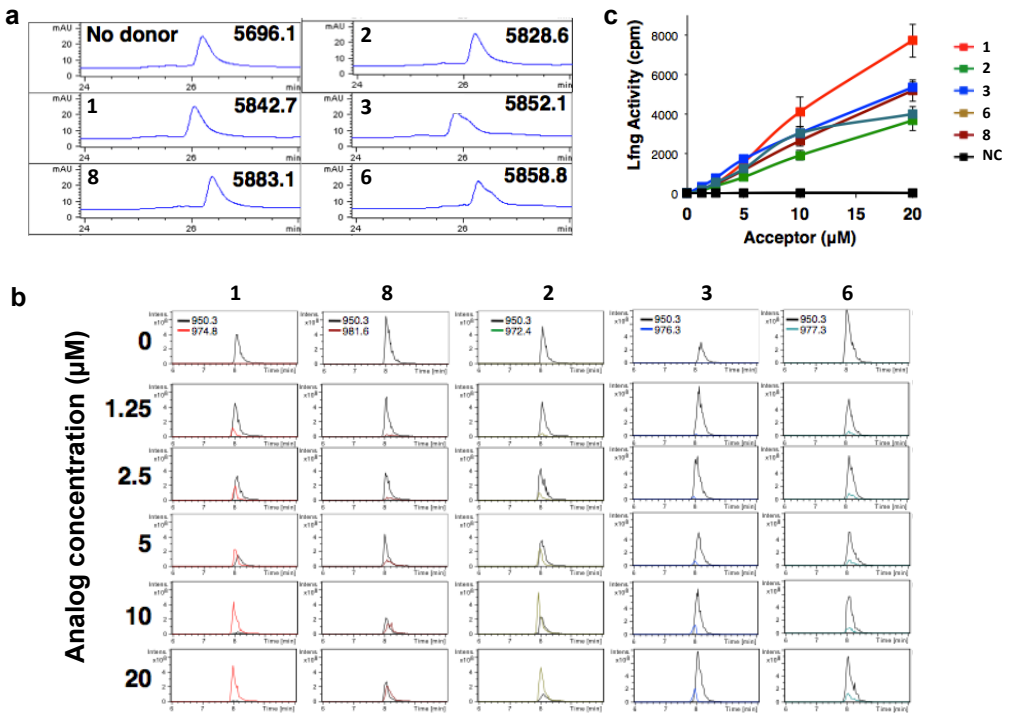

Figure 3.2: GDP-Fucose analogs are Pofut1 substrates that are transferred to EGF repeats, and can be elongated by Lfng *in vitro*. (a) Indicated (top left) GDP-fucose analogs were incubated with Pofut1 and hFA9 EGF repeats overnight at 37°C. hFA9 EGF repeats were purified using HPLC and the addition of each analog was confirmed by mass spectrometry (m/z shown). (b) Twenty-minute incubations of varying concentrations of GDP-fucose analogs with Pofut1 and hFA9 EGF repeat demonstrate that Pofut1 utilizes some analogs less efficiently than unmodified GDP-fucose. Extracted ion chromatograms (EICs) showing relative levels of unmodified EGF repeats (black peaks) and EGF repeats modified with the corresponding analog (colored peaks) were generated. (c) Lfng transferred [^{3}H]GlcNAc from UDP-[^{3}H]GlcNAc to fucose analog-modified hFA9 EGF repeats from A (as indicated). An unmodified EGF repeat was used as a negative control (NC). The data were from three independent assays. All bars represent mean ± SEM. Performed by Dr. Hideyuki Takeuchi, Stony Brook University.

Using mass spectral glycoproteomic methods, we confirmed that HEK293T cells treated with compounds **10** and **11** (the peracetylated versions of **3** and **4**, respectively) incorporated the corresponding fucose analog into a secreted Notch1 ECD fragment. Figure 3.3 shows the selection and fragmentation of a Notch1 peptide from EGF6 that contains an *O*-fucose consensus sequence. In the sample treated with control peracetylated fucose (**9**), we identified an ion corresponding to the mass of this peptide plus the mass of a fucose and an ion with a clear neutral loss of the fucose after fragmentation (Fig. 3.3a). In the samples

treated with test compounds **10** and **11**, we used the same strategy to identify ions corresponding to the mass of the EGF6 peptide plus the mass of the corresponding fucose analog and again observed a clear neutral loss of the analog after fragmentation (Fig. 3.3b and 3.3c). Searches for the ions representing the fucose analog and fucose-modified glycoforms of this peptide resulted in the extracted ion chromatograms (EICs) shown in Figure 3.3d-f, which indicate that these analogs were incorporated into Notch1 EGF repeats at high stoichiometry. Similar analyses in the presence of Lfng demonstrated that EGF repeats modified with compounds **10** and **11** were efficiently elongated with GlcNAc in cell culture (Fig. 3.3g-l). All other peptides with *O*-fucose modification sites that were identified by mass spectrometry were similarly modified with these fucose analogs (Fig. 3.13 and 3.14).

Although compound **6** was transferred by Pofut1 *in vitro* (Fig. 3.2a) and had a strong inhibitory effect in Zebrafish embryos (Fig. 3.1c), in its peracetylated form (compound **12**, Fig. 3.4a), it was not incorporated into Notch1 EGF repeats in cell culture and did not affect the incorporation of unmodified fucose (Fig. 3.4b). Compound **13**, a known inhibitor of fucosyltransferase (FUT) enzymes (167), was also tested. We observed no effect on Notch fucosylation (Fig. 3.4c) or Notch signaling in the co-culture reporter assay (Fig. 3.4e). Compound **14** was also tested because other reports demonstrated that it had an inhibitory effect on FUT enzyme activity (167, 169). This compound was efficiently incorporated into Notch1 EGF repeats (Fig. 3.4d). However, it had no significant effect on Notch signaling in a co-culture reporter assay, consistent with the Zebrafish embryo data using the GDP version of this sugar analog (Fig. 3.1c, compound **5**). Thus, we focused on compounds **10** and **11** as potential candidates for development of inhibitors of Notch signaling *in vivo.*

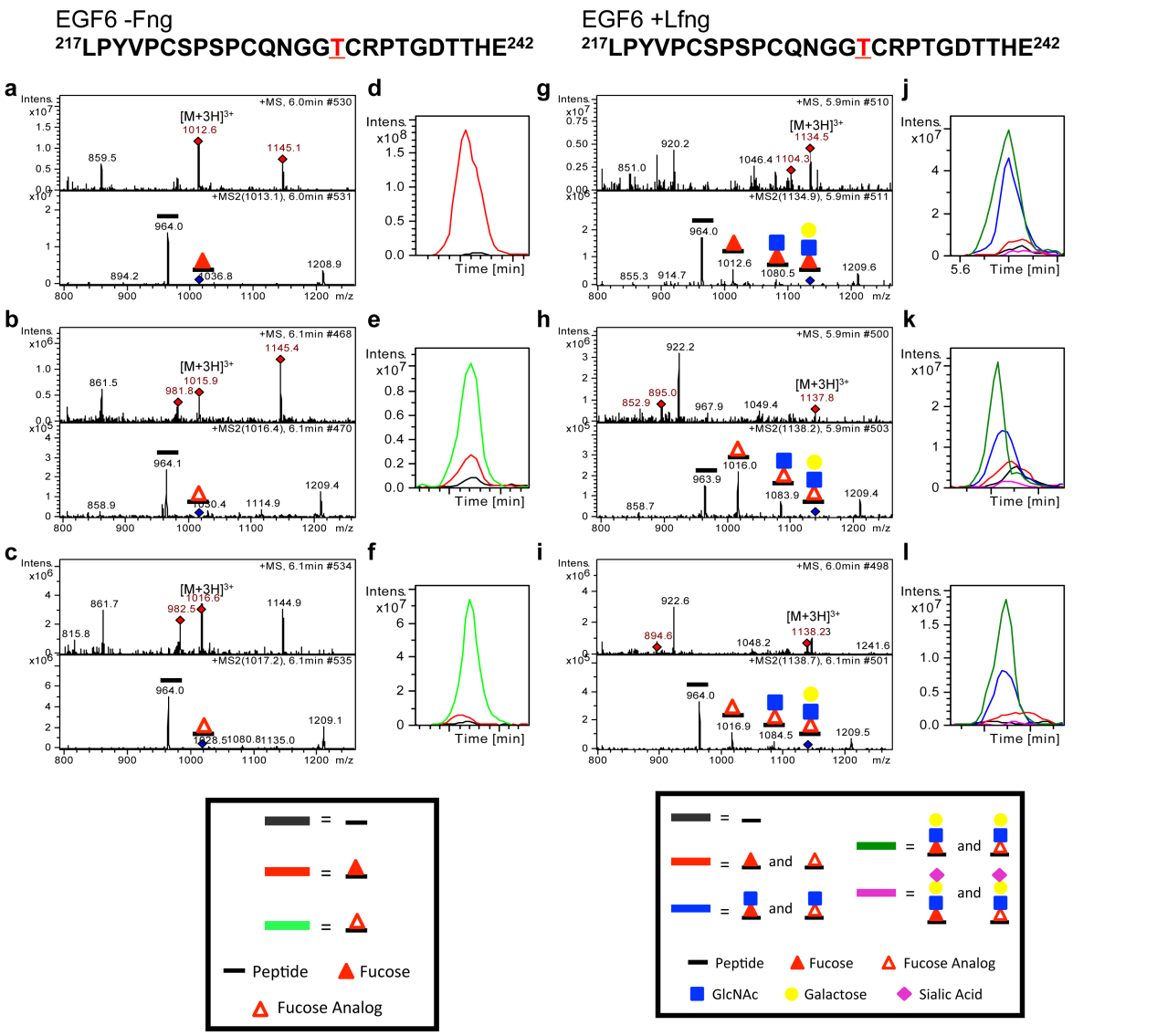

Figure 3.3: Peracetylated fucose analogs are efficiently incorporated into Notch EGF repeats and elongated by Lfng. EGF1-18-MycHis from mNotch1 was transfected into HEK293T cells expressing no Fng (a-f) or Lfng (g-l) and the cells were grown in the presence of compounds **9** (a, g), **10** (b, h), or **11** (c, i) for 72 hours. Purified EGF1-18-MycHis was digested and subjected to nano-LC-MS/MS analysis. Spectra are shown for the triply-charged form ($[M+3H]^{3+}$) of the molecular ion resulting from peptide **^{217}LPYVPCSPSPCQNGGTCRPTGDTTHE^{242}** from mNotch1 EGF6 modified with fucose analogs. Mass spectrometry data for this peptide has been previously described without peracetylated fucose or fucose analog treatment (125). Top panels show MS spectra at ~6.0 min and bottom panels show MS/MS spectra confirming the assignment. (d-f) Extracted ion chromatograms (EIC) of the ions corresponding to glycoforms (see key) of this peptide show efficient incorporation of the corresponding compounds. (g-l) Similar experiments in the presence of Lfng demonstrate elongation of these fucose analogs with GlcNAc. See Figures 3.13 and 3.14 for m/z ratios used to generate EICs.

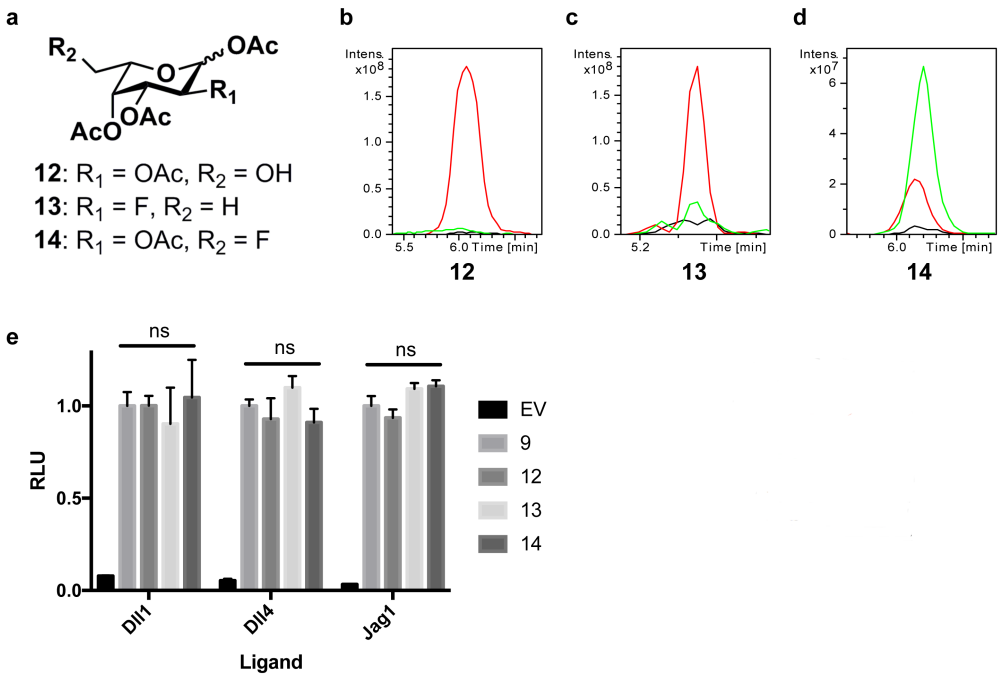

Figure 3.4: Fucosyltransferase inhibitors L-galactose, 2-fluoro-fucose and 6-fluoro-fucose do not reduce Notch signaling. (a) Structures of fucosyltransferase inhibitors. (b-d) EICs showing relative amounts of each glycoform of the same peptide from mNotch1 EGF6 as shown in Figure 3.3 ([217]**LPYVPCSPSPCQNGGTCRPTGDTTHE**[242]) produced by HEK293T cells grown in the presence of the indicated peracetylated fucose analog (See Figure 3.13 and 3.14 for mass spectra). (e) Co-culture Notch1 reporter assays were performed to evaluate the effects of these analogs on ligand-induced mNotch1 signaling.

3.4 Alkyne and alkene fucose specifically inhibit Dll-induced Notch signaling

To further evaluate the effect that incorporation of inhibitory fucose analogs into Notch EGF repeats has on Notch signaling, we used a cell-based co-culture Notch reporter assay. Treatment with peracetylated fucose (**9**) served as a control and did not inhibit Notch signaling levels under any of the tested conditions (Fig. 3.5). As reported previously, Notch signaling stimulated by Dll1 and Dll4 was enhanced by Lfng, whereas Notch signaling stimulated by Jag1 was reduced by Lfng for both Notch1 and Notch2 (Fig. 3.5) (304, 305). In contrast, treatment with fucose analogs **10** and **11** reduced Dll1-induced Notch1 signaling to background levels in the absence of Lfng (Fig. 3.5a). Similarly, Dll4-induced

Notch1 and Dll1- and Dll4-induced Notch2 signaling were all significantly inhibited by compounds **10** and **11** relative to DMSO and compound **9** treated controls (Fig. 3.5b, d, e). In each of these cases, co-expression of Lfng in Notch receptor-expressing cells partially rescued Notch signaling (Fig. 3.6a, b, d, e). Interestingly, these compounds had no significant effect on Jag1-induced Notch signaling in the absence of Lfng (Fig. 3.5c and f), although they did amplify the inhibitory effect of Lfng on Notch1 signaling (Fig. 3.6c). Both of these inhibitors were effective at nanomolar concentrations (Fig. 3.5g), and only caused a minimal (~10%) reduction in cell surface expression of Notch1 (Fig. 3.5h).

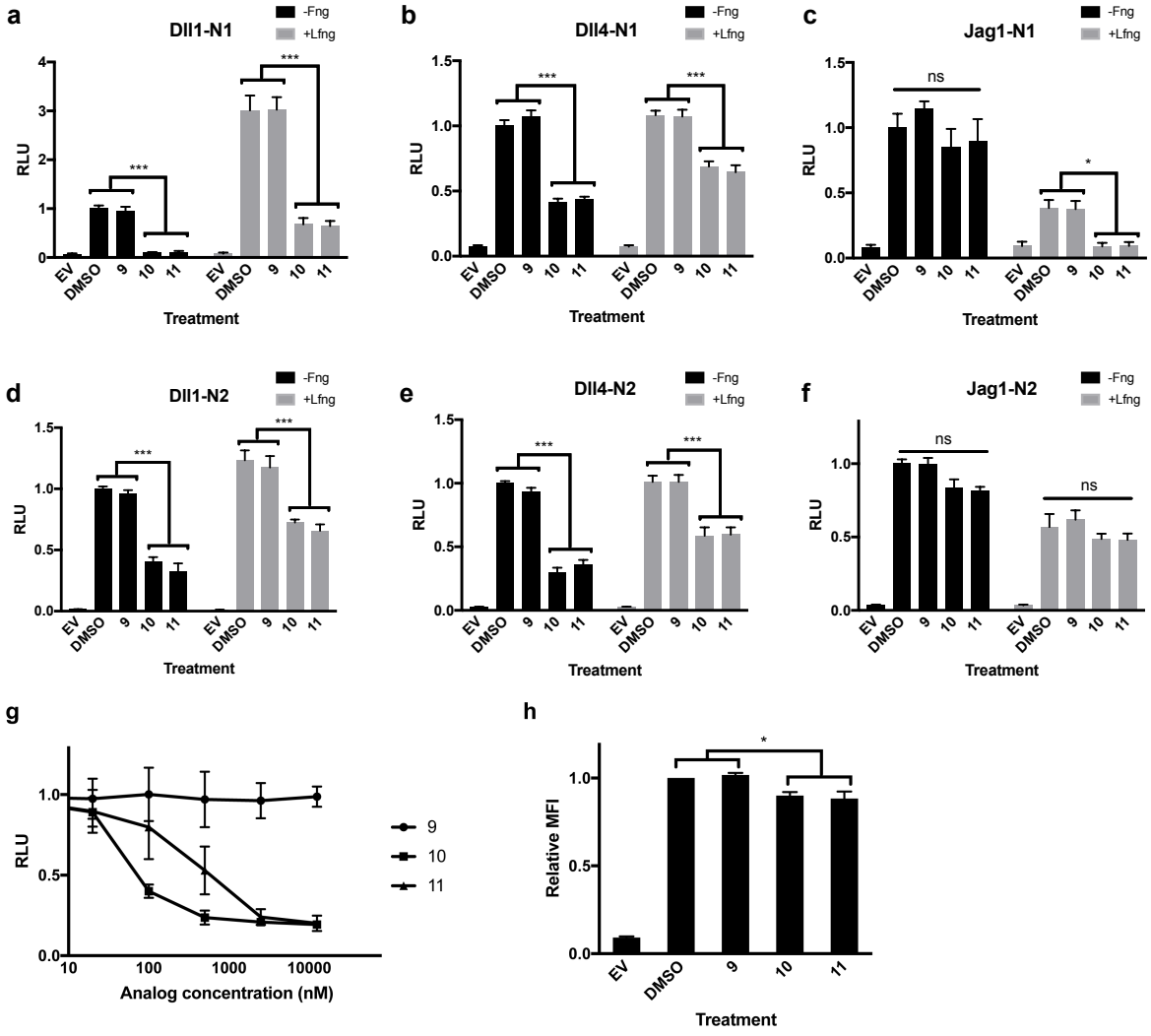

Figure 3.5: Peracetylated fucose analogs inhibit Dll1- and Dll4- but not Jag1-induced Notch signaling. NIH3T3 cells expressing mNotch1 (a-c) or mNotch2 (d-f) with or without Lfng, were co-cultured with cells expressing Dll1 (a, d), Dll4 (b, e), or Jag1 (c, f) in the presence of peracetylated fucose analogs (compounds **9, 10, 11**). Cells transfected with empty vector (EV) were used as a negative control and cells grown in DMSO were used as a control for normal Notch signaling. (g) Inhibition of Dll1-induced mNotch1 signaling was examined at varying concentrations of peracetylated fucose analogs. (h) Cell surface expression of mNotch1 was determined by flow cytometry using the NECD antibody after treatment of transfectants with the indicated compounds. All experiments were performed three independent times. In (a-f) data represents nine biological replicates (n=9) and in (g-h) three biological replicates were used (n=3) for each condition. All bars represent mean ± SEM. *p<0.05, **p<0.01, ***p<0.001, Tukey post-hoc test, adjusted p values.

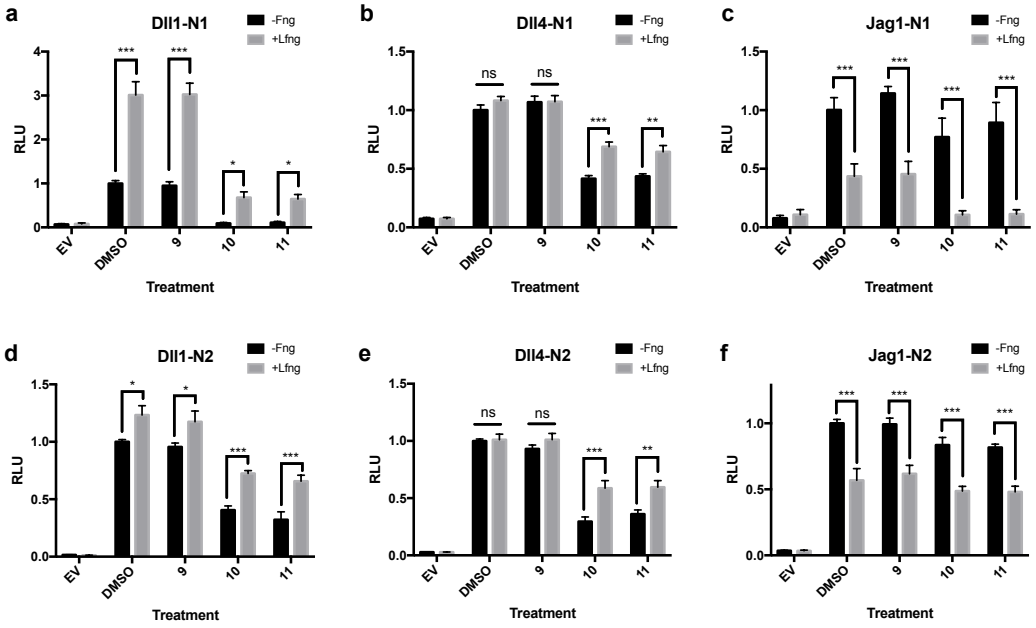

Figure 3.6: Lunatic Fringe partially rescues Notch signaling inhibition by fucose analogs. Co-culture assays from Figure 3.5 replotted to show the effects of Lfng on ligand-induced Notch1 (a-c) and Notch2 (d-f) signaling following incorporation of control versus inhibitory fucose analogs. All bars represent mean + SEM (n=9). *p<.05, **p<.01, ***p<.001, Sidaks multiple comparison test adjusted p values.

3.5 Inhibition of Notch signaling correlates with reduced ligand-receptor binding

Next, we used a flow cytometry based Notch ligand binding assay to determine if the decreased Notch signaling caused by fucose analogs **10** and **11** was a result of reduced ligand-receptor binding. Binding experiments with Dll1 and Dll4 correlated well with Notch signaling data. Dll1-Notch1 binding was reduced to background levels after

treatment with compounds **10** and **11** in the absence of Lfng (Fig. 3.7a). Dll1-Notch2, Dll4-Notch1 and Dll4-Notch2 binding were all significantly reduced, but to a lesser extent (Fig. 3.7b, d, e). All four of these binding interactions were partially rescued by Lfng (Fig. 3.7a, b, d, e); similar to what we saw in our signaling assays. Ligand binding is required in order to induce activation of Notch signaling. The reduced levels of Dll1-Notch1 binding shown here suggests that this reduced ligand-receptor binding is at least partially responsible for the effects of inhibitory fucose analogs on Dll-induced Notch signaling.

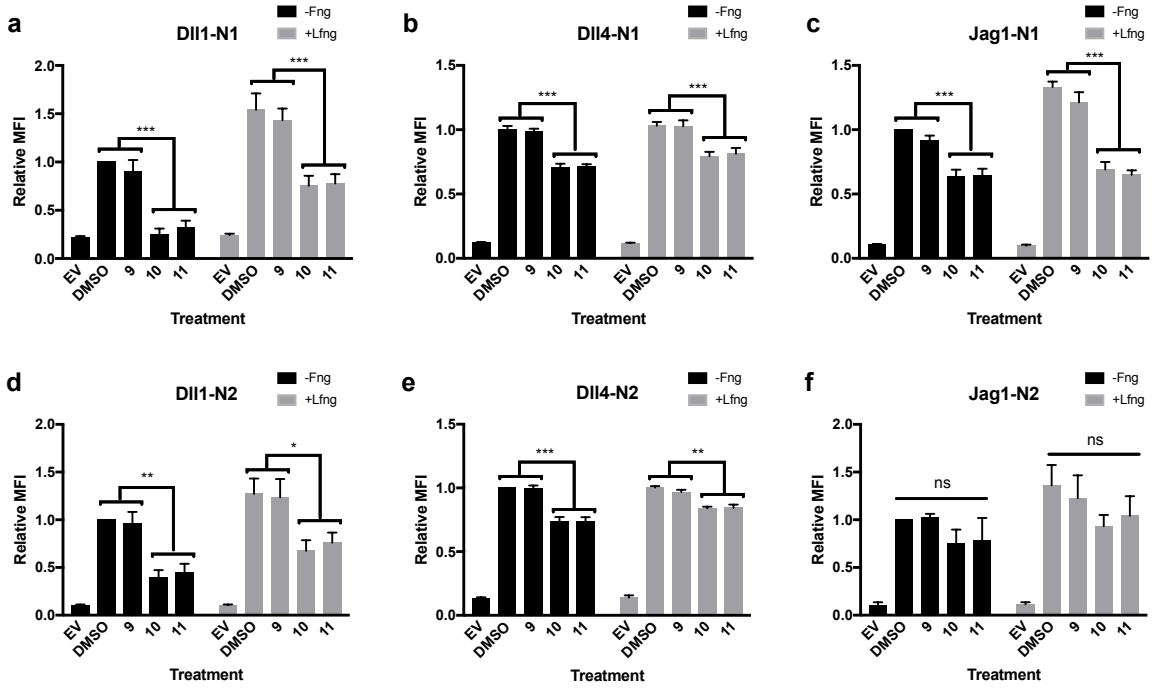

Figure 3.7: Alkyne and alkene fucose analogs inhibit Notch Dll ligand binding. Notch ligand binding experiments were performed to measure the effect of fucose analogs on the ability of mNotch1 (a-c) or mNotch2 (d-f) transfectants to bind soluble Dll1-Fc (a, d), Dll4-Fc (b, e), or Jag1-Fc (c, f) using cell-based flow cytometry assays. Experiments were performed on cells that were either not expressing (black) or expressing (gray) Lfng. EV transfected cells were used as a negative control and cells cultured in the presence of only DMSO served as a positive control. Six independent experiments were performed for all –Fng samples (n=6, black bars) and three independent experiments were performed for all +Lfng samples (n=3, gray bars). All bars represent mean ± SEM. *p<0.05, **p<0.01, ***p<0.001, Tukey post-hoc test, adjusted p values.

As others have reported, mammalian Jag1 binding activity does not necessarily correlate with signaling intensity (125, 305, 306). Relative to DMSO and compound **9** treated controls, treatment with compounds **10** and **11** caused a modest reduction in Jag1 binding to Notch1 and Notch2 in both the presence and absence of Lfng (Fig. 3.7c and f). This reduction in binding did not result in a significant effect of these inhibitors on Jag1-induced Notch signaling, although it did correlate with trends in Jag1-induced signaling. This supports the idea that Jag1 signaling is dependent on more than just ligand binding strength (125, 305, 306).

3.6 Modification of EGF repeats on Notch ligands is not responsible for the inhibitory effect of fucose analogs

In the co-culture Notch reporter assay, both ligand-expressing cells and Notch receptor-expressing cells were exposed to the same treatment conditions, and ligands also contain EGF repeats modified with *O*-fucose (111, 307). Thus, we assessed if exposure of the ligand-expressing cells to these conditions reduced their ability to induce Notch signaling and thereby contributed to the inhibitory effects of fucose analogs **10** and **11**. In order to do this, we used a reverse binding assay, in which cells overexpressing full-length Dll1 were grown in the presence of each of the experimental compounds and then stained with a soluble fragment containing the ligand-binding portion of the Notch1 ECD that was generated in the absence of any fucose analogs. None of the treatment conditions caused any significant change in the ability of Dll1 to bind NECD (Fig. 3.8a-b). Subsequently, we used a plate-coating assay, in which plates were coated with Notch ligands generated in untreated cells. Notch1 reporter cells were plated onto the bound ligands and incubated

with fucose analogs. The results showed the same pattern of inhibition of Notch signaling as in the co-culture Notch reporter assay (Fig. 3.8c). Taken together, these data strongly support the hypothesis that the incorporation of compounds **10** and **11** into EGF repeats on Notch receptors, not into EGF repeats of Notch ligands, is responsible for their inhibitory effect.

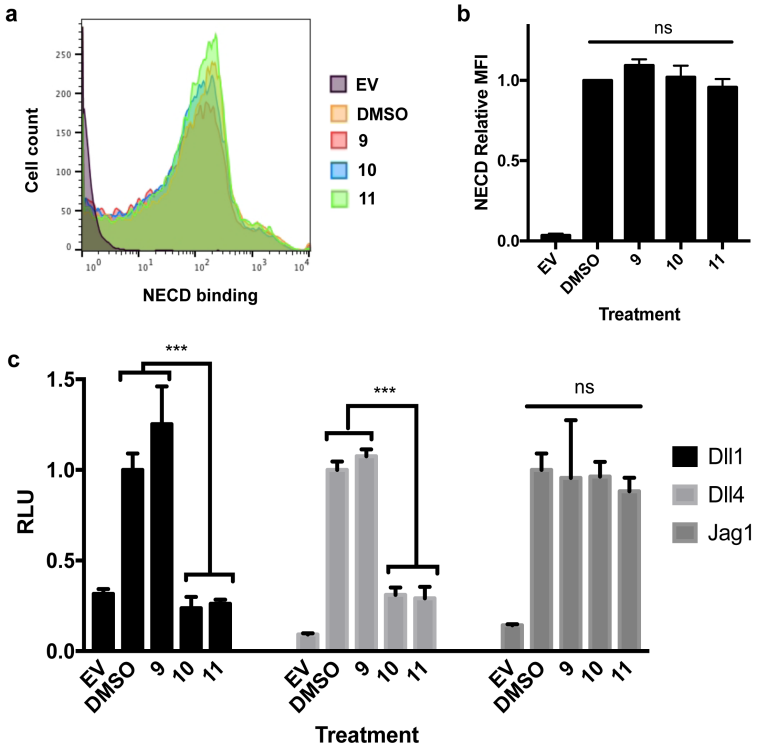

Figure 3.8: Modification of Notch receptors, not Notch ligands, with fucose analogs is responsible for Notch signaling inhibition. (a) Cells expressing full length Dll1 and grown in the presence of the indicated compounds were stained with soluble mNotch1 EGF1-13-Fc and binding was evaluated using flow cytometry. Data is representative of three independent experiments. (b) A bar graph showing the MFIs of results shown in panel a. (c) Soluble Notch ligands generated in the absence of fucose analogs were used to coat cell culture dishes. Luciferase-based signaling assays were performed for transfectants grown on dishes coated with Dll1, Dll4, or Jag1 in the presence of the indicated compounds. All bars represent mean + SEM (n=3). *p<0.05, **p<0.01, ***P<0.001. Tukey post-hoc test, adjusted p values.

3.7 Further insights into the mechanism of fucose analog inhibition of Notch signaling

In order to gain further insights into the mechanism by which compounds **10** and **11** inhibit Notch signaling, we generated Notch1 mutants that eliminated the *O*-fucose modification sites on EGF8, EGF12 or both. The fucose on EGF12 is involved in interactions at the interface of Notch-ligand interactions (123, 126, 308) and the fucose on EGF8 also plays an important role in Notch-ligand binding (125). We hypothesized that if steric clashes caused by incorporation of fucose analogs at either of these sites were responsible

for inhibition of Notch signaling, then eliminating the fucose at these sites might reduce the inhibition by fucose analogs.

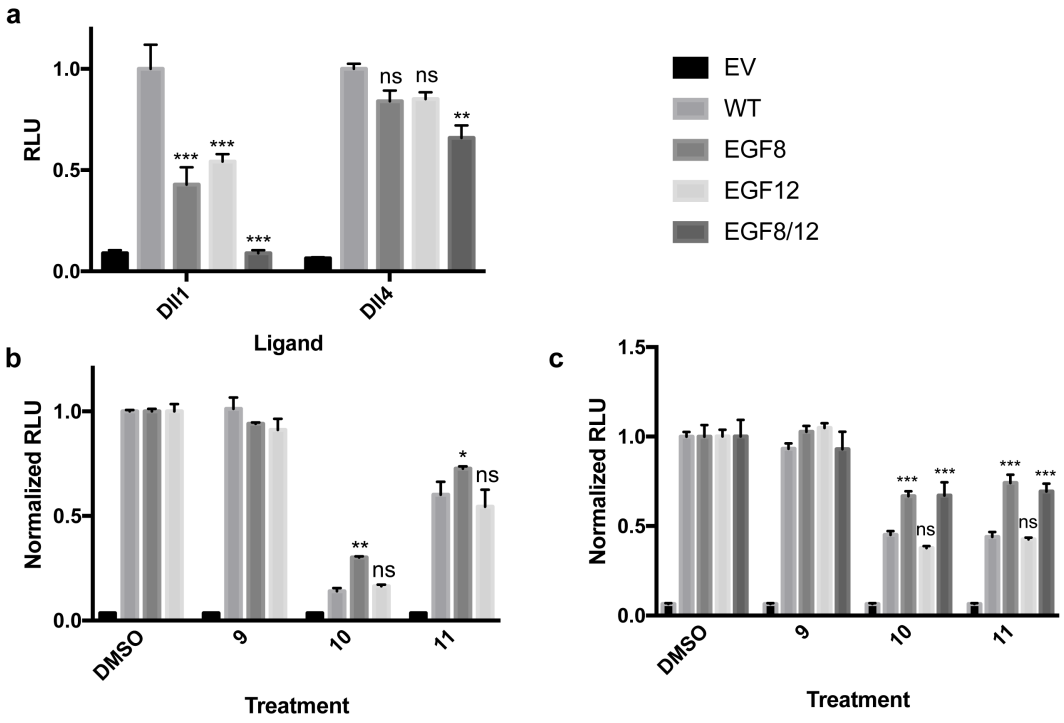

Figure 3.9: Minor steric clashes, at multiple EGF repeats, might contribute to the inhibitory effect of fucose analogs on Notch ligand binding and signaling. (a) Bar graph showing the effect of mutations at EGF8, 12 or both without normalization on Dll1 and Dll4-induced signaling. (b) Notch1 constructs with T to V mutations at fucose modification sites for EGF8 and EGF12 were generated and used in Notch luciferase reporter signaling assays in the presence and absence of 100 nM fucose analog. This concentration was chosen based on results in Figure 3.5 to achieve only partial elimination of Notch signaling to allow better evaluation of the effects mutations. Both analogs could still inhibit Dll1-induced mNotch1 signaling, suggesting that incorporation of the analogs at non-mutated sites allowed mNotch1 activation. (c) Similar experiments for Dll4-induced Notch signaling using 50 μM fucose analogs. An EGF8/12 double mutant was also tested. Each condition was compared to the DMSO control. All bars represent mean ± SEM (n=6). *p<0.05, **p<0.01, ***p<0.001, Tukey post-hoc test, adjusted p values.

As expected, in the DMSO and compound **9** treated controls, elimination of each of these sites caused a substantial reduction in Dll1-induced Notch signaling, although residual signaling remained (Fig. 3.9a). Treatment with 100 nM compounds **10** and **11** caused a further decrease in Notch signaling by these mutants, indicating that steric clashes

at either of these individual sites were not solely responsible for the inhibitory effects of the fucose analogs. Normalizing DMSO treated controls for each mutant to one allowed us to compare the relative decrease caused by each analog with each mutant. We saw decreased inhibition by compounds **10** and **11** in the EGF8 mutant, but the EGF12 mutant was inhibited as potently as WT Notch1 (Fig. 3.9b). An EGF8/12 double mutant entirely eliminated Dll1-induced Notch1 signaling in the absence of inhibitors (125) and therefore the effects of the fucose analogs could not be tested with this construct.

Similar experiments using Dll4-induced Notch signaling also demonstrated that elimination of the fucose site at EGF8, EGF12 or both did not entirely prevent the effect of the fucose analogs on Notch signaling. Elimination of the fucose site on EGF8 again resulted in a reduced level of Notch inhibition by compounds **10** and **11** compared with controls (Fig. 3.9c). Mutation of the EGF12 fucose site had no significant effect on the ability of the analogs to inhibit signaling and the EGF8/12 double mutant had a similar effect to the EGF8 single mutant data. These data suggest that incorporation at EGF8 plays a role in mediating the effects of fucose analogs **10** and **11**, but incorporation of these analogs at other sites must also be important.

3.8 Notch-dependent T-cell differentiation is inhibited by the alkyne fucose analog

To assess the functional consequences of remodeling Notch glycosylation, we investigated the impact of fucose analog **10** treatment on Notch-dependent T-cell differentiation in a co-culture assay. LSK (Lineage$^-$Sca1$^+$ckit$^+$) bone marrow stem cells isolated from mice heterozygous or wild type for all three Fringe enzymes (278) were overlaid on OP9-GFP cells alone or OP9-GFP cells expressing Dll1 (OP9-Dll1) or Dll4 (OP9-

Dll4) to promote differentiation. Both OP9-Dll1 and OP9-Dll4, but not OP9 alone, promoted differentiation to $CD25^+$ T-cell progenitors of LSK cells grown in the control compound **9** (Fig. 3.10a). However, after treatment with compound **10**, neither Dll1 nor Dll4 promoted T-cell differentiation (Fig. 3.10a and c). This same result was obtained when co-cultures were incubated with 1 μM DAPT to inhibit Notch signaling (data not shown). To examine B-cell production in LSK/OP9 co-cultures, a default pathway when T-cells are not produced in the thymus (309), $CD19^+$ cells produced from co-cultured LSK cells were quantified (Fig. 3.10b and d). A robust proportion of $CD19^+$ cells were produced when LSK cells were incubated with OP9 cells under all treatment conditions. This proportion decreased markedly when LSK cells were co-cultured with OP9-Dll1 or OP9-Dll4 stromal cells in the presence of DMSO or compound **9**. However, an increase in $CD19^+$ B-cells was observed when cells were co-cultured in compound **10** and OP9-Dll4 stromal cells.

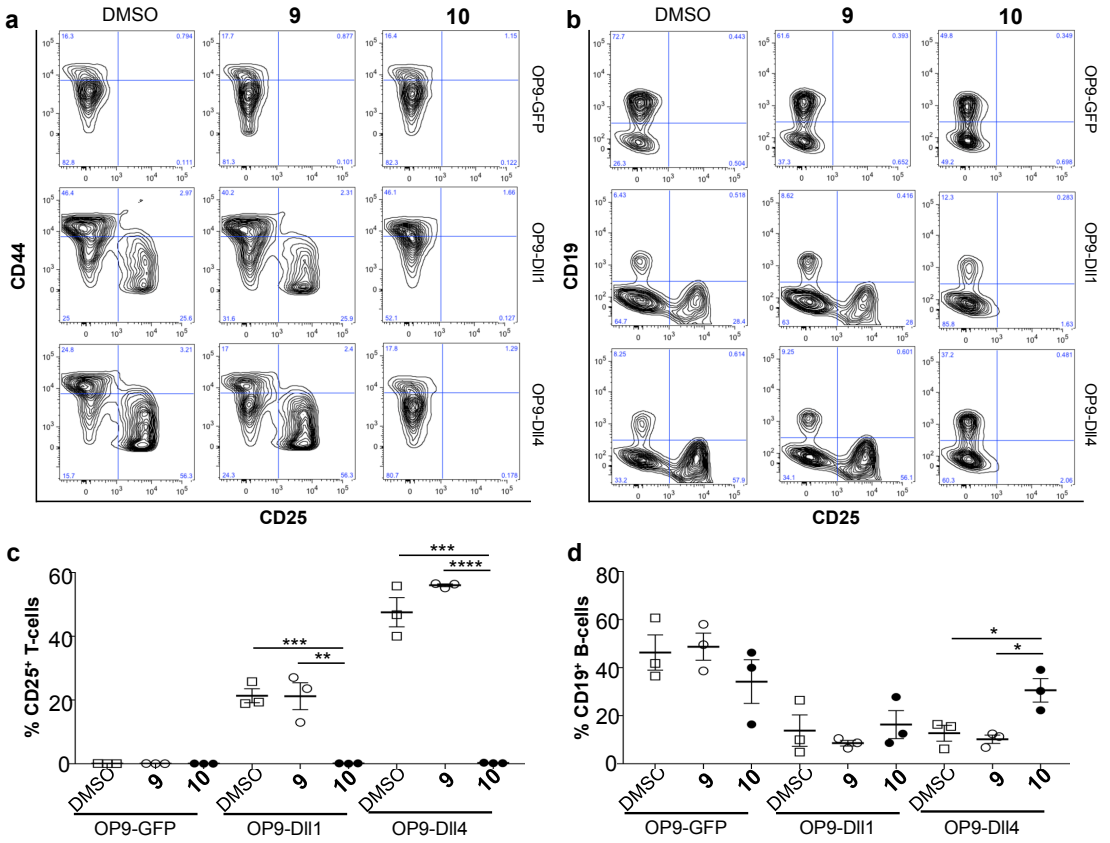

Figure 3.10: Fucose analog 10 inhibits the development of T-cell progenitors. Representative flow cytometric profiles of cells produced from bone marrow LSK cells co-cultured with OP9-GFP, OP9-Dll1 or OP9-Dll4 stromal cells in the presence of DMSO, compound **9** or compound **10** for 8 days. (a) Production of $CD25^+$ T-cell progenitors was evaluated by the expression of CD44 and CD25. (b) Production of B-cells was evaluated by the expression of CD19. (c) Percentage of $CD25^+$ T-cells from mice with a profile typical of panel a (n=3). (d) Percentage of $CD19^+$ B-cells from mice with a profile typical of panel b (n=3). Mean ± SEM, each symbol represents average data from duplicate wells of LSK cells from one mouse. Data shown are representative of three experiments performed in duplicate. *$p \leq 0.05$, **$p \leq 0.01$, ***$p \leq 0.001$, ****$p \leq 0.0001$, two-tailed Student t-test. Performed by Stanley lab, Einstein.

3.9 Inhibition of Notch signaling in cancer cells using fucose analogs

Glioma cell lines have been reported to rely on Dll1 mediated Notch signaling (310), so these were an ideal target for our inhibitors. We chose to look at the effects of fucose analogs on glioma cell growth to examine their therapeutic potential for the treatment of Notch dependent malignancies. Our inhibitors effectively reduced Notch signaling in the

glioma cell lines that we studied, although not to the same extent as a GSI (Fig. 3.11a). This is likely due to expression of Fringe enzymes and a variety of Notch receptors in these cells (Fig. 3.11c), which prevent complete inhibition of Notch signaling by our fucose analogs, but does not affect GSI induced inhibition. However, our inhibitors still caused significant reduction in proliferation of these cell lines at similar levels to GSI (Fig. 3.11b). The inhibitors had no effect on 3T3 cell proliferation (Fig. 3.11d).

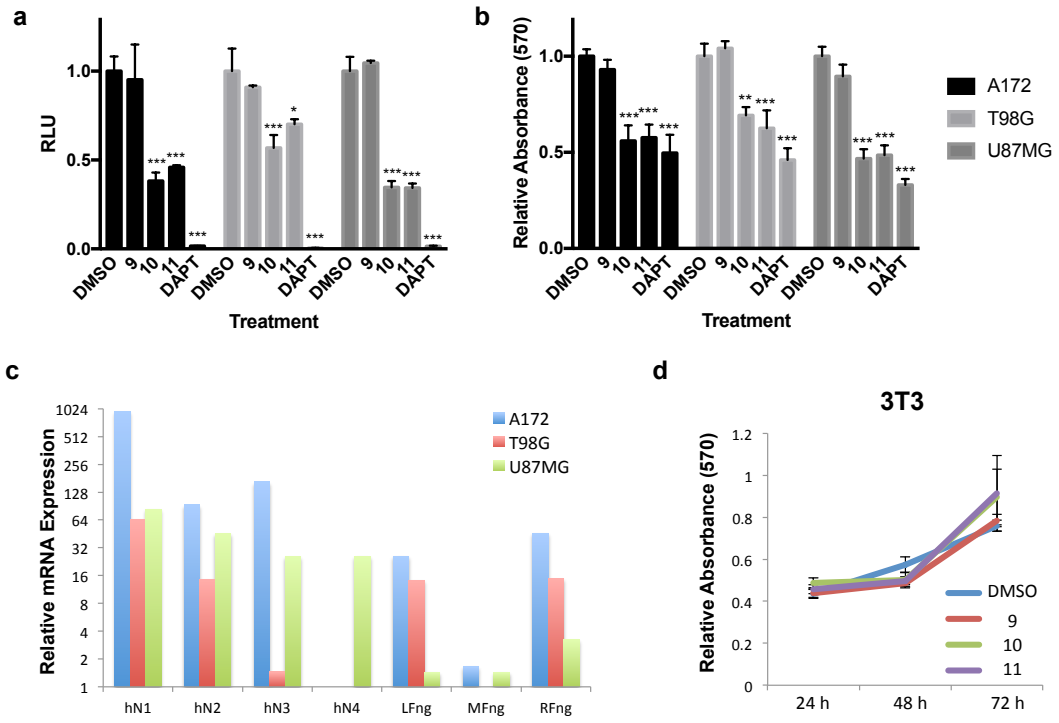

Figure 3.11: Fucose analogs can be used to inhibit glioma cell proliferation. (a) A luciferase based signaling assay was used to determine the effect of fucose analogs on Notch signaling in glioma cell lines after 24 hours of treatment. (b) Cells from three glioma cell lines dependent on Dll1 for growth (310) were grown in the presence of the indicated compounds for 96 hours. An MTT assay was used to assess cell proliferation. (c) RT-qPCR was used to assess relative levels of the four Notch homologues and three Fringe enzymes in each cell line. (d) Proliferation of control cells (NIH3T3 cells) is not affected by the presence of the fucose analogs.

Additionally, we examined the effect of compound **10** on signaling from Notch1 mutants found in human T-cell acute lymphoblastic leukemia (T-ALL). Some of these mutants have been shown to be activated in ligand independent manner (311). Initial experiments demonstrated that compound **10** inhibited Dll1-mediated Notch signaling from T-ALL mutants (Fig. 3.12a) in WT U2OS cells. Similar experiments in POFUT1 knockout cells demonstrated, as expected, that POFUT1 plays a critical role in promoting Notch signaling, even for constitutively active Notch mutants. These experiments also demonstrated that compound **10** did not further reduce the already low Notch signaling in the absence of POFUT1 (Fig. 3.12b). Interestingly, compound **10** did inhibit ligand independent Notch signaling in all T-ALL mutants tested (Fig. 3.12c).

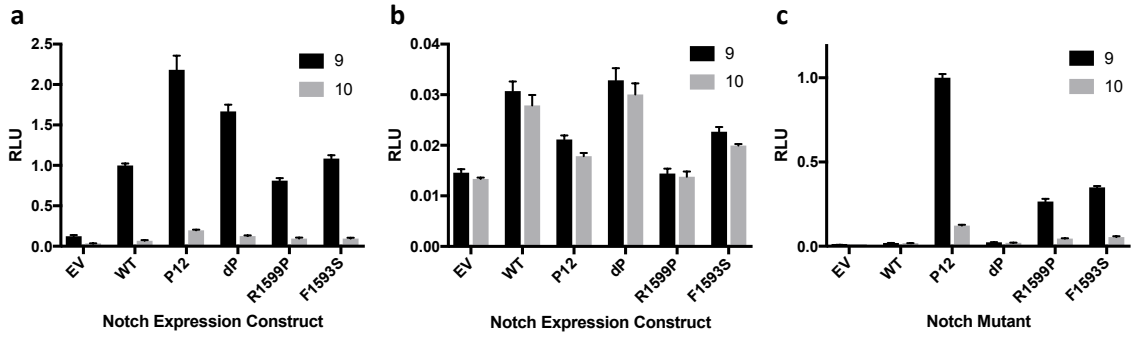

Figure 3.12: 6-Alkynyl fucose inhibits Notch signaling in constitutively active Notch mutants found in T-ALL. (a) Luciferase based co-culture assay showing the effect of compound **10** on Dll1-stimulated activation of Notch T-ALL mutants in WT U2OS cells. (b) Similar assay performed in POFUT1 knockout U2OS cells. (c) Luciferase based assay showing the effect of compound **10** on ligand independent activation of Notch T-ALL mutants. U2OS cells were provided generously by Dr. Stephen Blacklow's lab, Harvard University.

3.10 Discussion

We demonstrate here that fucose analogs serve as inhibitors of Notch signaling, preferentially inhibiting Notch activation from Delta-like ligands. These analogs are converted to GDP-fucose analogs, utilized by Pofut1 and incorporated into Notch EGF

repeats. Further, Lfng can elongate incorporated fucose analogs and alter their effect on Notch signaling strength. Here, we posit that this type of manipulation of Notch receptor glycosylation may lead to a better understanding of exactly how glycan modifications alter Notch function. We further show that this may then be directly applied toward the development of novel strategies that may allow us to gain control over Notch signaling in functional processes such as T-cell differentiation and cancer cell proliferation.

Interestingly, the effects of these inhibitory fucose analogs (**10** and **11**) differed between the various Notch-ligand interactions assessed. Among Delta ligands, we saw complete inhibition of Dll1-Notch1 signaling, but only partial inhibition of Dll4-Notch1, Dll1-Notch2, and Dll4-Notch2 signaling. Others have shown that the Dll1-Notch1 interaction is relatively weaker than the other interactions we examined (305, 312). This suggests that the inhibitory effect is more potent in the setting of lower receptor-ligand affinity complexes. This hypothesis could also explain why elongation by Lfng, which has been shown to enhance receptor-ligand affinity (305), is able to partially rescue the inhibitory effect of these analogs. Despite reduced binding affinity in the presence of inhibitory fucose analogs, Jag1-induced Notch signaling was relatively unaffected by these compounds. This could be due to an alternative signaling mechanism, which does not necessarily correlate with binding affinity. There was a trend toward decreased signaling in the Jag1 stimulated signaling assays, which may have been a result of slightly decreased cell surface expression of Notch.

We also show that peracetylated fucose analogs are taken up by cells, converted to their corresponding GDP-fucose derivatives and incorporated into Notch EGF repeats by Pofut1. It is notable that although GDP-L-galactose (**6**) inhibited Notch signaling in

Zebrafish embryos, peracetylated L-galactose (**12**) was not incorporated into EGF repeats (Fig. 3.4b). This was likely due to a failure of this compound to be converted to GDP-L-galactose by the fucose salvage pathway. Additionally, peracetylated 2F-Fuc (**13**), an established fucosyltransferase inhibitor, neither inhibited incorporation of fucose into Notch EGF repeats nor was it incorporated. Based on the cePofut1-GDP-fucose co-crystal structure, the hydroxyl group on carbon in the second position appears to play a critical role in the binding and transfer of GDP-fucose (313). This likely explains why a fucose derivative modified at the 2-carbon position would not be utilized by Pofut1. Perhaps at higher concentrations or with longer treatment durations, peracetylated 2F-Fuc (**13**) might cause feedback inhibition of GDP-fucose synthesis and effectively prevent the transfer of fucose to Notch EGF repeats, as others have seen in different systems (169).

Our data also indicate that the incorporation of fucose analogs **10** and **11** at EGF8 appears to play a role in mediating their inhibitory effects, while EGF12 is less important. This suggests that EGF8 plays an important role at the interface of Dll1/4 and Notch1 binding or is particularly important in regulating Notch's conformation. However, incorporation at EGF8 is still only partially responsible for the decrease that we see in Notch signaling caused by analogs **10** and **11**. Others have shown that mutations outside the ligand binding domain (126) and carbohydrate modifications on other Notch EGF repeats (125, 305, 314) play an important role in stabilizing the conformation of Notch and its ligands, thereby affecting their binding affinities. It is possible that the presence of fucose analogs, both within and outside of the ligand-binding domain, could cause conformational changes in Notch that destabilize Notch-ligand interactions.

The importance of excess Notch signaling in the etiology of human malignancy has stimulated intense interest in the development of Notch inhibitors as novel cancer therapeutics. However, complete inhibition of Notch with GSIs in the clinic has proven excessively toxic and new, more selective, strategies are much needed (292). More targeted inhibitors of specific components of the Notch signaling pathway are currently being developed in an attempt to reduce this toxicity (293-295). However, none of these efforts take advantage of Notch glycosylation, a crucial component in the Notch signaling pathway.

This work demonstrates that that fucose analogs can be used as targeted inhibitors of Notch signaling that can reduce proliferation of glioma cells. While Notch signaling was only partially reduced in these cell lines, this can be explained by the expression of a variety of Notch receptors and Fringe enzymes expressed in these cells and did not have much of an effect on the ability of these analogs to reduce glioma cell proliferation. Additionally, we demonstrate that we can reduce Notch signaling mediated by constitutively active T-ALL mutants in a manner dependent on POFUT1. Interestingly, 6-alkynyl fucose also caused a reduction in ligand independent signaling mediated by these mutants. This suggests that its role in reducing cell surface expression might play a more important role these systems (Fig. 3.5h), where higher receptor turnover might be required to allow for increased Notch signaling. It is also possible that the slower transfer of this fucose analog compared with L-fucose affects turnover rate or slows the transport of receptors from the ER to the cell surface (Fig. 3.2c).

In this work, we demonstrate that two fucose derivatives can be used as effective targeted inhibitors of Dll-mediated Notch signaling. We show that these inhibitors effectively inhibit T-cell differentiation in a Dll-dependent assay requiring the activity of

endogenous Notch receptors in mouse LSK cells and can be used to interfere with Notch signaling in cancer cell lines reducing proliferation. Such an agent that may effectively inhibit Notch signaling without excessive human toxicity would be a welcome addition to the current collection of anti-neoplastic treatment strategies.

Figure 3.13

EGF 5

^{182}CSQNPGLCRHGGTCHNE^{198}

Compound 9

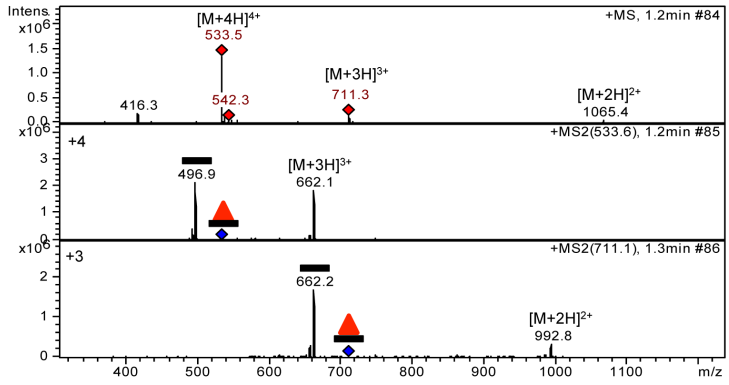

▬	496.9, 662.2, 992.8
▲	533.7, 711.1, 1065.9

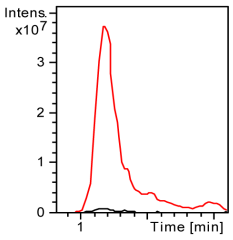

Compound 10

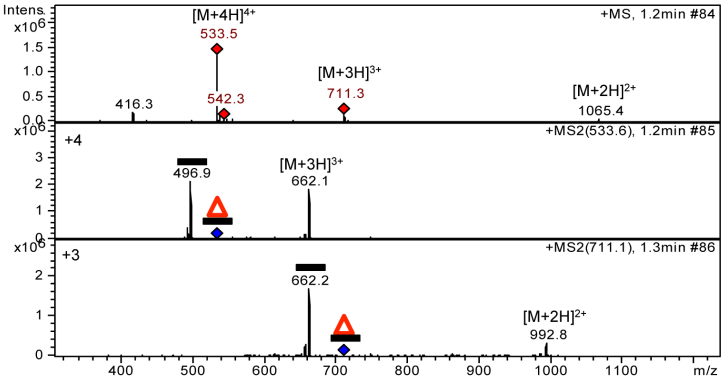

▬	496.9, 662.2, 992.8
▲	533.7, 711.1, 1065.9
△	535.9, 714.2, 1070.8

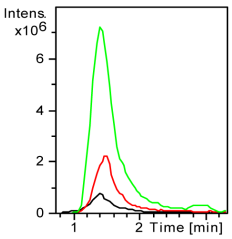

Compound 11

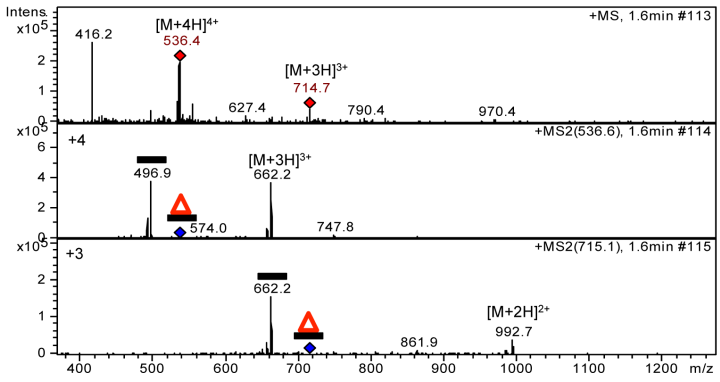

▬	496.9, 662.2, 992.8
▲	533.7, 711.1, 1065.9
△	536.4, 714.9, 1071.8

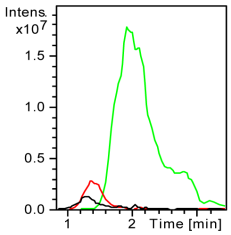

Compound 12

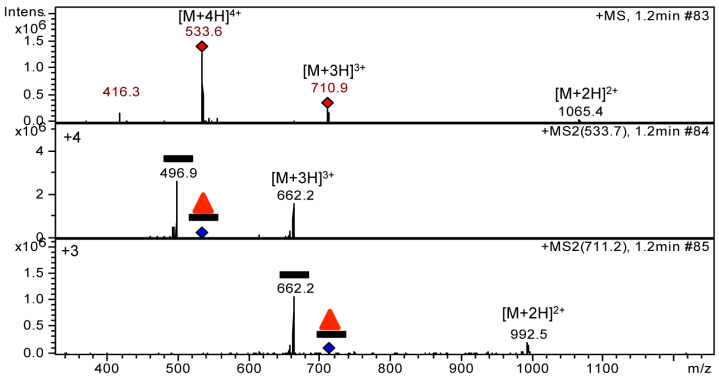

▬	496.9, 662.2, 992.8
▲	533.7, 711.1, 1065.9
△	537.3, 716.2, 1073.8

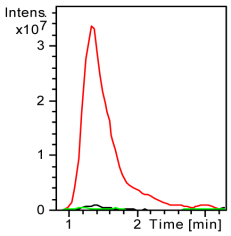

Compound 13

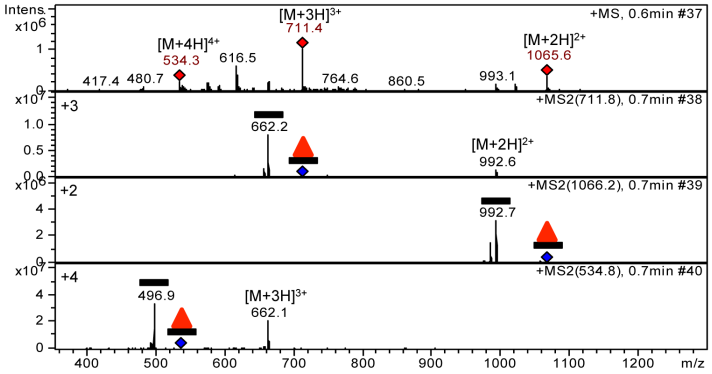

▬	496.9, 662.2, 992.8
▲	533.7, 711.1, 1065.9
△	534.2, 711.8, 1065.9

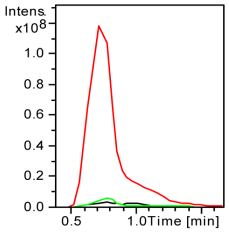

Compound 14

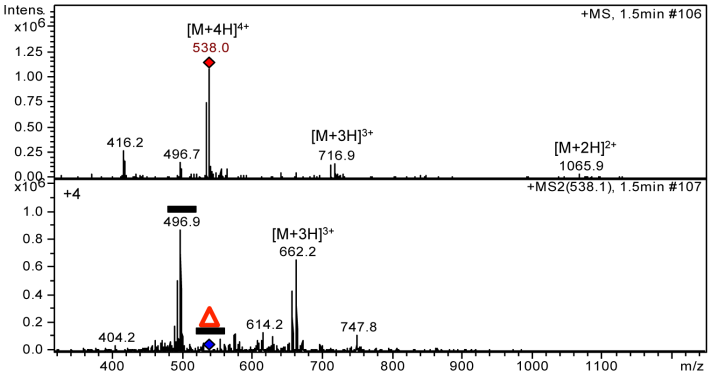

▬	496.9, 662.2, 992.8
▲	533.7, 711.1, 1065.9
△	538.2, 717.2, 1075.3

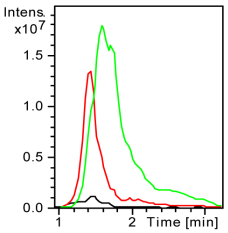

EGF 6

^{217}LPYVPCSPSPCQNGGTCRPTGDTTHE^{242}

Compound 9

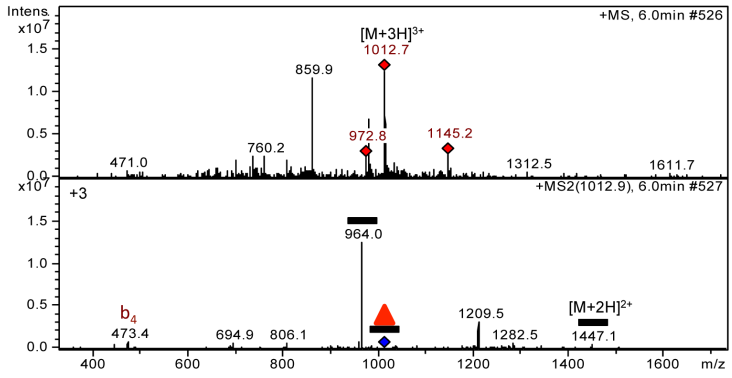

▬	964.0
▲	1013.1

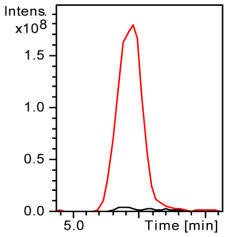

Compound 10

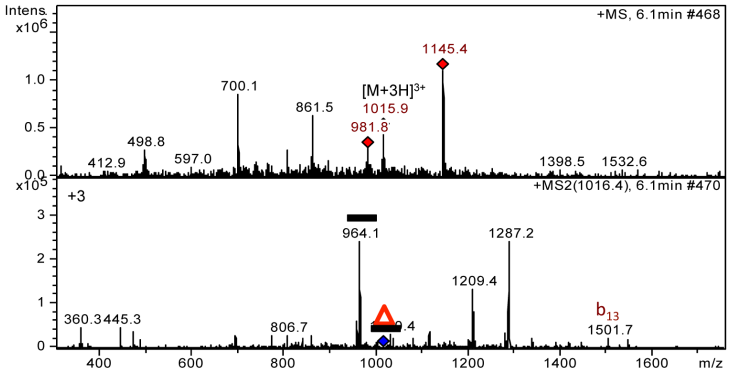

▬	964.0
▲	1013.1
△	1016.4

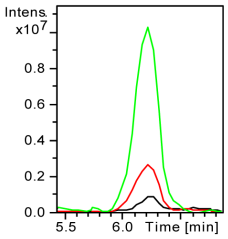

Compound 11

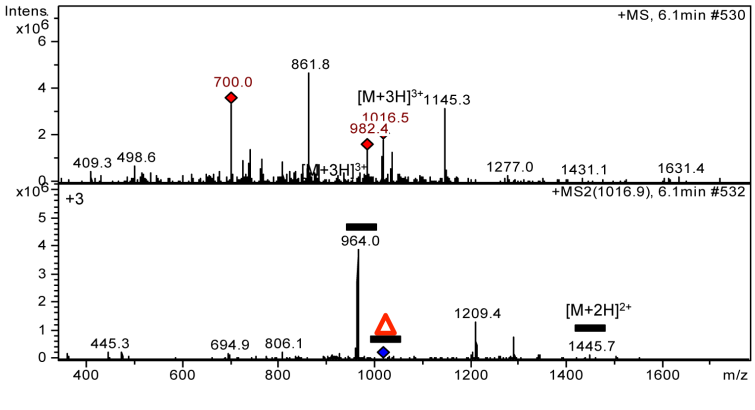

▬	964.0
▲	1013.1
△	1017.1

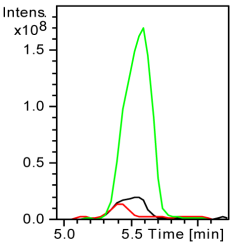

Compound 12

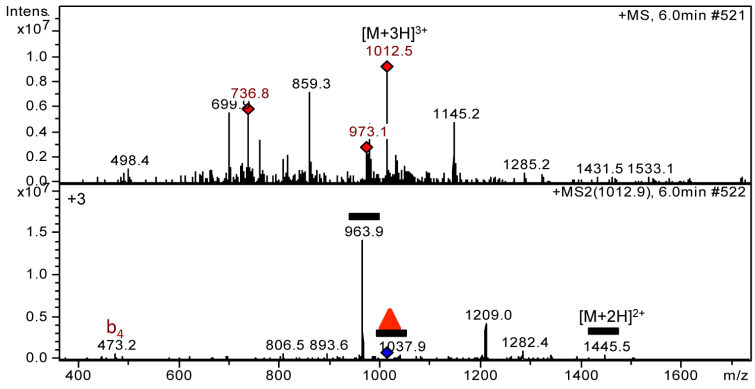

▬	964.0
▲	1013.1
△	1018.0

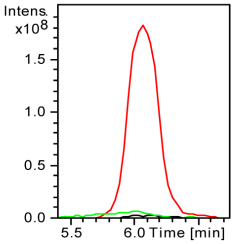

Compound 13

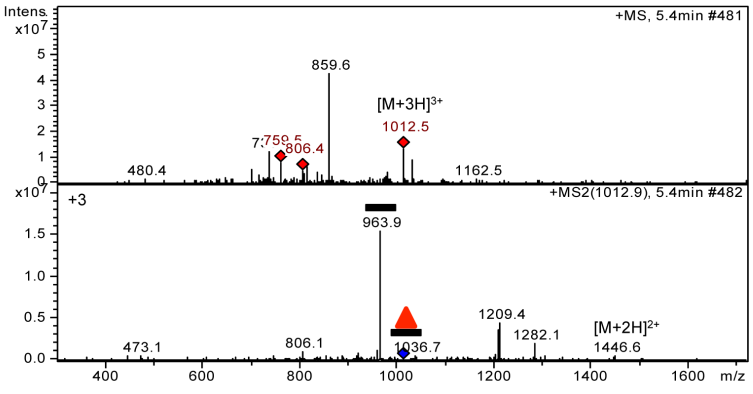

▬	964.0
▲	1013.1
△	1013.8

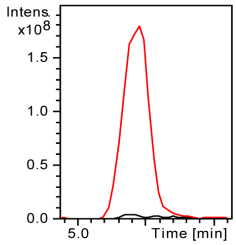

Compound 14

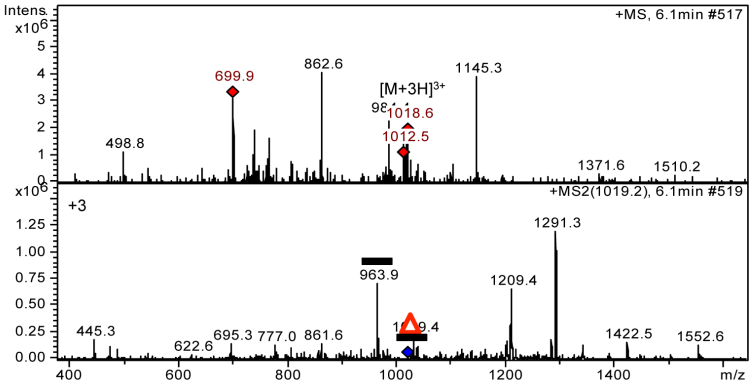

▬	964.0
▲	1013.1
△	1019.4

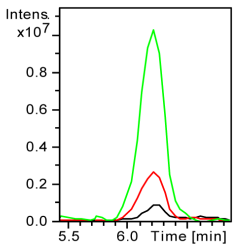

EGF 12

^{456}CISNPCQNDATCLDQIGE^{473}

Compound 9

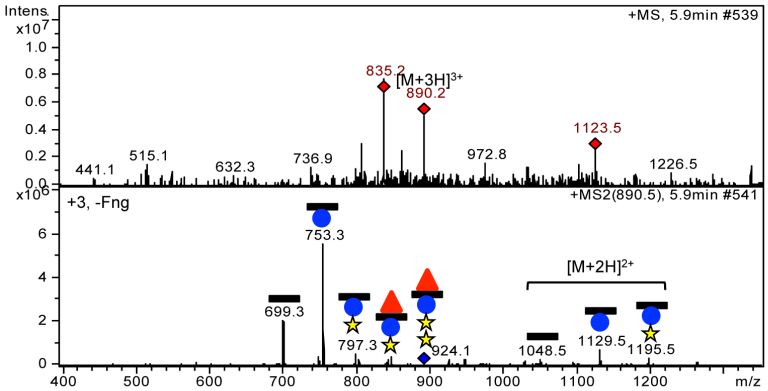

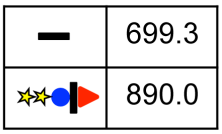

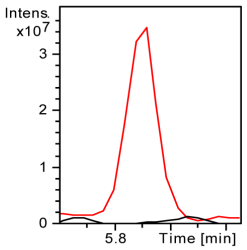

Compound 10

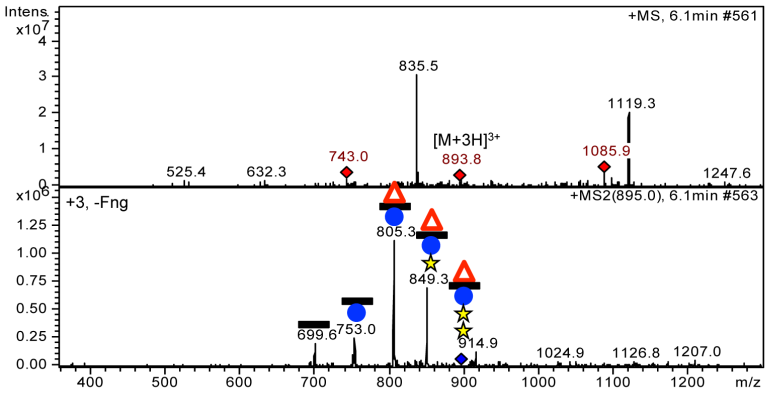

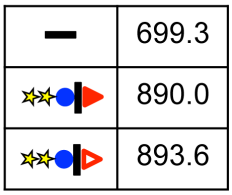

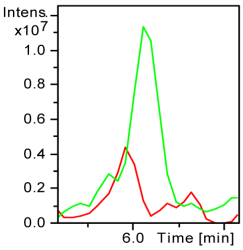

Compound 11

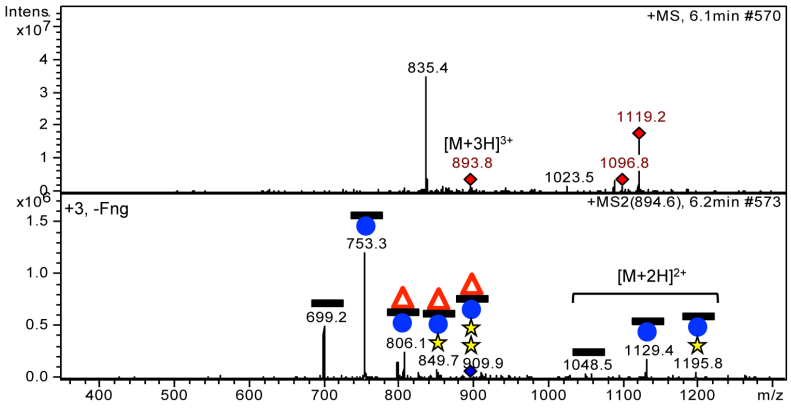

—	699.3
	890.0
	894.0

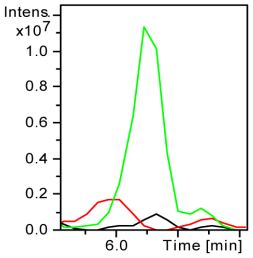

Compound 14

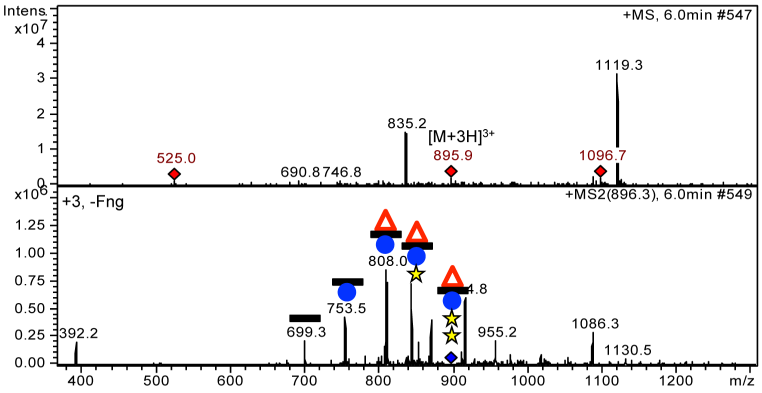

—	699.3
	890.0
	895.3

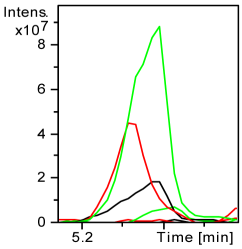

EGF 16

^{616}GTCQDRDNSYLC^{627}

Compound 9

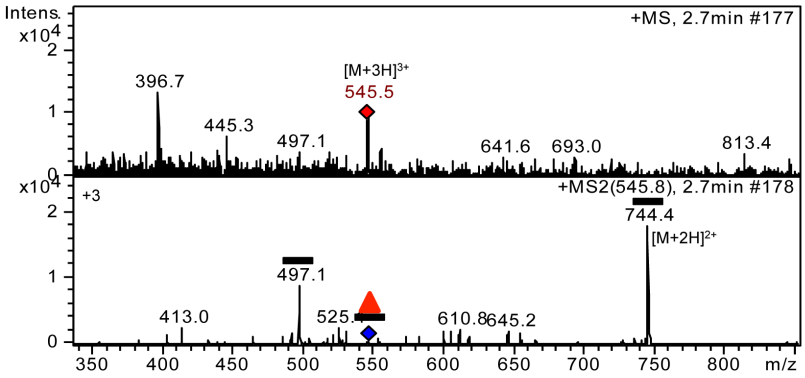

—	497.1
▲	545.8

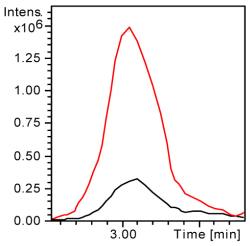

Compound 10

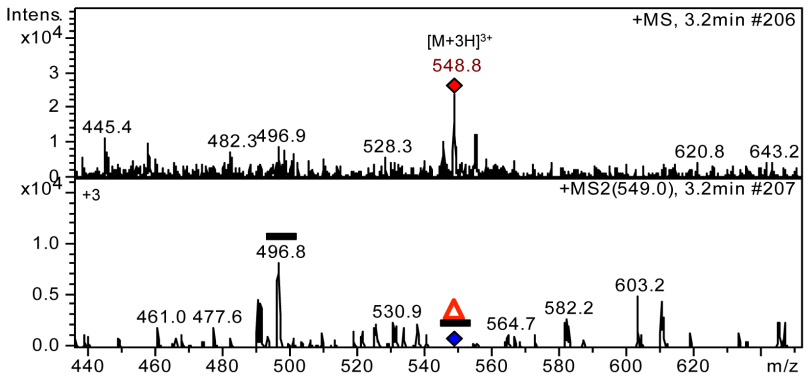

—	497.1
▲	545.8
△	549.0

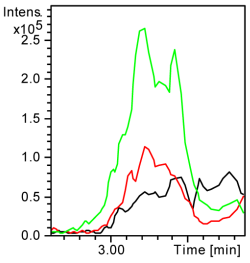

Compound 11

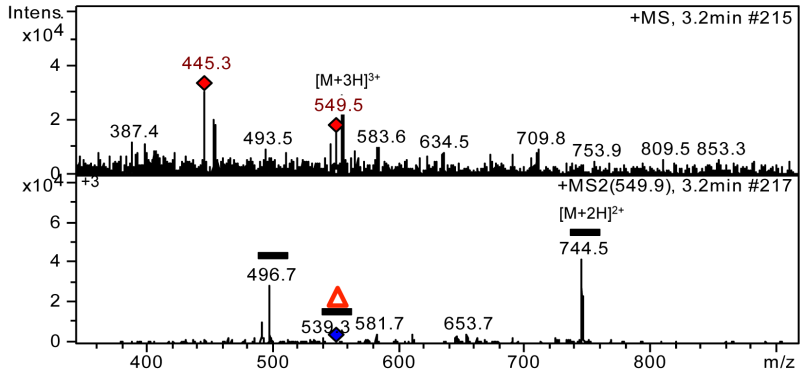

—	497.1
▲	545.8
△	549.5

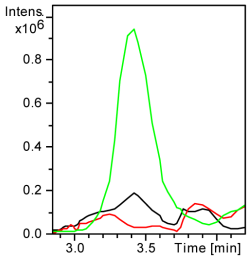

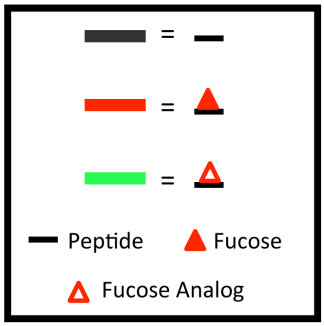

Figure 3.13. Mass spectra and extracted ion chromatograms (EICs) for *O*-fucose glycoform of additional peptides from EGF repeats containing an *O*-fucose consensus sequence in mNotch1 EGF1-18. Samples were generated in HEK293T cells transfected with plasmids encoding EGF1-18 and SEAP (EV). Cells were grown in the presence of the indicated compound as described in Materials and Methods (Chapter 2). Upper panels show an MS spectrum at a specific time, with the ion corresponding to the m/z of the peptide containing an *O*-fucose consensus sequence indicated. Lower panels show the MS/MS spectra confirming the identity of corresponding glycopeptides. Tables (right) show the m/z used for the EIC searches for glycoforms of the peptide and EICs represent relative amounts of these glycoforms. Mass spectrometry data for these peptides has been previously described without peracetylated fucose or fucose analog treatment (315). Key: black bar, peptide; red triangle, fucose; empty red triangle, fucose analog; blue square, GlcNAc; yellow circle, galactose; purple diamond, sialic acid.

EGF 6

^{217}LPYVPCSPSPCQNGGTCRPTGDTTHE^{242}

9

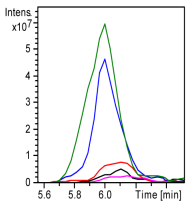

—	964.0
▶	1013.1
▶■	1080.8
▶■●	1134.8
▶■●◆	1231.9

10

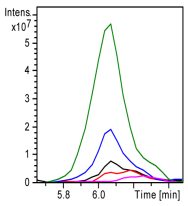

—	964.0
▶	1016.4
▶■	1084.1
▶■●	1138.1
▶■●◆	1235.2

11

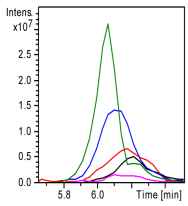

—	964.0
▶	1017.1
▶■	1084.8
▶■●	1138.8
▶■●◆	1235.9

14

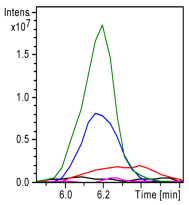

—	964.0
▶	1019.4
▶■	1086.1
▶■●	1140.1
▶■●◆	1237.2

EGF 12

^{456}CISNPCQNDATCLDQIGE^{473}

9

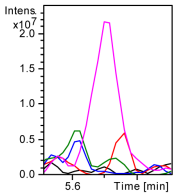

—	699.3
★★●▶	890.0
★★●▶■	957.7
★★●▶■●	1011.7
★★●▶■●◆	1108.8

10

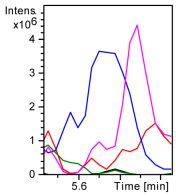

—	699.3
★★●▶	893.6
★★●▶■	961.3
★★●▶■●	1015.3
★★●▶■●◆	1112.4

11

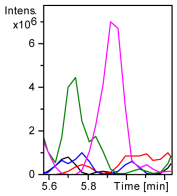

—	699.3
★★●▶	894.0
★★●▶■	961.7
★★●▶■●	1015.7
★★●▶■●◆	1112.8

14

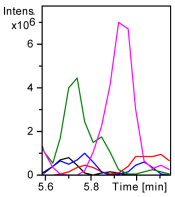

—	699.3
★★●▶	895.3
★★●▶■	963.0
★★●▶■●	1017.0
★★●▶■●◆	1114.1

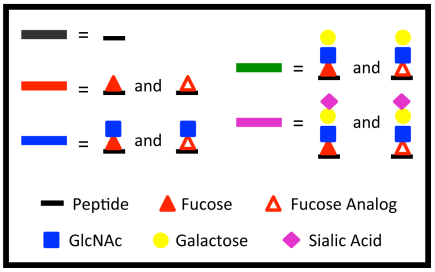

Figure 3.14. EICs for Lfng elongated peptides from EGF repeats containing an *O*-fucose consensus sequence in mNotch1 EGF1-18. Samples were generated in HEK293T cells co-transfected with plasmids encoding EGF1-18 and Lfng. Cells were grown in the presence of the indicated compound as described in Materials and Methods (Chapter 2). Tables (below each EIC) show the m/z used for the EIC searches for glycoforms of the peptide and EICs represent relative amounts of these glycoforms. Mass spectrometry data for these peptides has been previously described without peracetylated fucose or fucose analog treatment (315). EGF5 and 16 are not elongated by Lfng (315). Key: black bar, peptide; red triangle, fucose; empty red triangle, fucose analog; blue square, GlcNAc; yellow circle, galactose; purple diamond, sialic acid.

Contributions to this work

Lei Feng, a former member of Peng Wu's lab, generated data shown in Figure 3.1c. Hideyuki Takeuchi, a post-doc in our lab, generated data presented in Figure 3.2. Vivek Kumar, a post-doc in Pamela Stanley's lab, produced data shown in Figure 3.10. Lars Ulrik Nordstrøm, a former member of Peng Wu's lab, synthesized many of the fucose analogs used here (see Chapter 2).

Chapter 4: A novel mutation in human *POFUT1* eliminating an *N*-glycosylation sequon reduces its enzymatic activity and ability to rescue Notch signaling

4.1 Introduction

Notch signaling plays critical roles in regulating cell-fate decisions throughout development and into adulthood (287, 316). Dysregulation of Notch signaling can cause several human diseases including Alagille syndrome (214), CADASIL (317) and T-cell leukemia (318). Although over 100 potential targets contain the consensus sequence for modification by POFUT1 in mammals (Table 1.1) (319), elimination of *Pofut1* in mice results in embryonic lethality with a phenotype that is very similar to Notch knockout mice, suggesting that at least during development, Notch is its primary target. In addition to POFUT1's enzymatic activity, it may also play a role as a chaperone for Notch, which could also contribute to these phenotypes (118). The extent to which POFUT1's enzymatic activity is required for proper Notch signaling *in vivo* remains unclear.

There are some examples of the effect of reduced or defective POFUT1 in mammals. *Cax* mice contain a hypomorphic *Pofut1* gene caused by an insertion into its fourth exon and produce only about 25% of WT *Pofut1* mRNA levels. This results in defective Notch signaling-dependent somitogenesis (320). In this setting, some tissues (e.g. presomitic mesoderm) appear to be more sensitive to the expression level of Pofut1 than others. In humans, haploinsufficiency of *POFUT1* has been associated with Dowling Degos Disease (DDD), a rare dermatologic condition (136).

Here we describe a patient bearing an S162L missense mutation in the *POFUT1* gene. The patient displays some clinical features overlapping with defects resulting from loss of Notch signaling. We show that the S162L mutation disrupts POFUT1's second *N*-glycosylation site (Fig. 4.1a) and significantly reduces its enzymatic activity. We also

demonstrate that the S162L POFUT1 mutant has a weaker ability to rescue Notch signaling in a cell-based assay compared with WT POFUT1.

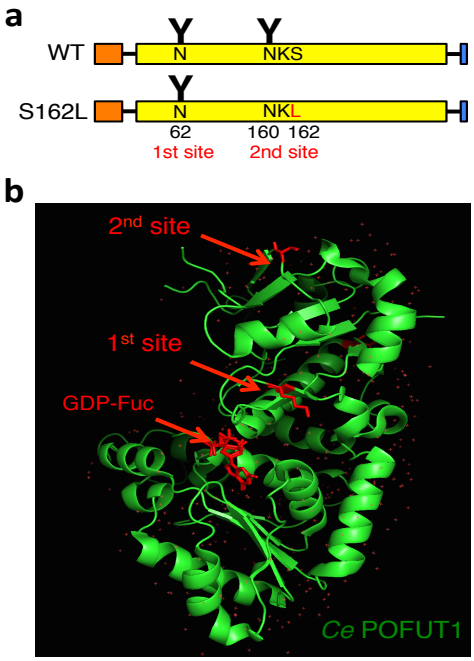

Figure 4.1: Patient mutation eliminates an *N*-glycosylation site on POFUT1. (a) Diagrams indicating the locations of *N*-glycan sites in WT and S162L mutant POFUT1. **Y** indicates predicted *N*-glycan sites. The mutated amino acid within the *N*-glycosylation consensus sequence is shown in red (b) The solved structure of *C. elegans* POFUT1 (313). The two *N*-glycan sites have been modeled in and are indicated by red arrows (note that *C. elegans* POFUT1 does not contain these sites). The GDP-fucose catalytic site is also indicated. Note that the 2nd site is the site mutated in this patient and appears to be far from the catalytic site of the enzyme.

4.2 Clinical features and identification of POFUT1 mutation

The patient displayed clinical features including failure to thrive, developmental delay, microcephaly, hypotonia, abnormal fat distribution, malnutrition, multiple fractures with osteopenia. Other symptoms included coagulopathy with low factor II, V, VII, IX, protein C and anti-thrombin III, which could not be explained by liver disease. Portal vein agenesis, regenerative nodular hyperplasia of the liver with persistent low-grade cholestasis, ventricular septal defect and aortic coarctation were also observed. The patient had a normal ophthalmologic exam and normal skeletal survey, with no evidence of vertebral abnormalities in contrast with what was seen in *Cax* mutant mice (320). Cardiac and vascular defects have been associated with Notch signaling.

A homozygous c.485C>T variant (p.S162L) in *POFUT1* was identified in this patient using Sanger sequencing (Fig. 4.1a). The mutation was also confirmed to be present in heterozygous form in both the mother (R12-22483) and father (R12-22489). POFUT1 mRNA levels in the fibroblasts from the affected patient (CDG402) was normal compared with those from control patients (GM0038 and GM3348) (Fig. 4.2a).

Based on the primary sequence of POFUT1, the S162L mutation eliminated the consensus sequence (^{160}NKS^{162}) for *N*-glycosylation on POFUT1 (the underlined asparagine residue is the predicted *N*-glycosylation site), one of two *N*-linked glycosylation consensus sequences on human POFUT1 (Fig. 1.1). Analysis of POFUT1 protein levels in extracts of patient fibroblasts showed that the POFUT1 levels were comparable to controls (Fig. 4.2b); however, the enzyme's size in the affected patient appeared to be smaller than its size in controls, presumably due to loss of *N*-glycosylation at N^{160}. PNGase F digestion to remove *N*-glycans on the protein caused a further decrease in size in the samples from the patient. This size was consistent with the size of POFUT1 from control fibroblasts digested with PNGase F (Fig. 4.2b). This data strongly suggests that WT POFUT1 is modified with *N*-glycans at two sites (N^{62} and N^{160}), while the S162L mutant is modified with an *N*-glycan chain at N^{62}, but not at N^{160}.

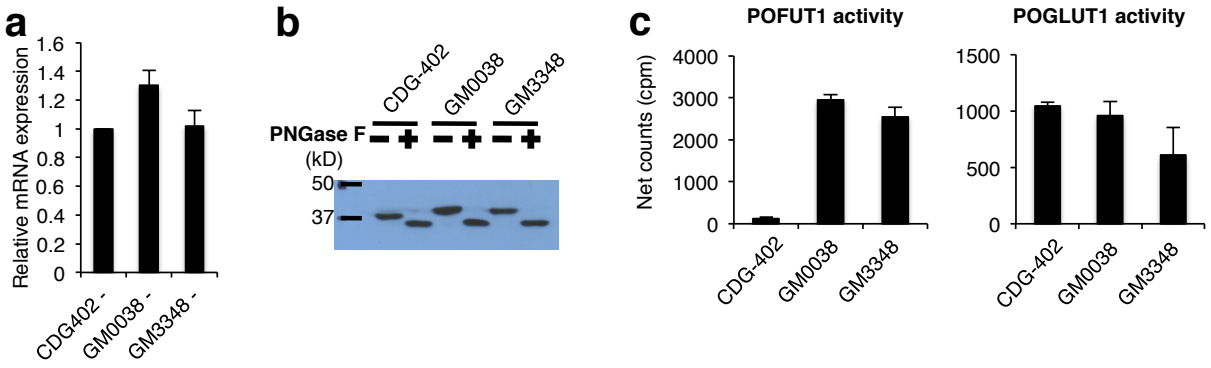

Figure 4.2: The S162L mutant disrupted an *N*-glycosylation site in POFUT1 leading to reduced enzymatic activity. (a) The mRNA expression levels of POFUT1 in fibroblasts from the patient and control individuals were detected by qPCR analysis. The data indicate mean + SEM from three independent experiments (n=9). (b) POFUT1 protein from fibroblast cells from the patient (CDG402) and control individuals (GM0038 and GM3348) were detected by Western blot before and after treatment with PNGase F. A representative image is shown from three biological replicates. (c) POFUT1 activity and POGLUT1 activity from the extracts of fibroblasts from the affected patient and control individuals. Assays were performed three independent times. Values indicate mean + SEM. Data in panels b and c provided by Dr. Hideyuki Takeuchi.

In order to examine whether the S162L mutation affects the ability of POFUT1 to modify its substrates with fucose, we measured enzymatic activity for POFUT1 extracted from patient fibroblasts. Using a bacterially expressed epidermal growth factor-like (EGF) repeat from human coagulation factor IX (FA9) as an acceptor substrate and GDP-fucose as the donor substrate, we measured POFUT1 activity in fibroblast extracts from the affected patient and controls (Fig. 4.2c). The POFUT1 activity in the fibroblast extracts from the patient was significantly lower than that from controls, although not eliminated. As a control for ER-associated enzymatic activity, we examined the activity of POGLUT1 from these extracts and found no significant difference between the patient and controls (Fig. 4.2c). Taken together with results showing that the S162L mutation did not reduce POFUT1 mRNA or protein levels significantly (Fig. 4.2a-b), this result suggests that the mutation had a direct effect on POFUT1 enzymatic activity.

4.3 POFUT1 mutant only partially rescues Notch signaling

The clinical features seen in the patient including defects in cardiogenesis and vasculogenesis overlap with some of the *Notch*-like phenotypes observed in mice lacking *Pofut1* (4). To examine whether the reduced enzymatic activity observed with the S162L POFUT1 mutant affects Notch activity, we performed cell-based Notch1 signaling assays in

POFUT1-null U2OS cells in which the Notch activity is profoundly reduced compared with control U2OS cells. As expected, transfection of WT POFUT1 rescued DLL1-mediated Notch1 activity in POFUT1-null cells (Fig. 4.3a). Transfection of the S162L mutant only partially rescued Notch1 activity, consistent with its decreased fucosyltransferase activity. DLL1 ligand-mediated signaling in control U2OS cells was not affected by overexpression of either WT or mutant POFUT1. To avoid saturation of POFUT1 activity in the cells, we varied the amount of POFUT1 expression plasmid against the constant NOTCH1 plasmid to carefully determine the appropriate NOTCH1:POFUT1 ratio. At the 1:0.1 ratio, the Notch activity upon the overexpression of WT POFUT1 was significantly lower than those at the 1:0.5 or 1:0.25 ratios (Fig. 4.3b). At all ratios tested, the S162L mutant of POFUT1 rescued the Notch activity to a significantly lower extent compared with WT POFUT1. Western blot analysis revealed that WT and S162L mutant POFUT1 were expressed at similar levels in these cells, consistent with the expression levels of the WT and S162L mutant of POFUT1 in the patient fibroblasts (Fig. 4.3c).

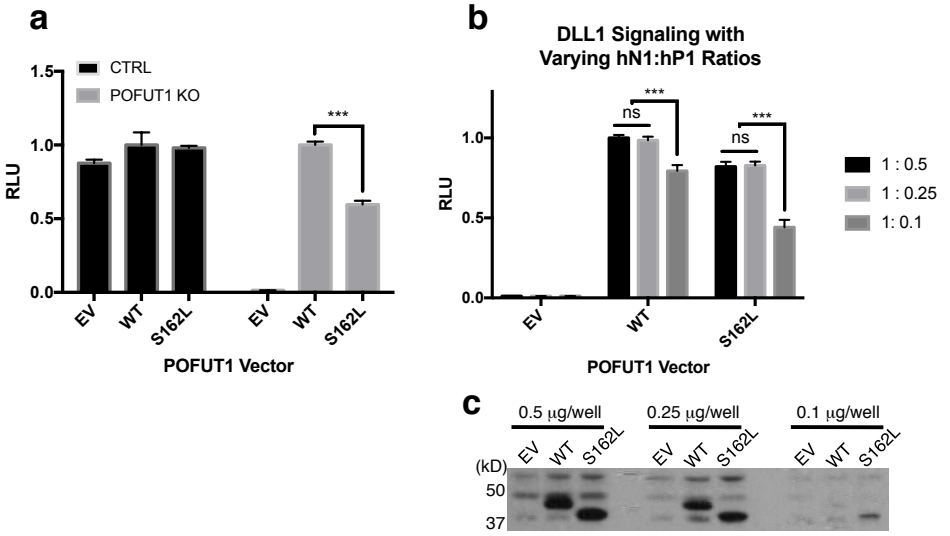

Figure 4.3. The POFUT1 S162L mutant did not fully rescue Notch activity in cells. (a) Luciferase reporter assays for DLL1-mediated NOTCH1 signaling were performed in WT or *POFUT1* knockout U2OS cells. Cells were transfected with NOTCH and either empty vector (EV), WT POFUT1 (WT) or mutant POFUT1 (S162L) at a 1:0.5 ratio. The experiment was performed two independent times with six biological replicates (n=6). Values indicate mean + SEM ***p<.001. (b) U2OS cells lacking *POFUT1* were co-transfected with EV, WT POFUT1 or mutant POFUT1 at varying NOTCH:POFUT1 ratios. Three biological replicates were performed for each condition. Values indicate mean + SEM ***p<.001. (c) Protein expression levels of overexpressed WT and S162L mutant POFUT1 were measured in U2OS cells at varying NOTCH:POFUT1 ratios by Western blot using an anti-His antibody.

4.4 Discussion

This work investigates a patient with an S162L missense mutation in *POFUT1*, who showed severe developmental and physiological defects, some of which are consistent with a Notch phenotype. We show that this mutant disrupted an *N*-glycosylation site at N^{160}, which was modified in WT POFUT1, and that the mutation resulted in significantly lower enzymatic activity compared to WT controls. Additionally, we showed that the S162L mutant of POFUT1 was less able to rescue Notch activity compared with WT POFUT1, which suggests that some of the phenotypes in the patient are likely due to altered Notch signaling.

The structure of *C. elegans* POFUT1, which has ~41% identity with higher eukaryotic enzymes, has been solved (313). Although *C. elegans* POFUT1 does not have any predicted *N*-glycosylation sites, the N^{160} residue of human POFUT1 mapped into the structure of *C. elegans* POFUT1 indicates that the residue is not near the enzyme's catalytic site or the predicted EGF binding pocket (313). This suggests that the *N*-glycans at N^{160} are unlikely to be involved in the enzyme's catalytic reaction (Fig. 4.1b). The reduced activity of the S162L mutant might be due to an allosteric effect caused by the mutation itself, loss of *N*-glycans at N^{160}, or both. Any of these possibilities might result in decreased enzyme-enzyme or

enzyme-substrate affinity. It is worth noting that both of POFUT1's *N*-glycosylation sites are well-conserved in mammals.

The observation that this mutation causes a significant decrease in the enzymatic activity of POFUT1 provides important biological insights into the requirement of this activity for Notch signaling *in vivo*. Previous reports have demonstrated that *Pofut1* knockout in mice results in embryonic lethality with Notch-like phenotypes, but heterozygous loss of *Pofut1* does not cause any detectable defects (4). It has also been reported that *Cax* mice, expressing only ~25% of WT *Pofut1* mRNA levels, show somitogenesis defects – a process dependent on Notch signaling (320). The patient described here did not display any skeletal abnormalities, but did show developmental defects consistent with defective Notch signaling including problems with cardiogenesis and vasculogenesis. Other defects in this patient are not typically associated with defective Notch signaling and more work will be needed to determine their cause. It is possible that other POFUT1 target proteins may be responsible (See Table 1.1).

Finally, this data suggests that *N*-glycosylation of POFUT1 is critical for its function. The elimination of this *N*-glycan site almost entirely eliminates enzymatic activity. The mechanism for this effect remains unclear and further work will be needed to determine the role this *N*-glycan plays in regulating POFUT1 activity.

Contributions to this work: Data presented in Fig. 4.1b-c was generated by Hideyuki Takeuchi, a post-doc in our lab. Dr. Hudson Freeze and members of his group made all clinical characterizations and conducted genome sequencing of the affected patient.

Chapter 5: Investigating the role of *POFUT1* amplification in hepatocellular carcinoma

5.1 Introduction

It is projected that there will be over 33,000 new cases of hepatocellular carcinoma (HCC) diagnosed and 23,000 HCC related deaths in the United States in 2014. Worldwide, HCC is the fourth most common cancer and the third leading cause of cancer death, resulting in over 500,000 deaths a year (321). Early stage HCC may be effectively treated with surgery, radiation or embolization techniques, but systemic treatment options have been extremely limited for more advanced disease, where the median survival is only 6-20 months (322). Sorafenib, a tyrosine kinase inhibitor with activity against the vascular endothelial growth factor receptor (VEGF-R), has been introduced as the first systemic therapy for HCC, suggesting the importance of neo-angiogenesis in supporting HCC progression, but has only modest activity (323). Notch signaling modulates VEGF signaling output and increased Notch signaling mediates resistance to anti-VEGF cancer therapies (324, 325). Thus, an increase in Notch signaling might partially explain the poor response of HCC to Sorafenib. Razumilava and Gores identified an increased Notch activity signature in approximately 30% of human HCC specimens, despite the absence of frequent mutations or copy number alterations in Notch genes (326). This increased Notch signaling may be a result of alterations in other Notch related genes, including those responsible for its post-translational modifications.

Increased activation of the Notch signaling pathway is also associated with a wide range of other human cancers including cervical, renal, lung, prostate, oral, and hematologic malignancies (142, 291, 327). This increased activity can promote cellular proliferation, tumor angiogenesis and epithelial to mesenchymal transition (EMT) (328). Notch activity also plays an important role in the maintenance of cancer stem cells (CSCs),

which are particularly important targets in the prevention of cancer relapse and metastasis (329).

Notch cell surface levels, signal strength and the resulting cellular effects appear to be dependent on each homologue's specific extracellular domain (330), which might be caused by differences in glycosylation patterns within these domains (120, 331). Protein *O*-Fucosyltransferase 1 (POFUT1) adds *O*-fucose to consensus sequences in Notch EGF repeats during Notch maturation (273, 332). Fucose modifications can be extended further via the addition of other carbohydrates by supplementary enzymes, further regulating Notch activity (273). Enzymes involved in post-translational protein processing can promote cancer survival and represent promising prognostic and therapeutic targets (333). Recent work suggests that POFUT1 is amplified in ~34% of HCC and promotes Notch signaling in these cells (141, 142). Additionally, amplifications of *POFUT1* have been linked with cervical cancer (334), oral squamous cell carcinoma (OSCC)(140), and glioblastomas (335). Genome database searches indicate that *POFUT1* is amplified in several additional cancer types including uterine and colorectal cancers (Fig. 5.1a) (336).

Although POFUT1's role as a fucosyltransferase and chaperone involved in post-translational processing of Notch is well established (4, 118, 124), its physiologic importance in the context of cancer and other diseases remains poorly understood. Additionally, POFUT1's role in promoting Notch cell surface expression, ligand binding and ultimately Notch signaling varies when examined in different contexts. For example, recent reports are in disagreement regarding the effects of POFUT1 knockdown on Notch1 cell surface expression (121, 124). Studies have identified increased Notch signaling in cancer, but in many cases the cause of this increased activity remains unclear (326). *POFUT1*

amplification or overexpression might be one mechanism responsible for this increased Notch activity. Prior work has demonstrated that increased POFUT1 contributes to cancer growth (140, 141) and is associated with several cancer types (334, 335), but no published report has examined the precise mechanisms causing this effect.

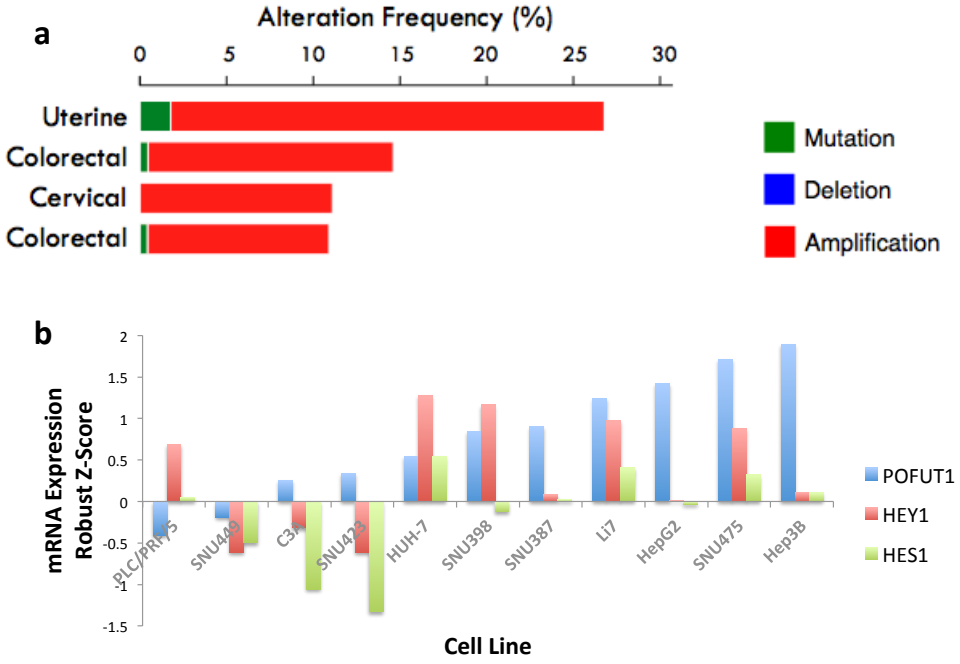

Figure 5.1: *POFUT1* is amplified in several cancer types and many hepatocellular carcinoma (HCC) cell lines. (a) *POFUT1* is amplified in greater than 10% of uterine, colorectal and cervical cancers according to some studies (336). (b) mRNA expression robust Z-scores for POFUT1 and Notch downstream reporters in a panel of HCC cell lines. *POFUT1* overexpression appears to correlate with an increased Notch activation signature in some, but not all cell lines (337).

5.2 Preliminary data indicating a role for POFUT1 in HCC

Preliminary data from Dr. Scott Powers' lab suggested that *POFUT1* causes an increase in Notch activity (Fig. 5.2). Overexpression of *POFUT1* in $p53^{-/-}$, Myc overexpressing mouse hepatoblasts (PHM1 cells) caused an increase in HEY1 expression, a downstream reporter for Notch signaling (Fig. 5.2a). HCC cell lines with amplified *POFUT1*, as determined by comparative genomic hybridization array (aCGH), expressed high levels

of HEY1 relative to HCC cell lines without *POFUT1* amplification. These elevated HEY1 levels were reversed using a γ-secretase inhibitor (GSI) to inhibit Notch activation (Fig. 5.2b-c). Additionally, GSI treatment has a significantly larger effect on cell growth of HCC cell lines with amplified *POFUT1* relative to other HCC cell lines tested (Fig. 5.2d).

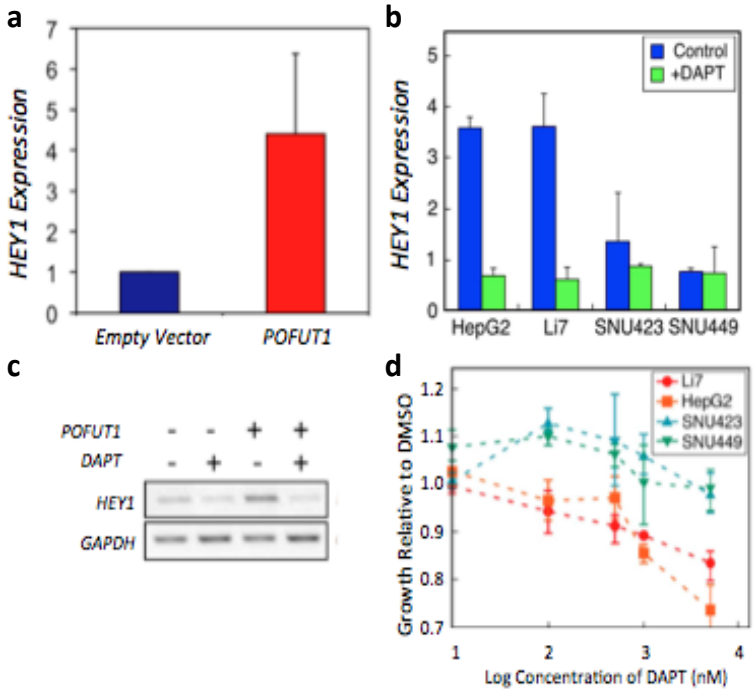

Figure 5.2: POFUT1 overexpression increases Notch activity and cell growth in hepatocytes. (a) *HEY1* mRNA levels are increased in immortalized mouse hepatocytes over-expressing POFUT1. (b) *POFUT1* amplified cell lines (HepG2 & Li7) show higher levels of *HEY1* mRNA expression than cell lines without *POFUT1* amplification (SNU423 & SNU449). Increased HEY1 expression is reversed by GSI treatment. (c) HEY1 protein levels are increased in hepatocytes overexpressing POFUT1. This is reversed by GSI treatment. (d) *POFUT1* amplified cell lines treated with a GSI show reduced cell growth relative to cells treated with DMSO. No effect is seen when cell lines without *POFUT1* amplification are treated. Performed by Dr. Eric Sawey, Powers lab.

Database searches supported the idea that *POFUT1* might be elevated in HCC and other types of cancer, but a correlation between *POFUT1* expression levels and expression levels of downstream Notch signaling reporters *HES1* and *HEY1* was seen in some, but not all HCC cell lines (Fig. 5.1b) (337).

5.3 Generation and characterization of cells overexpressing POFUT1

In order to begin my own characterization of the role of *POFUT1* in HCC, I began by overexpressing a Flag-tagged *POFUT1* construct in PHM1 cells and examining expression of

well-established Notch downstream reporters HEY1 and HES1. In order to optimize transfection efficiency for this cell line, I used two transfection reagents: Lipofectamine 2000 (L2K) and polyethylenimine (PEI). While both regents resulted in successful overexpression of POFUT1, L2K promoted more efficient protein expression (Fig. 5.3a), so L2K was used for the remainder of my experiments. Additionally, PHM1 cells stably over-expressing POFUT1 were generated and over-expression of POFUT1 was confirmed by Western blot with both anti-POFUT1 and anti-Flag antibodies (Fig. 5.3b).

I then used qPCR to evaluate the effects of this overexpression on Notch signaling. Primers for HEY1 and HES1 were validated on a DNA gel (Fig. 5.3c) and qPCR experiments were performed for PHM1 cells transiently overexpressing POFUT1 at three different time points (Fig. 5.3d). While we observed small increases in HEY1 and HES1 expression levels, these changes were not significantly different from WT PHM1 cells. Similar experiments were performed with cells stably over-expressing POFUT1 and again only very small differences were seen between experimental cells and controls (Fig. 5.3e). These results suggest that increased expression of POFUT1 in mouse hepatoblasts results in, at most, a minimal increase in Notch signaling.

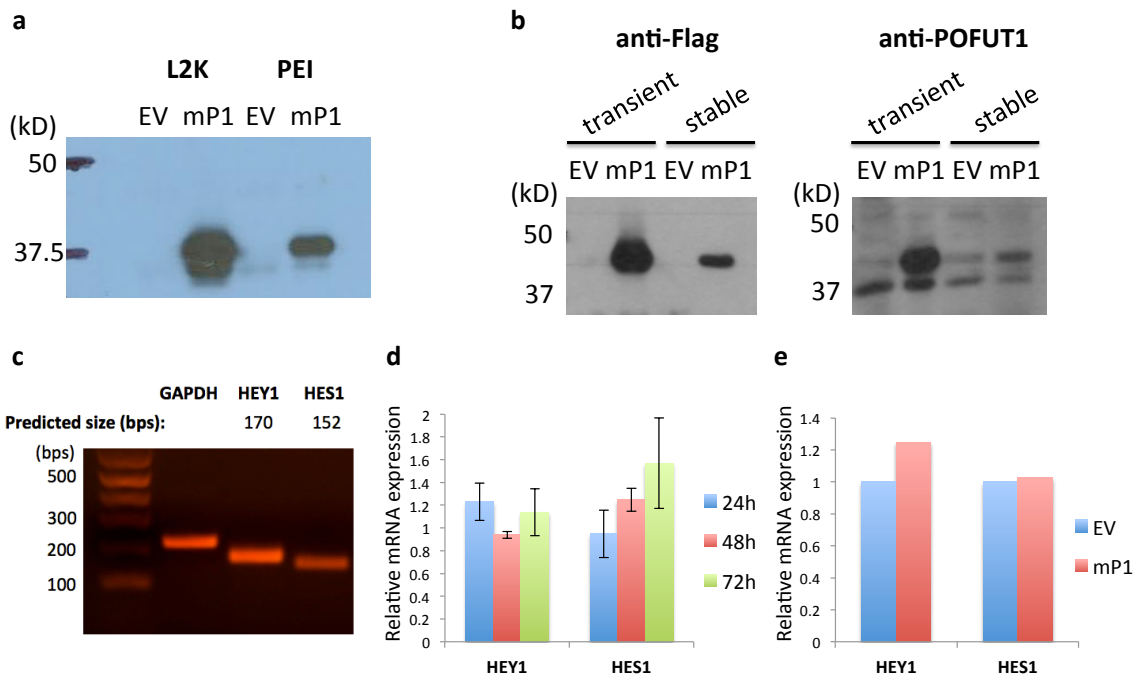

Figure 5.3: Overexpression of POFUT1 in PHM1 cells causes no significant increase in HEY1 or HES1 expression. (a) Western blot showing POFUT1 expression levels in empty vector (EV) and POFUT1 (mP1) transfected cells using Lipofectamine 2000 (L2K) or polyethylenimine (PEI) (b) Expression levels of POFUT1 in transiently and stably transfected PHM1 cells. (c) DNA gel validating primers used for qPCR analysis of HEY1 and HES1. (d) mRNA expression levels of HEY1 and HES1 in PHM1 cells transiently transfected with POFUT1 relative to EV transfected controls at 24 h, 48 h, or 72 h post-transfection. (e) mRNA expression levels of HEY1 and HES1 in cells stably expressing EV or POFUT1.

5.4 Generation and characterization of POFUT1 knock down cell lines

Although over-expression of POFUT1 in PHM1 cells did not appear to have a large effect on Notch signaling, I next examined the effects of POFUT1 knockdown in HCC and other cells. I first screened a panel of retroviral plasmids containing anti-POFUT1 shRNA in order to identify one that most efficiently knocked down POFUT1 levels effectively (Table 5.1). Each plasmid also contained a vector for GFP expression, allowing for selection and tracking of successfully transfected cells. These constructs were screened using HEK293T because they express high levels of endogenous POFUT1 and are easy to handle.

shRNA construct	Sequence (5' to 3')
296	GAAGGCTCGAGAAGGTATATTGCTGTTGACAGTGAGCGCCCATGTGTCCTACCAGAAGT ATAGTGAAGCCACAGATGTATACTTCTGGTAGGACACATGGATGCCTACTGCCTCGGAC TTCAAGGGGCTAGAATTCGAGCA
322	GAAGGCTCGAGAAGGTATATTGCTGTTGACAGTGAGCGCCCAGAAGTACTTCAAGCTGG ATAGTGAAGCCACAGATGTATCCAGCTTGAAGTACTTCTGGTTGCCTACTGCCTCGGACT TCAAGGGGCTAGAATTCGAGCA
366	GAAGGCTCGAGAAGGTATATTGCTGTTGACAGTGAGCGATCATCAGCTTGGAGGATTTC ATAGTGAAGCCACAGATGTATGAAATCCTCCAAGCTGATGACTGCCTACTGCCTCGGACT TCAAGGGGCTAGAATTCGAGCA
454	GAGGCTCGAGAAGGTATATTGCTGTTGACAGTGAGCGACCAGCGAAGCCCAGATAAGA ATAGTGAAGCCACAGATGTATTCTTATCTGGGCTTCGCTGGGTGCCTACTGCCTCGGACT TCAAGGGGCTAGAATTCGAGCA
513	GAAGGCTCGAGAAGGTATATTGCTGTTGACAGTGAGCGCTCTGGGATCAGTTTCATGTG ATAGTGAAGCCACAGATGTATCACATGAAACTGATCCCAGAATGCCTACTGCCTCGGACT TCAAGGGGCTAGAATTCGAGCA

Table 5.1: shRNA construct sequences screened for POFUT1 knock down.

I then generated retroviruses containing each of these constructs and transduced HEK293T cells with the resulting virus. After transduction, cells were sorted using fluorescence-activated cell sorting (FACS) to isolate GFP positive cells. GFP expression was confirmed using fluorescence microscopy (Fig. 5.4a). Cells were passaged and mRNA was isolated from cells containing each shRNA construct. RT-qPCR was used to quantify levels of POFUT1 mRNA from each sample and identify the most effective shRNA for POFUT1 knock down. Based on these results, we determined that the "513" construct knocked down POFUT1 mRNA levels most effectively (Fig. 5.4b). Knockdown was confirmed by Western blot for POFUT1 protein (Fig. 5.4c).

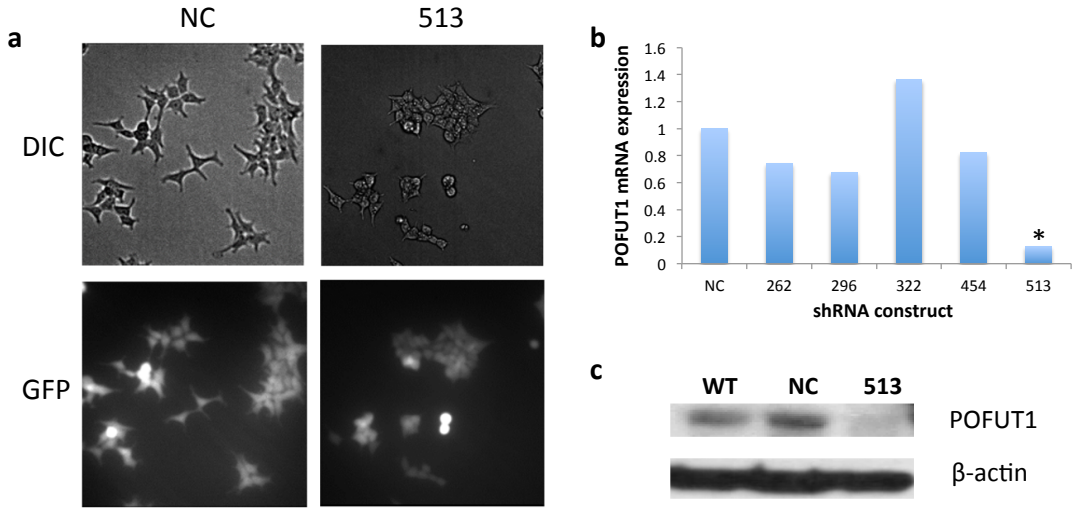

Figure 5.4: Identification of shRNA vector effective for POFUT1 knock down. (a) Images of cells showing negative control (NC) and POFUT1 knock down cells (513) taken using differential interference contrast (DIC) microscopy or fluorescence microscopy for GFP. Images show nearly all cells express GFP containing shRNA constructs. (b) RT-qPCR showing POFUT1 expression levels in HEK293T cells after transduction with a panel of shRNA containing plasmids. *indicates most effective knock down (c) Western blot showing knock down of POFUT1 protein levels in cells transduced with the 513 construct.

Further characterization of POFUT1 knock down HEK293T cells showed that cell surface expression of Notch was reduced in the absence of POFUT1 (Fig. 5.5a) Additionally, both Dll1 and Jag1 ligand binding were dramatically reduced compared to controls (Fig. 5.5b).

Using the 513 shRNA plasmid, which was most effective for POFUT1 knock down based on experiments in HEK293T cells, we then knocked down POFUT1 in HepG2 cells, an HCC cell line with amplified *POFUT1*. We confirmed expression of the GFP containing plasmid in these cells (Fig. 5.6a) and examined POFUT1 knock down levels by RT-qPCR and Western blot (Fig. 5.6b-c). We saw about a 40% knock down in mRNA levels, but only minimal change was detected at the protein level. Further experiments showed a minor reduction in the Notch downstream reporter gene HES1, but only a minimal decrease in HEY1 mRNA levels (Fig. 5.6d). We did, however, see a reduced rate of proliferation in

POFUT1 knock down cells compared with controls (Fig. 5.6e). Fucose analogs (see Chapter 3) did not significantly affect HepG2 cell proliferation (Fig. 5.6f).

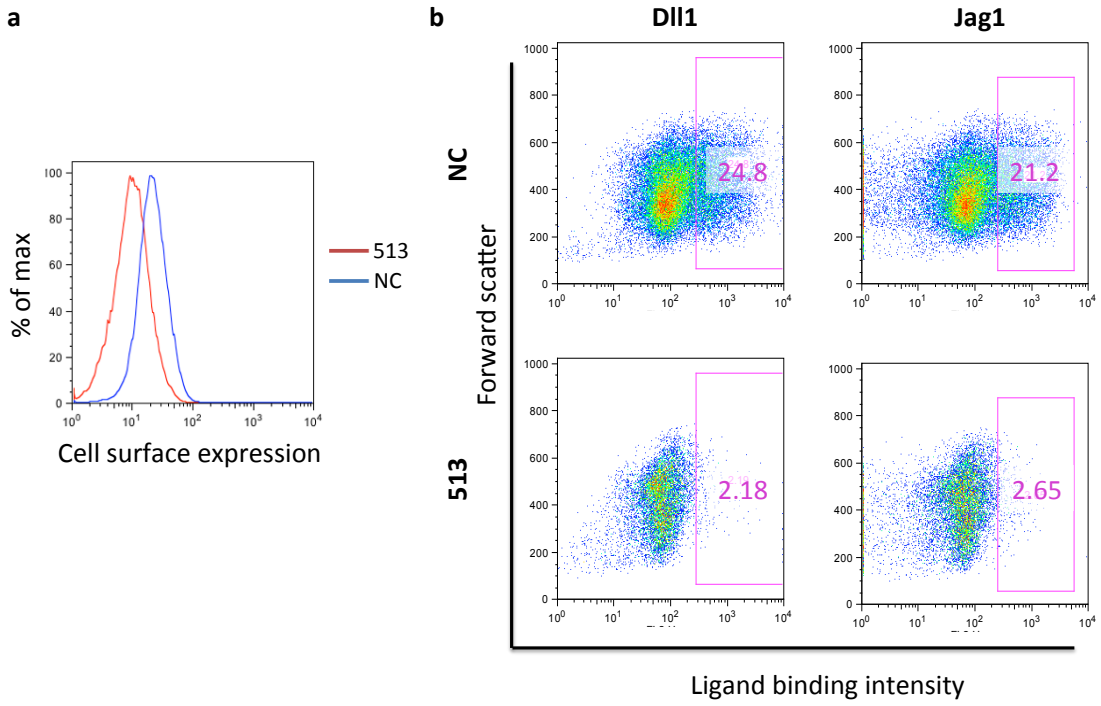

Figure 5.5: Knock down of POFUT1 reduces Notch cell surface expression and ligand binding (a) Histogram of Notch cell surface expression levels in negative control (NC) and POFUT1 knock down cell (513) HEK293T cells. (b) Plots of cells stained with soluble Delta-like ligand 1 (Dll1) or Jagged1 (Jag1). Percentage of ligand bound cells is indicated in each panel.

5.5 Discussion

The studies described here suggest a potential role for POFUT1 in promoting Notch signaling and proliferation in HCC. We demonstrate successful overexpression of POFUT1 in mouse hepatoblasts, but saw only a minimal effect on Notch signaling in these cells. Additionally, we efficiently knocked down POFUT1 in HEK293T cells causing a reduction in Notch cell surface expression and ligand binding. Finally, we show a partial knock down of POFUT1 in a human HCC cell line, which causes decreased proliferation of these cells.

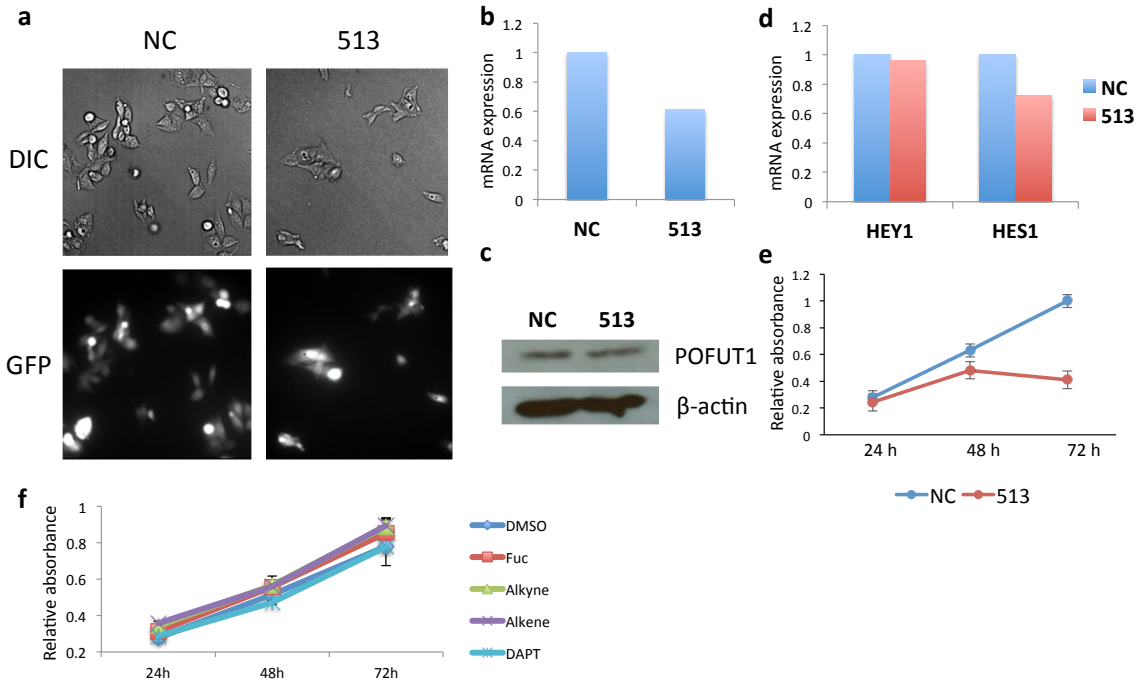

Figure 5.6: Knock down of POFUT1 in HepG2 cells may reduce Notch signaling and cell proliferation. (a) Images of HepG2 cells showing negative control (NC) and POFUT1 knock down cells (513) taken using differential interference contrast (DIC) microscopy or fluorescence microscopy for GFP. (b) POFUT1 mRNA expression levels in NC and 513 knock down cells. (c) POFUT1 protein expression levels in NC and 513 knock down HepG2 cells. (d) mRNA expression levels of Notch downstream reporters HEY1 and HES1 in NC and 513 knock down HepG2 cells. (e) MTT assay for NC and 513 cells measuring relative absorbance (570 nm) at 24, 48 and 72 hours after cells were plated. (f) MTT assay evaluating the effect of fucose analogs on HepG2 proliferation.

This work suggests that targeting Notch or factors causing its increased activation, such as POFUT1, may provide a mechanism for reducing HCC growth. Because Notch signaling plays an important role in regulating CSCs (338) and angiogenesis (328), inhibition of this pathway might be a useful tool for inhibiting these processes. Further work will be needed to determine the precise effects of *POFUT1* amplification on Notch signaling and cancer phenotype in the context of HCC. Additional work will be needed in order to develop tools that might be useful for the inhibition of Notch signaling and POFUT1. One possibility is the use of fucose analogs (discussed in Chapter 3) to inhibit Notch signaling that relies on the transfer of fucose by POFUT1.

Similarly, based on this work and the work of others (141), we might be able to use *POFUT1* amplification as a screening tool to identify cancers likely to respond to anti-Notch therapies and other anti-angiogenic treatments given the suggested role of Notch signaling in cancer dependent neo-vascularization. There has been much effort put into the development of γ-secretase inhibitors (GSIs), small molecules that inhibit Notch cleavage and activation, into anti-Notch signaling therapeutics for cancer. Unfortunately, these drugs have been shown to cause dangerous side-effects, most notably severe gastrointestinal tract toxicity (292). More recently, monoclonal antibodies targeting specific Notch homologues (339) or specific Notch activating ligands (294) have been developed in an effort to avoid this toxicity. However, no drugs have yet been developed to target Notch's post-translational modifiers, which might also serve as an effective mechanism to inhibit Notch signaling in disease states. This work suggests that targeting these post-translational modifiers might be a more effective way to target cells over-expressing *POFUT1* or the genes of other post-translational modifiers.

Finally, results presented here demonstrate only a small effect of POFUT1 on Notch signaling, potentially suggesting a role for other targets of POFUT1 in HCC. Work examining other POFUT1 target proteins in the context of HCC might reveal new insights into these cancers and more potential therapeutic targets for its treatment.

Contributions to this work: Data presented in Figure 5.2 was generated by Eric Sawey, a former graduate student from Dr. Scott Powers lab. Data presented in Figures 5.4, 5.5 and 5.6 was generated with the help of Allen Lee, a former undergraduate student working in our lab.

Chapter 6: Mouse Notch3 site mapping

6.1 Introduction

Protein *O*-fucosyltransferase 1 (POFUT1) is responsible for modifying EGF repeats containing the consensus sequence $C^2XXXX(\underline{S/T})C^3$ (see section 1.4). Although POFUT1 is predicted to modify about 100 proteins, its knockout in *Drosophila* or mice results in embryonic lethality with Notch-null phenotypes suggesting that Notch is its major target, at least throughout development (4, 340). The Fringe family of β3-GlcNAc-transferases can elongate *O*-fucose residues on EGF repeats with GlcNAc further regulating Notch activity (127). In mammals there are three Fringe enzymes: Lunatic Fringe (LFNG), Manic Fringe (MFNG) and Radical Fringe (RFNG). Only in mammals, GlcNAc residues can be further elongated to a trisaccharide by a β4-galactosyltransferase (341) or a tetrasaccharide by a sialyltransferase (120).

The three Fringe enzymes have varying specificities for different EGF repeats, although it remains unclear what factors determine this specificity (125). Nonetheless, these differing specificities result in distinct effects on Notch signaling (125). Thus, determining which EGF repeats are modified by which Fringe enzymes is important to gain a better understanding of the mechanism by which these carbohydrates regulate Notch signaling. Our lab and others have done much work using mass spectrometry to map *O*-fucose sites on Notch EGF repeats.

Mutations in Notch3 can lead to the human disease cerebral autosomal dominant arteriopathy with subcortical infarcts and leukoencephalopathy (CADASIL), which causes a number of physiological abnormalities that lead to dementia and strokes in patients (317). CADASIL mutations can directly impair elongation of *O*-fucose residues by Fringe enzymes (267), suggesting that GlcNAc modifications might play a role in the pathophysiology of this

disease. Notch3 is also overexpressed or constitutively active in a number of cancer types including lung cancer (342), hepatocellular carcinoma (343), breast cancer (344), colorectal cancer (345), and T-cell leukemia (346). Fringes have been implicated in regulating the activity of Notch3 in these contexts (347, 348).

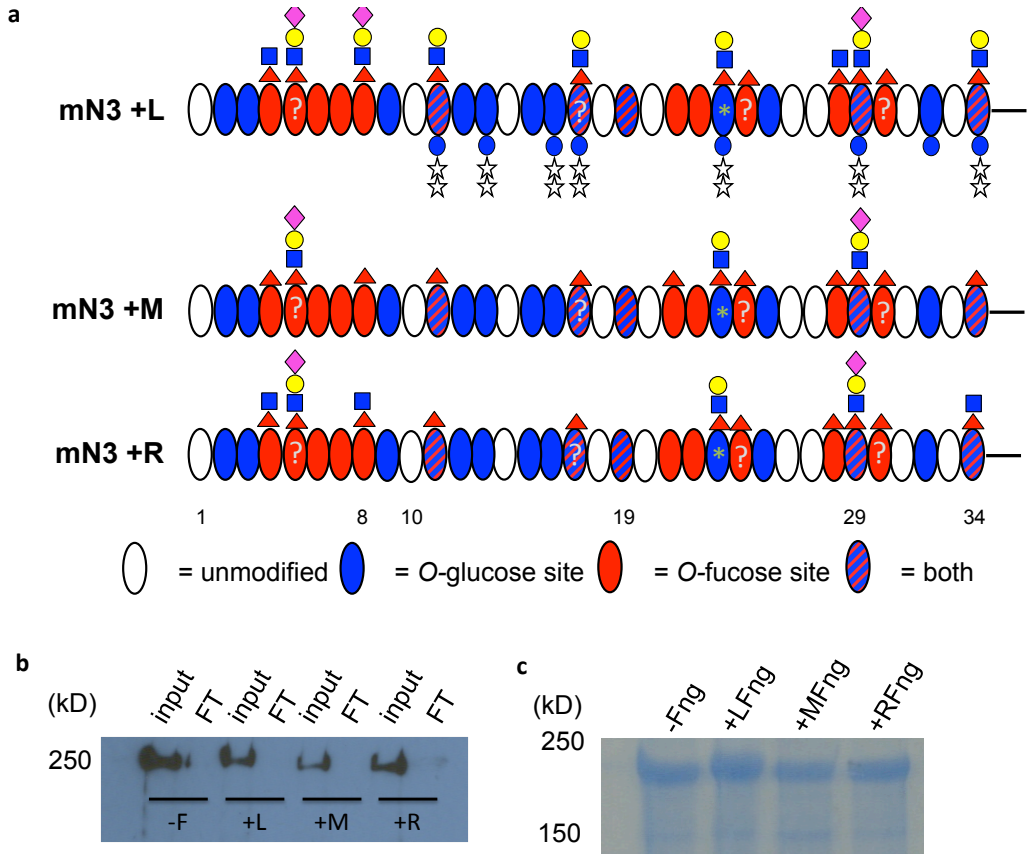

Figure 6.1: Mouse Notch3 site mapping summary. (a) Summary slide showing the 34 mNotch3 (mN3) EGF repeats and their modifications with LFNG (+L), MFNG (+M), or RFNG (+R). * indicates a site where a fucose modification was identified, but no consensus sequence was present. Peptides that require further work to confirm their identity are indicated with ?s. Spectra and EICs used to generate this summary are shown in Figure 6.3. (b) Western blot showing the input and flow through (FT) after purification of secreted mN3 EGF repeats in the absence of Fringe (-F) or with the three Fringe enzymes (+L, +M or +R). (c) Gel Code Blue stain showing purified mN3 ECD in the absence of Fringe or with each of the three Fringe enzymes.

For these reasons it is important to understand how POFUT1 and Fringe enzymes modify Notch3 EGF repeats. Here I mapped several *O*-fucose sites on mNotch3 and

evaluated the differential effects of the three Fringe enzymes on these modifications. I also begin to characterize the effects of different Fringe enzymes on Notch3-ligand binding.

6.2 Mouse Notch3 O-glycosylation site mapping

Based on the current consensus sequence for *O*-fucose modification on EGF repeats, mNotch3 has 14 predicted modification sites (Fig. 6.1a). In order to map glycan sites on mNotch3, I transfected HEK293T cells, which do not express endogenous Fringe enzymes, with a secreted form of mNotch3 and either empty vector, LFNG, MFNG, or RFNG. Protein was purified, reduced and alkylated, digested and analyzed by nano-LC-MS/MS (Fig. 6.1b-c, Fig. 6.3).

I was able to identify high stoichiometry *O*-fucose modifications at ten of the 14 predicted *O*-fucose sites on mNotch3 (Fig. 6.1a). At least one predicted modification site was identified as unmodified (EGF6). Additionally, I saw a fucose modification at one site without a classical consensus sequence for *O*-fucose (EGF23, CGPGTC, only 3 residues between C2 and the modified T). This modification has been seen previously in our lab (Eugene Tan's Undergraduate honor's thesis). These sites were modified differentially by the three Fringe enzymes. Of the ten sites modified with fucose, all but two were modified with GlcNAc by LFNG. Eight of these sites were not elongated with GlcNAc by MFNG and five were not elongated by RFNG. This data suggests that LFNG modifies Notch EGF repeats most efficiently. Interestingly, on mNotch3, RFNG modified EGF repeats more efficiently than MFNG, which represents a departure from what our lab has seen on mNotch1 (125).

There are also 14 predicted *O*-glucose modification sites on mNotch3. I was able to confirm the presence of glucose at seven of these sites. All but one of these modifications were efficiently modified to trisaccharide with xylose.

I also began to examine the effect of the three Fringe enzymes on mNotch3 ligand binding. While the Fringe effect was relatively small for mNotch3 relative to what our lab has seen in mNotch1 and mNotch2, there were some interesting findings. All three Fringes appeared to cause a slight increase in DLL1 binding (Fig. 6.2a). Only LFNG caused a slight increase in DLL4 binding, while RFNG caused a slight decrease in DLL4 binding (Fig. 6.2b). LFNG and MFNG also appeared to cause a slight increase in JAG1 binding to mNotch3 (Fig. 6.2c). Further work will be needed to evaluate the importance of these findings and determine their effect on mNotch3 signaling.

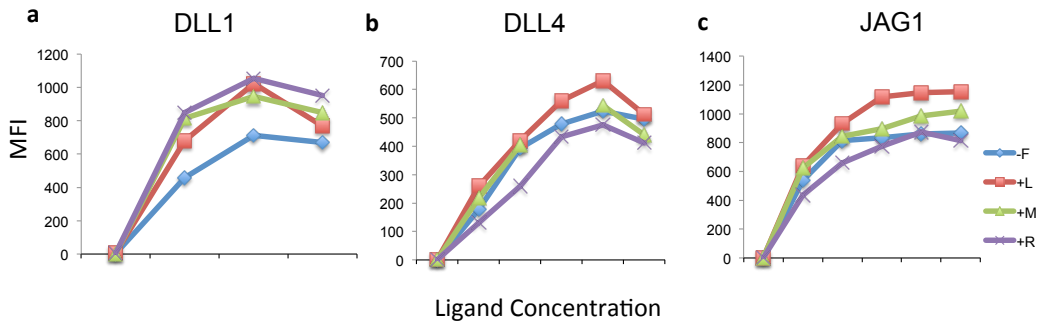

Figure 6.2: Ligand binding experiments with mNotch3. Cells were transfected with mNotch3 and either empty vector (-F), LFNG (+L), MFNG (+M), or RFNG (+R). Cells were isolated and stained with soluble (a) DLL1, (b) DLL4 or (c) JAG1. Ligand concentration increases along the x-axis.

6.3 Discussion

Here, I have begun to map the *O*-glycosylation sites on mNotch3 and investigate their effects on ligand binding. While more work will be needed to fully validate these results, they do provide some interesting information. Based on the sites that I have

mapped so far, it appears that LFNG most efficiently elongates *O*-fucose residues on mNotch3 EGF repeats, a result consistent with previous work on mNotch1 (125). However, I see more elongation of mNotch3 *O*-fucose residues by RFNG than MFNG, which is different from what our lab has seen in mNotch1 and 2. This may be a way for cells to differentially regulate Notch signaling from different receptors.

I also identified an *O*-fucose modification on EGF23 in the absence of a classical consensus sequence. This EGF repeat has only three residues between C^2 and the modified threonine, while the classical consensus sequence requires four residues between these amino acids. Similar sites on Notch1 and DLL1 are not modified based on previous literature (110, 111). Further evaluation, such as electron transfer dissociation (ETD) fragmentation, will be needed to confirm that this fucose is on the indicated threonine.

Finally, preliminary data suggests some differences between the effects of Fringe elongation on mNotch3 binding compared with mNotch1 and 2. Notably, RFNG appeared to cause a slight decrease in DLL4 binding and did not affect JAG1 binding levels. More work will be needed in order to determine how these binding differences affect Notch3 signaling. The effects on binding were relatively very small, so it will be important to look into the extent of their effects on signaling.

Figure 6.3

EGF 4

^{144}ACACPPGYQGQSCQSDIDECRSGTTCRHGGTCLNTPGSF^{182}

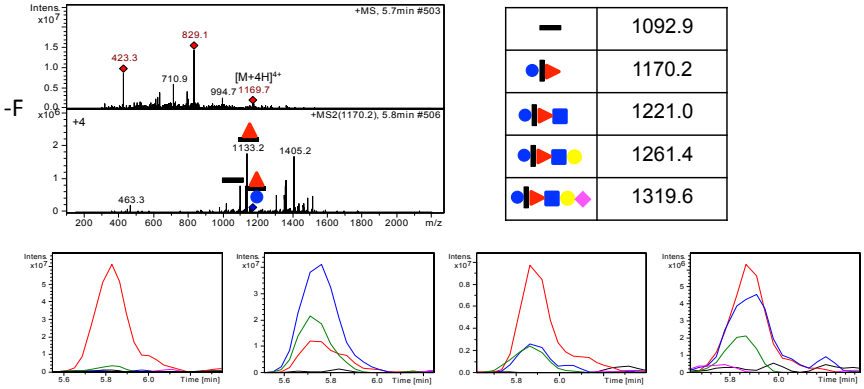

EGF 8

^{326}HGATCHDRVASF^{337}

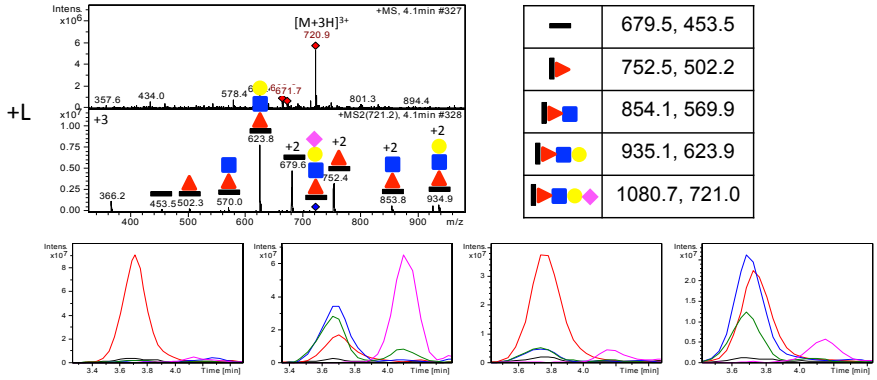

EGF 11

^{425}TGPRCETDVNECLSGPCRNQATCLDRIGQF^{454}

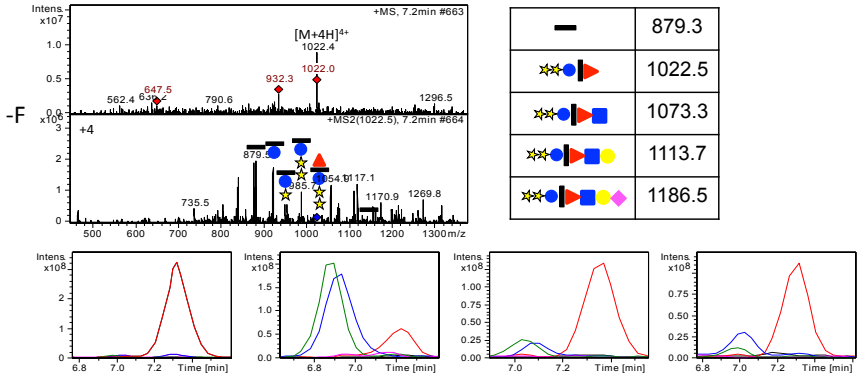

EGF 13

^{508}DVDECASTPCRNGAKCVDQPDGYECRCADGF^{538}

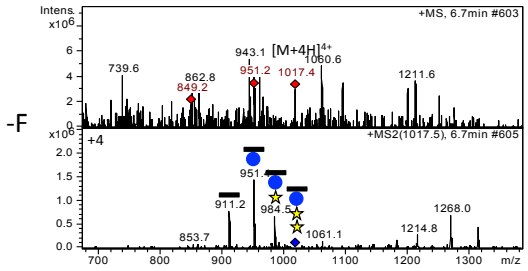

EGF 16

^{195}LCRCPPGTTGVNCEVNIDDCASNPCTF^{221}

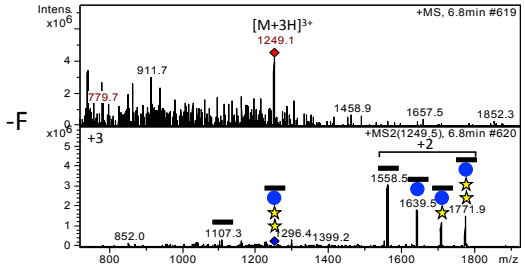

EGF 19

^{735}APDACESQPCQAGGTCTSDGIGFRCTCAPGF^{765}

-F

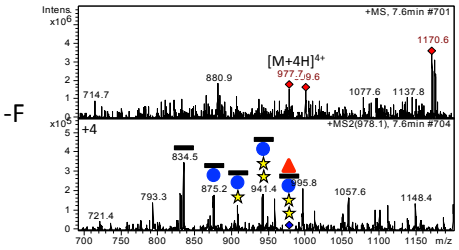

—	834.5
	977.9
	1028.6
	1069.1
	1141.9

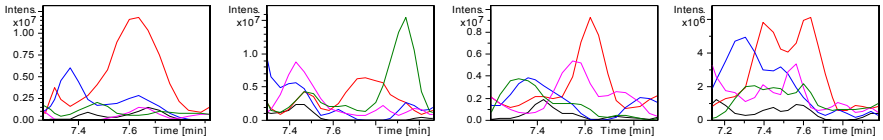

EGF 21

^{808}CQQDVDECAGASPCGPHGTCTNLPGNFR^{835}

-F

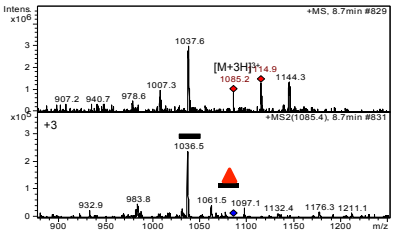

—	1036.5
	1085.4
	1153.1
	1207.1
	1304.2

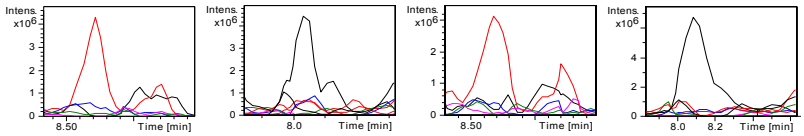

EGF 23

^{881}AGPRCARDVDECLSSPCGPGTCTDHVASF^{909}

-F

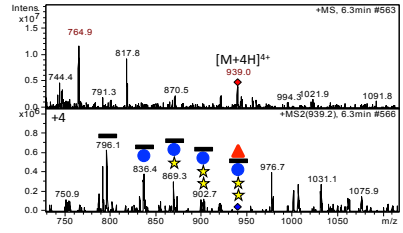

—	796.1
	939.2
	989.9
	1030.4
	1103.2

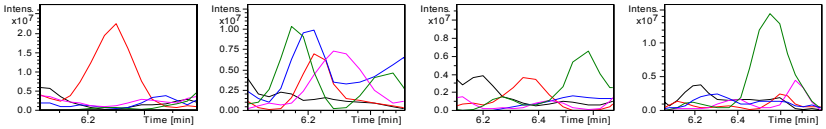

EGF 28

^{1071}CVCPEGRTGSHCEHEVDPCTAQPCQHGGTCRGY^{110}

-F

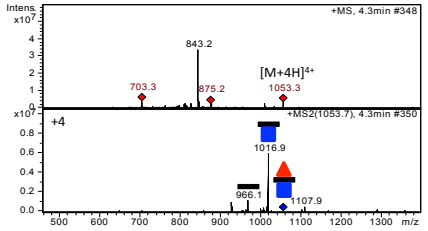

	966.1
	1053.7
	1104.5
	1144.9
	1217.7

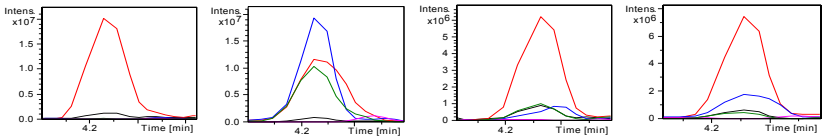

EGF 29

^{1111}CPAGYAGDSCEDNIDECASQPCQNGGSCIDL^{1141}

-F

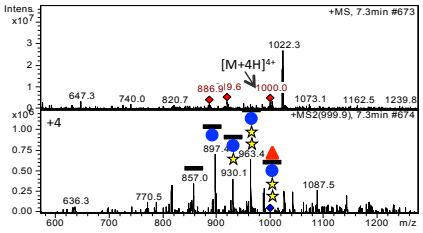

	857.0
	999.9
	1050.7
	1091.1
	1163.9

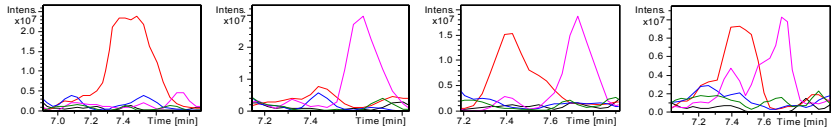

EGF 34

^{1321}SGPSCRVSRASPSGATNASCASAPCLHGGSCLPVQSVPFF^{1360}

+L

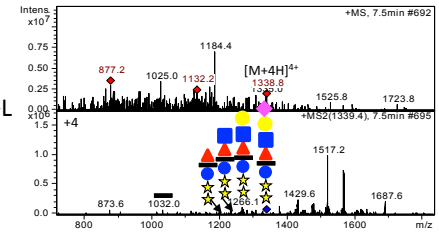

	1031.7
	1174.7
	1225.5
	1265.9
	1338.7

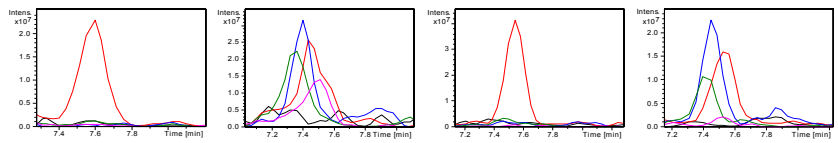

Figure 6.3: Spectra and EICs for mNotch *O*-glycosylation sites. Samples were generated in HEK293T cells co-transfected with plasmids encoding mNotch3 EGF1-34 and either empty vector, LFNG, MFNG, or RFNG. Spectra are representative of data from all four samples and to the left of each spectra it is indicated which sample that spectra came from (-F = EV, +L = LFNG, +M = MFNG, +R = RFNG). Above spectra the EGF repeat and peptide sequence is indicated. Sites predicted to be modified with glucose are highlighted in blue and fucose modification sites are highlighted in red. Tables (next to each spectra) show the m/z used for the EIC searches for glycoforms of the peptide and EICs represent relative amounts of each glycoform. EICs represent empty vector, LFNG, MFNG, and RFNG samples from left to right. Key: black bar, peptide; red triangle, fucose; empty red triangle, fucose analog; blue square, GlcNAc; yellow circle, galactose; purple diamond, sialic acid; blue circle, glucose; yellow star, xylose.

EGF	Sequence	[M+H]$^+$	Deglyco product	Predicted mass	*O*-glycoform
4	^{144}ACAACPPGYQGQSCQSDIDECRSGTT CRHGGTCLNTPGSF^{182}	4676.2	4368.6	4368.7	G + Fuc
8	^{326}HGATCHDRVASF^{337}	1504.6	1358.5	1358.5	Fuc
11	^{425}TGPRCETDVNECLSGPCRNQATCLD RIGQF^{454}	4087.0	3514.2	3513.9	GXX + Fuc
13	^{508}DVDECASTPCRNGAKCVDQPDGYEC RCADGF^{538}	4067.0	3641.8	3641.9	GXX
16	^{195}LCRCPPGTTGVNCEVNIDDCASNPC TF^{221}	3542.8	3116.0	3116.5	GXX
19	^{735}APDACESQPCQAGGTCTSDGIGFRCT CAPGF^{765}	3908.6	3335.0	3337.6	GXX + Fuc
21	^{808}CQQDVDECAGASPCGPHGTCTNLPG NFR^{835}	3254.2	3107.5	3107.3	Fuc
23	^{881}AGPRCARDVDECLSSPCGPGTCTDH VASF^{909}	3753.8	3181.4	3181.5	GXX + Fuc
28	^{1071}CVCPEGRTGSHCEHEVDPCTAQPC QHGGTCRGY^{110}	4211.8	3861.5	3862.1	GlcNAc + Fuc
29	^{1111}CPAGYAGDSCEDNIDECASQPCQNG GSCIDL^{1141}	3996.6	3423.0	3422.9	GXX + Fuc
34	^{1321}SGPSCRVSRASPSGATNASCASAPC LHGGSCLPVQSVPFF^{1360}	4695.8	4123.6	4123.8	GXX + Fuc

Table 6.1: Peptides from the MS analysis of mNotch3. Calculated and observed masses of the glycopeptides in Figure 6.3. All peptides were generated from chymotryptic digests except EGF21, which was generated from a tryptic digest. Glycoform of the peptide in the 1$^+$ charge state ([M+H]$^+$) is indicated (Fuc, Fucose; G, Glucose; X, Xylose; GlcNAc, *N*-acetylglucosamine). Predicted fucose (red), glucose (blue) and GlcNAc (green) modification sites are indicated on peptide sequences.

Chapter 7: ADAMTS17 requires *O*-fucosylation of TSRs for its secretion

7.1 Introduction

Extracellular proteases perform many important functions throughout the formation, remodeling and destruction of the extracellular matrix. The 19 members of the A Disintegrin And Metalloproteinase with ThromboSpondin motifs (ADAMTS) family remodel matrix and play important roles in many physiological and pathological processes (349). These proteins are all secreted zinc metalloproteinases with thrombospondin type-1 repeats (TSR), many of which have consensus sequences ($C^{1-2}XX(S/T)C^{2-3}$) for *O*-fucose modification by POFUT2 (see Table 1.2). These *O*-fucose residues can be elongated with glucose by B3GLCT. Many of these proteins require these carbohydrate modifications for efficient secretion into the extracellular space (143, 147, 149).

ADAMTS17 is an orphan member of the ADAMTS family and has no known substrates or biological functions. Mutations in *ADAMTS17*, however, do have well-established significance in human disease and can cause Weill-Marchesani-like syndrome. Individuals with this disorder have short stature, ectopia lentis, myopia, and glaucoma (250, 350). They do not, however, have the joint stiffness, brachydactyly or cardiac valve disease typically associated with Weill-Marchesani Syndrome (WMS) (351, 352). ADAMTS17 has also been linked with primary open angle glaucoma (353) and abnormal height (354, 355).

The ADAMTS17 protein has five TSRs, four of which contain a consensus sequence for *O*-fucose modification (Fig. 7.1a). Here, I show that three of these TSRs are efficiently modified with *O*-fucose and elongated with glucose. Additionally, I show that these modifications are required for efficient secretion of ADAMTS17.

7.2 ADAMTS17 O-fucose site mapping

In order to map *O*-fucose sites on ADAMTS17, I purified recombinant ADAMTS17 fragments, 1C and 25P (Fig. 7.1a), from the media of transiently transfected HEK293T cells. Purified fragments were reduced and alkylated, digested with proteases, and analyzed by LC-MS/MS. ADAMTS17 contains four predicted *O*-fucose modification sites, three of which (TSRs 1, 3 and 5) were efficiently modified with the *O*-fucose-glucose disaccharide. TSR4 was almost entirely unmodified (Fig. 7.1c, Fig. 7.3, Table 7.1).

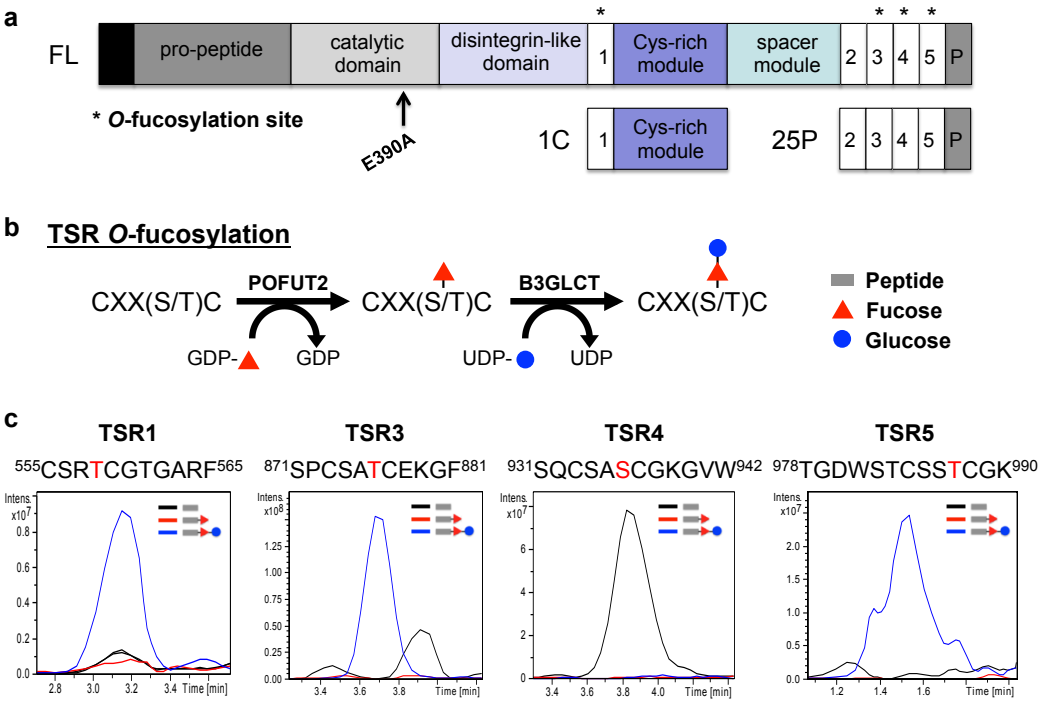

Figure 7.1: ADAMTS17 is *O*-fucosylated by POFUT2. (a) Constructs used for secretion assays and LC-MS/MS. *O*-Fucosylation sites are indicated by asterisks. (b) Schematic of TSR *O*-fucosylation with enzymes and substrates. (c) Extracted ion chromatograms (EICs) of the ions corresponding to unmodified (black), *O*-fucose (red), and *O*-fucose-glucose (blue) glycoforms of peptides as identified by nano-LC-MS/MS. The peptide from each TSR (as indicated) that was used for generation of EICs is shown above each chromatogram. Modified residues are indicated in red. Spectra for these glycopeptides, and the masses used to generate the EICs, are shown in Figure 7.3.

7.3 O-Fucosylation is required for ADAMTS17 secretion

In order to evaluate the importance of *O*-glycosylation for ADAMTS17 secretion, we utilized POFUT2 and B3GLCT CRISPR-Cas9 knockout HEK293T cells, eliminating *O*-fucosylation of TSRs or elongation with glucose, respectively. The 1C and 25P ADAMTS17 fragments and full length ADAMTS17 bearing an E390A mutation (ADAMTS17^{EA}) (Fig. 7.1a) were used to evaluate secretion of ADAMTS17 proteins with variable numbers of modified TSRs. ADAMTS17^{EA} was used instead of WT ADAMTS17 in order to eliminate its auto-catalytic activity, which allows for easier detection of protein in the media (269). IgG was used as a secretion control because it does not contain any TSRs.

Analysis of lysates from transfectants demonstrated minimal effect of POFUT1 or B3GLCT knock outs on production of ADAMTS17 protein in HEK293T cells (Fig. 7.2a). However, levels of ADAMTS17 secreted into the media were reduced in knock out cell lines (Fig. 7.2b). Quantification of Western blot bands confirmed that the B3GLCT and POFUT2 knockouts had no significant effect on protein levels in cell lysates (Fig. 7.2c). However, in the B3GLCT knockout secretion of 1C was not affected, but secretion of 25P and ADAMTS17^{EA} were each significantly reduced, correlating with the presence of 1, 2 or 3 *O*-fucosylation sites, respectively (Fig. 7.2d). In the absence of POFUT2, secretion of 1C into the medium was significantly reduced and secretion of 25P and ADAMTS17^{EA} were nearly eliminated (Fig. 7.2d). These results demonstrate that ADAMTS17 is extensively modified with *O*-fucose-glucose disaccharide and that these modifications play an important role in the regulation of ADAMTS17 secretion.

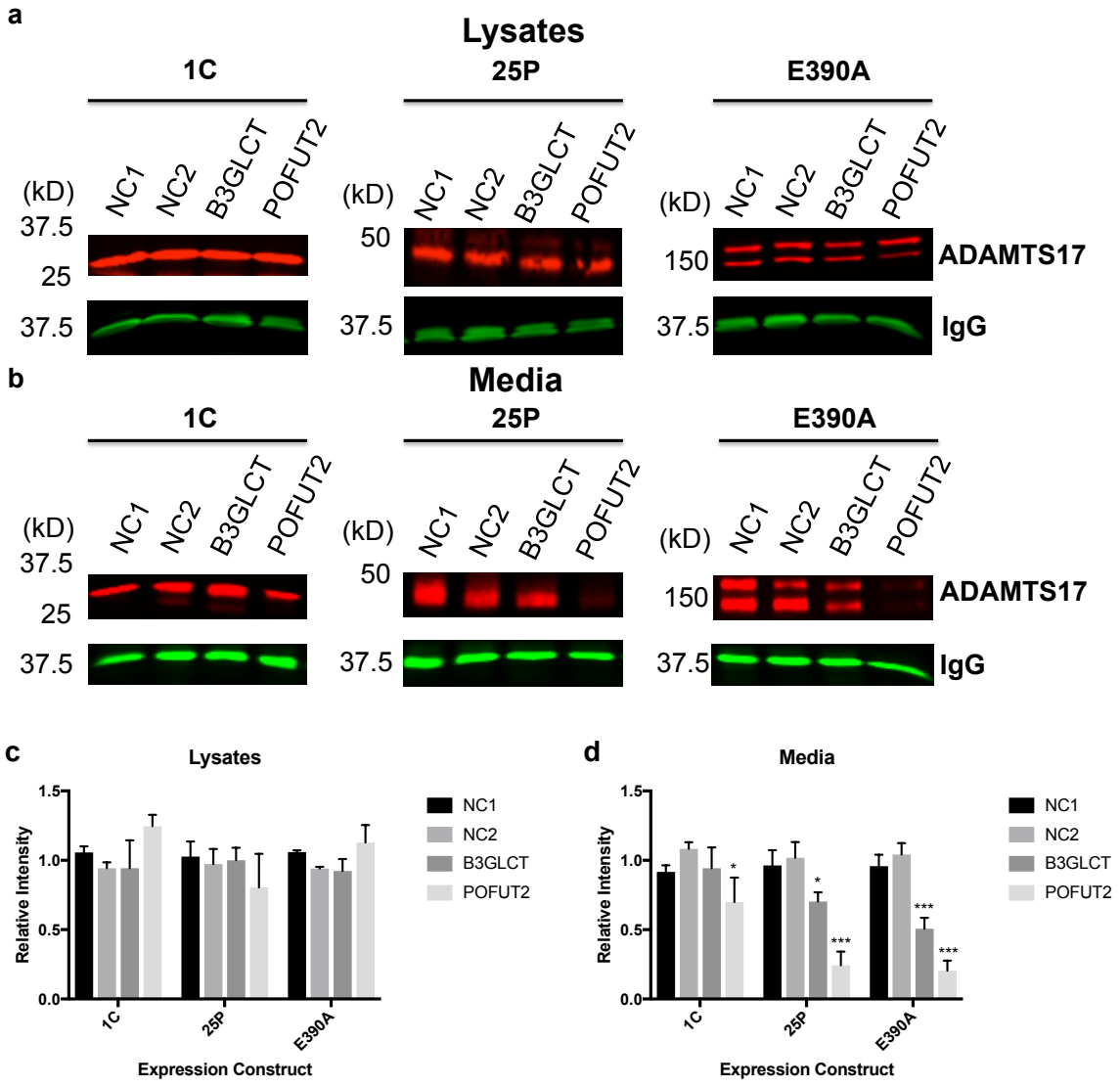

Figure 7.2: *O*-Fucosylation of TSRs on ADAMTS17 is required for its efficient secretion. (a-b) Representative images from Western blot analysis of (a) lysates and (b) media from negative control (NC1 and NC2) HEK293T cells or B3GLCT or POFUT2-null HEK293T cells that were transiently transfected with ADAMTS17-1C (1C), ADAMTS17-25P (25P) and ADAMTS17^{EA} (E390A). Co-transfected IgG (green) was used as a secretion control for quantification because it does not contain TSRs. (c-d) Quantification of the integrated densities of the respective bands normalized to IgG (n=3) for (c) lysates and (d) media samples. Statistical significance was calculated using a two-sided Student t-test and compared to the band intensity measured after secretion from the average of NC1 and NC2 cells. *p<.05, **p<.01, ***p<.001

7.4 Discussion

O-Fucosylation is an unusual modification found on TSR-containing proteins, including the ADAMTS family members, all of which contain the consensus sequence for this modification in one or more TSRs (119). Here, I show that ADAMTS17 is in fact modified by POFUT2 and elongated by B3GLCT at three sites. Additionally, I demonstrate that knock out of either of these glycosyltransferases results in impaired secretion of this protein.

My mass spectrometry data shows that three of four TSRs containing a consensus sequence for POFUT2 modification are efficiently modified with disaccharide. It is of note that the three sites that are efficiently modified by POFUT2 are all modified with fucose at threonine residues. The TSR that is not modified contains a serine at this position. This supports previous work suggesting that threonine is the preferred substrate for POFUT2 relative to serine (114).

These results support the idea that *O*-fucosylation serves as a quality control mechanism allowing only for the secretion of proteins with properly folded TSRs (147). It has previously been shown that other members of the ADAMTS family, including ADAMTS9, ADAMTS13, ADAMTSL1, and ADAMTSL2 (143, 147, 149, 150), are subject to similar regulation. Here, I additionally demonstrate that ADAMTS17 is not only subject to this type of regulation, but protein fragments with a greater number of *O*-fucosylation sites appear to be more affected by elimination of POFUT2 and B3GLCT.

Interestingly, in Peters Plus Syndrome, a disorder caused by mutations in B3GLCT, patients exhibit ocular anterior segment dysgenesis, short stature and brachydactyly (151). These are all features that are also associated with mutations in ADAMTS17 (250, 350).

Our data suggests that elimination of B3GLCT causes reduced secretion of ADAMTS17, which might be partially responsible for these Peters Plus Syndrome phenotypes.

Figure 7.3

TSR 1

^{555}CSRTCGTGARF^{565}

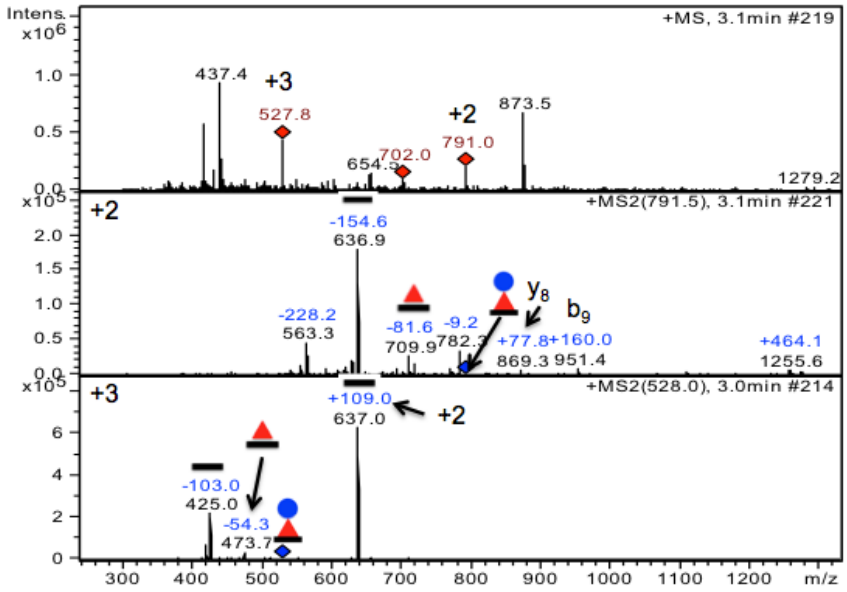

—	425.0, 636.9
▲	473.7, 709.9
● ▲	528.0, 791.5

TSR 3

^{871}SPCSATCEKGF^{881}

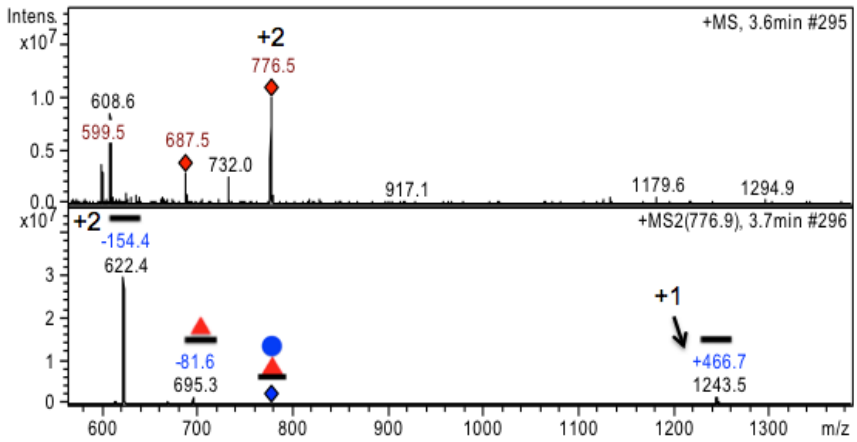

—	622.4
▲	695.3
● ▲	776.5

TSR 4

^{931}SQCSASCGKGVW^{942}

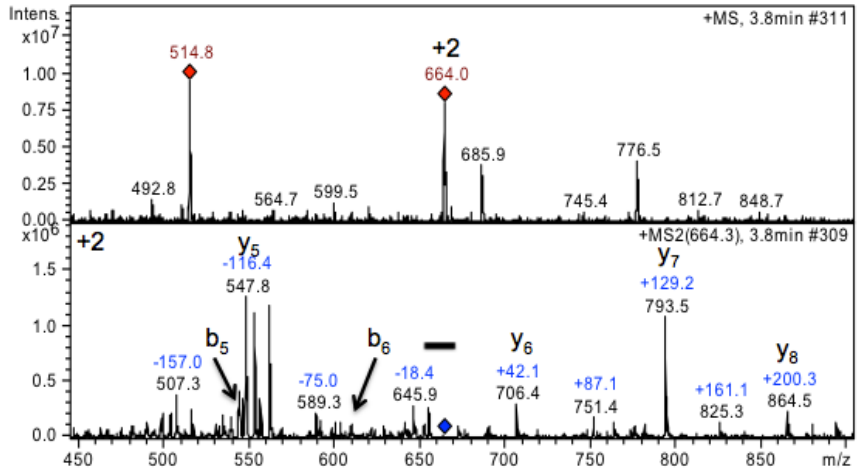

—	664.0
▲	737.0
●▲	818.0

TSR 5

^{978}TGDWSTCSSTCGK^{990}

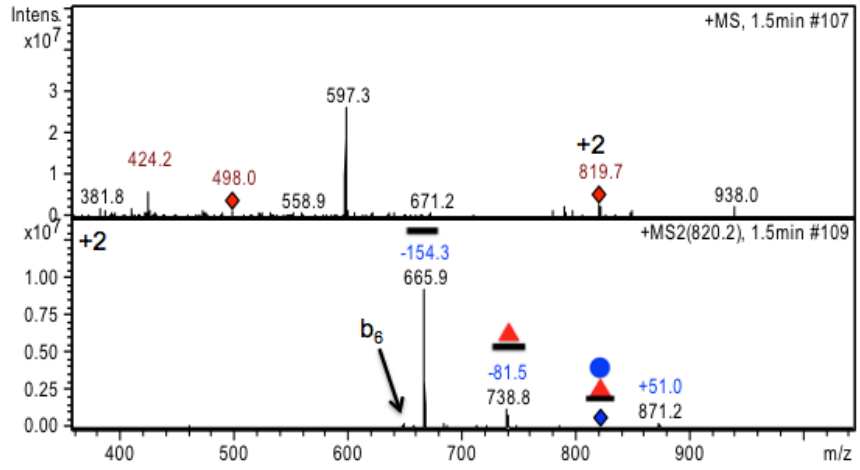

—	665.9
▲	738.8
●▲	820.2

Figure 7.3: Mass spectra of *O*-glycosylation on ADAMTS17. ADAMTS17 fragments were purified from HEK293T cells and prepared for mass spectrometry. Peptides corresponding to TSRs with fucose modification sites were identified and are indicated above each spectrum. The top panel for each peptide shows the MS spectra at a specific retention time. Red diamonds indicate ions chosen for fragmentation. Bottom panels represent the MS2 spectra corresponding to the appropriate parent ion. Blue diamonds in the MS2 spectra indicate the position of the parent ion. Peaks representing different glycoforms of each peptide and predicted b and y ions are indicated. Tables to the right of the spectra show ions searched in the EICs in Fig. 7.1c. Red triangles represent fucose (dHexose). Blue circles are glucose (Hexose).

TSR	Sequence	Charge (n)	$[M+nH]^{n+}$	$[M+nH-Hex]^{n+}$	$[M+nH-dHex-Hex]^{n+}$	Calculated mass
1	^{555}CSRTCGTGARF^{565}	2	791.5	709.9	636.9	636.8
1	^{555}CSRTCGTGARF^{565}	3	528.0	473.7	425.0	424.9
3	^{871}SPCSATCEKGF^{881}	2	776.9	695.3	622.4	622.3
4	^{931}SQCSASCGKGVW^{942}	2	--	--	664.3	663.8
5	^{978}TGDWSTCSSTCGK^{990}	2	820.2	738.8	665.9	666.3

Table 7.1: Peptides from the MS analysis of ADAMTS17: Calculated and observed masses of the glycopeptides in Figures 7.1 and 7.3. All peptides were generated from chymotryptic digests except TSR5, which was generated from a tryptic digest. Three forms of each peptide were detected: fully modified with fucose and glucose ($[M+nH]^{n+}$), the monosaccharide form modified only with fucose ($[M+nH-Hex]^{n+}$) and unmodified form ($[M+nH-dHex-Hex]^{n+}$). Average mass of the peptide was used for theoretical calculations. Note that for TSR 1 two different charge states of the same peptide were observed.

Chapter 8: Characterization of two novel Notch modifying protein *O*-glucosyltransferases: POGLUT2 and POGLUT3

8.1 Introduction

EGF repeats can be modified with several *O*-linked carbohydrate modifications. *O*-Fucose modifications have been the major focus of this dissertation to this point and are discussed in detail in previous chapters. However, EGF repeats can also be modified with *O*-GlcNAc (298) and *O*-glucose (356) (Fig. 8.1a). EGF Domain Specific *O*-linked *N*-Acetylglucosamine Transferase (EOGT) is responsible for the addition of *O*-GlcNAc modifications between the fifth and sixth cysteines of EGF repeats (357). These modifications appear to be important for normal Notch signaling (358) and mutations in EOGT have been associated with Adams-Oliver syndrome, a rare congenital disorder in humans causing scalp and terminal limb defects (359, 360). The enzyme Protein *O*-Glucosyltransferase 1 (POGLUT1) modifies EGF-repeats with *O*-glucose between the first and second cysteines (356). It is also required for normal Notch signaling (356) and its knockout in mice results in embryonic lethality with strong Notch phenotypes including somitogenesis and cardiogenesis defects (361).

In addition to these well-studied modifications, mass spectrometry data from another group suggested that EGF repeat 11 on Notch1 can be modified with an additional *O*-linked hexose between its third and fourth cysteines (312). Significantly, this is a distinct location from *O*-glucose modification added by POGLUT1 (Fig. 8.1a). A recent co-crystal structure of Notch1 and Delta-like ligand 4 (DLL4) also identified this *O*-linked hexose residue. Further, the crystal structure suggested that this sugar is located at the Notch1-DLL4 binding site and participates directly in the binding interaction between Notch1 and DLL4 (Fig. 8.1b) (126).

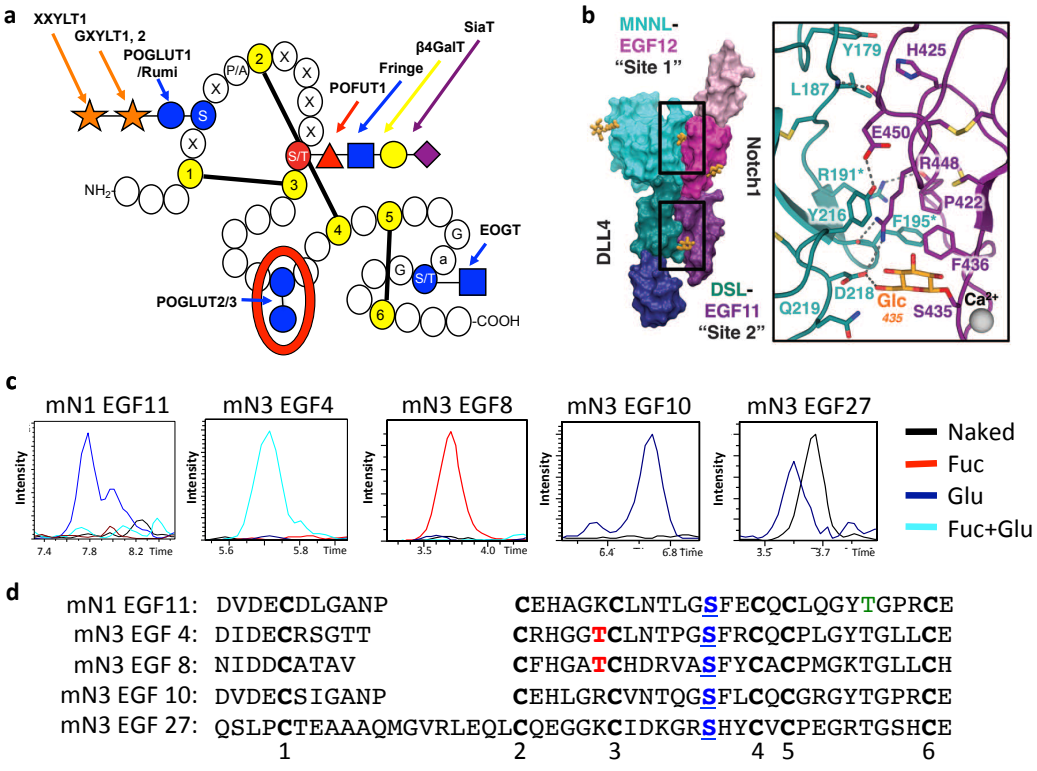

Figure 8.1: EGF repeats can be modified with a hexose between their third and fourth cysteines. (a) Cartoon showing *O*-linked carbohydrate modifications on EGF repeats and the enzymes responsible for their transfer. The novel *O*-glucose modification is highlighted by a red oval (331). (b) Co-crystal structure showing this novel *O*-glucose modification at the binding site between Notch1 and DLL4 (126). (c) Extracted ion chromatograms (EICs) showing EGF repeats with potential novel *O*-glucose sites. See Figure 8.6 for spectra, peptide information and m/z ratios used to generate EICs. (d) Sequences of EGF repeats shown in Figures 8.1c. Conserved cysteines are bolded. *O*-Fucose modification sites are highlighted in red and novel *O*-glucose modification sites highlighted in blue. Dr. Hideyuki Takeuchi generated EIC for mNotch1 (mN1) EGF11.

The finding of a novel *O*-linked hexose on an EGF repeat suggested that a novel enzyme must be responsible for its addition. CAP10-domain (a fungal glycosyltransferase domain) containing proteins, KDELC1 and KDELC2, show homology with POGLUT1 (Fig. 8.2a), but cannot modify EGF repeats at POGLUT1 consensus sequences or rescue POGLUT1 knockout (362). These enzymes have endoplasmic reticulum (ER) localization sequences (KDEL) and are presumably localized to the ER. KDELC1 has recently been

implicated to play a role in hepatic dysfunction (363), but the function of these enzymes remains poorly understood.

Here, we confirm the presence of an *O*-glucose residue between the third and fourth cysteines of EGF 11 on mouse Notch1 (mNotch1). Additionally, we identify other similar glucose modification sites on mNotch1 and mNotch3 EGF repeats. We demonstrate that KDELC1 and KDELC2 are protein *O*-glucosyltransferases that transfer glucose to these sites. Finally, we show that these modifications play an important role in regulating Notch cell surface expression and signaling.

8.2 POGLUT2 and POGLUT3 modify novel O-glucose sites on EGF repeats

Using nano-LC-MS/MS we identified an unusual hexose residue on peptides from EGF11 on mNotch1 and EGFs 4, 10 and 27 on mNotch3 (Fig. 8.1c). This modification at EGF 11 has been previously described (126, 312), but to our knowledge this modification has not been identified on other EGF repeats. Interestingly, we did not see any modification on EGF8 of mNotch3 (Fig. 8.1c), which contains a similar sequences between its third and fourth cysteines (Fig. 8.1c-d). Further work will be needed to determine a true consensus sequence for this modification.

Due to their homology with POGLUT1 (Fig. 8.2a), we next assessed whether KDELC1 or KDELC2 were able to modify a peptide from mNotch1 EGFs 11-13 containing this site. Since neither the mass spectral data (Fig. 8.1c) nor the electron density in the crystal structure (126) could distinguish between hexoses, we used both UDP-glucose and UDP-galactose as donor substrates. We incubated a fragment of mNotch1 with each of the UDP-hexoses and either POGLUT1, KDELC1 or KDELC2. The products were digested with

trypsin and analyzed by nano-LC-MS/MS (Fig. 8.2b). Results demonstrated that both KDELC1 and KDELC2 were able to transfer an *O*-glucose onto the peptide from EGF11, but POGLUT1 could not. *O*-Galactose was not transferred by any of the three enzymes (Fig. 8.2b). Thus KDELC1 and KDELC2 are protein *O*-glucosyltransferases and will be referred to as POGLUT2 and POGLUT3, respectively.

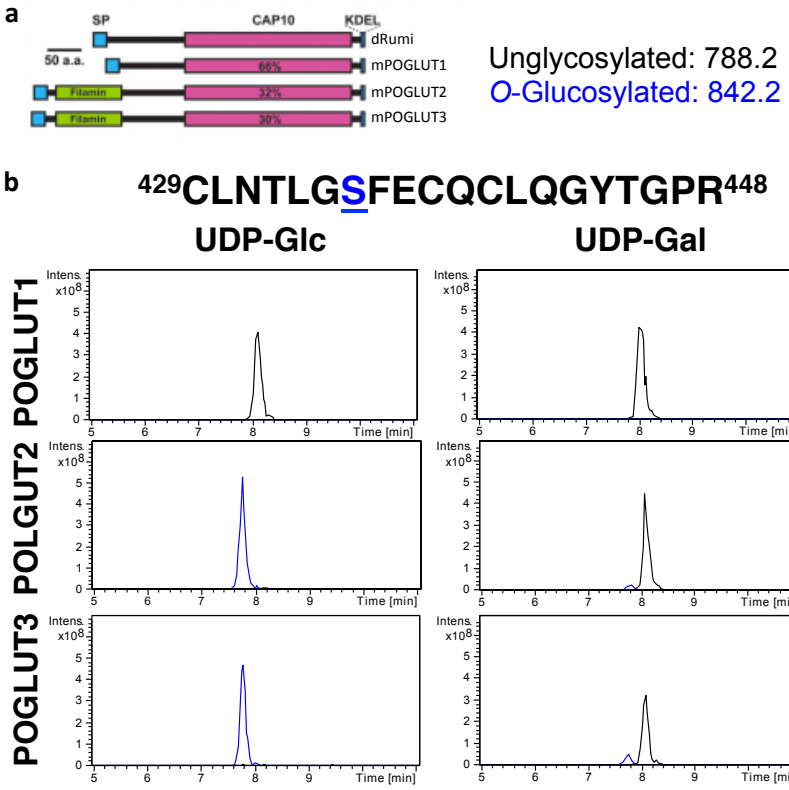

Figure 8.2: KDELC1 and KDELC2 modify a novel *O*-glucose site on mNotch1 EGF11 (a) Structures of mouse CAP10 containing proteins and their homology to *Drosophila* Rumi (dRumi) (361). (b) EGF repeats 11-13 from mNotch1 was incubated with POGLUT1, KDELC1, or KDELC2 and either UDP-glucose (UDP-Glc) or UDP-galactose (UDP-Gal). Products were reduced/alkylated, digested with trypsin, and analyzed by nano-LC-MS/MS. EICs of modified (blue lines) or unmodified (black lines) peptide from EGF11 (shown above) are shown. Masses used to generate EICs are indicated. Data presented in this figure was generated by Dr. Hideyuki Takeuchi.

8.3 Elimination of the novel O-glucose modification site causes decreased cell surface expression of Notch and reduced Notch signaling

We next set out to determine whether these glucose residues play a role in regulating Notch signaling. In order to do this, we eliminated the serine residue on mNotch1 EGF11 that is modified with *O*-glucose (S435A) using site directed mutagenesis. We chose this site because it was modified at high stoichiometry based on our mass spectrometry data (Fig. 8.1c) and is located at the binding site between Notch1 and Delta-like ligands (Fig. 8.1b) (126). We then examined cell surface expression and ligand binding ability of this mutant compared to a WT control (Fig. 8.3). Neither cell surface expression nor ligand binding by DLL1 or Jagged1 (JAG1) was affected by this mutation alone (Fig. 8.3).

In order to further probe this question, we generated mNotch1 double mutants, bearing both the S435A mutation and mutations at *O*-fucose modification sites on either EGF8 or EGF12. *O*-Fucose residues at these sites play important roles in regulating Notch-ligand binding and Notch signaling (125, 126). We hypothesized that *O*-glucose residues might serve a redundant function with *O*-fucose at these sites and that we might see a more dramatic reduction in Notch ligand binding and signaling in the double mutants compared with the *O*-fucose site single mutants. Our data showed that the S435A/EGF8 double mutant bound both DLL1 and JAG1 ligands significantly less efficiently than the EGF8 single mutant. Binding levels for both DLL1 and JAG1 in the S435A/EGF12 double mutant, however, did not differ significantly from the EGF12 single mutant (Fig. 8.3a-b). Interestingly, cell surface expression of the S435A/EGF8 double mutant was dramatically reduced relative to the EGF8 single mutant, suggesting that reduced cell surface expression

of Notch receptors is at least partially responsible for the reduction in ligand binding seen in this mutant. Cell surface expression of other mutants was relatively unaffected (Fig. 8.3c-d).

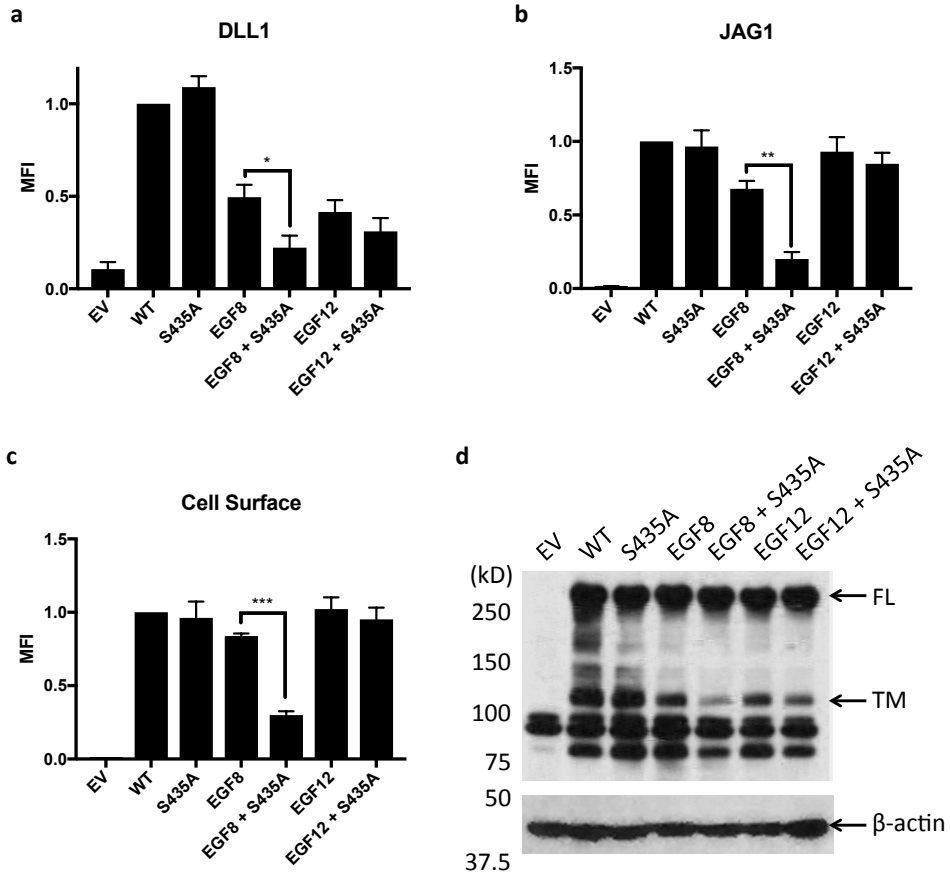

Figure 8.3: *O*-Glucose on mNotch1 EGF11 is involved in regulation of Notch ligand binding and cell surface expression. (a) Cell based ligand-binding assays with Delta-like ligand 1 (DLL1) and mNotch1 mutants. (b) Cell based ligand-binding assays with Jagged1 (JAG1) and mNotch1 mutants. (c) Cell surface expression levels of mNotch1 based on cell surface antibody staining. (d) Western blot showing expression levels of full length (FL) and transmembrane (TM) mNotch1 in mutants. The S435A/EGF8 mutant has markedly lower levels of TM protein. One-way ANOVAs with Tukey's post hoc analysis were used to assess statistical significance, *p<.05, **p<.01, ***p<.001.

Cell-based co-culture assays showed similar results. The S435A mutation did not significantly affect either DLL1 or JAG1 induced Notch signaling on its own (Fig. 8.4a-b). The S435A/EGF8 double mutant showed significantly reduced DLL1-mediated signaling

compared to the EGF8 single mutant. Interestingly, DLL1 mediating signaling in the S435A/EGF12 double mutant was significantly reduced relative to the EGF12 single mutant (Fig. 8.4a). There were no significant differences in JAG1 mediated signaling between the double mutants and single mutant controls.

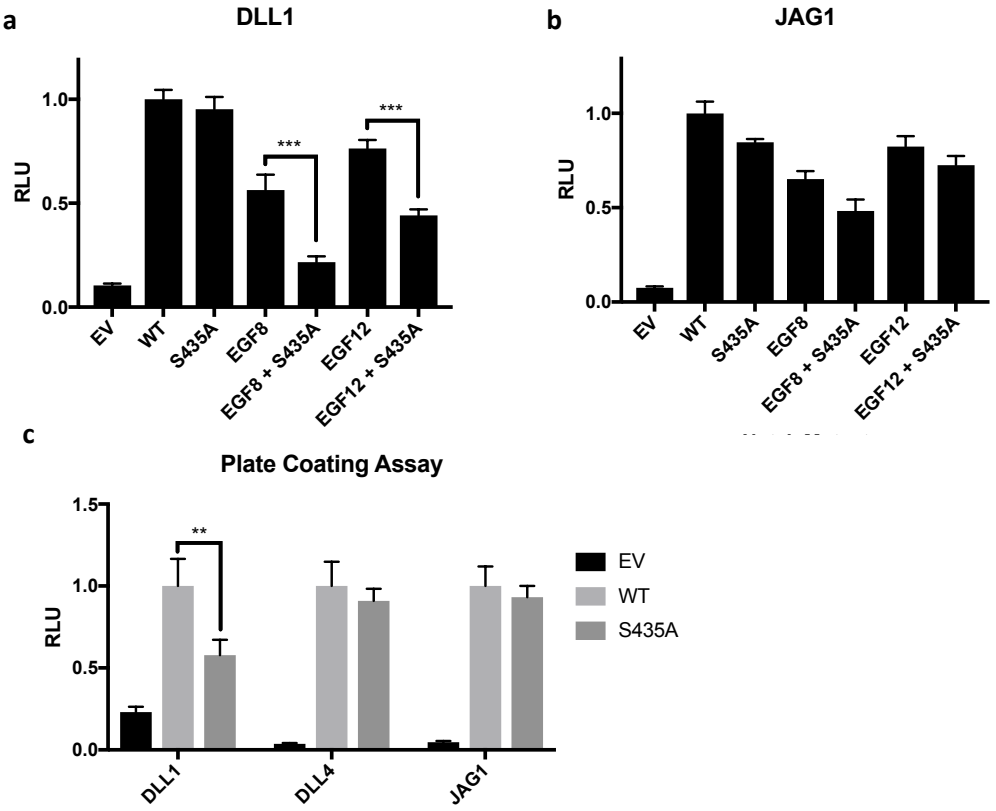

Figure 8.4: *O*-Glucose on mNotch1 EGF11 is important for Notch signaling. (a) Cell based signaling assays with Delta-like ligand 1 (DLL1) and mNotch1 mutants. (b) Cell based signaling assays with Jagged1 (JAG1) and mNotch1 mutants. (c) Plate coating assays for DLL1, DLL4, and JAG1 mediated signaling with Notch mutants at low concentrations of ligand. ANOVAs with Tukey's post hoc analysis were used to assess statistical significance, *p<.05, **p<.01, ***p<.001.

However, we did see a trend towards decreased activity in both of the double mutants compared with their respective controls (Fig. 8.4b). We also used a plate-coating assay with low concentrations of ligand to evaluate the effect of the S435A mutation under weaker signaling conditions. Interestingly, under these conditions the S435A mutation

caused a decrease in DLL1 mediated Notch signaling (Fig. 8.4c). DLL4 and JAG1 mediated signaling were not significantly affected by the S435A mutation (Fig. 8.4c). We confirmed expression of POGLUT2 and POGLUT3 in cell lines used for these analyses to reduce the likelihood that the binding and signaling defects seen in the mutants were unrelated to enzymatic modification of EGF repeats (Fig. 8.5).

a

	Primer		
	GAPDH	POGLUT2	POGLUT3
293T	16.08333	24.55	22.31
3T3	15.76666	23.79333	22.62

b

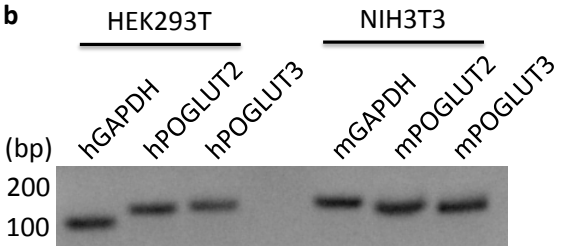

Figure 8.5: POGLUT2 and POGLUT3 are expressed in HEK293T cells and NIH3T3 cells. (a) Total mRNA was isolated from HEK293T and NIH3T3 cells. Random primers were used to generate cDNA. Primers specific for POGLUT2 or POGLUT3 were used in a RT-qPCR reaction to estimate mRNA levels of each of these genes. Table indicates average cycle number at which samples crossed a threshold level of amplified cDNA. (b) DNA gel showing bands amplified from qPCR reaction demonstrating that primers were specific for the intended genes.

8.4 Discussion

O-Glycosylation of EGF repeats plays an extremely important role in the regulation of protein behavior. The data shown here confirms the presence of a novel *O*-glucosylation site on Notch EGF repeats. We identify several EGF repeats on mNotch1 and mNotch3 that are substrates for this modification. Further, we show that the enzymes responsible for these modifications are POGLUT2 and POGLUT3 (formerly KDCLC1 and KDELC2). Finally, our data indicates that modification of this site on mNotch1 EGF11 plays an important role in regulating Notch behavior.

Previous work has suggested the presence of a hexose residue on S^{435} of mNotch1 EGF11 (126, 312). We confirmed the presence of this residue using mass spectrometry and

identified several other similar sites on other Notch EGF repeats. Further, we demonstrated that UDP-glucose, not UDP-galactose, is the substrate added to these EGF repeats. We also identified an EGF repeat that appears to have a similar sites between its third and fourth cysteines, but was not modified. However, we did not identify any characteristic features of modified sites that were not seen on this unmodified site. Further work examining more EGF repeats on Notch and other proteins will be important in determining a consensus sequence for this modification.

We also identify the enzymes responsible for catalyzing this reaction. POGLUT2 and POGLUT3 were previously orphan enzymes without a known function. Based on their homology with POGLUT1, we were able to identify them as candidate *O*-glucosyltransferases that might be responsible for this unusual glucose modification (361). Further work will be needed in order to characterize differences between these two enzymes and examine their specificities for different EGF repeats. While they both modified EGF11 of mNotch1, this may not be true for other modification sites.

Finally, we demonstrate that these enzymes play an important role in regulating Notch activity. While elimination of EGF11 alone had only a minimal effect on Notch behavior, this modification appeared to have a redundant function with *O*-fucose residues at EGFs 8 and 12. Interestingly, it appeared to be especially important in promoting cell surface expression and Notch signaling in the absence of fucose on EGF8. This suggests a role for these carbohydrate modifications in protein folding and/or transport through the ER and Golgi apparatus.

We also identified an important effect on Notch signaling and binding in the absence of these same *O*-fucose residues. While much of this effect, especially for the S435A/EGF8

double mutant, was likely caused by decreased cell surface expression, there did appear to be an additional decrease in DLL1 mediated signaling in the S435A/EGF12 double mutant. Both the *O*-fucose on EGF12 and this novel *O*-glucose on EGF11 of mNotch1 are located at the binding site between Delta-like ligands and the Notch1 receptor (126) and this data suggest that they both contribute to enhancing ligand-receptor binding affinity. This data was supported by the plate coating assay data, which also suggested that under weaker signaling conditions the S435A mutation disrupted DLL1 mediated Notch signaling. Together, this data suggests that in weaker signaling conditions (i.e. the absence of *O*-fucose on EGF12 or low concentrations of ligand), the glucose on EGF11 becomes important for promoting Notch-DLL binding and signaling.

mNotch1 EGF11

^{429}CLNTLG**S**FECQCLQGYTGPR^{448}

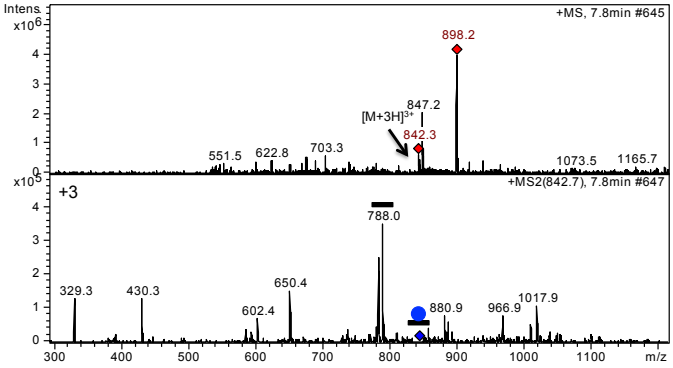

▬	788.7
●	842.7

mNotch3 EGF4

^{144}ACACPPGYQGQSCQSDIDECRSGTTCRHGG**T**CLNTPG**S**F^{182}

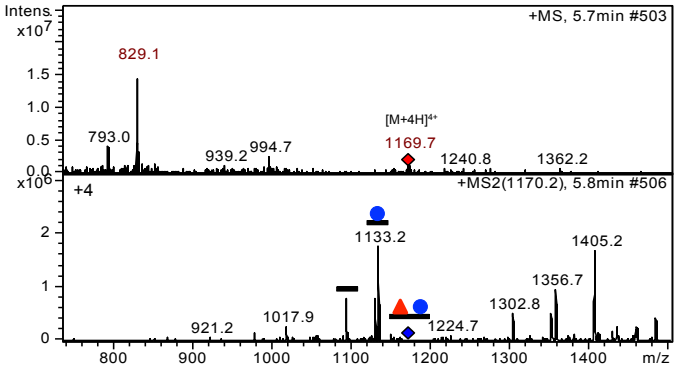

▬	1092.9
▲	1129.4
●	1133.3
●▲	1169.8

mNotch3 EGF8

^{326}HGA**T**CHDRVA**S**F^{337}

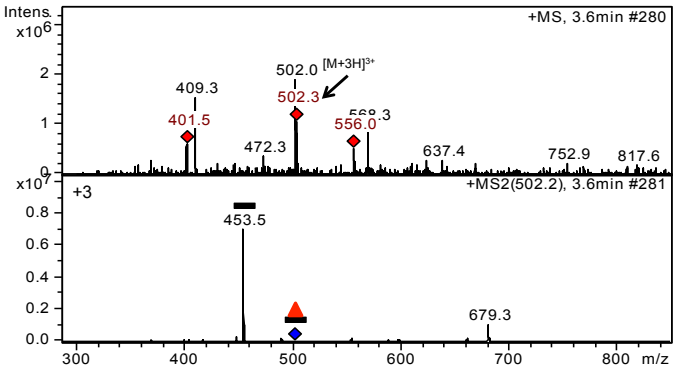

▬	453.5
▲	502.2
●	507.5
●▲	556.2

mNotch3 EGF10

^{409}CVNTQGSFLCQCGR^{422}

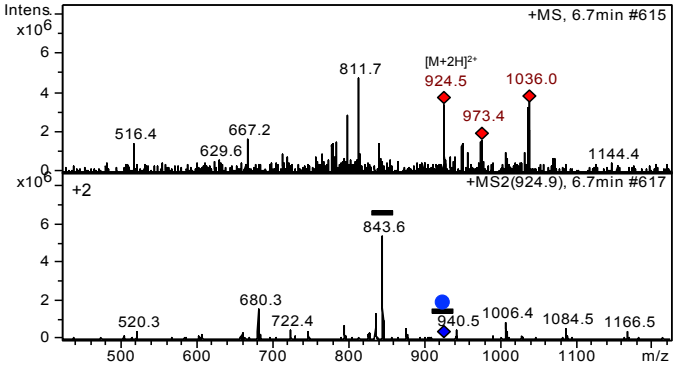

▬	843.6
●	924.5

mNotch3 EGF27

^{1066}GRSHYCVCPEGR^{1077}

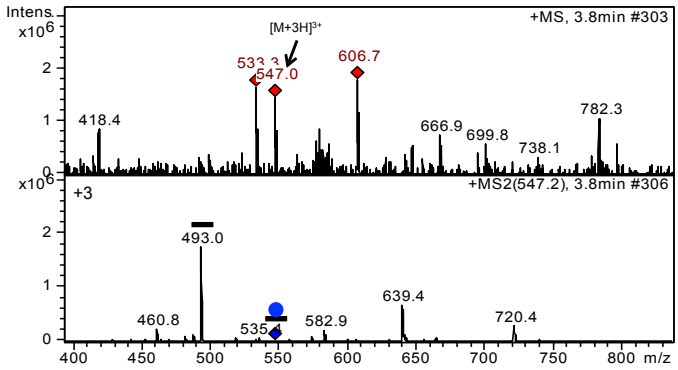

▬	493.0
●	547.1

Figure 8.6: Mass spectra of novel *O*-glucose sites on Notch receptors. A secreted form of the extracellular domain of mNotch1 or mNotch3 was overexpressed in HEK293T cells, purified and prepared for mass spectrometry. Peptides corresponding to EGF repeats with potential novel *O*-glucose modification sites were identified and are indicated above each spectrum with predicted glucose modification sites shown in blue and fucose modification sites shown in red. The top panel for each peptide shows the MS spectra at a specific retention time. Red diamonds indicate ions chosen for fragmentation. Bottom panels represent the MS2 spectra corresponding to the appropriate parent ion. Blue diamonds in the MS2 spectra indicate the position of the parent ion. Peaks representing different glycoforms of each peptide and predicted b and y ions are indicated. Tables to the right of the spectra show ions searched in the EICs in Fig. 8.1c. Red triangles represent fucose (dHexose). Blue circles are glucose (Hexose).

EGF	Sequence	[M+H]$^+$	Deglyco product	Predicted mass	*O*-glycoform
mN1 EGF11	^{429}CLNTLG**S**FECQCLCLQGYTGPR^{182}	2526.1	2364.1	--	Glu
mN3 EGF4	^{144}ACAACPPGYQGQSCQSDIDECRSG TTCRHGG**T**CLNTPG**S**F^{182}	4676.2	4368.6	4368.7	Glu + Fuc
mN3 EGF8	^{326}HGA**T**CHDRVASF^{337}	1504.6	1358.5	1358.5	Fuc
mN3 EGF10	^{409}CVNTQG**S**FLCQCGR^{422}	1848.0	1686.2	1687.0	Glu
mN3 EGF27	^{1066}GR**S**HYCVCPEGR^{1077}	1639.3	1477.0	1478.6	Glu

Table 8.1: Peptides from the MS analysis of potential novel *O*-glucosylation sites: Calculated and observed masses of the glycopeptides in Figures 8.1 and 8.6. Glycoform of the peptide in the 1$^+$ charge state ([M+H]$^+$) is indicated (Fuc, Fucose; Glu, Glucose). Predicted fucose (red) and glucose (blue) modification sites are indicated on peptide sequences.

Chapter 9: Conclusions and future directions

9.1 Conclusions

In this dissertation I have outlined my work studying the roles of *O*-linked glycans in regulating protein behavior. The major focus of this work was to characterize the effects of fucose analogs on Notch signaling. Previous work, from our lab and others, suggested that fucose analogs could be tolerated by POFUT1 and affect protein behavior. Here, I demonstrated that they could be used to specifically inhibit Delta-like ligand mediated Notch signaling. This result is significant because it suggests that altering glycan modifications on Notch receptors can have different effects on different Notch activating ligands. To our knowledge, this is the first small-molecule inhibitor that has different effects on the two families of Notch ligands. These fucose analogs expand the panel of tools available for the inhibition of Notch signaling and provide a unique specificity that allows for an inhibition of Notch activation more broad than with monoclonal antibodies, but more specific than with γ-secretase inhibitors. Here, I additionally showed that they could be used to slow proliferation of glioma cells and inhibit signaling in constitutively active T-ALL mutant Notch receptors, suggesting at least some therapeutic potential. Further, these fucose analogs have the potential to help us better understand mechanisms behind Notch signaling, especially as we examine differences between Delta-like ligand and Jagged ligand mediated signaling.

I also began to characterize the effects of increased or decreased *O*-fucosylation in several systems. This work demonstrates the importance of *O*-fucose in human physiology and pathology. I first described a patient with a POFUT1 mutation causing deficient fucosyltransferase activity. We showed that this mutation eliminated an *N*-glycosylation consensus sequence on POFUT1 and dramatically reduced its enzymatic activity. I showed

that this resulted in reduced Notch signaling, suggesting one potential mechanism for some of this patient's congenital defects. Next, I examined the role of POFUT1 in hepatocellular carcinoma. I was able to generate POFUT1 knockout cell lines and demonstrated that this knockout affected Notch signaling and hepatocellular carcinoma proliferation. Finally, I examined the effect of *O*-fucosylation on ADAMTS17 secretion. Mutations in this metalloproteinase can cause Weill Marchesani-like syndrome in humans. I showed that reduced glycosylation was required for efficient secretion of ADAMTS17, which may explain some phenotypes associated with POFUT2 knockout in mice.

Additionally, I began to map *O*-glycan sites on mouse Notch3 revealing some interesting findings. In my search for carbohydrate modifications on Notch3, I identified a novel *O*-glucose modification on some Notch EGF repeats. This prompted further work to characterize these modifications. Our lab was able to identify the enzymes responsible for catalyzing these *O*-glucose additions. I also began to characterize the effects of these novel glycans on Notch signaling. These results suggest that under weaker signaling conditions these residues become important for promoting Notch cell surface expression and ligand induced signaling.

9.2 Questions requiring further examination

While the work presented here helps to advance our understanding of Notch signaling and *O*-glycosylation, there remain many questions to be answered. Further work will be needed to pinpoint the mechanism behind fucose analog inhibition of Notch signaling. Once this is more precisely understood, we can begin to rationally generate new sugar analogs or other tools that can be used to more precisely target Notch signaling

initiated by specific ligands. We now know that POFUT1 tolerates modifications at the C6 position of fucose, so altering the modifications at this site might affect ligand specificity of Notch receptors containing this fucose analog modifications. Generating analogs at other carbon positions will also be interesting and if utilized by POFUT1, modifications at other positions might also alter ligand specificity or block Fringe elongation. Experiments to examine the effects of fucose analogs *in vivo* will also be useful in determining their off target effects. It is likely that the utility of blocking Notch for inhibition of cancer proliferation will be more pronounced *in vivo* where Notch signaling that is involved in complex systems including angiogenesis, cancer stem cell maintenance, cell-cell interactions, etc. becomes relevant.

More work will also be needed to improve our understanding of the role of *O*-glycans in disease. As we improve our understanding of the role of *O*-fucosyltransferases in regulating protein function as it relates to human disease, this will open up the door to new potential therapies to treat these disorders. As genomic sequencing becomes more readily available, it is likely that we will continue to identify mutations in these types of genes similar to those described here. Understanding the role these enzymes play in regulating protein behavior will be extremely important as we try to better understand and treat these disorders. Hepatocellular carcinoma may be one potential target for a specific POFUT1 inhibitor, but much more work will need to be done to better understand the role this enzyme plays in the disease. Additionally, a better understanding of which proteins are POFUT1 and POFUT2 targets and how they are affected by *O*-fucosylation will be important for interpreting disease symptoms.

Lastly, more work will be needed to fully map and understand the role of *O*-fucose residues on specific EGF repeats, as has been done for Notch1. Work will be needed to complete the glycosylation site mapping of this Notch3 and examine the effects of individual site mutants on Notch-ligand binding and signaling. It will also be extremely important to continue to characterize the role that the novel *O*-glucose that we identified at sites on mouse Notch1 and mouse Notch3 plays in regulating Notch cell surface expression and signaling. Further site mapping will be needed in order to determine a consensus sequence for this unusual *O*-glucose modification. POGLUT2 and POGLUT3 knockout cell lines and potentially knockout mice will be useful in determining the role these enzymes play in regulating Notch signaling and perhaps their role in regulating other proteins.

Chapter 10: References

1. Werz DB, Ranzinger R, Herget S, Adibekian A, von der Lieth C-W, Seeberger PH. Exploring the structural diversity of mammalian carbohydrates ("glycospace") by statistical databank analysis. ACS chemical biology. 2007;2(10):685-91.
2. Stanley P, Schachter H, Taniguchi N. N-glycans2009.
3. Du J, Takeuchi H, Leonhard-Melief C, Shroyer KR, Dlugosz M, Haltiwanger RS, Holdener BC. O-fucosylation of thrombospondin type 1 repeats restricts epithelial to mesenchymal transition (EMT) and maintains epiblast pluripotency during mouse gastrulation. Developmental biology. 2010;346(1):25-38.
4. Shi S, Stanley P. Protein O-fucosyltransferase 1 is an essential component of Notch signaling pathways. Proceedings of the National Academy of Sciences. 2003;100(9):5234-9.
5. Wang X, Inoue S, Gu J, Miyoshi E, Noda K, Li W, Mizuno-Horikawa Y, Nakano M, Asahi M, Takahashi M. Dysregulation of TGF-β1 receptor activation leads to abnormal lung development and emphysema-like phenotype in core fucose-deficient mice. Proceedings of the National Academy of Sciences of the United States of America. 2005;102(44):15791-6.
6. Tonetti M, Sturla L, Bisso A, Benatti U, De Flora A. Synthesis of GDP-L-fucose by the human FX protein. Journal of Biological Chemistry. 1996;271(44):27274-9.
7. Ginsburg V. Formation of guanosine diphosphate L-fucose from guanosine diphosphate D-mannose. Journal of Biological Chemistry. 1960;235(8):2196-201.
8. Yurchenco PD, Atkinson PH. Fucosyl-glycoprotein and precursor pools in HeLa cells. Biochemistry. 1975;14(14):3107-14.
9. Kaufman R, Ginsburg V. The metabolism of L-fucose by HeLa cells. Experimental cell research. 1968;50(1):127-32.
10. Coffey J, Miller ON, Sellinger OZ. The metabolism of L-fucose in the rat. Journal of Biological Chemistry. 1964;239:4011-7.
11. Wiese TJ, Dunlap JA, Yorek MA. L-fucose is accumulated via a specific transport system in eukaryotic cells. Journal of Biological Chemistry. 1994;269(36):22705-11.
12. Ishihara H, Massaro DJ, Heath EC. The Metabolism of l-Fucose III. THE ENZYMATIC SYNTHESIS OF β-l-FUCOSE 1-PHOSPHATE. Journal of Biological Chemistry. 1968;243(6):1103-9.
13. Lühn K, Wild MK, Eckhardt M, Gerardy-Schahn R, Vestweber D. The gene defective in leukocyte adhesion deficiency II encodes a putative GDP-fucose transporter. Nature genetics. 2001;28(1):69-72.
14. Ishikawa HO, Ayukawa T, Nakayama M, Higashi S, Kamiyama S, Nishihara S, Aoki K, Ishida N, Sanai Y, Matsuno K. Two pathways for importing GDP-fucose into the endoplasmic reticulum lumen function redundantly in the O-fucosylation of Notch in Drosophila. Journal of Biological Chemistry. 2010;285(6):4122-9.
15. Ashikov A, Routier F, Fuhlrott J, Helmus Y, Wild M, Gerardy-Schahn R, Bakker H. The human solute carrier gene SLC35B4 encodes a bifunctional nucleotide sugar transporter with specificity for UDP-xylose and UDP-N-acetylglucosamine. Journal of Biological Chemistry. 2005;280(29):27230-5.
16. Lu L, Hou X, Shi S, Körner C, Stanley P. Slc35c2 promotes Notch1 fucosylation and is required for optimal Notch signaling in mammalian cells. Journal of Biological Chemistry. 2010;285(46):36245-54.
17. Becker DJ, Lowe JB. Fucose: biosynthesis and biological function in mammals. Glycobiology. 2003;13(7):41R-53R.
18. Lowe JB. 7 The blood group-specific human glycosyltransferases. Bailliere's clinical haematology. 1993;6(2):465-92.

19. Dipta T, Hossain A. The bombay blood group: are we out of risk? Mymensingh medical journal: MMJ. 2011;20(3):536-40.
20. Kelly RJ, Ernst LK, Larsen RD, Bryant JG, Robinson JS, Lowe JB. Molecular basis for H blood group deficiency in Bombay (Oh) and para-Bombay individuals. Proceedings of the National Academy of Sciences. 1994;91(13):5843-7.
21. Davey R, Tourault M, Holland P. The Clinical Significance of Anti‐H in an Individual with the Oh (Bombay) Phenotype. Transfusion. 1978;18(6):738-42.
22. Wang B, Koda Y, Soejima M, Kimura H. Two Missense Mutations of H Type α (1, 2) Fucosyltransferase Gene (FUT1) Responsible for Para‐Bombay Phenotype. Vox sanguinis. 1997;72(1):31-5.
23. Lin‐Chu M, Broadberry R. Blood transfusion in the para‐Bombay phenotype. British journal of haematology. 1990;75(4):568-72.
24. Levy G, Ginsburg D. Getting at the variable expressivity of von Willebrand disease. Thrombosis and haemostasis. 2001;86(1):144-8.
25. Wolpin BM, Kraft P, Gross M, Helzlsouer K, Bueno-de-Mesquita HB, Steplowski E, Stolzenberg-Solomon RZ, Arslan AA, Jacobs EJ, LaCroix A. Pancreatic cancer risk and ABO blood group alleles: results from the pancreatic cancer cohort consortium. Cancer research. 2010;70(3):1015-23.
26. Edgren G, Hjalgrim H, Rostgaard K, Norda R, Wikman A, Melbye M, Nyrén O. Risk of gastric cancer and peptic ulcers in relation to ABO blood type: a cohort study. American journal of epidemiology. 2010;172(11):1280-5.
27. Slater G, Itzkowitz S, Azar S, Aufses Jr AH. Clinicopathologic correlations of ABO and Rhesus blood type in colorectal cancer. Diseases of the colon & rectum. 1993;36(1):5-7.
28. Hutson AM, Atmar RL, Graham DY, Estes MK. Norwalk virus infection and disease is associated with ABO histo-blood group type. Journal of Infectious Diseases. 2002;185(9):1335-7.
29. Ilver D, Arnqvist A, Ögren J, Frick I-M, Kersulyte D, Incecik ET, Berg DE, Covacci A, Engstrand L, Borén T. Helicobacter pylori adhesin binding fucosylated histo-blood group antigens revealed by retagging. Science. 1998;279(5349):373-7.
30. Huang P, Farkas T, Zhong W, Tan M, Thornton S, Morrow AL, Jiang X. Norovirus and histo-blood group antigens: demonstration of a wide spectrum of strain specificities and classification of two major binding groups among multiple binding patterns. Journal of virology. 2005;79(11):6714-22.
31. Wands AM, Fujita A, McCombs JE, Cervin J, Dedic B, Rodriguez AC, Nischan N, Bond MR, Mettlen M, Trudgian DC. Fucosylation and protein glycosylation create functional receptors for cholera toxin. Elife. 2015;4:e09545.
32. Xu J, Bjursell MK, Himrod J, Deng S, Carmichael LK, Chiang HC, Hooper LV, Gordon JI. A genomic view of the human-Bacteroides thetaiotaomicron symbiosis. Science. 2003;299(5615):2074-6.
33. Pacheco AR, Curtis MM, Ritchie JM, Munera D, Waldor MK, Moreira CG, Sperandio V. Fucose sensing regulates bacterial intestinal colonization. Nature. 2012;492(7427):113-7.
34. Kashyap PC, Marcobal A, Ursell LK, Smits SA, Sonnenburg ED, Costello EK, Higginbottom SK, Domino SE, Holmes SP, Relman DA. Genetically dictated change in host mucus carbohydrate landscape exerts a diet-dependent effect on the gut microbiota. Proceedings of the National Academy of Sciences. 2013;110(42):17059-64.
35. Pickard JM, Maurice CF, Kinnebrew MA, Abt MC, Schenten D, Golovkina TV, Bogatyrev SR, Ismagilov RF, Pamer EG, Turnbaugh PJ. Rapid fucosylation of intestinal epithelium sustains host-commensal symbiosis in sickness. Nature. 2014;514(7524):638-41.

36. Pham TAN, Clare S, Goulding D, Arasteh JM, Stares MD, Browne HP, Keane JA, Page AJ, Kumasaka N, Kane L. Epithelial IL-22RA1-mediated fucosylation promotes intestinal colonization resistance to an opportunistic pathogen. Cell host & microbe. 2014;16(4):504-16.
37. Hoskins LC. The ABO blood group antigens and their secretion by healthy and diseased gastric mucosa. Annals of the New York Academy of Sciences. 1967;140(2):848-60.
38. Ikehara Y, Nishihara S, Yasutomi H, Kitamura T, Matsuo K, Shimizu N, Inada K-i, Kodera Y, Yamamura Y, Narimatsu H. Polymorphisms of two fucosyltransferase genes (Lewis and Secretor genes) involving type I Lewis antigens are associated with the presence of anti-Helicobacter pylori IgG antibody. Cancer epidemiology biomarkers & prevention. 2001;10(9):971-7.
39. Rausch P, Rehman A, Künzel S, Häsler R, Ott SJ, Schreiber S, Rosenstiel P, Franke A, Baines JF. Colonic mucosa-associated microbiota is influenced by an interaction of Crohn disease and FUT2 (Secretor) genotype. Proceedings of the National Academy of Sciences. 2011;108(47):19030-5.
40. Rho J-h, Wright DP, Christie DL, Clinch K, Furneaux RH, Roberton AM. A novel mechanism for desulfation of mucin: identification and cloning of a mucin-desulfating glycosidase (sulfoglycosidase) from Prevotella strain RS2. Journal of bacteriology. 2005;187(5):1543-51.
41. Wacklin P, Mäkivuokko H, Alakulppi N, Nikkilä J, Tenkanen H, Räbinä J, Partanen J, Aranko K, Mättö J. Secretor genotype (FUT2 gene) is strongly associated with the composition of Bifidobacteria in the human intestine. PloS one. 2011;6(5):e20113.
42. Xavier R, Podolsky D. Unravelling the pathogenesis of inflammatory bowel disease. Nature. 2007;448(7152):427-34.
43. van Heel DA, Fisher SA, Kirby A, Daly MJ, Rioux JD, Lewis CM, Consortium GSM-AGotIIG. Inflammatory bowel disease susceptibility loci defined by genome scan meta-analysis of 1952 affected relative pairs. Human molecular genetics. 2004;13(7):763-70.
44. Serpa J, Mendes N, SILVA LFS, ALMEIDA R, LE PENDU J, DAVID L. Two new FUT2 (fucosyltransferase 2 gene) missense polymorphisms, 739G→ A and 839T→ C, are partly responsible for non-secretor status in a Caucasian population from Northern Portugal. Biochemical Journal. 2004;383(3):469-74.
45. McGovern DP, Jones MR, Taylor KD, Marciante K, Yan X, Dubinsky M, Ippoliti A, Vasiliauskas E, Berel D, Derkowski C. Fucosyltransferase 2 (FUT2) non-secretor status is associated with Crohn's disease. Human molecular genetics. 2010;19(17):3468-76.
46. Pohle W, Acosta L, Ru H, Krug M. Incorporation of [3H] fucose in rat hippocampal structures after conditioning by perforanth path stimulation and after LTP-producing tetanization. Brain research. 1987;410(2):245-56.
47. Krug M, Wagner M, Staak S, Smalla K-H. Fucose and fucose-containing sugar epitopes enhance hippocampal long-term potentiation in the freely moving rat. Brain research. 1994;643(1-2):130-5.
48. Kalovidouris SA, Gama CI, Lee LW, Hsieh-Wilson LC. A role for fucose α (1-2) galactose carbohydrates in neuronal growth. Journal of the American Chemical Society. 2005;127(5):1340-1.
49. St John JA, Claxton C, Robinson MW, Yamamoto F, Domino SE, Key B. Genetic manipulation of blood group carbohydrates alters development and pathfinding of primary sensory axons of the olfactory systems. Developmental biology. 2006;298(2):470-84.
50. Lipscomb BW, Treloar HB, Klenoff J, Greer CA. Cell surface carbohydrates and glomerular targeting of olfactory sensory neuron axons in the mouse. Journal of Comparative Neurology. 2003;467(1):22-31.

51. Murrey HE, Gama CI, Kalovidouris SA, Luo W-I, Driggers EM, Porton B, Hsieh-Wilson LC. Protein fucosylation regulates synapsin Ia/Ib expression and neuronal morphology in primary hippocampal neurons. Proceedings of the National Academy of Sciences of the United States of America. 2006;103(1):21-6.
52. Liedtke S, Geyer H, Wuhrer M, Geyer R, Frank G, Gerardy-Schahn R, Zähringer U, Schachner M. Characterization of N-glycans from mouse brain neural cell adhesion molecule. Glycobiology. 2001;11(5):373-84.
53. Pestean A, Krizbai I, Böttcher H, Párducz Á, Joó F, Wolff JR. Identification of the Ulex europaeus agglutinin-I-binding protein as a unique glycoform of the neural cell adhesion molecule in the olfactory sensory axons of adult rats. Neuroscience letters. 1995;195(2):117-20.
54. Murrey HE, Ficarro SB, Krishnamurthy C, Domino SE, Peters EC, Hsieh-Wilson LC. Identification of the Plasticity-Relevant Fucose-α (1− 2)-Galactose Proteome from the Mouse Olfactory Bulb. Biochemistry. 2009;48(30):7261-70.
55. Lowe JB. Selectin ligands, leukocyte trafficking, and fucosyltransferase genes. Kidney international. 1997;51(5):1418-26.
56. Imai Y, Singer MS, Fennie C, Lasky LA, Rosen SD. Identification of a carbohydrate-based endothelial ligand for a lymphocyte homing receptor. The Journal of cell biology. 1991;113(5):1213-21.
57. Homeister JW, Thall AD, Petryniak B, Malý P, Rogers CE, Smith PL, Kelly RJ, Gersten KM, Askari SW, Cheng G. The α (1, 3) fucosyltransferases FucT-IV and FucT-VII exert collaborative control over selectin-dependent leukocyte recruitment and lymphocyte homing. Immunity. 2001;15(1):115-26.
58. Malý P, Thall AD, Petryniak B, Rogers CE, Smith PL, Marks RM, Kelly RJ, Gersten KM, Cheng G, Saunders TL. The α (1, 3) fucosyltransferase Fuc-TVII controls leukocyte trafficking through an essential role in L-, E-, and P-selectin ligand biosynthesis. Cell. 1996;86(4):643-53.
59. Nimrichter L, Burdick MM, Aoki K, Laroy W, Fierro MA, Hudson SA, Von Seggern CE, Cotter RJ, Bochner BS, Tiemeyer M. E-selectin receptors on human leukocytes. Blood. 2008;112(9):3744-52.
60. Yakubenia S, Frommhold D, Schölch D, Hellbusch CC, Körner C, Petri B, Jones C, Ipe U, Bixel MG, Krempien R. Leukocyte trafficking in a mouse model for leukocyte adhesion deficiency II/congenital disorder of glycosylation IIc. Blood. 2008;112(4):1472-81.
61. Marquardt T, Lühn K, Srikrishna G, Freeze HH, Harms E, Vestweber D. Correction of leukocyte adhesion deficiency type II with oral fucose. Blood. 1999;94(12):3976-85.
62. Etzioni A, Sturla L, Antonellis A, Green ED, Gershoni‐Baruch R, Berninsone PM, Hirschberg CB, Tonetti M. Leukocyte adhesion deficiency (LAD) type II/carbohydrate deficient glycoprotein (CDG) IIc founder effect and genotype/phenotype correlation. American journal of medical genetics. 2002;110(2):131-5.
63. Hidalgo A, Ma S, Peired AJ, Weiss LA, Cunningham-Rundles C, Frenette PS. Insights into leukocyte adhesion deficiency type 2 from a novel mutation in the GDP-fucose transporter gene. Blood. 2003;101(5):1705-12.
64. Kannagi R. Carbohydrate-mediated cell adhesion involved in hematogenous metastasis of cancer. Glycoconjugate journal. 1997;14(5):577-84.
65. Zenita K, Kirihata Y, Kitahara A, Shigeta K, Higuchi K, Hirashima K, Murachi T, Miyake M, Takeda T, Kannagi R. Fucosylated type‐2 chain polylactosamine antigens in human lung cancer. International journal of cancer. 1988;41(3):344-9.
66. JESCHKE U, MYLONAS I, SHABANI N, KUNERT-KEIL C, SCHINDLBECK C, GERBER B, FRIESE K. Expression of sialyl lewis X, sialyl Lewis A, E-cadherin and cathepsin-D in human breast

cancer: immunohistochemical analysis in mammary carcinoma in situ, invasive carcinomas and their lymph node metastasis. Anticancer research. 2005;25(3A):1615-22.
67. Zipin A, Israeli-Amit M, Meshel T, Sagi-Assif O, Yron I, Lifshitz V, Bacharach E, Smorodinsky NI, Many A, Czernilofsky PA. Tumor-Microenvironment Interactions The Fucose-Generating FX Enzyme Controls Adhesive Properties of Colorectal Cancer Cells. Cancer research. 2004;64(18):6571-8.
68. Kudo T, Ikehara Y, Togayachi A, Morozumi K, Watanabe M, Nakamura M, Nishihara S, Narimatsu H. Up-regulation of a set of glycosyltransferase genes in human colorectal cancer. Laboratory investigation; a journal of technical methods and pathology. 1998;78(7):797-811.
69. Itai S, Nishikata J, Yoneda T, Ohmori K, Yamabe H, Arii S, Tobe T, Kannagi R. Tissue distribution of 2‐3 and 2‐6 sialyl lewis A antigens and significance of the ratio of two antigens for the differential diagnosis of malignant and benign disorders of the digestive tract. Cancer. 1991;67(6):1576-87.
70. Yuan K, Kucik D, Singh RK, Listinsky CM, Listinsky JJ, Siegal GP. Alterations in human breast cancer adhesion-motility in response to changes in cell surface glycoproteins displaying alpha-L-fucose moieties. International journal of oncology. 2008;32(4):797.
71. Zhang Z, Sun P, Liu J, Fu L, Yan J, Liu Y, Yu L, Wang X, Yan Q. Suppression of FUT1/FUT4 expression by siRNA inhibits tumor growth. Biochimica et Biophysica Acta (BBA)-Molecular Cell Research. 2008;1783(2):287-96.
72. Haltiwanger RS. Fucose is on the TRAIL of colon cancer. Gastroenterology. 2009;137(1):36.
73. Moriwaki K, Noda K, Furukawa Y, Ohshima K, Uchiyama A, Nakagawa T, Taniguchi N, Daigo Y, Nakamura Y, Hayashi N. Deficiency of GMDS leads to escape from NK cell-mediated tumor surveillance through modulation of TRAIL signaling. Gastroenterology. 2009;137(1):188-98. e2.
74. Yonezawa N, Mitsui S, Kudo K, Nakano M. Identification of an N-glycosylated region of pig zona pellucida glycoprotein ZPB that is involved in sperm binding. European journal of biochemistry. 1997;248(1):86-92.
75. Lefebvre R, Lo MC, Suarez SS. Bovine sperm binding to oviductal epithelium involves fucose recognition. Biology of Reproduction. 1997;56(5):1198-204.
76. Johnston DS, Wright WW, Shaper JH, Hokke CH, Van den Eijnden DH, Joziasse DH. Murine Sperm-Zona Binding, A Fucosyl Residue Is Required for a High Affinity Sperm-binding Ligand A SECOND SITE ON SPERM BINDS A NONFUCOSYLATED, β-GALACTOSYL-CAPPED OLIGOSACCHARIDE. Journal of Biological Chemistry. 1998;273(4):1888-95.
77. Pang P-C, Chiu PC, Lee C-L, Chang L-Y, Panico M, Morris HR, Haslam SM, Khoo K-H, Clark GF, Yeung WS. Human sperm binding is mediated by the sialyl-Lewisx oligosaccharide on the zona pellucida. Science. 2011;333(6050):1761-4.
78. Bird J, Kimber S. Oligosaccharides containing fucose linked α (1–3) and α (1–4) to N-acetylglucosamine cause decompaction of mouse morulae. Developmental biology. 1984;104(2):449-60.
79. Ohata S, Kinoshita S, Aoki R, Tanaka H, Wada H, Tsuruoka-Kinoshita S, Tsuboi T, Watabe S, Okamoto H. Neuroepithelial cells require fucosylated glycans to guide the migration of vagus motor neuron progenitors in the developing zebrafish hindbrain. Development. 2009;136(10):1653-63.
80. Kudo T, Fujii T, Ikegami S, Inokuchi K, Takayama Y, Ikehara Y, Nishihara S, Togayachi A, Takahashi S, Tachibana K. Mice lacking α1, 3-fucosyltransferase IX demonstrate disappearance of Lewis x structure in brain and increased anxiety-like behaviors. Glycobiology. 2007;17(1):1-9.

81. Maroni L, Hohenester S, van de Graaf S, Tolenaars D, van Lienden K, Verheij J, Marzioni M, Karlsen T, Oude ER, Beuers U. Knockout of the Primary Sclerosing Cholangitis-Risk Gene Fut2 Causes Liver Disease in Mice. Hepatology (Baltimore, Md). 2017.
82. Wang X, Gu J, Miyoshi E, Honke K, Taniguchi N. Phenotype changes of Fut8 knockout mouse: core fucosylation is crucial for the function of growth factor receptor (s). Methods in enzymology. 2006;417:11-22.
83. Kreidberg JA, Donovan MJ, Goldstein SL, Rennke H, Shepherd K, Jones RC, Jaenisch R. Alpha 3 beta 1 integrin has a crucial role in kidney and lung organogenesis. Development. 1996;122(11):3537-47.
84. Shields RL, Lai J, Keck R, O'Connell LY, Hong K, Meng YG, Weikert SH, Presta LG. Lack of fucose on human IgG1 N-linked oligosaccharide improves binding to human FcγRIII and antibody-dependent cellular toxicity. Journal of Biological Chemistry. 2002;277(30):26733-40.
85. Ferrara C, Grau S, Jäger C, Sondermann P, Brünker P, Waldhauer I, Hennig M, Ruf A, Rufer AC, Stihle M. Unique carbohydrate–carbohydrate interactions are required for high affinity binding between FcγRIII and antibodies lacking core fucose. Proceedings of the National Academy of Sciences. 2011;108(31):12669-74.
86. Shinkawa T, Nakamura K, Yamane N, Shoji-Hosaka E, Kanda Y, Sakurada M, Uchida K, Anazawa H, Satoh M, Yamasaki M. The absence of fucose but not the presence of galactose or bisecting N-acetylglucosamine of human IgG1 complex-type oligosaccharides shows the critical role of enhancing antibody-dependent cellular cytotoxicity. Journal of Biological Chemistry. 2003;278(5):3466-73.
87. Yamane-Ohnuki N, Satoh M, editors. Production of therapeutic antibodies with controlled fucosylation. MAbs; 2009: Taylor & Francis.
88. Beck A, Reichert JM, editors. Marketing approval of mogamulizumab: a triumph for glyco-engineering. MAbs; 2012: Taylor & Francis.
89. Ishii T, Ishida T, Utsunomiya A, Inagaki A, Yano H, Komatsu H, Iida S, Imada K, Uchiyama T, Akinaga S. Defucosylated humanized anti-CCR4 monoclonal antibody KW-0761 as a novel immunotherapeutic agent for adult T-cell leukemia/lymphoma. Clinical Cancer Research. 2010;16(5):1520-31.
90. Illidge T, Klein C, Sehn LH, Davies A, Salles G, Cartron G. Obinutuzumab in hematologic malignancies: Lessons learned to date. Cancer treatment reviews. 2015;41(9):784-92.
91. Hamadani M, Fanale MA, Bello CM, Kipps TJ, Offner F, Verhoef G, Federico M, Gregory SA, Sonet A, Assouline S. Safety profile and clinical response to MEDI-551, a humanized monoclonal anti-CD19, in a phase 1/2 study in adults with relapsed or refractory advanced B-cell malignancies. Blood. 2013;122(21):1810-.
92. Sathish J, editor. Checkpoint Modulators in Cancer Immunotherapy. Forum on Immunopathological Diseases and Therapeutics; 2014: Begel House Inc.
93. Gardai SJ, Epp A, Linares G, Westendorf L, Sutherland MK, Neff-LaFord H, Drachman JG, Peng S, Law C-L, editors. A sugar engineered non-fucosylated anti-CD40 antibody, SEA-CD40, with enhanced immune stimulatory activity alone and in combination with immune checkpoint inhibitors. ASCO Annual Meeting Proceedings; 2015.
94. Wei AH, Durrant ST, Hertzberg MS, Swords RT, Lewis ID, Jonas B, Cortes JE, Yarranton G, Walling JM. A phase I study of KB004, a novel non-fucosylated humaneered® antibody, targeted against the receptor tyrosine kinase EphA3, in advanced hematologic malignancies. Blood. 2013;122(21):3838-.
95. Wang X, Gu J, Ihara H, Miyoshi E, Honke K, Taniguchi N. Core fucosylation regulates epidermal growth factor receptor-mediated intracellular signaling. Journal of Biological Chemistry. 2006;281(5):2572-7.

96. Wang X, Fukuda T, Li W, Gao C-x, Kondo A, Matsumoto A, Miyoshi E, Taniguchi N, Gu J. Requirement of Fut8 for the expression of vascular endothelial growth factor receptor-2: a new mechanism for the emphysema-like changes observed in Fut8-deficient mice. Journal of biochemistry. 2009;145(5):643-51.
97. Adamczyk B, Tharmalingam T, Rudd PM. Glycans as cancer biomarkers. Biochimica et Biophysica Acta (BBA)-General Subjects. 2012;1820(9):1347-53.
98. Miyoshi E, Moriwaki K, Nakagawa T. Biological function of fucosylation in cancer biology. Journal of biochemistry. 2008;143(6):725-9.
99. Aoyagi Y, Isokawa O, Suda T, Watanabe M, Suzuki Y, Asakura H. The fucosylation index of α - fetoprotein as a possible prognostic indicator for patients with hepatocellular carcinoma. Cancer. 1998;83(10):2076-82.
100. Flores A, Marrero JA. Emerging trends in hepatocellular carcinoma: focus on diagnosis and therapeutics. Clinical Medicine Insights Oncology. 2014;8:71.
101. Saldova R, Fan Y, Fitzpatrick JM, Watson RWG, Rudd PM. Core fucosylation and α2-3 sialylation in serum N-glycome is significantly increased in prostate cancer comparing to benign prostate hyperplasia. Glycobiology. 2011;21(2):195-205.
102. Kyselova Z, Mechref Y, Al Bataineh MM, Dobrolecki LE, Hickey RJ, Vinson J, Sweeney CJ, Novotny MV. Alterations in the serum glycome due to metastatic prostate cancer. Journal of proteome research. 2007;6(5):1822-32.
103. Okuyama N, Ide Y, Nakano M, Nakagawa T, Yamanaka K, Moriwaki K, Murata K, Ohigashi H, Yokoyama S, Eguchi H. Fucosylated haptoglobin is a novel marker for pancreatic cancer: a detailed analysis of the oligosaccharide structure and a possible mechanism for fucosylation. International journal of cancer. 2006;118(11):2803-8.
104. Miyoshi E, Nakano M. Fucosylated haptoglobin is a novel marker for pancreatic cancer: detailed analyses of oligosaccharide structures. Proteomics. 2008;8(16):3257-62.
105. Goggins M. Molecular markers of early pancreatic cancer. Journal of Clinical Oncology. 2005;23(20):4524-31.
106. Zhao Y, Sato Y, Isaji T, Fukuda T, Matsumoto A, Miyoshi E, Gu J, Taniguchi N. Branched N - glycans regulate the biological functions of integrins and cadherins. FEBS journal. 2008;275(9):1939-48.
107. Zhao Y, Itoh S, Wang X, Isaji T, Miyoshi E, Kariya Y, Miyazaki K, Kawasaki N, Taniguchi N, Gu J. Deletion of core fucosylation on α3β1 integrin down-regulates its functions. Journal of Biological Chemistry. 2006;281(50):38343-50.
108. Chen C-Y, Jan Y-H, Juan Y-H, Yang C-J, Huang M-S, Yu C-J, Yang P-C, Hsiao M, Hsu T-L, Wong C-H. Fucosyltransferase 8 as a functional regulator of nonsmall cell lung cancer. Proceedings of the National Academy of Sciences. 2013;110(2):630-5.
109. Yan L-M, Lin B, Zhu L-C, Hao Y-Y, Qi Y, Wang C-Z, Gao S, Liu S-C, Zhang S-L, Iwamori M. Enhancement of the adhesive and spreading potentials of ovarian carcinoma RMG-1 cells due to increased expression of integrin α5β1 with the Lewis Y-structure on transfection of the α1, 2-fucosyltransferase gene. Biochimie. 2010;92(7):852-7.
110. Shao L, Moloney DJ, Haltiwanger R. Fringe modifies O-fucose on mouse Notch1 at epidermal growth factor-like repeats within the ligand-binding site and the Abruptex region. Journal of Biological Chemistry. 2003;278(10):7775-82.
111. Müller J, Rana NA, Serth K, Kakuda S, Haltiwanger RS, Gossler A. O-fucosylation of the notch ligand mDLL1 by POFUT1 is dispensable for ligand function. PloS one. 2014;9(2):e88571.
112. Luo Y, Koles K, Vorndam W, Haltiwanger RS, Panin VM. Protein O-fucosyltransferase 2 adds O-fucose to thrombospondin type 1 repeats. Journal of Biological Chemistry. 2006;281(14):9393-9.

113. Luo Y, Nita-Lazar A, Haltiwanger RS. Two distinct pathways for O-fucosylation of epidermal growth factor-like or thrombospondin type 1 repeats. Journal of Biological Chemistry. 2006;281(14):9385-92.
114. Valero-González J, Leonhard-Melief C, Lira-Navarrete E, Jiménez-Osés G, Hernández-Ruiz C, Pallarés MC, Yruela I, Vasudevan D, Lostao A, Corzana F. A proactive role of water molecules in acceptor recognition by protein O-fucosyltransferase 2. Nature chemical biology. 2016;12(4):240-6.
115. Wang Y, Spellman MW. Purification and characterization of a GDP-fucose: polypeptide fucosyltransferase from Chinese hamster ovary cells. Journal of Biological Chemistry. 1998;273(14):8112-8.
116. Rampal R, Luther KB, Haltiwanger RS. Notch signaling in normal and disease States: possible therapies related to glycosylation. Current molecular medicine. 2007;7(4):427-45.
117. Leonhard-Melief C, Haltiwanger RS. Chapter Eighteen-O-Fucosylation of Thrombospondin Type 1 Repeats. Methods in enzymology. 2010;480:401-16.
118. Okajima T, Xu A, Lei L, Irvine KD. Chaperone activity of protein O-fucosyltransferase 1 promotes notch receptor folding. Science. 2005;307(5715):1599-603.
119. Vasudevan D, Haltiwanger RS. Novel roles for O-linked glycans in protein folding. Glycoconjugate journal. 2014;31(6-7):417-26.
120. Moloney DJ, Shair LH, Lu FM, Xia J, Locke R, Matta KL, Haltiwanger RS. Mammalian Notch1 is modified with two unusual forms ofO-linked glycosylation found on epidermal growth factor-like modules. Journal of Biological Chemistry. 2000;275(13):9604-11.
121. Okamura Y, Saga Y. Pofut1 is required for the proper localization of the Notch receptor during mouse development. Mechanisms of development. 2008;125(8):663-73. Epub 2008/06/13. doi: 10.1016/j.mod.2008.04.007. PubMed PMID: 18547789.
122. Yao D, Huang Y, Huang X, Wang W, Yan Q, Wei L, Xin W, Gerson S, Stanley P, Lowe JB. Protein O-fucosyltransferase 1 (Pofut1) regulates lymphoid and myeloid homeostasis through modulation of Notch receptor ligand interactions. Blood. 2011;117(21):5652-62.
123. Rampal R, Arboleda-Velasquez JF, Nita-Lazar A, Kosik KS, Haltiwanger RS. Highly conserved O-fucose sites have distinct effects on Notch1 function. Journal of Biological Chemistry. 2005;280(37):32133-40.
124. Stahl M, Uemura K, Ge C, Shi S, Tashima Y, Stanley P. Roles of Pofut1 and O-fucose in mammalian Notch signaling. Journal of Biological Chemistry. 2008;283(20):13638-51.
125. Kakuda S, Haltiwanger R. Deciphering the Fringe-mediated Notch Code. Developmental Cell. 2017;In Press.
126. Luca VC, Jude KM, Pierce NW, Nachury MV, Fischer S, Garcia KC. Structural basis for Notch1 engagement of Delta-like 4. Science. 2015;347(6224):847-53.
127. Moloney DJ, Panin VM, Johnston SH, Chen J, Shao L, Wilson R, Wang Y, Stanley P, Irvine KD, Haltiwanger RS. Fringe is a glycosyltransferase that modifies Notch. Nature. 2000;406(6794):369-75.
128. Irvine KD, Wieschaus E. fringe, a Boundary-specific signaling molecule, mediates interactions between dorsal and ventral cells during Drosophila wing development. Cell. 1994;79(4):595-606.
129. Klein T, Arias AM. Interactions among Delta, Serrate and Fringe modulate Notch activity during Drosophila wing development. Development. 1998;125(15):2951-62.
130. Panin VM, Papayannopoulos V, Wilson R, Irvine KD. Fringe modulates Notch-ligand interactions. Nature. 1997;387(6636):908-12.
131. Johnston SH, Rauskolb C, Wilson R, Prabhakaran B, Irvine KD, Vogt TF. A family of mammalian Fringe genes implicated in boundary determination and the Notch pathway. Development. 1997;124(11):2245-54.

132. LeBon L, Lee TV, Sprinzak D, Jafar-Nejad H, Elowitz MB. Fringe proteins modulate Notch-ligand cis and trans interactions to specify signaling states. Elife. 2014;3:e02950.
133. Zhang N, Gridley T. Defects in somite formation in lunatic fringe-deficient mice. Nature. 1998;394(6691):374-7.
134. Evrard YA, Lun Y, Aulehla A, Gan L, Johnson RL. Lunatic fringe is an essential mediator of somite segmentation and patterning. Nature. 1998;394(6691):377-81.
135. Harvey BM, Rana NA, Moss H, Leonardi J, Jafar-Nejad H, Haltiwanger RS. Mapping sites of O-glycosylation and fringe elongation on Drosophila Notch. Journal of Biological Chemistry. 2016:jbc. M116. 732537.
136. Li M, Cheng R, Liang J, Yan H, Zhang H, Yang L, Li C, Jiao Q, Lu Z, He J. Mutations in POFUT1, encoding protein O-fucosyltransferase 1, cause generalized Dowling-Degos disease. The American Journal of Human Genetics. 2013;92(6):895-903.
137. Chen M, Li Y, Liu H, Fu Xa, Yu Y, Yu G, Wang C, Bao F, Liany H, Wang Z. Analysis of POFUT1 gene mutation in a Chinese family with Dowling-Degos disease. PloS one. 2014;9(8):e104496.
138. Kim M-L, Chandrasekharan K, Glass M, Shi S, Stahl MC, Kaspar B, Stanley P, Martin PT. O-fucosylation of muscle agrin determines its ability to cluster acetylcholine receptors. Molecular and Cellular Neuroscience. 2008;39(3):452-64.
139. Milde-Langosch K, Karn T, Schmidt M, Zu Eulenburg C, Oliveira-Ferrer L, Wirtz RM, Schumacher U, Witzel I, Schütze D, Müller V. Prognostic relevance of glycosylation-associated genes in breast cancer. Breast cancer research and treatment. 2014;145(2):295-305.
140. Yokota S, Ogawara K, Kimura R, Shimizu F, Baba T, Minakawa Y, Higo M, Kasamatsu A, Endo-Sakamoto Y, Shiiba M. Protein O-fucosyltransferase 1: a potential diagnostic marker and therapeutic target for human oral cancer. International journal of oncology. 2013;43(6):1864-70.
141. Ma L, Dong P, Liu L, Gao Q, Duan M, Zhang S, Chen S, Xue R, Wang X. Overexpression of protein O-fucosyltransferase 1 accelerates hepatocellular carcinoma progression via the Notch signaling pathway. Biochemical and biophysical research communications. 2016;473(2):503-10.
142. Sawey ET, Chanrion M, Cai C, Wu G, Zhang J, Zender L, Zhao A, Busuttil RW, Yee H, Stein L, French DM, Finn RS, Lowe SW, Powers S. Identification of a therapeutic strategy targeting amplified FGF19 in liver cancer by Oncogenomic screening. Cancer cell. 2011;19(3):347-58. Epub 2011/03/15. doi: 10.1016/j.ccr.2011.01.040. PubMed PMID: 21397858; PMCID: 3061399.
143. Benz BA, Nandadasa S, Takeuchi M, Grady RC, Takeuchi H, LoPilato RK, Kakuda S, Somerville RP, Apte SS, Haltiwanger RS. Genetic and biochemical evidence that gastrulation defects in Pofut2 mutants result from defects in ADAMTS9 secretion. Developmental Biology. 2016.
144. Perbal B. CCN proteins: multifunctional signalling regulators. The Lancet. 2004;363(9402):62-4.
145. Niwa Y, Suzuki T, Dohmae N, Simizu S. O‐fucosylation of CCN1 is required for its secretion. FEBS letters. 2015;589(21):3287-93.
146. Tang BL. ADAMTS: a novel family of extracellular matrix proteases. The international journal of biochemistry & cell biology. 2001;33(1):33-44.
147. Vasudevan D, Takeuchi H, Johar SS, Majerus E, Haltiwanger RS. Peters plus syndrome mutations disrupt a noncanonical ER quality-control mechanism. Current Biology. 2015;25(3):286-95.

148. Dubail J, Vasudevan D, Wang LW, Earp SE, Jenkins MW, Haltiwanger RS, Apte SS. Impaired ADAMTS9 secretion: A potential mechanism for eye defects in Peters Plus Syndrome. Scientific reports. 2016;6.
149. Ricketts LM, Dlugosz M, Luther KB, Haltiwanger RS, Majerus EM. O-fucosylation is required for ADAMTS13 secretion. Journal of Biological Chemistry. 2007;282(23):17014-23.
150. Wang LW, Dlugosz M, Somerville RP, Raed M, Haltiwanger RS, Apte SS. O-Fucosylation of Thrombospondin Type 1 Repeats in ADAMTS-like-1/Punctin-1 Regulates Secretion IMPLICATIONS FOR THE ADAMTS SUPERFAMILY. Journal of Biological Chemistry. 2007;282(23):17024-31.
151. Oberstein SAL, Kriek M, White SJ, Kalf ME, Szuhai K, den Dunnen JT, Breuning MH, Hennekam RC. Peters Plus syndrome is caused by mutations in B3GALTL, a putative glycosyltransferase. The American Journal of Human Genetics. 2006;79(3):562-6.
152. Srivastava G, Kaur K, Hindsgaul O, Palcic M. Enzymatic transfer of a preassembled trisaccharide antigen to cell surfaces using a fucosyltransferase. Journal of Biological Chemistry. 1992;267(31):22356-61.
153. Laughlin ST, Baskin JM, Amacher SL, Bertozzi CR. In vivo imaging of membrane-associated glycans in developing zebrafish. Science. 2008;320(5876):664-7.
154. Laughlin ST, Bertozzi CR. In vivo imaging of Caenorhabditis elegans glycans. ACS chemical biology. 2009;4(12):1068-72.
155. Anderson CT, Wallace IS, Somerville CR. Metabolic click-labeling with a fucose analog reveals pectin delivery, architecture, and dynamics in Arabidopsis cell walls. Proceedings of the National Academy of Sciences. 2012;109(4):1329-34.
156. Hsu T-L, Hanson SR, Kishikawa K, Wang S-K, Sawa M, Wong C-H. Alkynyl sugar analogs for the labeling and visualization of glycoconjugates in cells. Proceedings of the National Academy of Sciences. 2007;104(8):2614-9.
157. Sawa M, Hsu T-L, Itoh T, Sugiyama M, Hanson SR, Vogt PK, Wong C-H. Glycoproteomic probes for fluorescent imaging of fucosylated glycans in vivo. Proceedings of the National Academy of Sciences. 2006;103(33):12371-6.
158. Liu T-W, Kaji H, Togayachi A, Ito H, Sato T, Narimatsu H. A chemoenzymatic approach toward the identification of fucosylated glycoproteins and mapping of N-glycan sites. Glycobiology. 2012;22(5):630-7.
159. Al-Shareffi E, Chaubard JL, Leonhard-Melief C, Wang SK, Wong CH, Haltiwanger RS. 6-alkynyl fucose is a bioorthogonal analog for O-fucosylation of epidermal growth factor-like repeats and thrombospondin type-1 repeats by protein O-fucosyltransferases 1 and 2. Glycobiology. 2013;23(2):188-98. Epub 2012/10/10. doi: 10.1093/glycob/cws140. PubMed PMID: 23045360; PMCID: 3531295.
160. Kizuka Y, Funayama S, Shogomori H, Nakano M, Nakajima K, Oka R, Kitazume S, Yamaguchi Y, Sano M, Korekane H. High-Sensitivity and Low-Toxicity Fucose Probe for Glycan Imaging and Biomarker Discovery. Cell Chemical Biology. 2016;23(7):782-92.
161. Gloster TM, Vocadlo DJ. Developing inhibitors of glycan processing enzymes as tools for enabling glycobiology. Nature chemical biology. 2012;8(8):683-94.
162. Rillahan CD, Brown SJ, Register AC, Rosen H, Paulson JC. High‐Throughput Screening for Inhibitors of Sialyl‐and Fucosyltransferases. Angewandte Chemie International Edition. 2011;50(52):12534-7.
163. Dalziel M, Crispin M, Scanlan CN, Zitzmann N, Dwek RA. Emerging principles for the therapeutic exploitation of glycosylation. Science. 2014;343(6166):1235681.
164. Fuster MM, Esko JD. The sweet and sour of cancer: glycans as novel therapeutic targets. Nature Reviews Cancer. 2005;5(7):526-42.
165. Hosoguchi K, Maeda T, Furukawa J-i, Shinohara Y, Hinou H, Sekiguchi M, Togame H, Takemoto H, Kondo H, Nishimura S-I. An efficient approach to the discovery of potent

inhibitors against glycosyltransferases. Journal of medicinal chemistry. 2010;53(15):5607-19.
166. Lee LV, Mitchell ML, Huang S-J, Fokin VV, Sharpless KB, Wong C-H. A potent and highly selective inhibitor of human α-1, 3-fucosyltransferase via click chemistry. Journal of the American Chemical Society. 2003;125(32):9588-9.
167. Rillahan CD, Antonopoulos A, Lefort CT, Sonon R, Azadi P, Ley K, Dell A, Haslam SM, Paulson JC. Global metabolic inhibitors of sialyl- and fucosyltransferases remodel the glycome. Nat Chem Biol. 2012;8(7):661-8. doi: 10.1038/nchembio.999. PubMed PMID: 22683610; PMCID: PMC3427410.
168. Villalobos JA, Bo RY, Wallace IS. 2-fluoro-L-fucose is a metabolically incorporated inhibitor of plant cell wall polysaccharide fucosylation. PloS one. 2015;10(9):e0139091.
169. Okeley NM, Alley SC, Anderson ME, Boursalian TE, Burke PJ, Emmerton KM, Jeffrey SC, Klussman K, Law C-L, Sussman D. Development of orally active inhibitors of protein and cellular fucosylation. Proceedings of the National Academy of Sciences. 2013;110(14):5404-9.
170. Rose SP, Jork R. Long-term memory formation in chicks is blocked by 2-deoxygalactose, a fucose analog. Behavioral and neural biology. 1987;48(2):246-58.
171. Krug M, Jork R, Reymann K, Wagner M, Matthies H. The amnesic substance 2-deoxy-D-galactose suppresses the maintenance of hippocampal LTP. Brain research. 1991;540(1-2):237-42.
172. Lorenzini CGA, Baldi E, Bucherelli C, Sacchetti B, Tassoni G. 2-Deoxy-D-galactose effects on passive avoidance memorization in the rat. Neurobiology of learning and memory. 1997;68(3):317-24.
173. Huze C, Bauche S, Richard P, Chevessier F, Goillot E, Gaudon K, Ben Ammar A, Chaboud A, Grosjean I, Lecuyer HA, Bernard V, Rouche A, Alexandri N, Kuntzer T, Fardeau M, Fournier E, Brancaccio A, Ruegg MA, Koenig J, Eymard B, Schaeffer L, Hantai D. Identification of an agrin mutation that causes congenital myasthenia and affects synapse function. American journal of human genetics. 2009;85(2):155-67. Epub 2009/07/28. doi: 10.1016/j.ajhg.2009.06.015. PubMed PMID: 19631309; PMCID: Pmc2725239.
174. Maselli RA, Fernandez JM, Arredondo J, Navarro C, Ngo M, Beeson D, Cagney O, Williams DC, Wollmann RL, Yarov-Yarovoy V, Ferns MJ. LG2 agrin mutation causing severe congenital myasthenic syndrome mimics functional characteristics of non-neural (z-) agrin. Human genetics. 2012;131(7):1123-35. Epub 2011/12/30. doi: 10.1007/s00439-011-1132-4. PubMed PMID: 22205389.
175. Robinson A, Escuin S, Doudney K, Vekemans M, Stevenson RE, Greene ND, Copp AJ, Stanier P. Mutations in the planar cell polarity genes CELSR1 and SCRIB are associated with the severe neural tube defect craniorachischisis. Human mutation. 2012;33(2):440-7. Epub 2011/11/19. doi: 10.1002/humu.21662. PubMed PMID: 22095531.
176. Bamford RN, Roessler E, Burdine RD, Saplakoglu U, dela Cruz J, Splitt M, Goodship JA, Towbin J, Bowers P, Ferrero GB, Marino B, Schier AF, Shen MM, Muenke M, Casey B. Loss-of-function mutations in the EGF-CFC gene CFC1 are associated with human left-right laterality defects. Nat Genet. 2000;26(3):365-9. Epub 2000/11/04. doi: 10.1038/81695. PubMed PMID: 11062482.
177. Goldmuntz E, Bamford R, Karkera JD, dela Cruz J, Roessler E, Muenke M. CFC1 mutations in patients with transposition of the great arteries and double-outlet right ventricle. American journal of human genetics. 2002;70(3):776-80. Epub 2002/01/19. doi: 10.1086/339079. PubMed PMID: 11799476; PMCID: Pmc384955.
178. den Hollander AI, ten Brink JB, de Kok YJ, van Soest S, van den Born LI, van Driel MA, van de Pol DJ, Payne AM, Bhattacharya SS, Kellner U, Hoyng CB, Westerveld A, Brunner HG, Bleeker-Wagemakers EM, Deutman AF, Heckenlively JR, Cremers FP, Bergen AA. Mutations

in a human homologue of Drosophila crumbs cause retinitis pigmentosa (RP12). Nat Genet. 1999;23(2):217-21. Epub 1999/10/03. doi: 10.1038/13848. PubMed PMID: 10508521.
179. den Hollander AI, Heckenlively JR, van den Born LI, de Kok YJ, van der Velde-Visser SD, Kellner U, Jurklies B, van Schooneveld MJ, Blankenagel A, Rohrschneider K, Wissinger B, Cruysberg JR, Deutman AF, Brunner HG, Apfelstedt-Sylla E, Hoyng CB, Cremers FP. Leber congenital amaurosis and retinitis pigmentosa with Coats-like exudative vasculopathy are associated with mutations in the crumbs homologue 1 (CRB1) gene. American journal of human genetics. 2001;69(1):198-203. Epub 2001/06/05. PubMed PMID: 11389483; PMCID: Pmc1226034.
180. McKay GJ, Clarke S, Davis JA, Simpson DA, Silvestri G. Pigmented paravenous chorioretinal atrophy is associated with a mutation within the crumbs homolog 1 (CRB1) gene. Investigative ophthalmology & visual science. 2005;46(1):322-8. Epub 2004/12/30. doi: 10.1167/iovs.04-0734. PubMed PMID: 15623792.
181. Miyamoto T, Inoue H, Sakamoto Y, Kudo E, Naito T, Mikawa T, Mikawa Y, Isashiki Y, Osabe D, Shinohara S, Shiota H, Itakura M. Identification of a novel splice site mutation of the CSPG2 gene in a Japanese family with Wagner syndrome. Investigative ophthalmology & visual science. 2005;46(8):2726-35. Epub 2005/07/27. doi: 10.1167/iovs.05-0057. PubMed PMID: 16043844.
182. Kloeckener-Gruissem B, Neidhardt J, Magyar I, Plauchu H, Zech JC, Morle L, Palmer-Smith SM, Macdonald MJ, Nas V, Fry AE, Berger W. Novel VCAN mutations and evidence for unbalanced alternative splicing in the pathogenesis of Wagner syndrome. European journal of human genetics : EJHG. 2013;21(3):352-6. Epub 2012/06/29. doi: 10.1038/ejhg.2012.137. PubMed PMID: 22739342; PMCID: Pmc3573191.
183. Aminoff M, Carter JE, Chadwick RB, Johnson C, Grasbeck R, Abdelaal MA, Broch H, Jenner LB, Verroust PJ, Moestrup SK, de la Chapelle A, Krahe R. Mutations in CUBN, encoding the intrinsic factor-vitamin B12 receptor, cubilin, cause hereditary megaloblastic anaemia 1. Nat Genet. 1999;21(3):309-13. Epub 1999/03/18. doi: 10.1038/6831. PubMed PMID: 10080186.
184. Kristiansen M, Aminoff M, Jacobsen C, de La Chapelle A, Krahe R, Verroust PJ, Moestrup SK. Cubilin P1297L mutation associated with hereditary megaloblastic anemia 1 causes impaired recognition of intrinsic factor-vitamin B(12) by cubilin. Blood. 2000;96(2):405-9. Epub 2000/07/11. PubMed PMID: 10887099.
185. Bulman MP, Kusumi K, Frayling TM, McKeown C, Garrett C, Lander ES, Krumlauf R, Hattersley AT, Ellard S, Turnpenny PD. Mutations in the human delta homologue, DLL3, cause axial skeletal defects in spondylocostal dysostosis. Nat Genet. 2000;24(4):438-41. Epub 2000/03/31. doi: 10.1038/74307. PubMed PMID: 10742114.
186. Groenestege WM, Thebault S, van der Wijst J, van den Berg D, Janssen R, Tejpar S, van den Heuvel LP, van Cutsem E, Hoenderop JG, Knoers NV, Bindels RJ. Impaired basolateral sorting of pro-EGF causes isolated recessive renal hypomagnesemia. The Journal of clinical investigation. 2007;117(8):2260-7. Epub 2007/08/03. doi: 10.1172/jci31680. PubMed PMID: 17671655; PMCID: Pmc1934557.
187. Collin RW, Littink KW, Klevering BJ, van den Born LI, Koenekoop RK, Zonneveld MN, Blokland EA, Strom TM, Hoyng CB, den Hollander AI, Cremers FP. Identification of a 2 Mb human ortholog of Drosophila eyes shut/spacemaker that is mutated in patients with retinitis pigmentosa. American journal of human genetics. 2008;83(5):594-603. Epub 2008/11/04. doi: 10.1016/j.ajhg.2008.10.014. PubMed PMID: 18976725; PMCID: Pmc2668042.
188. Abd El-Aziz MM, Barragan I, O'Driscoll CA, Goodstadt L, Prigmore E, Borrego S, Mena M, Pieras JI, El-Ashry MF, Safieh LA, Shah A, Cheetham ME, Carter NP, Chakarova C, Ponting CP, Bhattacharya SS, Antinolo G. EYS, encoding an ortholog of Drosophila spacemaker, is

mutated in autosomal recessive retinitis pigmentosa. Nat Genet. 2008;40(11):1285-7. Epub 2008/10/07. doi: 10.1038/ng.241. PubMed PMID: 18836446; PMCID: Pmc2719291.
189. Huang Y, Zhang J, Li C, Yang G, Liu M, Wang QK, Tang Z. Identification of a novel homozygous nonsense mutation in EYS in a Chinese family with autosomal recessive retinitis pigmentosa. BMC medical genetics. 2010;11:121. Epub 2010/08/11. doi: 10.1186/1471-2350-11-121. PubMed PMID: 20696082; PMCID: Pmc2927534.
190. Audo I, Sahel JA, Mohand-Said S, Lancelot ME, Antonio A, Moskova-Doumanova V, Nandrot EF, Doumanov J, Barragan I, Antinolo G, Bhattacharya SS, Zeitz C. EYS is a major gene for rod-cone dystrophies in France. Human mutation. 2010;31(5):E1406-35. Epub 2010/03/25. doi: 10.1002/humu.21249. PubMed PMID: 20333770.
191. Bernardi F, Liney DL, Patracchini P, Gemmati D, Legnani C, Arcieri P, Pinotti M, Redaelli R, Ballerini G, Pemberton S, et al. Molecular defects in CRM+ factor VII deficiencies: modelling of missense mutations in the catalytic domain of FVII. Br J Haematol. 1994;86(3):610-8. Epub 1994/03/01. PubMed PMID: 8043443.
192. O'Brien DP, Gale KM, Anderson JS, McVey JH, Miller GJ, Meade TW, Tuddenham EG. Purification and characterization of factor VII 304-Gln: a variant molecule with reduced activity isolated from a clinically unaffected male. Blood. 1991;78(1):132-40. Epub 1991/07/01. PubMed PMID: 2070047.
193. Leonard BJ, Chen Q, Blajchman MA, Ofosu FA, Sridhara S, Yang D, Clarke BJ. Factor VII deficiency caused by a structural variant N57D of the first epidermal growth factor domain. Blood. 1998;91(1):142-8. Epub 1998/02/07. PubMed PMID: 9414278.
194. Girelli D, Russo C, Ferraresi P, Olivieri O, Pinotti M, Friso S, Manzato F, Mazzucco A, Bernardi F, Corrocher R. Polymorphisms in the factor VII gene and the risk of myocardial infarction in patients with coronary artery disease. The New England journal of medicine. 2000;343(11):774-80. Epub 2000/09/14. doi: 10.1056/nejm200009143431104. PubMed PMID: 10984565.
195. Landau D, Rosenberg N, Zivelin A, Staretz-Chacham O, Kapelushnik J. Familial factor VII deficiency with foetal and neonatal fatal cerebral haemorrhage associated with homozygosis to Gly180Arg mutation. Haemophilia : the official journal of the World Federation of Hemophilia. 2009;15(3):774-8. Epub 2009/05/13. doi: 10.1111/j.1365-2516.2009.02004.x. PubMed PMID: 19432927.
196. Jiang M, Wang Z, Yu Z, Bai X, Su J, Cao L, Zhang W, Ruan C. A novel missense mutation close to the charge-stabilizing system in a patient with congenital factor VII deficiency. Blood coagulation & fibrinolysis : an international journal in haemostasis and thrombosis. 2011;22(4):264-70. Epub 2011/03/05. doi: 10.1097/MBC.0b013e3283447388. PubMed PMID: 21372693.
197. de la Salle C, Charmantier JL, Ravanat C, Ohlmann P, Hartmann ML, Schuhler S, Bischoff R, Ebel C, Roecklin D, Balland A, et al. The Arg-4 mutant factor IX Strasbourg 2 shows a delayed activation by factor XIa. Nouvelle revue francaise d'hematologie. 1993;35(5):473-80. Epub 1993/01/01. PubMed PMID: 8295821.
198. Suehiro K, Kawabata S, Miyata T, Takeya H, Takamatsu J, Ogata K, Kamiya T, Saito H, Niho Y, Iwanaga S. Blood clotting factor IX BM Nagoya. Substitution of arginine 180 by tryptophan and its activation by alpha-chymotrypsin and rat mast cell chymase. The Journal of biological chemistry. 1989;264(35):21257-65. Epub 1989/12/15. PubMed PMID: 2592373.
199. Green PM, Bentley DR, Mibashan RS, Nilsson IM, Giannelli F. Molecular pathology of haemophilia B. The EMBO journal. 1989;8(4):1067-72. Epub 1989/04/01. PubMed PMID: 2743975; PMCID: Pmc400915.
200. Simioni P, Tormene D, Tognin G, Gavasso S, Bulato C, Iacobelli NP, Finn JD, Spiezia L, Radu C, Arruda VR. X-linked thrombophilia with a mutant factor IX (factor IX Padua). The New

England journal of medicine. 2009;361(17):1671-5. Epub 2009/10/23. doi: 10.1056/NEJMoa0904377. PubMed PMID: 19846852.
201. Schloesser M, Hofferbert S, Bartz U, Lutze G, Lammle B, Engel W. The novel acceptor splice site mutation 11396(G-->A) in the factor XII gene causes a truncated transcript in cross-reacting material negative patients. Hum Mol Genet. 1995;4(7):1235-7. Epub 1995/07/01. PubMed PMID: 8528215.
202. Bernardi F, Marchetti G, Patracchini P, del Senno L, Tripodi M, Fantoni A, Bartolai S, Vannini F, Felloni L, Rossi L, et al. Factor XII gene alteration in Hageman trait detected by TaqI restriction enzyme. Blood. 1987;69(5):1421-4. Epub 1987/05/01. PubMed PMID: 2882793.
203. Dewald G, Bork K. Missense mutations in the coagulation factor XII (Hageman factor) gene in hereditary angioedema with normal C1 inhibitor. Biochem Biophys Res Commun. 2006;343(4):1286-9. Epub 2006/04/28. doi: 10.1016/j.bbrc.2006.03.092. PubMed PMID: 16638441.
204. Cichon S, Martin L, Hennies HC, Muller F, Van Driessche K, Karpushova A, Stevens W, Colombo R, Renne T, Drouet C, Bork K, Nothen MM. Increased activity of coagulation factor XII (Hageman factor) causes hereditary angioedema type III. American journal of human genetics. 2006;79(6):1098-104. Epub 2006/12/23. doi: 10.1086/509899. PubMed PMID: 17186468; PMCID: Pmc1698720.
205. Cappello S, Gray MJ, Badouel C, Lange S, Einsiedler M, Srour M, Chitayat D, Hamdan FF, Jenkins ZA, Morgan T, Preitner N, Uster T, Thomas J, Shannon P, Morrison V, Di Donato N, Van Maldergem L, Neuhann T, Newbury-Ecob R, Swinkells M, Terhal P, Wilson LC, Zwijnenburg PJ, Sutherland-Smith AJ, Black MA, Markie D, Michaud JL, Simpson MA, Mansour S, McNeill H, Gotz M, Robertson SP. Mutations in genes encoding the cadherin receptor-ligand pair DCHS1 and FAT4 disrupt cerebral cortical development. Nat Genet. 2013;45(11):1300-8. Epub 2013/09/24. doi: 10.1038/ng.2765. PubMed PMID: 24056717.
206. Debeer P, Schoenmakers EF, Twal WO, Argraves WS, De Smet L, Fryns JP, Van De Ven WJ. The fibulin-1 gene (FBLN1) is disrupted in a t(12;22) associated with a complex type of synpolydactyly. Journal of medical genetics. 2002;39(2):98-104. Epub 2002/02/12. PubMed PMID: 11836357; PMCID: Pmc1735038.
207. Greene LM, Twal WO, Duffy MJ, McDermott EW, Hill AD, O'Higgins NJ, McCann AH, Dervan PA, Argraves WS, Gallagher WM. Elevated expression and altered processing of fibulin-1 protein in human breast cancer. British journal of cancer. 2003;88(6):871-8. Epub 2003/03/20. doi: 10.1038/sj.bjc.6600802. PubMed PMID: 12644824; PMCID: Pmc2377096.
208. Putnam EA, Zhang H, Ramirez F, Milewicz DM. Fibrillin-2 (FBN2) mutations result in the Marfan-like disorder, congenital contractural arachnodactyly. Nat Genet. 1995;11(4):456-8. Epub 1995/12/01. doi: 10.1038/ng1295-456. PubMed PMID: 7493032.
209. Park ES, Putnam EA, Chitayat D, Child A, Milewicz DM. Clustering of FBN2 mutations in patients with congenital contractural arachnodactyly indicates an important role of the domains encoded by exons 24 through 34 during human development. Am J Med Genet. 1998;78(4):350-5. Epub 1998/08/26. PubMed PMID: 9714438.
210. Babcock D, Gasner C, Francke U, Maslen C. A single mutation that results in an Asp to His substitution and partial exon skipping in a family with congenital contractural arachnodactyly. Human genetics. 1998;103(1):22-8. Epub 1998/09/16. PubMed PMID: 9737771.
211. Belleh S, Zhou G, Wang M, Der Kaloustian VM, Pagon RA, Godfrey M. Two novel fibrillin-2 mutations in congenital contractural arachnodactyly. Am J Med Genet. 2000;92(1):7-12. Epub 2000/05/08. PubMed PMID: 10797416.
212. Gupta PA, Putnam EA, Carmical SG, Kaitila I, Steinmann B, Child A, Danesino C, Metcalfe K, Berry SA, Chen E, Delorme CV, Thong MK, Ades LC, Milewicz DM. Ten novel FBN2 mutations in congenital contractural arachnodactyly: delineation of the molecular pathogenesis and

clinical phenotype. Human mutation. 2002;19(1):39-48. Epub 2001/12/26. doi: 10.1002/humu.10017. PubMed PMID: 11754102.
213. Callewaert BL, Loeys BL, Ficcadenti A, Vermeer S, Landgren M, Kroes HY, Yaron Y, Pope M, Foulds N, Boute O, Galan F, Kingston H, Van der Aa N, Salcedo I, Swinkels ME, Wallgren-Pettersson C, Gabrielli O, De Backer J, Coucke PJ, De Paepe AM. Comprehensive clinical and molecular assessment of 32 probands with congenital contractural arachnodactyly: report of 14 novel mutations and review of the literature. Human mutation. 2009;30(3):334-41. Epub 2008/11/14. doi: 10.1002/humu.20854. PubMed PMID: 19006240.
214. Oda T, Elkahloun AG, Pike BL, Okajima K, Krantz ID, Genin A, Piccoli DA, Meltzer PS, Spinner NB, Collins FS, Chandrasekharappa SC. Mutations in the human Jagged1 gene are responsible for Alagille syndrome. Nat Genet. 1997;16(3):235-42. Epub 1997/07/01. doi: 10.1038/ng0797-235. PubMed PMID: 9207787.
215. Krantz ID, Colliton RP, Genin A, Rand EB, Li L, Piccoli DA, Spinner NB. Spectrum and frequency of jagged1 (JAG1) mutations in Alagille syndrome patients and their families. American journal of human genetics. 1998;62(6):1361-9. Epub 1998/06/19. doi: 10.1086/301875. PubMed PMID: 9585603; PMCID: Pmc1377154.
216. Eldadah ZA, Hamosh A, Biery NJ, Montgomery RA, Duke M, Elkins R, Dietz HC. Familial Tetralogy of Fallot caused by mutation in the jagged1 gene. Hum Mol Genet. 2001;10(2):163-9. Epub 2001/01/12. PubMed PMID: 11152664.
217. Ali M, McKibbin M, Booth A, Parry DA, Jain P, Riazuddin SA, Hejtmancik JF, Khan SN, Firasat S, Shires M, Gilmour DF, Towns K, Murphy AL, Azmanov D, Tournev I, Cherninkova S, Jafri H, Raashid Y, Toomes C, Craig J, Mackey DA, Kalaydjieva L, Riazuddin S, Inglehearn CF. Null mutations in LTBP2 cause primary congenital glaucoma. American journal of human genetics. 2009;84(5):664-71. Epub 2009/04/14. doi: 10.1016/j.ajhg.2009.03.017. PubMed PMID: 19361779; PMCID: Pmc2680998.
218. Kumar A, Duvvari MR, Prabhakaran VC, Shetty JS, Murthy GJ, Blanton SH. A homozygous mutation in LTBP2 causes isolated microspherophakia. Human genetics. 2010;128(4):365-71. Epub 2010/07/10. doi: 10.1007/s00439-010-0858-8. PubMed PMID: 20617341.
219. Haji-Seyed-Javadi R, Jelodari-Mamaghani S, Paylakhi SH, Yazdani S, Nilforushan N, Fan JB, Klotzle B, Mahmoudi MJ, Ebrahimian MJ, Chelich N, Taghiabadi E, Kamyab K, Boileau C, Paisan-Ruiz C, Ronaghi M, Elahi E. LTBP2 mutations cause Weill-Marchesani and Weill-Marchesani-like syndrome and affect disruptions in the extracellular matrix. Human mutation. 2012;33(8):1182-7. Epub 2012/04/28. doi: 10.1002/humu.22105. PubMed PMID: 22539340.
220. Twigg SR, Lloyd D, Jenkins D, Elcioglu NE, Cooper CD, Al-Sannaa N, Annagur A, Gillessen-Kaesbach G, Huning I, Knight SJ, Goodship JA, Keavney BD, Beales PL, Gileadi O, McGowan SJ, Wilkie AO. Mutations in multidomain protein MEGF8 identify a Carpenter syndrome subtype associated with defective lateralization. American journal of human genetics. 2012;91(5):897-905. Epub 2012/10/16. doi: 10.1016/j.ajhg.2012.08.027. PubMed PMID: 23063620; PMCID: Pmc3487118.
221. Logan CV, Lucke B, Pottinger C, Abdelhamed ZA, Parry DA, Szymanska K, Diggle CP, van Riesen A, Morgan JE, Markham G, Ellis I, Manzur AY, Markham AF, Shires M, Helliwell T, Scoto M, Hubner C, Bonthron DT, Taylor GR, Sheridan E, Muntoni F, Carr IM, Schuelke M, Johnson CA. Mutations in MEGF10, a regulator of satellite cell myogenesis, cause early onset myopathy, areflexia, respiratory distress and dysphagia (EMARDD). Nat Genet. 2011;43(12):1189-92. Epub 2011/11/22. doi: 10.1038/ng.995. PubMed PMID: 22101682.
222. Boyden SE, Mahoney LJ, Kawahara G, Myers JA, Mitsuhashi S, Estrella EA, Duncan AR, Dey F, DeChene ET, Blasko-Goehringer JM, Bonnemann CG, Darras BT, Mendell JR, Lidov HG, Nishino I, Beggs AH, Kunkel LM, Kang PB. Mutations in the satellite cell gene MEGF10 cause a recessive congenital myopathy with minicores. Neurogenetics. 2012;13(2):115-24. Epub

2012/03/01. doi: 10.1007/s10048-012-0315-z. PubMed PMID: 22371254; PMCID: Pmc3332380.
223. Hayward CP, Rivard GE, Kane WH, Drouin J, Zheng S, Moore JC, Kelton JG. An autosomal dominant, qualitative platelet disorder associated with multimerin deficiency, abnormalities in platelet factor V, thrombospondin, von Willebrand factor, and fibrinogen and an epinephrine aggregation defect. Blood. 1996;87(12):4967-78. Epub 1996/06/15. PubMed PMID: 8652809.
224. Garg V, Muth AN, Ransom JF, Schluterman MK, Barnes R, King IN, Grossfeld PD, Srivastava D. Mutations in NOTCH1 cause aortic valve disease. Nature. 2005;437(7056):270-4. Epub 2005/07/19. doi: 10.1038/nature03940. PubMed PMID: 16025100.
225. McDaniell R, Warthen DM, Sanchez-Lara PA, Pai A, Krantz ID, Piccoli DA, Spinner NB. NOTCH2 mutations cause Alagille syndrome, a heterogeneous disorder of the notch signaling pathway. American journal of human genetics. 2006;79(1):169-73. Epub 2006/06/15. doi: 10.1086/505332. PubMed PMID: 16773578; PMCID: Pmc1474136.
226. Isidor B, Lindenbaum P, Pichon O, Bezieau S, Dina C, Jacquemont S, Martin-Coignard D, Thauvin-Robinet C, Le Merrer M, Mandel JL, David A, Faivre L, Cormier-Daire V, Redon R, Le Caignec C. Truncating mutations in the last exon of NOTCH2 cause a rare skeletal disorder with osteoporosis. Nat Genet. 2011;43(4):306-8. Epub 2011/03/08. doi: 10.1038/ng.778. PubMed PMID: 21378989.
227. Simpson MA, Irving MD, Asilmaz E, Gray MJ, Dafou D, Elmslie FV, Mansour S, Holder SE, Brain CE, Burton BK, Kim KH, Pauli RM, Aftimos S, Stewart H, Kim CA, Holder-Espinasse M, Robertson SP, Drake WM, Trembath RC. Mutations in NOTCH2 cause Hajdu-Cheney syndrome, a disorder of severe and progressive bone loss. Nat Genet. 2011;43(4):303-5. Epub 2011/03/08. doi: 10.1038/ng.779. PubMed PMID: 21378985.
228. Joutel A, Vahedi K, Corpechot C, Troesch A, Chabriat H, Vayssiere C, Cruaud C, Maciazek J, Weissenbach J, Bousser MG, Bach JF, Tournier-Lasserve E. Strong clustering and stereotyped nature of Notch3 mutations in CADASIL patients. Lancet. 1997;350(9090):1511-5. Epub 1997/12/06. doi: 10.1016/s0140-6736(97)08083-5. PubMed PMID: 9388399.
229. Dichgans M, Filippi M, Bruning R, Iannucci G, Berchtenbreiter C, Minicucci L, Uttner I, Crispin A, Ludwig H, Gasser T, Yousry TA. Quantitative MRI in CADASIL: correlation with disability and cognitive performance. Neurology. 1999;52(7):1361-7. Epub 1999/05/05. PubMed PMID: 10227618.
230. Fouillade C, Chabriat H, Riant F, Mine M, Arnoud M, Magy L, Bousser MG, Tournier-Lasserve E, Joutel A. Activating NOTCH3 mutation in a patient with small-vessel-disease of the brain. Human mutation. 2008;29(3):452. Epub 2008/02/15. doi: 10.1002/humu.9527. PubMed PMID: 18273901.
231. Martignetti JA, Tian L, Li D, Ramirez MC, Camacho-Vanegas O, Camacho SC, Guo Y, Zand DJ, Bernstein AM, Masur SK, Kim CE, Otieno FG, Hou C, Abdel-Magid N, Tweddale B, Metry D, Fournet JC, Papp E, McPherson EW, Zabel C, Vaksmann G, Morisot C, Keating B, Sleiman PM, Cleveland JA, Everman DB, Zackai E, Hakonarson H. Mutations in PDGFRB cause autosomal-dominant infantile myofibromatosis. American journal of human genetics. 2013;92(6):1001-7. Epub 2013/06/05. doi: 10.1016/j.ajhg.2013.04.024. PubMed PMID: 23731542; PMCID: Pmc3675260.
232. Nicole S, Davoine CS, Topaloglu H, Cattolico L, Barral D, Beighton P, Hamida CB, Hammouda H, Cruaud C, White PS, Samson D, Urtizberea JA, Lehmann-Horn F, Weissenbach J, Hentati F, Fontaine B. Perlecan, the major proteoglycan of basement membranes, is altered in patients with Schwartz-Jampel syndrome (chondrodystrophic myotonia). Nat Genet. 2000;26(4):480-3. Epub 2000/12/02. doi: 10.1038/82638. PubMed PMID: 11101850.

233. Arikawa-Hirasawa E, Wilcox WR, Le AH, Silverman N, Govindraj P, Hassell JR, Yamada Y. Dyssegmental dysplasia, Silverman-Handmaker type, is caused by functional null mutations of the perlecan gene. Nat Genet. 2001;27(4):431-4. Epub 2001/03/30. doi: 10.1038/86941. PubMed PMID: 11279527.
234. Miyata T, Zheng YZ, Sakata T, Kato H. Protein C Osaka 10 with aberrant propeptide processing: loss of anticoagulant activity due to an amino acid substitution in the protein C precursor. Thromb Haemost. 1995;74(4):1003-8. Epub 1995/10/01. PubMed PMID: 8560401.
235. Romeo G, Hassan HJ, Staempfli S, Roncuzzi L, Cianetti L, Leonardi A, Vicente V, Mannucci PM, Bertina R, Peschle C, et al. Hereditary thrombophilia: identification of nonsense and missense mutations in the protein C gene. Proc Natl Acad Sci U S A. 1987;84(9):2829-32. Epub 1987/05/01. PubMed PMID: 2437584; PMCID: Pmc304753.
236. Couture P, Demers C, Morissette J, Delage R, Jomphe M, Couture L, Simard J. Type I protein C deficiency in French Canadians: evidence of a founder effect and association of specific protein C gene mutations with plasma protein C levels. Thromb Haemost. 1998;80(4):551-6. Epub 1998/11/03. PubMed PMID: 9798967.
237. Hong SE, Shugart YY, Huang DT, Shahwan SA, Grant PE, Hourihane JO, Martin ND, Walsh CA. Autosomal recessive lissencephaly with cerebellar hypoplasia is associated with human RELN mutations. Nat Genet. 2000;26(1):93-6. Epub 2000/09/06. doi: 10.1038/79246. PubMed PMID: 10973257.
238. Anastasio N, Ben-Omran T, Teebi A, Ha KC, Lalonde E, Ali R, Almureikhi M, Der Kaloustian VM, Liu J, Rosenblatt DS, Majewski J, Jerome-Majewska LA. Mutations in SCARF2 are responsible for Van Den Ende-Gupta syndrome. American journal of human genetics. 2010;87(4):553-9. Epub 2010/10/05. doi: 10.1016/j.ajhg.2010.09.005. PubMed PMID: 20887961; PMCID: Pmc2948800.
239. Degen SJ, Rajput B, Reich E. The human tissue plasminogen activator gene. The Journal of biological chemistry. 1986;261(15):6972-85. Epub 1986/05/25. PubMed PMID: 3009482.
240. Hart TC, Gorry MC, Hart PS, Woodard AS, Shihabi Z, Sandhu J, Shirts B, Xu L, Zhu H, Barmada MM, Bleyer AJ. Mutations of the UMOD gene are responsible for medullary cystic kidney disease 2 and familial juvenile hyperuricaemic nephropathy. Journal of medical genetics. 2002;39(12):882-92. Epub 2002/12/10. PubMed PMID: 12471200; PMCID: Pmc1757206.
241. Rampoldi L, Caridi G, Santon D, Boaretto F, Bernascone I, Lamorte G, Tardanico R, Dagnino M, Colussi G, Scolari F, Ghiggeri GM, Amoroso A, Casari G. Allelism of MCKD, FJHN and GCKD caused by impairment of uromodulin export dynamics. Hum Mol Genet. 2003;12(24):3369-84. Epub 2003/10/23. doi: 10.1093/hmg/ddg353. PubMed PMID: 14570709.
242. Paterson AD, Rommens JM, Bharaj B, Blavignac J, Wong I, Diamandis M, Waye JS, Rivard GE, Hayward CP. Persons with Quebec platelet disorder have a tandem duplication of PLAU, the urokinase plasminogen activator gene. Blood. 2010;115(6):1264-6. Epub 2009/12/17. doi: 10.1182/blood-2009-07-233965. PubMed PMID: 20007542.
243. Colige A, Sieron AL, Li SW, Schwarze U, Petty E, Wertelecki W, Wilcox W, Krakow D, Cohn DH, Reardon W, Byers PH, Lapiere CM, Prockop DJ, Nusgens BV. Human Ehlers-Danlos syndrome type VII C and bovine dermatosparaxis are caused by mutations in the procollagen I N-proteinase gene. American journal of human genetics. 1999;65(2):308-17. Epub 1999/07/27. doi: 10.1086/302504. PubMed PMID: 10417273; PMCID: Pmc1377929.
244. Kutz WE, Wang LW, Dagoneau N, Odrcic KJ, Cormier-Daire V, Traboulsi EI, Apte SS. Functional analysis of an ADAMTS10 signal peptide mutation in Weill-Marchesani syndrome demonstrates a long-range effect on secretion of the full-length enzyme. Human mutation. 2008;29(12):1425-34. Epub 2008/06/21. doi: 10.1002/humu.20797. PubMed PMID: 18567016.

245. Dagoneau N, Benoist-Lasselin C, Huber C, Faivre L, Megarbane A, Alswaid A, Dollfus H, Alembik Y, Munnich A, Legeai-Mallet L, Cormier-Daire V. ADAMTS10 mutations in autosomal recessive Weill-Marchesani syndrome. American journal of human genetics. 2004;75(5):801-6. Epub 2004/09/16. doi: 10.1086/425231. PubMed PMID: 15368195; PMCID: Pmc1182109.
246. Levy GG, Nichols WC, Lian EC, Foroud T, McClintick JN, McGee BM, Yang AY, Siemieniak DR, Stark KR, Gruppo R, Sarode R, Shurin SB, Chandrasekaran V, Stabler SP, Sabio H, Bouhassira EE, Upshaw JD, Jr., Ginsburg D, Tsai HM. Mutations in a member of the ADAMTS gene family cause thrombotic thrombocytopenic purpura. Nature. 2001;413(6855):488-94. Epub 2001/10/05. doi: 10.1038/35097008. PubMed PMID: 11586351.
247. Kokame K, Matsumoto M, Soejima K, Yagi H, Ishizashi H, Funato M, Tamai H, Konno M, Kamide K, Kawano Y, Miyata T, Fujimura Y. Mutations and common polymorphisms in ADAMTS13 gene responsible for von Willebrand factor-cleaving protease activity. Proc Natl Acad Sci U S A. 2002;99(18):11902-7. Epub 2002/08/16. doi: 10.1073/pnas.172277399. PubMed PMID: 12181489; PMCID: Pmc129366.
248. Schneppenheim R, Budde U, Oyen F, Angerhaus D, Aumann V, Drewke E, Hassenpflug W, Haberle J, Kentouche K, Kohne E, Kurnik K, Mueller-Wiefel D, Obser T, Santer R, Sykora KW. von Willebrand factor cleaving protease and ADAMTS13 mutations in childhood TTP. Blood. 2003;101(5):1845-50. Epub 2002/10/24. doi: 10.1182/blood-2002-08-2399. PubMed PMID: 12393505.
249. Antoine G, Zimmermann K, Plaimauer B, Grillowitzer M, Studt JD, Lammle B, Scheiflinger F. ADAMTS13 gene defects in two brothers with constitutional thrombotic thrombocytopenic purpura and normalization of von Willebrand factor-cleaving protease activity by recombinant human ADAMTS13. Br J Haematol. 2003;120(5):821-4. Epub 2003/03/05. PubMed PMID: 12614216.
250. Morales J, Al-Sharif L, Khalil DS, Shinwari JM, Bavi P, Al-Mahrouqi RA, Al-Rajhi A, Alkuraya FS, Meyer BF, Al Tassan N. Homozygous mutations in ADAMTS10 and ADAMTS17 cause lenticular myopia, ectopia lentis, glaucoma, spherophakia, and short stature. The American Journal of Human Genetics. 2009;85(5):558-68.
251. Aldahmesh MA, Alshammari MJ, Khan AO, Mohamed JY, Alhabib FA, Alkuraya FS. The syndrome of microcornea, myopic chorioretinal atrophy, and telecanthus (MMCAT) is caused by mutations in ADAMTS18. Human mutation. 2013;34(9):1195-9. Epub 2013/07/03. doi: 10.1002/humu.22374. PubMed PMID: 23818446.
252. Le Goff C, Morice-Picard F, Dagoneau N, Wang LW, Perrot C, Crow YJ, Bauer F, Flori E, Prost-Squarcioni C, Krakow D, Ge G, Greenspan DS, Bonnet D, Le Merrer M, Munnich A, Apte SS, Cormier-Daire V. ADAMTSL2 mutations in geleophysic dysplasia demonstrate a role for ADAMTS-like proteins in TGF-beta bioavailability regulation. Nat Genet. 2008;40(9):1119-23. Epub 2008/08/05. doi: 10.1038/ng.199. PubMed PMID: 18677313; PMCID: Pmc2675613.
253. Ahram D, Sato TS, Kohilan A, Tayeh M, Chen S, Leal S, Al-Salem M, El-Shanti H. A homozygous mutation in ADAMTSL4 causes autosomal-recessive isolated ectopia lentis. American journal of human genetics. 2009;84(2):274-8. Epub 2009/02/10. doi: 10.1016/j.ajhg.2009.01.007. PubMed PMID: 19200529; PMCID: Pmc2668005.
254. Christensen AE, Fiskerstrand T, Knappskog PM, Boman H, Rodahl E. A novel ADAMTSL4 mutation in autosomal recessive ectopia lentis et pupillae. Investigative ophthalmology & visual science. 2010;51(12):6369-73. Epub 2010/08/13. doi: 10.1167/iovs.10-5597. PubMed PMID: 20702823.
255. Ikinciogullari A, Tekin M, Dogu F, Reisli I, Tanir G, Yi Z, Garrison N, Brilliant MH, Babacan E. Meningococccal meningitis and complement component 6 deficiency associated with

oculocutaneous albinism. European journal of pediatrics. 2005;164(3):177-9. Epub 2004/11/27. doi: 10.1007/s00431-004-1582-y. PubMed PMID: 15565285.
256. Schultz DW, Klein ML, Humpert AJ, Luzier CW, Persun V, Schain M, Mahan A, Runckel C, Cassera M, Vittal V, Doyle TM, Martin TM, Weleber RG, Francis PJ, Acott TS. Analysis of the ARMD1 locus: evidence that a mutation in HEMICENTIN-1 is associated with age-related macular degeneration in a large family. Hum Mol Genet. 2003;12(24):3315-23. Epub 2003/10/23. doi: 10.1093/hmg/ddg348. PubMed PMID: 14570714.
257. Fredrikson GN, Westberg J, Kuijper EJ, Tijssen CC, Sjoholm AG, Uhlen M, Truedsson L. Molecular characterization of properdin deficiency type III: dysfunction produced by a single point mutation in exon 9 of the structural gene causing a tyrosine to aspartic acid interchange. Journal of immunology (Baltimore, Md : 1950). 1996;157(8):3666-71. Epub 1996/10/15. PubMed PMID: 8871668.
258. Fredrikson GN, Gullstrand B, Westberg J, Sjoholm AG, Uhlen M, Truedsson L. Expression of properdin in complete and incomplete deficiency: normal in vitro synthesis by monocytes in two cases with properdin deficiency type II due to distinct mutations. Journal of clinical immunology. 1998;18(4):272-82. Epub 1998/08/26. PubMed PMID: 9710744.
259. van den Bogaard R, Fijen CA, Schipper MG, de Galan L, Kuijper EJ, Mannens MM. Molecular characterisation of 10 Dutch properdin type I deficient families: mutation analysis and X-inactivation studies. European journal of human genetics : EJHG. 2000;8(7):513-8. Epub 2000/07/26. doi: 10.1038/sj.ejhg.5200496. PubMed PMID: 10909851.
260. Hirose Y, Chiba K, Karasugi T, Nakajima M, Kawaguchi Y, Mikami Y, Furuichi T, Mio F, Miyake A, Miyamoto T, Ozaki K, Takahashi A, Mizuta H, Kubo T, Kimura T, Tanaka T, Toyama Y, Ikegawa S. A functional polymorphism in THBS2 that affects alternative splicing and MMP binding is associated with lumbar-disc herniation. American journal of human genetics. 2008;82(5):1122-9. Epub 2008/05/06. doi: 10.1016/j.ajhg.2008.03.013. PubMed PMID: 18455130; PMCID: Pmc2427305.
261. Hurvitz JR, Suwairi WM, Van Hul W, El-Shanti H, Superti-Furga A, Roudier J, Holderbaum D, Pauli RM, Herd JK, Van Hul EV, Rezai-Delui H, Legius E, Le Merrer M, Al-Alami J, Bahabri SA, Warman ML. Mutations in the CCN gene family member WISP3 cause progressive pseudorheumatoid dysplasia. Nat Genet. 1999;23(1):94-8. Epub 1999/09/02. doi: 10.1038/12699. PubMed PMID: 10471507.
262. Rana NA, Nita-Lazar A, Takeuchi H, Kakuda S, Luther KB, Haltiwanger RS. O-glucose trisaccharide is present at high but variable stoichiometry at multiple sites on mouse Notch1. J Biol Chem. 2011;286(36):31623-37. Epub 2011/07/16. doi: 10.1074/jbc.M111.268243. PubMed PMID: 21757702; PMCID: 3173066.
263. Nye JS, Kopan R, Axel R. An activated Notch suppresses neurogenesis and myogenesis but not gliogenesis in mammalian cells. Development. 1994;120(9):2421-30.
264. Shimizu K, Chiba S, Kumano K, Hosoya N, Takahashi T, Kanda Y, Hamada Y, Yazaki Y, Hirai H. Mouse jagged1 physically interacts with notch2 and other notch receptors assessment by quantitative methods. Journal of Biological Chemistry. 1999;274(46):32961-9.
265. Takeuchi H, Kantharia J, Sethi MK, Bakker H, Haltiwanger RS. Site-specific O-Glucosylation of the Epidermal Growth Factor-like (EGF) Repeats of Notch EFFICIENCY OF GLYCOSYLATION IS AFFECTED BY PROPER FOLDING AND AMINO ACID SEQUENCE OF INDIVIDUAL EGF REPEATS. Journal of Biological Chemistry. 2012;287(41):33934-44.
266. Fellmann C, Hoffmann T, Sridhar V, Hopfgartner B, Muhar M, Roth M, Lai DY, Barbosa IA, Kwon JS, Guan Y. An optimized microRNA backbone for effective single-copy RNAi. Cell reports. 2013;5(6):1704-13.
267. Arboleda-Velasquez JF, Rampal R, Fung E, Darland DC, Liu M, Martinez MC, Donahue CP, Navarro-Gonzalez MF, Libby P, D'Amore PA. CADASIL mutations impair Notch3 glycosylation by Fringe. Human molecular genetics. 2005;14(12):1631-9.

268. Beatus P, Lundkvist J, Oberg C, Lendahl U. The notch 3 intracellular domain represses notch 1-mediated activation through Hairy/Enhancer of split (HES) promoters. Development. 1999;126(17):3925-35.
269. Hubmacher D, Schneider M, Berardinelli S, Takeuchi H, Willard B, Reinhard D, Haltiwanger RS, Apte S. Unusual life cycle and impact on microfibril assembly of ADAMTS17, a secreted metalloprotease mutated in genetic eye disease. Scientific reports. In Press.
270. Thomas M, Lu JJ, Ge Q, Zhang C, Chen J, Klibanov AM. Full deacylation of polyethylenimine dramatically boosts its gene delivery efficiency and specificity to mouse lung. Proceedings of the National Academy of Sciences of the United States of America. 2005;102(16):5679-84.
271. Kakuda S, Haltiwanger RS. Analyzing the posttranslational modification status of Notch using mass spectrometry. Methods Mol Biol. 2014;1187:209-21. doi: 10.1007/978-1-4939-1139-4_16. PubMed PMID: 25053492.
272. Yamamoto S, Charng W-L, Rana NA, Kakuda S, Jaiswal M, Bayat V, Xiong B, Zhang K, Sandoval H, David G, Wang H, Haltiwanger RS, Bellen HJ. A mutation in EGF repeat-8 of Notch discriminates between Serrate/Jagged and Delta family ligands. Science. 2012;338:1229-32.
273. Rana NA, Haltiwanger RS. Fringe benefits: functional and structural impacts of O-glycosylation on the extracellular domain of Notch receptors. Current opinion in structural biology. 2011;21(5):583-9. Epub 2011/09/20. doi: 10.1016/j.sbi.2011.08.008. PubMed PMID: 21924891; PMCID: 3195399.
274. Wewers MD, Crystal RG. Alpha-1 antitrypsin augmentation therapy. Copd. 2013;10 Suppl 1:64-7. Epub 2013/04/03. doi: 10.3109/15412555.2013.764402. PubMed PMID: 23527997.
275. Kimmel CB, Ballard WW, Kimmel SR, Ullmann B, Schilling TF. Stages of embryonic development of the zebrafish. Developmental dynamics. 1995;203(3):253-310.
276. White RM, Sessa A, Burke C, Bowman T, LeBlanc J, Ceol C, Bourque C, Dovey M, Goessling W, Burns CE. Transparent adult zebrafish as a tool for in vivo transplantation analysis. Cell stem cell. 2008;2(2):183-9.
277. Parsons MJ, Pisharath H, Yusuff S, Moore JC, Siekmann AF, Lawson N, Leach SD. Notch-responsive cells initiate the secondary transition in larval zebrafish pancreas. Mechanisms of development. 2009;126(10):898-912.
278. Song Y, Kumar V, Wei H-X, Qiu J, Stanley P. Lunatic, Manic, and Radical Fringe Each Promote T and B Cell Development. The Journal of Immunology. 2016;196(1):232-43.
279. Van de Walle I, De Smet G, Gärtner M, De Smedt M, Waegemans E, Vandekerckhove B, Leclercq G, Plum J, Aster JC, Bernstein ID. Jagged2 acts as a Delta-like Notch ligand during early hematopoietic cell fate decisions. Blood. 2011;117(17):4449-59.
280. Wang W, Hu T, Frantom PA, Zheng T, Gerwe B, Del Amo DS, Garret S, Seidel RD, Wu P. Chemoenzymatic synthesis of GDP-L-fucose and the Lewis X glycan derivatives. Proceedings of the National Academy of Sciences. 2009;106(38):16096-101.
281. MacDonald MJ, Hesp CR, Schipper DJ, Pesant M, Beauchemin AM. Highly enantioselective intermolecular hydroamination of allylic amines with chiral aldehydes as tethering catalysts. Chemistry–A European Journal. 2013;19(8):2597-601.
282. Kaliappan KP, Subrahmanyam AV. A new versatile strategy for C-aryl glycosides. Organic letters. 2007;9(6):1121-4.
283. Alley SC, Jeffrey SC, Sussman D, Benjamin DR, Toki B, Burke PJ. Methods and compositions for making antibodies and antibody derivatives with reduced core fucosylation. Google Patents; 2012.
284. Artavanis-Tsakonas S, Rand MD, Lake RJ. Notch signaling: cell fate control and signal integration in development. Science. 1999;284(5415):770-6.

285. Hori K, Sen A, Artavanis-Tsakonas S. Notch signaling at a glance. J Cell Sci. 2013;126(10):2135-40.
286. Lai EC. Notch signaling: control of cell communication and cell fate. Development. 2004;131(5):965-73.
287. Kopan R, Ilagan MXG. The canonical Notch signaling pathway: unfolding the activation mechanism. Cell. 2009;137(2):216-33.
288. Ellisen LW, Bird J, West DC, Soreng AL, Reynolds TC, Smith SD, Sklar J. TAN-1, the human homolog of the Drosophila notch gene, is broken by chromosomal translocations in T lymphoblastic neoplasms. Cell. 1991;66(4):649-61.
289. Teodorczyk M, Schmidt MH. Notching on cancer's door: Notch signaling in brain tumors. Frontiers in oncology. 2015;4:341.
290. Wu G, Wilson G, George J, Qiao L. Modulation of Notch signaling as a therapeutic approach for liver cancer. Current gene therapy. 2015;15(2):171-81.
291. Espinoza I, Pochampally R, Xing F, Watabe K, Miele L. Notch signaling: targeting cancer stem cells and epithelial-to-mesenchymal transition. OncoTargets and therapy. 2013;6:1249-59. Epub 2013/09/18. doi: 10.2147/OTT.S36162. PubMed PMID: 24043949; PMCID: 3772757.
292. Yin L, Velazquez OC, Liu Z-J. Notch signaling: emerging molecular targets for cancer therapy. Biochemical pharmacology. 2010;80(5):690-701.
293. Wu Y, Cain-Hom C, Choy L, Hagenbeek TJ, de Leon GP, Chen Y, Finkle D, Venook R, Wu X, Ridgway J. Therapeutic antibody targeting of individual Notch receptors. Nature. 2010;464(7291):1052-7.
294. Sagert J, West J, Vasiljeva O, Richardson J, Desnoyers L, Liu S, Yang A, Wong C, Menendez E, Polu K, Lowman H. Abstract C158: Tumor-specific inhibition of jagged-dependent notch signaling using a Probody™ therapeutic. Molecular Cancer Therapeutics. 2013;12(11 Supplement):C158. doi: 10.1158/1535-7163.targ-13-c158.
295. Tran IT, Sandy AR, Carulli AJ, Ebens C, Chung J, Shan GT, Radojcic V, Friedman A, Gridley T, Shelton A. Blockade of individual Notch ligands and receptors controls graft-versus-host disease. The Journal of clinical investigation. 2013;123(4):1590-604.
296. Lafkas D, Shelton A, Chiu C, de Leon Boenig G, Chen Y, Stawicki SS, Siltanen C, Reichelt M, Zhou M, Wu X. Therapeutic antibodies reveal Notch control of transdifferentiation in the adult lung. Nature. 2015.
297. Wharton KA, Johansen KM, Xu T, Artavanis-Tsakonas S. Nucleotide sequence from the neurogenic locus notch implies a gene product that shares homology with proteins containing EGF-like repeats. Cell. 1985;43(3):567-81.
298. Matsuura A, Ito M, Sakaidani Y, Kondo T, Murakami K, Furukawa K, Nadano D, Matsuda T, Okajima T. O-linked N-acetylglucosamine is present on the extracellular domain of notch receptors. Journal of Biological Chemistry. 2008;283(51):35486-95.
299. Bruckner K, Perez L, Clausen H, Cohen S. Glycosyltransferase activity of Fringe modulates Notch-Delta interactions. Nature. 2000;406(6794):411-4.
300. Okajima T, Xu A, Irvine KD. Modulation of notch-ligand binding by protein O-fucosyltransferase 1 and fringe. Journal of Biological Chemistry. 2003;278(43):42340-5.
301. Herrmann M, von der Lieth CW, Stehling P, Reutter W, Pawlita M. Consequences of a subtle sialic acid modification on the murine polyomavirus receptor. Journal of virology. 1997;71(8):5922-31.
302. Descheny L, Gainers ME, Walcheck B, Dimitroff CJ. Ameliorating skin-homing receptors on malignant T cells with a fluorosugar analog of N-acetylglucosamine: P-selectin ligand is a more sensitive target than E-selectin ligand. Journal of investigative dermatology. 2006;126(9):2065-73.

303. Gloster TM, Zandberg WF, Heinonen JE, Shen DL, Deng L, Vocadlo DJ. Hijacking a biosynthetic pathway yields a glycosyltransferase inhibitor within cells. Nature chemical biology. 2011;7(3):174-81.
304. Hicks C, Johnston SH, Collazo A, Vogt TF, Weinmaster G. Fringe differentially modulates Jagged1 and Delta1 signalling through Notch1 and Notch2. Nature cell biology. 2000;2(8):515-20.
305. Taylor P, Takeuchi H, Sheppard D, Chillakuri C, Lea SM, Haltiwanger RS, Handford PA. Fringe-mediated extension of O-linked fucose in the ligand-binding region of Notch1 increases binding to mammalian Notch ligands. Proceedings of the National Academy of Sciences. 2014;111(20):7290-5.
306. Yang L-T, Nichols JT, Yao C, Manilay JO, Robey EA, Weinmaster G. Fringe glycosyltransferases differentially modulate Notch1 proteolysis induced by Delta1 and Jagged1. Molecular biology of the cell. 2005;16(2):927-42.
307. Panin VM, Shao L, Lei L, Moloney DJ, Irvine KD, Haltiwanger RS. Notch Ligands Are Substrates for ProteinO-Fucosyltransferase-1 and Fringe. Journal of Biological Chemistry. 2002;277(33):29945-52.
308. Shi S, Ge C, Luo Y, Hou X, Haltiwanger RS, Stanley P. The threonine that carries fucose, but not fucose, is required for Cripto to facilitate Nodal signaling. Journal of Biological Chemistry. 2007;282(28):20133-41.
309. Koch U, Lacombe TA, Holland D, Bowman JL, Cohen BL, Egan SE, Guidos CJ. Subversion of the T/B lineage decision in the thymus by lunatic fringe-mediated inhibition of Notch-1. Immunity. 2001;15(2):225-36.
310. Purow BW, Haque RM, Noel MW, Su Q, Burdick MJ, Lee J, Sundaresan T, Pastorino S, Park JK, Mikolaenko I. Expression of Notch-1 and its ligands, Delta-like-1 and Jagged-1, is critical for glioma cell survival and proliferation. Cancer research. 2005;65(6):2353-63.
311. Grabher C, von Boehmer H, Look AT. Notch 1 activation in the molecular pathogenesis of T-cell acute lymphoblastic leukaemia. Nature Reviews Cancer. 2006;6(5):347-59.
312. Andrawes MB, Xu X, Liu H, Ficarro SB, Marto JA, Aster JC, Blacklow SC. Intrinsic selectivity of Notch 1 for Delta-like 4 over Delta-like 1. Journal of Biological Chemistry. 2013;288(35):25477-89.
313. Lira-Navarrete E, Valero-González J, Villanueva R, Martínez-Júlvez M, Tejero T, Merino P, Panjikar S, Hurtado-Guerrero R. Structural insights into the mechanism of protein O-fucosylation. PLoS One. 2011;6(9):e25365.
314. Hiruma-Shimizu K, Hosoguchi K, Liu Y, Fujitani N, Ohta T, Hinou H, Matsushita T, Shimizu H, Feizi T, Nishimura S-I. Chemical synthesis, folding, and structural insights into O-fucosylated epidermal growth factor-like repeat 12 of mouse Notch-1 receptor. Journal of the American Chemical Society. 2010;132(42):14857-65.
315. Kakuda S, Haltiwanger RS. Deciphering the Fringe-mediated Notch Code. Developmental Cell. 2016.
316. Bray SJ. Notch signalling in context. Nature Reviews Molecular Cell Biology. 2016;17(11):722-35.
317. Joutel A, Corpechot C, Ducros A, Vahedi K, Chabriat H, Mouton P, Alamowitch S, Domenga V, Cécillion M, Maréchal E. Notch3 mutations in CADASIL, a hereditary adult-onset condition causing stroke and dementia. Nature. 1996;383(6602):707-10.
318. Weng AP, Ferrando AA, Lee W, Morris JP, Silverman LB, Sanchez-Irizarry C, Blacklow SC, Look AT, Aster JC. Activating mutations of NOTCH1 in human T cell acute lymphoblastic leukemia. Science. 2004;306(5694):269-71.
319. Rampal R, Luther KB, Haltiwanger RS. Notch signaling in normal and disease States: possible therapies related to glycosylation. Curr Mol Med. 2007;7(4):427-45. Epub 2007/06/23. PubMed PMID: 17584081.

320. Schuster-Gossler K, Harris B, Johnson KR, Serth J, Gossler A. Notch signalling in the paraxial mesoderm is most sensitive to reduced Pofut1 levels during early mouse development. BMC developmental biology. 2009;9(1):1.
321. American Cacner Society: Cancer Facts and Figures 2014. Atlanta, Ga: American Cancer Society; 2014.
322. A new prognostic system for hepatocellular carcinoma: a retrospective study of 435 patients: the Cancer of the Liver Italian Program (CLIP) investigators. Hepatology (Baltimore, Md). 1998;28(3):751-5. doi: 10.1002/hep.510280322.
323. Bruix J, Sherman M, American Association for the Study of Liver D. Management of hepatocellular carcinoma: an update. Hepatology. 2011;53(3):1020-2. Epub 2011/03/05. doi: 10.1002/hep.24199. PubMed PMID: 21374666; PMCID: 3084991.
324. Li JL, Sainson RC, Oon CE, Turley H, Leek R, Sheldon H, Bridges E, Shi W, Snell C, Bowden ET, Wu H, Chowdhury PS, Russell AJ, Montgomery CP, Poulsom R, Harris AL. DLL4-Notch signaling mediates tumor resistance to anti-VEGF therapy in vivo. Cancer research. 2011;71(18):6073-83. Epub 2011/08/02. doi: 10.1158/0008-5472.CAN-11-1704. PubMed PMID: 21803743.
325. Siekmann AF, Covassin L, Lawson ND. Modulation of VEGF signalling output by the Notch pathway. BioEssays : news and reviews in molecular, cellular and developmental biology. 2008;30(4):303-13. Epub 2008/03/19. doi: 10.1002/bies.20736. PubMed PMID: 18348190.
326. Razumilava N, Gores GJ. Notch-driven carcinogenesis: the merging of hepatocellular cancer and cholangiocarcinoma into a common molecular liver cancer subtype. Journal of hepatology. 2013;58(6):1244-5. Epub 2013/01/29. doi: 10.1016/j.jhep.2013.01.017. PubMed PMID: 23352938; PMCID: 3818720.
327. South AP, Cho RJ, Aster JC. The double-edged sword of Notch signaling in cancer. Seminars in cell & developmental biology. 2012;23(4):458-64. Epub 2012/02/09. doi: 10.1016/j.semcdb.2012.01.017. PubMed PMID: 22309843; PMCID: 3360804.
328. Leong KG, Karsan A. Recent insights into the role of Notch signaling in tumorigenesis. Blood. 2006;107(6):2223-33. Epub 2005/11/18. doi: 10.1182/blood-2005-08-3329. PubMed PMID: 16291593.
329. Pannuti A, Foreman K, Rizzo P, Osipo C, Golde T, Osborne B, Miele L. Targeting Notch to target cancer stem cells. Clinical cancer research : an official journal of the American Association for Cancer Research. 2010;16(12):3141-52. Epub 2010/06/10. doi: 10.1158/1078-0432.CCR-09-2823. PubMed PMID: 20530696; PMCID: 3008160.
330. Liu Z, Chen S, Boyle S, Zhu Y, Zhang A, Piwnica-Worms DR, Ilagan MX, Kopan R. The extracellular domain of Notch2 increases its cell-surface abundance and ligand responsiveness during kidney development. Developmental cell. 2013;25(6):585-98. Epub 2013/06/29. doi: 10.1016/j.devcel.2013.05.022. PubMed PMID: 23806616; PMCID: 3710456.
331. Takeuchi H, Haltiwanger RS. Role of glycosylation of Notch in development. Seminars in cell & developmental biology. 2010;21(6):638-45. Epub 2010/03/17. doi: 10.1016/j.semcdb.2010.03.003. PubMed PMID: 20226260; PMCID: 2898917.
332. Wang Y, Shao L, Shi S, Harris RJ, Spellman MW, Stanley P, Haltiwanger RS. Modification of epidermal growth factor-like repeats with O-fucose. Molecular cloning and expression of a novel GDP-fucose protein O-fucosyltransferase. The Journal of biological chemistry. 2001;276(43):40338-45. Epub 2001/08/29. doi: 10.1074/jbc.M107849200. PubMed PMID: 11524432.
333. Dejeans N, Glorieux C, Guenin S, Beck R, Sid B, Rousseau R, Bisig B, Delvenne P, Buc Calderon P, Verrax J. Overexpression of GRP94 in breast cancer cells resistant to oxidative stress promotes high levels of cancer cell proliferation and migration: implications for tumor

recurrence. Free radical biology & medicine. 2012;52(6):993-1002. Epub 2012/01/17. doi: 10.1016/j.freeradbiomed.2011.12.019. PubMed PMID: 22245095.
334. Scotto L, Narayan G, Nandula SV, Arias-Pulido H, Subramaniyam S, Schneider A, Kaufmann AM, Wright JD, Pothuri B, Mansukhani M, Murty VV. Identification of copy number gain and overexpressed genes on chromosome arm 20q by an integrative genomic approach in cervical cancer: potential role in progression. Genes, chromosomes & cancer. 2008;47(9):755-65. Epub 2008/05/29. doi: 10.1002/gcc.20577. PubMed PMID: 18506748.
335. Joseph R Moskal RA. Glycokinomics: Emerging Therapeutic Approaches for Malignant Brain Tumors. Journal of Glycomics & Lipidomics. 2013;03(01). doi: 10.4172/2153-0637.1000109.
336. Cerami E, Gao J, Dogrusoz U, Gross B, Sumer SO, Aksoy BA, Jacobsen A, Byrne CJ, Heuer ML, Larsson E, Antipin Y, Reva B, Goldberg AP, Sander C, Schultz N. The cBio Cancer Genomics Portal: An Open Platform for Exploring Multidimensional Cancer Genomics Data. Cancer Discovery. 2012;2(5):401-4. doi: 10.1158/2159-8290.CD-12-0095
337. Barretina J, Caponigro G, Stransky N, Venkatesan K, Margolin AA, Kim S, Wilson CJ, Lehár J, Kryukov GV, Sonkin D. The Cancer Cell Line Encyclopedia enables predictive modelling of anticancer drug sensitivity. Nature. 2012;483(7391):603-7.
338. Sainz B, Jr., Heeschen C. Standing out from the crowd: cancer stem cells in hepatocellular carcinoma. Cancer cell. 2013;23(4):431-3. Epub 2013/04/20. doi: 10.1016/j.ccr.2013.03.023. PubMed PMID: 23597561.
339. Groth C, Fortini ME. Therapeutic approaches to modulating Notch signaling: current challenges and future prospects. Seminars in cell & developmental biology. 2012;23(4):465-72. Epub 2012/02/09. doi: 10.1016/j.semcdb.2012.01.016. PubMed PMID: 22309842; PMCID: 3372654.
340. Okajima T, Irvine KD. Regulation of notch signaling by o-linked fucose. Cell. 2002;111(6):893-904.
341. Chen J, Moloney DJ, Stanley P. Fringe modulation of Jagged1-induced Notch signaling requires the action of β4galactosyltransferase-1. Proceedings of the National Academy of Sciences. 2001;98(24):13716-21.
342. Dang TP, Gazdar AF, Virmani AK, Sepetavec T, Hande KR, Minna JD, Roberts JR, Carbone DP. Chromosome 19 translocation, overexpression of Notch3, and human lung cancer. Journal of the National Cancer Institute. 2000;92(16):1355-7.
343. Hu L, Xue F, Shao M, Deng A, Wei G. Aberrant expression of Notch3 predicts poor survival for hepatocellular carcinomas. Bioscience trends. 2013;7(3):152-6.
344. Yamaguchi N, Oyama T, Ito E, Satoh H, Azuma S, Hayashi M, Shimizu K, Honma R, Yanagisawa Y, Nishikawa A. NOTCH3 signaling pathway plays crucial roles in the proliferation of ErbB2-negative human breast cancer cells. Cancer research. 2008;68(6):1881-8.
345. Serafin V, Persano L, Moserle L, Esposito G, Ghisi M, Curtarello M, Bonanno L, Masiero M, Ribatti D, Stürzl M. Notch3 signalling promotes tumour growth in colorectal cancer. The Journal of pathology. 2011;224(4):448-60.
346. Bellavia D, Campese AF, Alesse E, Vacca A, Felli MP, Balestri A, Stoppacciaro A, Tiveron C, Tatangelo L, Giovarelli M. Constitutive activation of NF‐κB and T‐cell leukemia/lymphoma in Notch3 transgenic mice. The EMBO journal. 2000;19(13):3337-48.
347. Xu K, Usary J, Kousis PC, Prat A, Wang D-Y, Adams JR, Wang W, Loch AJ, Deng T, Zhao W. Lunatic fringe deficiency cooperates with the Met/Caveolin gene amplicon to induce basal-like breast cancer. Cancer cell. 2012;21(5):626-41.
348. Yi F, Amarasinghe B, Dang TP. Manic fringe inhibits tumor growth by suppressing Notch3 degradation in lung cancer. American journal of cancer research. 2013;3(5):490.

349. Apte SS. A disintegrin-like and metalloprotease (reprolysin-type) with thrombospondin type 1 motif (ADAMTS) superfamily: functions and mechanisms. Journal of Biological Chemistry. 2009;284(46):31493-7.
350. Khan AO, Aldahmesh MA, Al-Ghadeer H, Mohamed JY, Alkuraya FS. Familial spherophakia with short stature caused by a novel homozygous ADAMTS17 mutation. Ophthalmic genetics. 2012;33(4):235-9.
351. Tsilou E, MacDonald IM. Weill-Marchesani Syndrome2013.
352. Faivre L, Dollfus H, Lyonnet S, Alembik Y, Mégarbané A, Samples J, Gorlin RJ, Alswaid A, Feingold J, Le Merrer M. Clinical homogeneity and genetic heterogeneity in Weill–Marchesani syndrome. American Journal of Medical Genetics Part A. 2003;123(2):204-7.
353. Forman OP, Pettitt L, Komáromy AM, Bedford P, Mellersh C. A Novel Genome-Wide Association Study Approach Using Genotyping by Exome Sequencing Leads to the Identification of a Primary Open Angle Glaucoma Associated Inversion Disrupting ADAMTS17. PloS one. 2015;10(12):e0143546.
354. van Duyvenvoorde HA, Lui JC, Kant SG, Oostdijk W, Gijsbers A, Hoffer M, Karperien M, Walenkamp M, Noordam C, Voorhoeve PG. Copy number variants in patients with short stature. Eur J Hum Genet. 2014;22(5):602-9.
355. Allen HL, Estrada K, Lettre G, Berndt SI, Weedon MN, Rivadeneira F, Willer CJ, Jackson AU, Vedantam S, Raychaudhuri S. Hundreds of variants clustered in genomic loci and biological pathways affect human height. Nature. 2010;467(7317):832-8.
356. Acar M, Jafar-Nejad H, Takeuchi H, Rajan A, Ibrani D, Rana NA, Pan H, Haltiwanger RS, Bellen HJ. Rumi is a CAP10 domain glycosyltransferase that modifies Notch and is required for Notch signaling. Cell. 2008;132(2):247-58.
357. Sakaidani Y, Ichiyanagi N, Saito C, Nomura T, Ito M, Nishio Y, Nadano D, Matsuda T, Furukawa K, Okajima T. O-linked-N-acetylglucosamine modification of mammalian Notch receptors by an atypical O-GlcNAc transferase Eogt1. Biochemical and biophysical research communications. 2012;419(1):14-9.
358. Müller R, Jenny A, Stanley P. The EGF repeat-specific O-GlcNAc-transferase Eogt interacts with notch signaling and pyrimidine metabolism pathways in Drosophila. PloS one. 2013;8(5):e62835.
359. Shaheen R, Aglan M, Keppler-Noreuil K, Faqeih E, Ansari S, Horton K, Ashour A, Zaki MS, Al-Zahrani F, Cueto-González AM. Mutations in EOGT confirm the genetic heterogeneity of autosomal-recessive Adams-Oliver syndrome. The American Journal of Human Genetics. 2013;92(4):598-604.
360. Cohen I, Silberstein E, Perez Y, Landau D, Elbedour K, Langer Y, Kadir R, Volodarsky M, Sivan S, Narkis G. Autosomal recessive Adams-Oliver syndrome caused by homozygous mutation in EOGT, encoding an EGF domain-specific O-GlcNAc transferase. European Journal of Human Genetics. 2014;22(3).
361. Fernandez-Valdivia R, Takeuchi H, Samarghandi A, Lopez M, Leonardi J, Haltiwanger RS, Jafar-Nejad H. Regulation of mammalian Notch signaling and embryonic development by the protein O-glucosyltransferase Rumi. Development. 2011;138(10):1925-34.
362. Takeuchi H, Fernández-Valdivia RC, Caswell DS, Nita-Lazar A, Rana NA, Garner TP, Weldeghiorghis TK, Macnaughtan MA, Jafar-Nejad H, Haltiwanger RS. Rumi functions as both a protein O-glucosyltransferase and a protein O-xylosyltransferase. Proceedings of the National Academy of Sciences. 2011;108(40):16600-5.
363. Wang X, Lv X, Zhang J, Yu H, Liu N, Guan J, Wei H, Ma L. KDELC1, a novel endoplasmic reticulum resident glycoprotein in hepatic dysfunction. INTERNATIONAL JOURNAL OF CLINICAL AND EXPERIMENTAL MEDICINE. 2016;9(6):10529-36.